



Geochemical evolution of the acid crater lake of Poás volcano (Costa Rica)

Insights into volcanic-hydrothermal processes



Geochemical evolution of the acid crater lake of Poás volcano (Costa Rica): Insights into volcanic-hydrothermal processes

María Martínez Cruz



Universiteit Utrecht

November 2008

Front cover: Poás Volcano photographed from the air in May 2004 by Bernhard Edmaier.
The acid lake looks quiescent and shows an unusual dark greenish colour.

Graphic design and figures:
GeoMedia [6997], Faculty of Geosciences, Utrecht University

Geochemical evolution of the acid crater lake of Poás volcano (Costa Rica): Insights into volcanic-hydrothermal processes

Evolución de la geoquímica del lago cratérico ácido del volcán Poás (Costa Rica):

Una mirada a procesos volcánico-hidrotermales

(con resumen en español)

PROEFSCHRIFT

ter verkrijging van de graad van doctor aan de Universiteit Utrecht

op gezag van de rector magnificus, prof.dr. J.C. Stoof,

ingevolge het besluit van het college voor promoties

in het openbaar te verdedigen op

dinsdag 25 november 2008 des middags te 12.45 uur

door

María Martínez Cruz

geboren op 2 Augustus 1965

te Liberia-Guanacaste, Costa Rica

Promotor:
Prof. dr. B.H.W.S. de Jong

Co-promotor:
Dr. M.J. van Bergen

This research was financially supported by scholarship programmes of Utrecht University and Universidad Nacional, the Petrology Group of the Department of Earth Sciences, OVSICORI and the Laboratory of Atmospheric Chemistry of the School of Chemistry of Universidad Nacional, as well as by grants provided by the Commission of Incentives of the Costa Rican Council for Scientific and Technological Research (CONICIT) of the Ministry of Science and Technology of Costa Rica (MICIT).

La Vorágine

¿Cuál es aquí la poesía de los retiros, dónde están las mariposas que parecen flores traslúcidas,
los pájaros mágicos, el arroyo cantor?

¡Pobre fantasía de los poetas que sólo conocen las soledades domesticadas!

¡Nada de ruiseñores enamorados, nada de jardín versallesco, nada de panoramas sentimentales! Aquí, los respuestas de sapos hidrópicos, las malezas de cerros misántropos, los rebalses de caños podridos. Aquí, la parásita afrodisíaca que llena el suelo de abejas muertas; la diversidad de flores inmundas que se contraen con sexuales palpitaciones y su olor pegajoso emborracha como una droga; la liana maligna cuya pelusa enceguece los animales; la “pringamosa” que inflama la piel, la pepa del “curujú” que parece irisado globo y sólo contiene ceniza cáustica, la uva purgante, el corozo amargo.

José Eustasio Rivera, “La Vorágine” page 149.

La novela por excelencia de La Selva que presenta el honor y
la violencia, el caos y la lucha titánica del ser humano
por su supervivencia

“The novel by excellence of The Jungle
that presents the honour and the violence,
the chaos and the titanic struggling of human beings for survival”

Dedicated to my wonderful, tiny and brave mother Isabella,
To my brother Jose Manuel and my sister Mayra and nephews

To the memory of my Dutch grandparents,
Dirk Johannes de Ruyter and Cornelia Mooy Vermeulen

To the memory of Henry Rodríguez Miranda,
a Good Friend of everybody at OVSICORI-UNA.
We miss you Henry!

To Uli Schmidt and Jason S. Herrin whose love, friendship,
and support inspired me and who made my life immensely easier
while I worked on this thesis

Members of the Examining Committee:

Prof. A. Bernard

Laboratoire de Géochimie, Université Libre de Bruxelles, Belgium

Prof. E. Malavassi Rojas

Volcanological and Seismological Observatory of Costa Rica, Universidad Nacional, Costa Rica

Prof. B. Takano

Graduate School of Arts and Sciences, University of Tokyo, Japan

Prof. J. Valdés González

Laboratory of Atmospheric Chemistry, Universidad Nacional, Costa Rica

Prof. J.C. Varekamp

Department of Earth and Environmental Sciences, Wesleyan University, USA

Contents

Foreword	9
Chapter 1 General Introduction	11
Chapter 2 Background, setting and historical activity of Poás Volcano	15
Chapter 3 Chemical evolution and volcanic activity of the active crater lake of Poás volcano, Costa Rica, 1993-1997	35
Chapter 4 A long-term record of polythionates in the acid crater lake of Poás volcano: Insights into the subaqueous input of fumarolic gases	47
Chapter 5 Three decades of dynamic evolution of the acid crater lake of Poás volcano, Costa Rica	73
Chapter 6 Volatile fluxes from Poás volcano: inferences from acid flank springs and fumarolic emissions	117
Appendices	125
Appendices to Chapter 4	126
Appendix to Chapter 5	132
Appendix with photo documentation	133
References	141
Summaries in English, Spanish and Dutch	149
Acknowledgements	159
Curriculum Vitae	162

Foreword

By Dr. Eduardo Malavassi Rojas

Costa Rica has 5 active volcanoes and some of them present (permanent or episodic) magmatic degassing that affects severely the surrounding environment. Therefore, the challenges are to learn how volcanic processes operate in order to attempt the prediction of volcanic eruptions using a combination of volcano geophysical and geochemical techniques, but also to learn how to reduce the impact of volcanic emissions over human settlements and their economic activities that develop around the emission centers. As an example of volcanic impact, losses to crops caused by the period of enhanced acidic deposition in 1994 at the surroundings of Poás volcano approached 1.5 million dollars based on estimates made by the Costa Rican Agricultural Extension Agency. About two thirds of the economic loss came from lower productivity in coffee plantations.

These challenges were accepted by Universidad Nacional (UNA) in 1974, when only a few months after its foundation, the School of Geographical Sciences hosted a Latin American meeting to discuss about national seismographic networks. In addition, the Volcanology Section of the School of Geographical Sciences of UNA started to work under the leadership of a Chilean geographer, Juan Cevo, who only a few years before participated in the documentation of the eruption of Villa Rica Volcano in Chile. The Volcanology Section organized visits to the active volcanoes of Costa Rica and purchased furniture and reagents to organize a very basic chemistry laboratory. Visits to the volcanoes were made periodically after 1978 with a clear aim of initiating volcano monitoring. Nevertheless, systematic monitoring of Costa Rican volcanoes started in 1980 when a faculty member from UNA returned to Costa Rica after finishing graduate work at the University of Hawaii and an internship period at the Hawaiian Volcano Observatory (HVO). In addition, start-up funds were made available to Dr. Eduardo Malavassi to organize a volcano observatory by the Costa Rican Council for Scientific and Technological Research of the Ministry of Science and Technology of Costa Rica at Universidad Nacional. In 1980, the Volcanological and Seismological Observatory of Costa Rica at UNA (OVSICORI-UNA) became the first volcano observatory in Spanish speaking Latin America with permanent full time personnel. During twenty-six years OVSICORI-UNA has developed the monitoring of five active volcanoes in Costa Rica using four methodologies: seismology, ground deformation, description of external changes associated with volcanic activity and geochemistry. Additionally, there has been a process of training of human resources, accumulation of expertise and baselines of active volcanism in Costa Rica. Ten members of OVSICORI have devoted their time to volcano monitoring and research over the last 15 years.

Interaction with foreign scientists produced important exchanges that sponsored the initiation of volcano geochemistry in Costa Rica in 1982-83. For example, Dr. Jean Louis

Chemineé and collaborators from France in association with OVSICORI personnel sampled high-temperature fumaroles using Giggenbach evacuated bottles at Arenal and Poás volcanoes. Also, Dr. Richard Stoiber from Dartmouth College and his senior graduate student, Dr. Stanley Williams, in association with OVSICORI personnel made the first COSPEC measurements at Poás and Arenal volcanoes, and started acid rain studies at Poás volcano. An initiative of Dr. Stoiber provided Costa Rica and Nicaragua, in 1983, with basic classic analytical equipment to measure sulphate, chloride and fluoride from fumarole condensates, acid rain, lake, and spring waters collected from the active volcanoes. The grant provided to Dr. Richard Stoiber by the Arthur L. Day Fund of the American Endowment for the Arts, permitted OVSICORI's primary chemistry laboratory to grow into a volcanic waters and condensates geochemistry laboratory, which was in operation for over a decade. OVSICORI's personnel were trained in sampling and analytical techniques by Dr. Stoiber and Dr. Williams.

In 1984, OVSICORI-UNA received through the University of California in Santa Cruz an AID grant to Dr. Karen McNally to install a permanent seismographic network and a programme to reduce earthquake hazards in Costa Rica. The new seismographic network expanded the volcano-monitoring programme by establishing one station near the summit of each active volcano in Costa Rica to monitor both volcanic and tectonic seismicity.

In 1992, the Laboratory of Atmospheric Chemistry of the School of Chemistry of UNA (LAQAT) was founded and started joint activities with OVSICORI-UNA in the topics of volcanic emissions and geochemistry of volcanic lake systems. The new arrangement with LAQAT allowed for the introduction of HPLC instrumentation for the analysis of volcanic fluids, the supervision of Dr. Juan Valdés González, an analytical chemist graduated from the Max Plank Institute in Germany and the appointment of a chemist, María Martínez, devoted to the analytical process. Thus, over the following decade the group (OVSICORI-LAQAT) acquired more data and basic understanding of the geochemistry of volcanic lake systems and volcanic emissions (for instance, Martínez *et al.*, 2000), but it became obvious that, in order to get better insights of geochemical processes, the group needed to send at least one of its faculty members to work under the leadership of scientists that were undertaking major studies on the geochemistry of active volcanoes. The opportunity was obtained thanks to Dr. Manfred J. van Bergen from University of Utrecht in the Netherlands, the Scholarship Programmes of Utrecht University and Universidad Nacional, the Petrology Group of the Faculty of Geosciences of Utrecht University, the OVSICORI-UNA, and the Commission of Incentives of the Costa Rican Council for Scientific and Technological Research (CONICIT) of the Ministry of Science and Technology of Costa Rica (MICIT)

which together made it possible for María Martínez to carry out studies on the geochemistry of volcanic fluids at Utrecht University.

In 2002, thanks to the support provided by the Government of Costa Rica to the public universities and the support of the authorities of Universidad Nacional, OVSICORI-UNA obtained resources to construct a modern building with a large area devoted to the Volcano Geochemistry Laboratory. In parallel, the Costa Rican Congress approved special funding for OVSICORI-UNA that financed state-of-the-art sampling and analytical instrumentation for both field and laboratory routine work, essential tools for systematic monitoring and research on volcanic processes and associated environmental impact. The Volcano Geochemistry Laboratory was equipped with new instrumentation and became operational in the middle of 2006.

The research on the geochemistry of the crater lake-hydrothermal system of Poás volcano that is being carried out at OVSICORI-UNA has been supported since 1999 until present by the Japanese Government through the Japanese International Cooperation Agency (JICA) that sponsored the visits of Dr. Bokuichiro Takano (Graduate School of Arts and Sciences of Tokyo University, Japan) and Dr. Takeshi Ohba (Volcanic Fluid Research Center of Tokyo Institute of Technology, Japan) in 1999 and 2004, respectively. In addition, from 2004 to present Dr. Yasuyuki Miura (Department of Chemistry of Faculty of Science of Tokai University, Japan) has been also supporting our research on sulphur speciation in volcanic fluids. This cooperation has improved significantly the knowledge on sampling and analytical techniques that OVSICORI-UNA

is using to monitor the chemistry of crater lake systems and fumarolic gases, as well as to improve the understanding of volcanic processes.

OVSICORI-UNA is the only volcano monitoring programme in Central America that has been able to investigate for more than twenty five years the geochemistry of volcanic systems for volcano monitoring purposes, despite of often having to face a lack of funding and training limitations during that period of time. The success in volcano geochemistry and other volcano monitoring areas makes an obligation to have academic exchange with other research centres and to provide assistance to other volcano monitoring projects in Latin America during volcanic crises or by organizing training opportunities for their staff members. A good example of these training opportunities is the UNESCO funded workshop on volcano monitoring that has been organized by OVSICORI-UNA every two years for two decades, graduating around 160 scientists from Latin-America's volcano monitoring programmes.

In the context of OVSICORI-UNA long-term goals, María Martínez's Ph.D. thesis represents the culmination of a period when broad baselines of the active volcanoes in Costa Rica were acquired, as well as basic understanding of volcano geochemistry for each volcano. In fact, María Martínez's Ph.D. thesis represents the initiation of a new period for volcano geochemistry in Costa Rica, as more detailed geochemical data and comprehensive knowledge on volcanic processes and geochemistry of volcanic fluids are being obtained through her research with multiple applications to volcano monitoring and research.

General introduction

1.1 The significance of volcanic lakes

Volcanic lakes emplaced in active craters are of considerable interest from a volcano research and monitoring point of view, since they are usually the external expression of subsurface hydrothermal systems, which form the link with deeper-seated magma bodies. Changes in the conditions of a cooling magma reservoir or intrusion of fresh magma will be accompanied by heat effects, transport of mobile materials and perturbation of the hydrothermal system, the transmission of which to the surface will generate detectable changes in the properties of a lake. Hence, investigating the physico-chemical status and evolution of an active volcanic lake provides insights into magmatic-hydrothermal processes in the interior of the volcanic edifice, including those that might create hazards.

Because magmatic-hydrothermal systems are usually complex and dynamic, a set of different parameters should preferably be measured and combined with systematic field observations to arrive at meaningful interpretations. For the same reason, it is of fundamental importance that data are obtained at regular intervals over long periods of time. The results of such efforts will contribute to successful disaster prevention of volcanic hazards such as lahars and flooding, releases of harmful gas and eruptive events, particularly if they are integrated with geophysical methods of volcano surveillance.

Despite the fact that a considerable number of the World's active volcanoes host lakes, relatively few have been systematically studied till date. Time-series data covering longer periods of time are only available for a small minority. Volcanoes with lakes on which substantial data sets have been published include Ruapehu, New Zealand (Giggenbach and Glover, 1975; Christenson and Wood, 1993; Takano *et al.*, 1994b; Christenson, 2000), Kawah Ijen, Indonesia (Delmelle and Bernard, 1994; 2000; Takano *et al.*, 2004); Kusatsu-Shirane, Japan (Takano and Watanuki, 1990; Ohba *et al.*, 1994; 2000; 2008; Takano *et al.*, 2008), Kawah Putih, Indonesia (Sriwana *et al.*, 2000), Pinatubo, Philippines (Stimac *et al.*, 2003), Santa Ana, El Salvador (Bernard *et al.*, 2004), El Chichón, Mexico (Casadevall *et al.*, 1984b; Taran *et al.*, 1998; Armienta *et al.*, 2000; Rouwet *et al.*, 2008) and Copahue, Argentina (Varekamp *et al.*, 2001 and references therein). Most of these lakes are characterised by higher-than-ambient temperatures, low pH,



Figure 1.1 Colour version and full caption on page 133.

high concentrations of dissolved elements, colour changes and sulphur-rich sediments, properties that are largely derived from the influx of gas and hydrothermal water.

The stable existence of active volcanic lakes depends on a balance between supplies and losses of water and heat (Pasternack and Varekamp, 1997). Two major processes control their chemical properties: (1) input and dissolution-hydrolysis of magmatic volatiles in water bodies forming highly acid brines, and (2) partial or wholesale dissolution of rock, enriching the waters in rock-forming elements (Giggenbach, 1974; Delmelle and Bernard, 1994; Varekamp *et al.*, 2001; Takano *et al.*, 2004). This combined uptake of magmatic volatiles and water-rocks interaction make acid volcanic lakes among the chemically most extreme aqueous environments on Earth.

1.2 Monitoring magmatic-hydrothermal processes at Poás volcano through study of its acid crater lake

The acid lake of Poás (Laguna Caliente) is one of the very few lakes at active and potentially dangerous volcanoes that have been continuously monitored since decades (this thesis; Rowe *et al.*, 1992a,b; Martínez *et al.*, 2000; Venzke *et al.*, 2002-; see further in this thesis for other references). Within the broad

spectrum of volcano-hosted lakes, it ranks among the high-activity lakes, occasionally reaching peak-activity status when it becomes too hot to exist in steady state (Pasternack and Varekamp, 1997). The lake is part of one of the most dynamic magmatic-hydrothermal systems known, as is reflected by persistent drastic fluctuations in temperature, volume and chemical composition, and by periods of eruptive activity. This physico-chemical evolution, together with varying gas emission rates from fumarolic vents and changing properties of associated thermal springs, is driven by heat and mass fluxes that are intercepted by the lake-hydrothermal system but are ultimately derived from magma at shallow depth. Degassing and eruptions from Poás have been confined to the currently active crater since historical times (Figs 1.1 and 1.2). All of these aspects make Laguna Caliente a highly attractive object for study, both from a hazard mitigation point of view, and for gaining fundamental insight into internal processes of a volcano-hosted lake-hydrothermal system. Relatively easy access to the volcano is a practical advantage for frequent sampling and field measurements. Poás is one of the very few active volcanoes in Costa Rica that has been frequently visited by scientists since the late 1960s. OVSICORI-UNA personnel have regularly monitored it since 1978.

1.3 This thesis

This thesis presents a comprehensive overview of the chemical evolution of Laguna Caliente, covering three decades of activity since monitoring began. Based on extensive sets of analytical data, newly generated and compiled from published and



Figure 1.2. Colour version and full caption on page 133.

unpublished sources, its continuously changing characteristics are documented as completely as possible. Together with field observations and chemical data on other, equally dynamic hydrothermal manifestations in the active crater, the variations in the lake's properties over different time scales are used to explore the deeper-rooted controls in the underlying magmatic-hydrothermal system. The results shed new light on the origin of the behaviour of Poás in recent times, and set a baseline for future monitoring strategies and hazard prediction.

Chapter 2 introduces the setting of Poás volcano as part of the Central American Volcanic Arc, and examines its historical activity, which has been characterised by almost continuous degassing through subaerial fumarolic vents and the lake area, alternating with periods of phreatic eruptions and rare phreato-magmatic events. Background information is provided on climate conditions in the summit region and on acid seepage springs at the NW flank of the volcano, which have a chemical impact on the Agrio River basin. A brief comparison is made with other acid crater lakes in Costa Rica.

Chapter 3 discusses changes in the chemistry of the crater lake and acid rain at Cerro Pelón over the period 1993–1997, when the lake volume was extremely low and sometimes reduced to isolated mud pools. It discusses trends in seismicity and fumarole activity at the summit, which accompanied a significant increase in heat and gas fluxes through the lake bottom in 1994 when it completely dried out. The height of eruption plumes and downwind environmental impact of the gas emissions is evaluated. From this time on, a new lake began to form, reaching a record level by 1997. It is considered that the drastic changes observed in 1994 were the consequence of a preceding hydrofracturing event or the ascent of a small magma body beneath the crater.

Chapter 4 concentrates on subaqueous fumarolic input and presents time-series trends of polythionate concentrations in the lake. It is shown that different polythionate species, which are formed in the lake by reaction with inflowing SO_2 and H_2S , provide a sensitive record of changing compositions and flow rates of gas released into the lake. Results are compared with observed variations in the composition of subaerial fumaroles. Together with other chemical parameters, the observed rises, changing proportions and disappearances of polythionate species are interpreted in terms of fluctuations in the state of activity of the magmatic hydrothermal system. A close relationship between the behaviour of polythionates and seismic phenomena is discussed.

Chapter 5 discusses the long-term geochemical evolution of the lake, springs, and fumaroles in the active crater. A comprehensive set of analytical results is presented, covering three decades (1978–early 2008) and including data for thermal springs, fumarolic gases and condensates. Various approaches to data interpretation are applied to unravelling multiple processes that regulate the properties of the lake system. Trends in major-anion concentrations and proportions serve to assess the rate and composition of magma-derived volatile and the modulating effects of the hydrothermal system. The behaviour

of major cations and signatures of rare earth elements are used to explore the nature and extent of water-rock interaction. SOLVEQ modelling is employed to assess the saturation state of minerals in the lake and to predict the stability of minerals in the subsurface that potentially control cation budgets. Time-series trends in the composition and temperature of thermal springs and fumaroles are used to corroborate the evidence for changing conditions in the summit system, as inferred from the lake properties. Implications for the causes of long-term periodic variations in the state of volcanic activity and recurrence of phreatic eruptions are discussed.

Chapter 6 presents an overview of estimated minimum fluxes of volatiles emitted by Poás volcano. Special attention is paid

to a substantial discharge via acid-chloride-sulphate springs on the northwest flank, which form the headwaters of the Agrio River, a tributary of Río Toro Amarillo. Evidence of a presumed connection with the summit hydrothermal reservoir is tested, using chemical time-series for the lake and the springs. Output rates via spring discharge and fumarolic emissions are compared for different monitoring intervals. Implications of contrasting stabilities of these sources in time are discussed.

Appendices to various chapters are added to provide relevant background information, including a photo documentation of the changing appearances of the lake and surrounding crater area, as observed in the field.

Background, setting and historical activity of Poás Volcano

2.1 Geological setting

Costa Rica is located at the western margin of the Caribbean Plate. Offshore the Middle American Trench (MAT) marks the boundary where the Cocos Plate begins subducting beneath the Caribbean Plate and Panamá Block (Protti *et al.*, 1995; Husen *et al.*, 2003; Marshall *et al.*, 2003). Here the direction of convergence is 025° – 030° and the subduction rate varies between 8.6 cm/yr in north-western Costa Rica to 9.2 cm/yr in the southeast (De Mets, 2001; Protti *et al.*, 2001). Numerous seismic events have been registered within the national territory associated with the subduction process, and moreover with internal deformation in the Central Costa Rica Deformed Belt (a diffuse zone of active faulting across central Costa Rica) and with magmatic activity along the volcano-plutonic arc (Husen *et al.*, 2003) (Figs. 2.1 and 2.2).

The subduction of the Cocos plate under Central America, on the western margin of the Caribbean plate, is the main process controlling Tertiary and Quaternary tectonic activity in the region. Costa Rica is located at the southern terminus of this collision zone (Fig. 2.1), where the interaction of these plates with the Nazca plate and with the Panamá block creates a complicated tectonic setting. Subduction of the Cocos plate under Costa Rica occurs at rates from 86 to 95 mm/yr from northern to southern Costa Rica, respectively (computed from De Mets *et al.*, 1990). As a consequence of this subduction process, an active volcanic chain runs from Guatemala to central Costa Rica. Remnants of late Tertiary volcanism of basic composition are widely exposed trenchward from this arc in northern and central Costa Rica and mainly toward the back-arc in the south. Along the western margin of Costa Rica, this subduction process has also uplifted and exposed ultramafic ophiolitic units of late Jurassic to early Tertiary age. In southern Costa Rica, the shallow subduction of young oceanic lithosphere (Protti and Schwartz, 1994) hinders active volcanism, and a batholith of intermediate composition (the Talamanca Cordillera) constitutes the inner arc. The Talamanca Cordillera lies on the Panamá block. The western boundary of the Panamá block with the Caribbean plate is a wide fan-shaped transcurrent shear zone that runs from the Caribbean Sea to the Pacific Ocean, across central Costa Rica (Fig. 2.1). Suggestions and evidence in favour of the existence of this developing plate

boundary have been given by Ponce and Case (1987), Jacob and Pacheco (1991), Güendel and Pacheco (1992), Goes *et al.* (1993), Fan *et al.* (1993), Fisher *et al.* (1994), and Protti and Schwartz (1994). Incipient subduction of the Caribbean plate under the northern margin of the Panamá block seems to be ongoing along the north Panamá deformed belt (Silver *et al.*, 1990), where the 1991 Valle de la Estrella earthquake occurred (Goes *et al.*, 1993; Fan *et al.*, 1993; Protti and Schwartz, 1994).

The multiplate interaction in Costa Rica explains the higher seismic activity of this country with respect to the rest of Central America, with seismic sources of different genesis and depths (Fig. 2.2). Events less than 30-km deep occur (a) associated with the subduction of the Cocos plate under the Caribbean plate and Panamá block; (b) along the Panamá fracture zone, the plate boundary between the Cocos and Nazca plates (Fig. 2.1); (c) as interplate activity between the Caribbean plate and the Panamá block; (d) as intraplate deformation of these tectonic units; and (e) associated with the active volcanic arc. Intermediate-depth earthquakes (down to 200 km) occur as internal deformation of the subducted Cocos plate.

The intermediate-depth seismicity under central Costa Rica reveals a tear on the subducted Cocos Plate (the Quesada Sharp Contortion, Protti *et al.*, 1995), which is recognizable below 70 km (Fig. 2.1 and 2.2). To the northwest the Cocos Plate dips at 80 degrees, and seismicity reaches depths of 220 km beneath the Nicaragua border to 135 km at the tear. To the southeast the Cocos Plate dips at 60 degrees, and the seismicity does not exceed below 125 km behind the volcanic arc, nor below 60 km below the Talamanca Range (Protti *et al.*, 1995). The projection of the tear to the trench coincides with an abrupt change in the bathymetry of the Cocos Plate along a northeast alignment (the rough/smooth boundary of Hey [1977]). This bathymetry change marks the boundary between lithosphere of the Cocos Plate created along the East Pacific Rise and that created along the Galapagos spreading centre. The northeast extension of the rough/smooth boundary, which becomes the Quesada Sharp Contortion (QSC) after subducting (Fig. 2.1), was interpreted as a relic of the original transform fault along which the Farallon Plate broke into Cocos and Nazca Plates. It is the contrast in age, and therefore in density of the Cocos plate what produces the QSC slab tear at this boundary separating steeper slab dips

to the northeast from shallower slab dips to the southwest (Protti *et al.*, 1995).

A number of geochemical studies have assessed the role of subducted material in generating arc lavas by comparing the concentration of fluid-mobile elements (e.g., B, Ba) to the concentration of immobile elements (e.g., La, Zr) in arc basalts. Volcanic front lavas contain up to 0.5% subducted sediment, or a fluid derived from the subducted sediment (Carr *et al.*, 1990). Ratios such as B/La, Ba/La, and $^{10}\text{Be}/\text{Be}$ indicate that the subducted slab signal is greatest in the Nicaragua arc where the slab dips steeply and is at a minimum in the Costa Rica arc (Carr *et al.*, 1990; Morris *et al.*, 1990; Leeman *et al.*, 1994). The rapid along-strike change in arc geochemistry occurs close to the border between Nicaragua and Costa Rica where the position of the volcanic front shifts, some 150 km northwest of

the major change in slab geometry represented by the Quesada Sharp Contortion (Fig. 2.1) (Peacock *et al.*, 2005).

The subduction zone that lies beneath most of Central America gave rise to many volcanoes that have contributed significantly to the geographical and biological evolution of Central American countries. In Costa Rica at least 290 volcanic centres or apparatuses have been recognized (Alvarado, 2000), however only eight of the volcanoes are under monitoring or geothermal exploitation due to volcanic manifestations. Subduction has produced intense volcanic activity since the Middle Tertiary, consisting of andesitic-rhyolitic ignimbrites, lavas, domes, dykes, lahars and pyroclastic deposits (Pichler and Weyl, 1975; Castillo *et al.*, 1988; Kussmaul, 1987; Malavassi, 1991; Alvarado *et al.*, 1992; Vogel *et al.*, 2004; MacMillan *et al.*, 2004; and references therein).

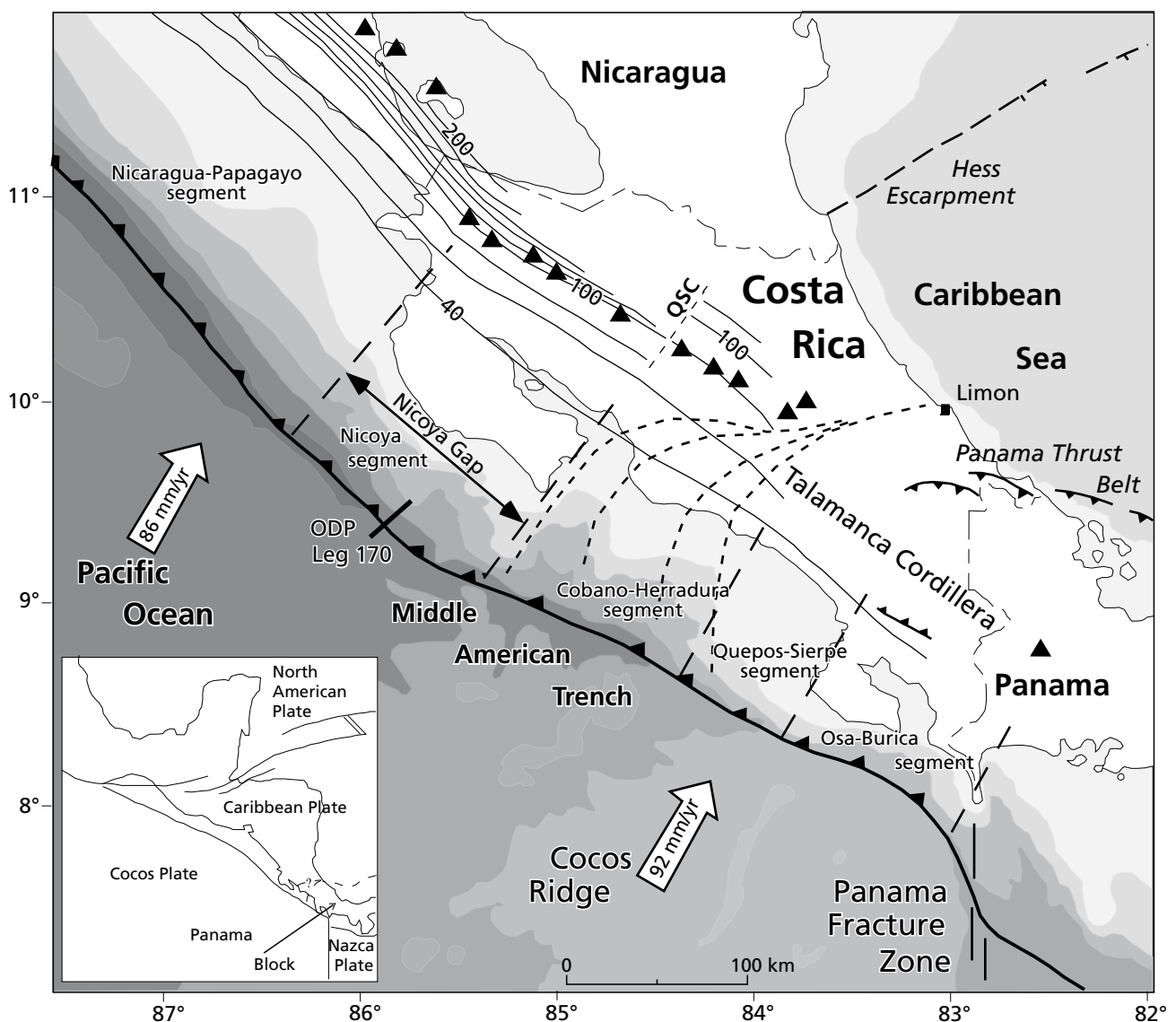


Figure 2.1. Tectonic setting of southern Central America and geometry of the top of the Wadati-Benioff zone (20-km interval contours) from Protti *et al.* (1994). Filled triangles represent main Quaternary stratovolcanoes. Convergence velocities between the Cocos and Caribbean plates were derived from De Mets *et al.* (1990). QSC: Quesada sharp contortion, located at the boundary between the northern and central sections of Costa Rica. ODP Leg 170: Ocean Drilling Project. Inset: major plate boundaries in Central America and map location. Dashed lines across central Costa Rica schematically represent the shear zone that marks the boundary between the Caribbean plate and the Panama block (adapted from Protti *et al.*, 2001).

The Central America Volcanic Arc (CAVA) in Costa Rica extends from Orosí volcano in the northwest (near the border with Nicaragua) to Turrialba volcano in central Costa Rica, while south-eastern Costa Rica shows a gap in the volcanic arc. The Costa Rica Volcanic Arc (CRVA) can be divided into two mountain ranges (cordilleras): Cordillera de Guanacaste and Cordillera Central. The Cordillera de Guanacaste is a chain of volcanoes in NW Costa Rica which contains from NW to SE Quaternary volcanoes such as Orosí, Rincón de la Vieja, Miravalles, Tenorio and Arenal (Fig. 2.3). These volcanoes have transitional geochemical signatures between the Cordillera Central volcanoes and the Nicaraguan volcanoes, which have a depleted mantle source and a high subduction signal (Carr *et al.*, 1990; Morris *et al.*, 1990; Leeman *et al.*, 1994; Husen *et al.*, 2003; Peacock *et al.*, 2005). The Cordillera Central consists of Quaternary volcanoes from NW to SE such as Poás, Barva,

Irazú and Turrialba. The volcanic activity in Costa Rica in the last 25000 years has mainly been characterized by phreatic and phreato-magmatic eruptions with rare plinian eruptive events (Alvarado, 1992).

2.1.1 Poás Volcano

According to historical documentation, Poás ($10^{\circ}11'26''\text{N}$ - $84^{\circ}13'56''\text{W}$, data from World Geodetic System 1984), one of the most active volcanoes of Costa Rica, has shown nearly constant fumarolic degassing for ca. 175 years. It is located NW of the Central Valley within the Cordillera Central, about 35 km NW of San José, where half of the population of Costa Rica (~2.3 million people) is settled (Fig. 2.3). It is a broad basaltic-andesite stratovolcano with maximum elevation of 2708 m.a.s.l. that formed during the Quaternary after the migration of the volcanic front, from the SW to its present location of the

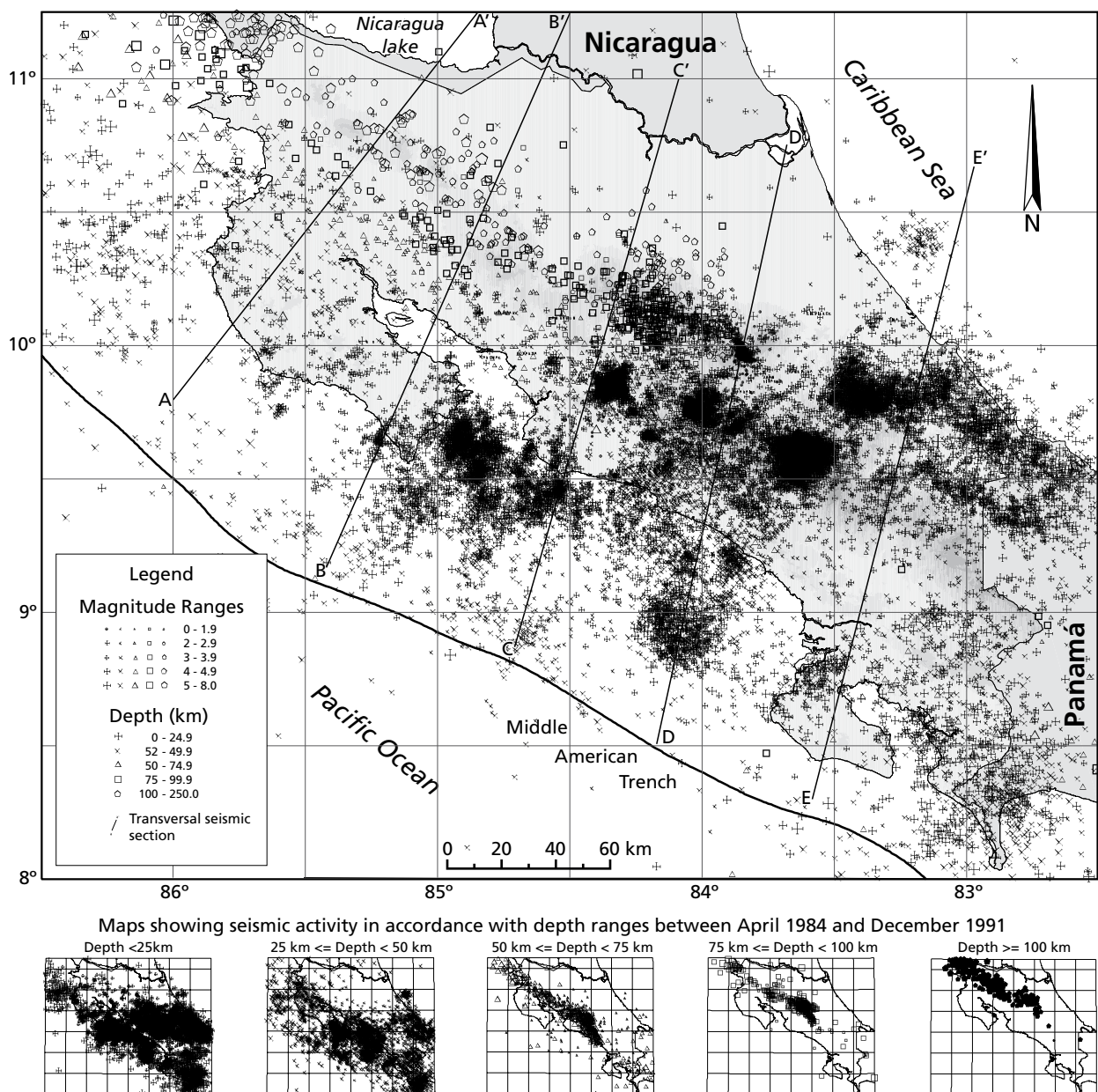


Figure 2.2. Seismicity along horizontal and vertical sections for the northern, central and southern parts of Costa Rica recorded by OVSICORI's Seismic Network between 1984 and 1999. Map constructed by Víctor González (OVSICORI-UNA).

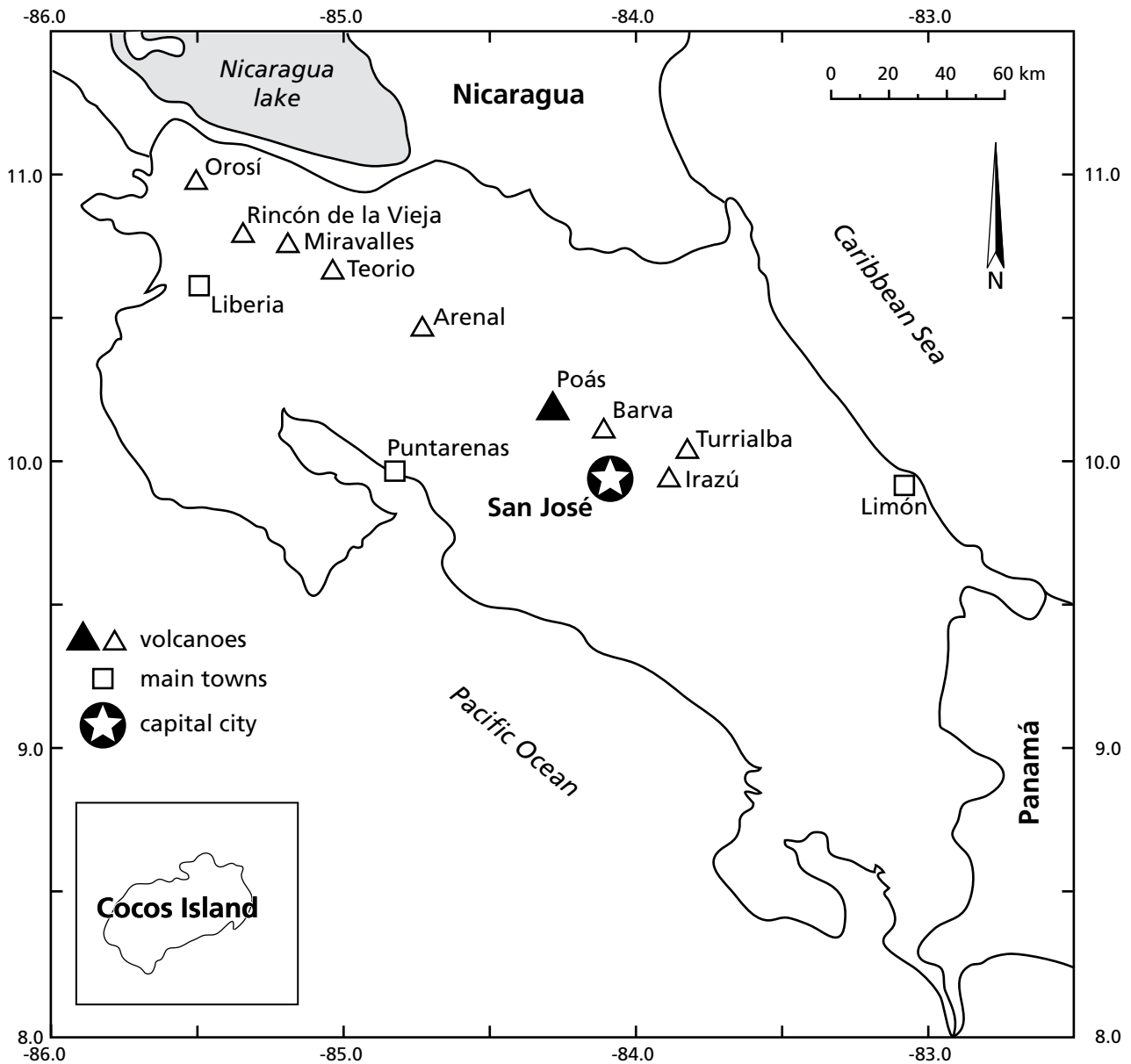


Figure 2.3. Distribution of main Quaternary volcanoes. Filled triangle: Poás volcano; open triangles: other active volcanoes.



Figure 2.4. Colour version and full caption on page 133.

Central volcanic range. In this region, Quaternary volcanic rocks overlay Tertiary Sedimentary rocks of Miocene age that are exposed in the Central Valley and along the Aguas Zarcas river gorge, north of Platanar volcano (Malavassi, E., pers. comm. 2006). The current active crater of Poás volcano is about 1130 m in diameter (along its N-S axis) and 252 m deep (Van der Laat, R. pers. comm. 2006), and its floor lies at an elevation of about 2300 m.a.s.l. (Rowe *et al.*, 1992a).

The Poás massif consists of two volcanic clusters. The western volcanic cluster includes the Platanar, Pelón, Porvenir, Palmira, and Viejo stratovolcanoes. The eastern volcanic cluster located along the Poás rift zone, a north-south lineation of volcanic edifices and maars of 30 kilometres long, includes the Sabana Redonda, Poás, Botos, Von Frantzius and Cerro Congo cones as well as the Bosque Alegre caldera and the Río Cuarto maar (Malavassi *et al.*, 1993). Despite that some of the volcanoes on

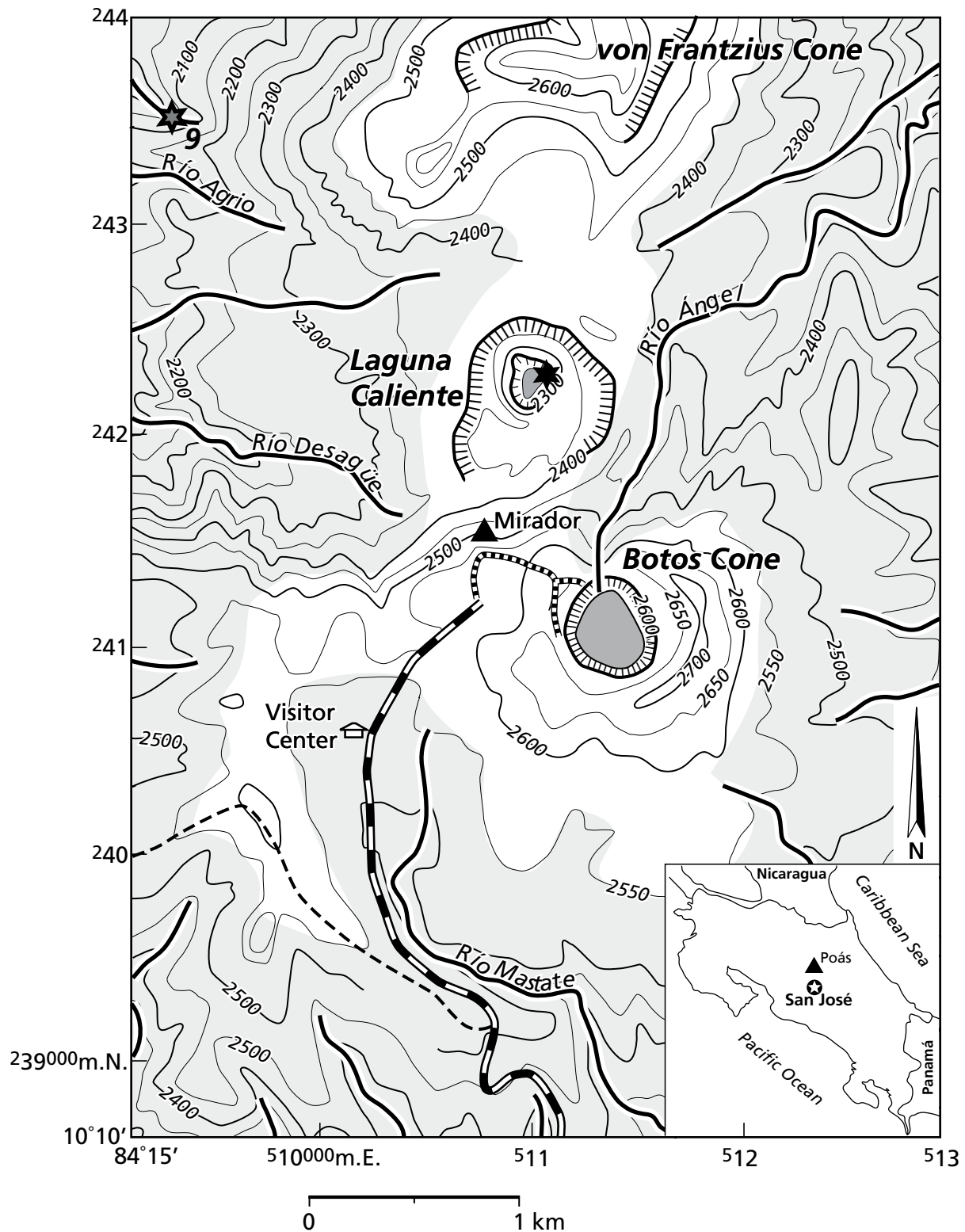


Figure 2.5. Topographic map of the summit area of Poás Volcano. The active crater with the acid crater lake (Laguna Caliente) is situated between the Von Frantzius and Botos cones. Inset shows the location of Poás Volcano in the Central Mountain Range (map adapted from Poás sheet 3346 I (1:50,000) of the Instituto Geográfico Nacional de Costa Rica, Edition 1-IGNCR 1967).

the west cluster are geomorphologically very young, Volcán Viejo is the only cone where mild fumarolic activity was reported during the 19th century, which disappeared during the 20th century (Alvarado, 2000). Poás volcano, located in the

eastern cluster, is the only cone that has been active in historical times in the Poás massif.

The currently active crater of Poás Volcano lies between the Von Frantzius cone to the north and Botos cone to the

southeast. The latter cone contains a cold freshwater lake (Figs. 2.4 and 2.5). The active crater contains a shallow hydrothermal system and frequently a hot, hyper-acidic crater lake (Rymer *et al.*, 2000). However, in several occasions during enhanced flux of heat and volatiles through the active crater, the crater lake has dried out (e.g. Rowe *et al.*, 1992b; Rymer *et al.*, 2000; Martínez *et al.*, 2000).

2.1.2 The acidic crater lake

The waters of the acidic crater lake of Poás, locally known as “*Laguna Caliente*” (Figs. 2.4 and 2.5), are extremely rich in chemical compounds which are derived from magma degassing and fluid-rock interaction in a predominantly igneous arc-crust environment. The physico-chemical parameters of the lake have been subjected to an on-going monitoring programme for ca. 30 years by the Observatorio Vulcanológico y Sismológico de Costa Rica at Universidad Nacional (OVSICORI-UNA), so that geochemical data of the acidic crater lake are available since 1978 until present.

The acidic crater lake is among the most active ones in the world, since more than 60 subaqueous eruptions have been documented during the last 175 years (Mastin and Witter, 2000; Martínez *et al.*, 2000; Venzke *et al.*, 2002-; OVSICORI open reports). The physico-chemical properties of the lake have shown frequent fluctuations in a relatively short period of time of only three decades. These fluctuations are influenced by rainfall, thermal power output, changes in the flux of chemicals, and summit seismic activity (see Chapters 3, 4 and 5). Thus the acidic crater lake of Poás is a highly dynamic site compared to other highly active acid crater lakes such as Kawah Ijen in Indonesia (Sumarti, 1998; Delmelle *et al.*, 2000) or Ruapehu in New Zealand (Christenson 1994, 2000).

The lake volume is variable with a diameter and depth up to 320 m and 55 m, respectively, when full (Van der Laat, R., pers. comm. 2006). Nevertheless, the lake has dried out four times in the course of ca. 30 years. Its pH has ranged between -0.87 and 1.75, while temperature has varied between 22 and 94°C. Moreover, the concentrations of chemical species have shown very large fluctuations (for instance, total sulphate and chloride concentrations have ranged in the orders of 3300-285,000 and 2500-115,000 ppm, respectively). The lake colour has varied from bluish, to greenish, to grey. The changes experienced by the acid crater lake of Poás volcano are described in detail throughout several of the chapters of this manuscript (see Chapters 3, 4, and 5).

2.1.3 Acid seepage at Poás volcano

Seepage of acid chloride-sulphate brines (pH and temperature ranging between 0.9-2.8 and 54-14°C, see Chapter 6 Table 6.1) occurs in a confined region on the northwestern flank of Poás volcano, within 2-5 km from the acid crater lake. This seepage emerges as acid springs, which together with nearly neutral streams form the Agrio River (Fig. 2.5).

A hydraulic connection between the Agrio River acid springs and the crater lake brine has been proposed by Alexander von Frantzius in 1861 (Vargas, 1979), Rowe *et al.* (1992a,b; 1995) and Sandford *et al.* (1995). The two latter authors have proposed that the acid seepage represents lake brine diluted with meteoric water in the subsurface during travelling from the crater lake

to the Agrio River watershed. This is based upon geologic, structural and hydro-geologic features, chemical and isotope data on the lake, the springs and the river, as well as numerical simulations of heat and mass-balance and solute transport for the period 1987-1989.

Transport modelling calculations yield an estimated travel time of 1-30 years for the acid crater lake brine to reach the seepage points on the NW flank (Sandford *et al.*, 1995). This agrees with the estimated age of the acid spring waters, which ranges between 3 and 17 years according to tritium data (Rowe *et al.*, 1995). Furthermore, we found that the acid crater lake showed an enrichment in major anions after 1989 (till present), but this change has not been observed in the Agrio acid springs collected since then (at least until 2002), implying that if the acid seepage were largely diluted acid lake water, the travel time should be at least 13 years (see Chapter 4, Fig. 4.12).

2.2 Poás Volcano historical activity

Formal reports on the activity of Poás volcano exist since 1828 when small eruptions were described (Vargas, 1979; Salguero, 1980), however, the oldest eruption mentioned in historical records dates back to 1747. Since then, the activity has been nearly continuous but with large fluctuations. It includes (1) persistent degassing with occasional intervals of intense fumarolic emissions such as in 1980-85, 1986-1991, 1994, 1999 and 2005-2008; (2) periods of phreatic explosions in the lake like those of the 1960's and mid 1980's, 1987-1991, 1994 and 2006-2008; and (3) rare phreato-magmatic eruptions such as occurred in 1953-1954 (Rowe *et al.*, 1992b, Martínez *et al.*, 2000, Malavassi, E., pers. comm. 2008; see also Chapters 3, 4 and 5). The largest reported eruption occurred in 1910 with a large steam and ash cloud reaching 4-8 km above the summit (Martínez *et al.*, 2000). Several phases with enhanced phreatic activity have occurred since then, as is described in the following sections (Martínez *et al.*, 2000).

The creation of the Poás Volcano National Park in 1971 (Boza and Mendoza, 1981) promoted interest about its natural history and activity, so that Poás volcano started being systematically monitored since the end of the seventies. Reports from various naturalists who visited the volcano during the XIX and early XX centuries, such as the Danish Andres Sandoe Oersted in 1863, were compiled by Vargas (1979). Boza and Mendoza (1981) prepared a summary of the natural history of the new national park which included reports of activity from the previous decades. Scientific accounts about the activity of Poás volcano became numerous since the late 1960s (Krushensky and Escalante, 1967; Raccichini and Bennett, 1977). Systematic volcano monitoring started around 1978 by the group at Universidad Nacional, presently known as OVSICORI-UNA. Since then, a number of authors have written about the volcanic processes, e.g., Boza and Mendoza, 1981; Malavassi and Barquero, 1982; Brantley *et al.*, 1987; Prosser, 1983, 1985; Prosser and Carr, 1987; Oppenheimer and Stevenson, 1989; Rymer and Brown, 1989; Fernández, 1990; Rowe, 1991, Rowe *et al.*, 1989, 1992a,b, 1995; Malavassi *et al.*, 1993; Rowe, 1994; Rowe *et al.*, 1995; Martínez *et al.*, 2000, 2003; Rymer *et al.*, 2000, 2004, 2005; Vaselli *et al.*, 2003, 2004;

Fournier, 2003; Fournier *et al.*, 2004; Mora *et al.*, 2004; Mora and Ramírez, 2004. In addition, the Smithsonian Institution, through Global Volcanism Program Information Series (Venzke *et al.*, 2002-) has been systematically compiling and informing the volcanological community worldwide about the evolution of Poás activity, as reported by the local volcanologists and sporadic visitors of the volcano.

The locus of main fumarolic degassing has been shifting within a confined region that comprises the acid lake and the CPC. However, between 1995 and mid 2000, fumarole opening events occurred at the south-western inner crater walls and later on, between 1999 and 2007, a new fumarolic developed at the eastern terrace (Fig. 2.20) (Martínez *et al.*, 2000; Rymer *et al.*, 2000; Venzke *et al.*, 2002-; Vaselli *et al.*, 2003; Fournier *et al.*, 2004; see also Chapters 3 and 4). The shifts in the location and vigour of fumarolic emissions have been an important factor in the nature and degree of activity observed since the late 1970s. Based upon the trends shown by a number of geochemical and geophysical parameters regularly monitored by OVSICORI since the late 1970s, five distinct successive main stages of activity are defined. Four of these were characterized by a moderate to strong input of magmatic-hydrothermal fluids and heat into the lake area, and one by relative quiescence. Many of the observed changes appeared to be related to the location of main fumarolic degassing within the active crater. The most salient events and features of these stages are described in the following sections.

2.2.1 Activity between 1830 and 1970: before Stage I

In 1834 a strong eruption of ash was reported. In the following years, i.e. 1838, 1860, 1879–1880, 1884, 1889–1890, 1895, 1899–91, 1903, 1905, 1908, 1910 numerous phreatic eruptions occurred. These eruptions were typically geyser-like explosions, similar to shallow submarine volcanic eruptions, occurring within the lake area and forming muddy water columns that reached altitudes of 100 m or more above the crater floor.

The largest phreatic eruption reported over the last two centuries occurred on 25 January 1910. The column of steam, mud, gases, blocks and ashes from this eruption reached heights of 4 to 8 km above the crater floor, and the ashes were dispersed towards the Central Valley (hosting ~60% of Costa Rica's population), also reaching parts of Cartago, the former capital city. During this eruption, most of the crater lake waters were

ejected, but the lake did not completely disappear (Calvert and Calvert, 1917). After this eruptive period, Poás activity slowed down, and there were only some small to moderate intermittent geyser-like explosions over the following ca. 40 years (1910, 1914–1916, 1925, 1929, 1941–46, and 1948–52 and nearly continuous fumarolic activity in the active crater.

Before 1951 a grey hot crater lake (39–64°C) covered the entire floor of the main crater (i.e. its diameter was considerably greater than that of the current lake, Fig. 2.6). Activity at the volcano changed markedly in 1952 when geyser-like phreatic eruptions through the lake turned more energetic, thus the crater was filled with vapours and gases, and the bottom and walls became covered with a layer of mud and rock fragments ejected by the eruptions. This enhancement in activity marked the onset of a transitional period from phreatic in 1952 to magmatic activity in 1953–1955 (Fig. 2.7). Two vents were active at the main crater during this eruption cycle: one that formed a small composite pyroclastic cone (CPC) 40 m height, referred by many authors as the “dome” or “crypto-dome” in the central part of the crater (Fig. 2.9 and Fig. 2.20 site 1), and another unnamed vent, that had formed about 150 metres to the north of the cone. This northern vent collapsed and was later filled with water to form the hyper-acid crater lake (Martínez *et al.*, 2000).

On May 17, 1953 there was a violent explosion eruption with a high column of water, mud and rock fragments, accompanied by large water vapour-plumes and lightening. Local residents living near the summit of the volcano felt earthquakes and heard roars. During the night, inhabitants of San Rafael de Varablanca (ca. 11 km SE of the volcano) and La Colonia de la Virgen del Socorro (ca. 9 km NE of the volcano) observed incandescent rock fragments being ejected from the active crater (Molina Carlos, pers. comm. 2004).

In mid-July, 1953 eruptions of ash, accompanied by electrical activity (twilights) and a reddish brilliance, due to diffraction of sunlight by volcanic particles suspended in the air, succeeded the phreatic eruptions. Ashes were deposited all around the active crater, being dispersed to the east (e.g. Vara Blanca), to the west and to the north (Malavassi Enrique, pers. comm. to Eduardo Malavassi 1990). Pastures were covered by the ashes, creating health problems in livestock. The emission of ashes also affected some of the watersheds. Large amounts of ashes fell around Botos Lake and in the valley of the Ángel River (Fig. 2.5). The ashes gave a milky aspect to the waters of the Ángel



Figure 2.6. Before the 1950s a hot lake (39–64°C) covered the entire floor of the main crater, and minor phreatic eruptions were often observed near the centre of the lake. Note that the composite pyroclastic cone (CPC) did not exist at that time. Photograph (looking west) taken on 14 March 1940, courtesy of Enrique Valverde Sanabria.



Figure 2.7. View of Poás crater looking north in 1953 during the last phreatic-magmatic period. Unknown photographer.

River and the Sarapiquí River, into which it discharges, killing a large amount of fish. Coffee crops and metallic structures (iron-zinc galvanized roofs) at Isla Bonita and Cinchona, about 7 km NE of the active crater, suffered some damage (Molina Carlos, pers. comm. 2004). The crater lake dried out completely, and the CPC was formed in the centre of the area previously occupied by the lake. This cone continued growing, up to 45 m, mainly by accumulation of pyroclastic material emitted during the 1953-55 eruptions. Lava flows were issued from the base of the CPC, and flowed 200 m north of the cone, forming a terrace NE of the CPC.

In 1965, after the phreato- and magmatic activity of 1953-1955, a new lake formed in the crater left by the explosions to the north of the CPC. It maintained a depth of about 50 m, circulating mildly acidic brines at about 40°C. The CPC was the main locus of fumarolic activity until 1968 when phreatic activity and strong exhalations resumed in the crater lake. The phreatic activity was characterized by columns of vapour, gases, water, mud and fragments ejected up to 2500 m above the bottom of the crater. The CPC was eroded by the waves produced by collapse of geyser-like eruptions and by partial failure of the cone due to fumarolic alteration, acquiring a dome-like shape, which explains why several investigators referred to this cone (actually a crypto-dome) as “the dome”.

In March 1964, the temperature of the CPC fumaroles ranged between 195-250°C (Casertano *et al.*, 1983). In 1968 phreatic activity resumed again in the lake area, which was accompanied by intense fumarolic degassing. A series of small geyser-like phreatic eruptions were recorded in 1969. These phreatic eruptions carried small amounts of materials to heights of approximately 30 m. Material did not spread out when falling, either because they were too coarse or too wet (Boza and Mendoza, 1981). These phreatic eruptions were characterized by columns of vapour, gases, water, mud and fragments ejected up to 2500 m above the bottom of the crater, as in 1968. One precursory signal of phreatic activity at Poás was the appearance of grey-yellowish spots of 25-50 m diameter near the centre of the acid crater lake. This change was followed by increments in the lake water temperature and by a change in the lake's colour from greenish turquoise to greyish turquoise, produced by the enhanced vigour of the subaqueous fumarolic discharges. In 1970, the temperature of fumaroles at the CPC was below 60°C (Malavassi, E., pers. comm. 2005).



Figure 2.8. Colour version and full caption on page 133.

2.2.2 Activity between 1972 and August 1980: Stage I

In the seventies, more specifically between 1972 and August 1980 (**Stage I**), fumarolic degassing and intermittent geyser-like phreatic eruptions occurred within the lake area although there was also weak fumarolic activity around the CPC (Fig. 2.20, site 1). The geyser-like phreatic eruptions produced in the grey-coloured lake in late 1977 ejected columns of steam, and muddy lake water above the lake surface to heights that ranged from several metres up to 2 km. Phreatic explosions in 1978 expelled through the crater lake greenish-yellow kidney-shaped droplets of molten sulphur with diameters 0.5-1 mm and lengths of 2 cm (called by OVSICORI's staff “cacarrutas”), and fragments of highly altered rocks encrusted with native sulphur (Bennett and Raccichini, 1978a,b; Bennett, 1979; Francis *et al.*, 1980; Casertano *et al.*, 1987). There was also convective bubbling in the lake that sometimes brought sediment to the surface as well as a yellowish froth (sulphur globules).

During the first half of 1980 there was a nearly continuous large plume of vapours and gases rising above the CPC. The lake showed a greyish-turquoise colouration (Fig. 2.8). There was a permanent sulphur odour at the vicinities of the active crater. By mid-June 1980 the conditions remained similar except that the typical H₂S odour was not perceived anymore. A grey-yellowish slick was observed floating on the surface of the lake, near its centre.

Intense swarms of A-type earthquakes (Casertano *et al.*, 1987) started being recorded beneath the active crater on July 27, 1980. The A-type quakes numbered in the order of the thousands within a two-week period (see Chapter 4 Fig. 4.6) (Casertano *et al.*, 1985). These swarms are believed to represent hydrofracturing of the chilled, brittle margin of the shallow magma body beneath the crater (Casertano *et al.*, 1987). On August 8, 1980 the lake turned to a grey colour but between September and December phreatic activity ceased and quiescence prevailed in the lake.

2.2.3 Activity between September 1980 and April 1986:

Stage II

Between September and December 1980, while the lake turned relatively quiescent, moderate hydrothermal explosions occurred at the interface between the lake and the northern side of the CPC ejecting small blocks and muddy lake water up to 320 m above the lake surface. Following these events, enhanced degassing started around the CPC, marking the beginning of **Stage II** (September 1980-April 1986). Between January 1981 and November 1988 intense high-temperature fumarolic activity was centred around the CPC. Peaks in temperature were attained between March and October 1981 after a rising from 92°C up to 1020°C (Figs. 2.9 and 2.11) (Barquero and Malavassi, 1981a,b; 1982; 1983). On April 8, 1981 at 8:00 p.m. incandescence was observed at the northern side of the CPC from the visitor's lookout (Mirador) and by the end of that month fumaroles around the cone reached 1020°C, the highest fumarolic temperatures recorded at Poás volcano over the last three decades (Casertano *et al.*, 1987). A vigorous volcanic plume rose above the CPC reaching heights higher than 200 m. On May 4, 1981 at 5:30 a.m. a strong release of vapour and gases occurred at the CPC and a plume of ~2000 m height was observed from the Central Valley and Irazú volcano. Large



Figure 2.9. Colour version and full caption on page 134.

amounts of native sulphur were deposited on the CPC and some of the sulphur melted, turning yellow-orange suggesting minima temperatures around 180°C.

The temperature of fumaroles on the CPC gradually decreased from 1020°C in mid-1981 to 420°C in May 1985 (Fig. 2.11) (Cheminée *et al.*, 1981; Barquero and Malavassi, 1983), and was reduced to boiling point by late 1988. The only anomaly was a second increment in temperature between July 1986 and September 1988, when it increased from 290 to 612°C, as can be seen in Fig. 2.11. This may be related to the renewal of phreatic activity in the lake, which started in June 1987 and continued until 1990. Boiling point temperatures have been observed at the CPC from 1989 on, with occasional exceptions (September 1998, October 1999, March 2000) when temperatures at fumaroles on the northern side of the CPC registered between 110–190°C (Fig. 2.11).

A remarkable observation is that despite of the incandescence at the CPC, the temperature of the lake was around 50°C, similar to temperatures registered at the end of 1980 (Fig. 2.11). Thus, the lake itself was not strongly affected by the very high temperatures and gas flux at the CPC, suggesting that the release of heat and volatiles through the CPC occurred throughout a very confined region. Casertano *et al.* (1987) suggested that in 1981–1983, during maximum heating of the CPC, the crater lake was still in continuous hydraulic connection (not necessarily equilibrium) with the rising hot fluids, consistent with a steady increase in lake temperature during those years (Fig. 2.11). In the beginning of 1983, the lake was consistently warmer than 60°C, had a greyish-turquoise colour and showed strong evaporation and streaks of floating sulphur spherules at its surface. By the end of October 1983 the lake water level had descended about 10 metres. On the other hand, fumarolic activity continued vigorously and with a strong sulphur odour around the CPC. COSPEC measurements of SO₂ flux indicated levels of about 800 tons per day in February 1982 (Casadevall *et al.*, 1984a).

In view of the drastic changes in the level of seismicity observed in mid 1980 followed afterwards by a sharp rise in temperature of the fumaroles around the CPC in early 1981, a portable seismometer was installed at the summit of Poás on March 19, 1981. Through May, this instrument recorded: (a) harmonic tremor at frequencies of 3–4 Hz for a few minutes to a few hours daily; (b) discrete events caused by internal rupturing; (c) signals produced by degassing; (d) explosion



Figure 2.10. Colour version and full caption on page 134.

events accompanying vapour eruptions; (e) very shallow (~1 km deep) B-type earthquakes; and (f) very few A-type earthquakes from depths of 1–10 km. An inverse relationship between the daily duration of harmonic tremor and the daily number of discrete earthquakes was evident, a feature that had also been observed at Arenal Volcano in 1975 by T. Matsumoto (Sáenz, R., pers. comm. 2005). Generally, recording of total hours of tremor increased significantly in 1981–1982 (1250–1800 hours) when high-temperature degassing was concentrated at the CPC. The annual number of B-type earthquakes was 12000 in 1983 (Fernández, 1990).

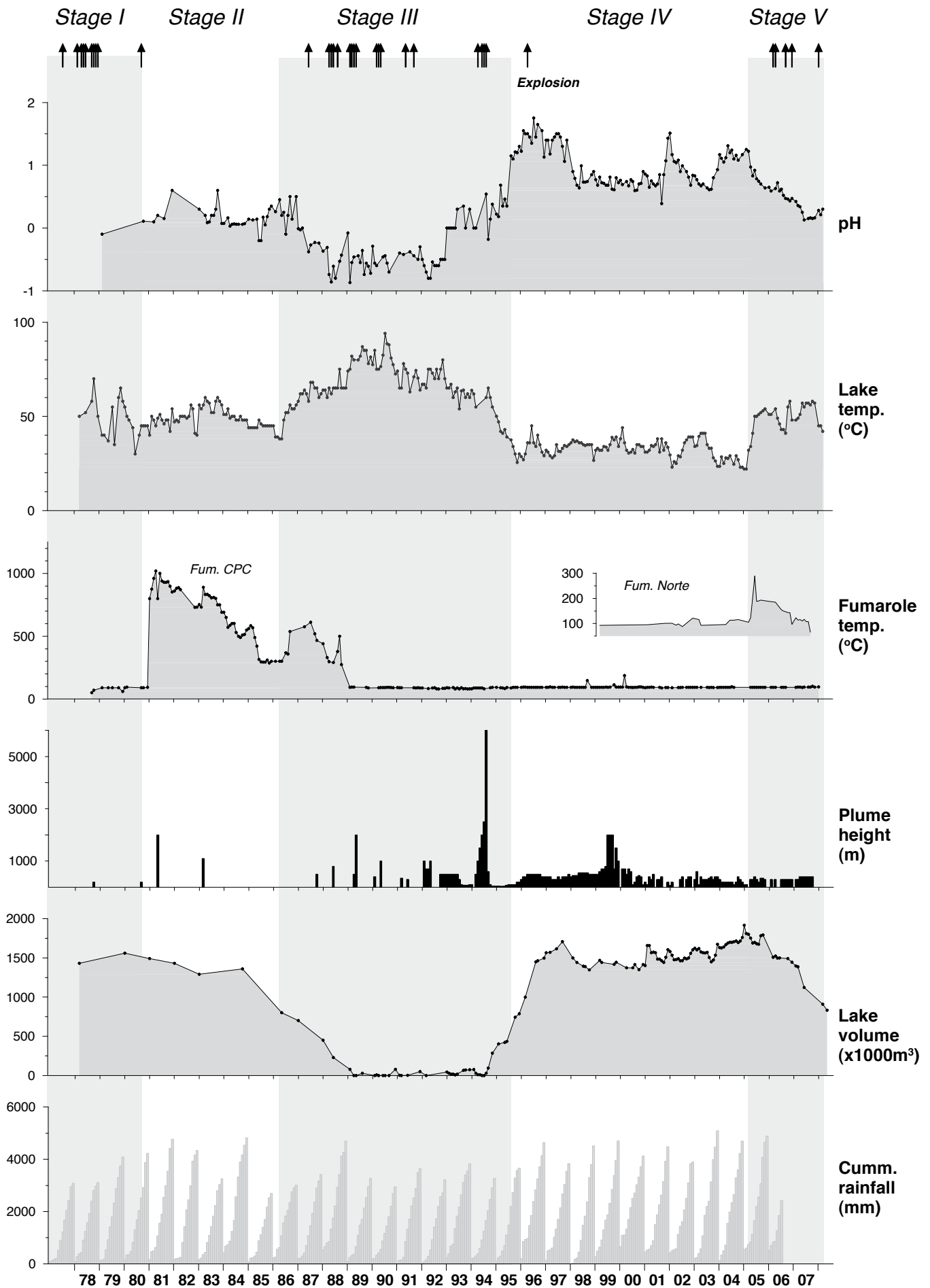
The events observed around the CPC between late 1980 and late 1983 probably heralded the start of a new magmatic cycle that has lasted till today. The new cycle has been explained as the result of several shallow magmatic intrusions beneath the CPC (sometime in the first half of 1980) and beneath the acidic crater lake (sometime in 1985, 1994, 2002), as indicated by gravity increases at crater-bottom stations, and increases in seismicity and power output through the active crater (Rymer and Brown, 1989; Martínez *et al.*, 2000; Rymer *et al.*, 2000).

2.2.4 Activity between May 1986 and August 1995: Stage III

Apart from moderate fluctuations in water level and temperature, and a period of mild to moderate phreatic activity between the 70s and late 1980, the lake system appeared relatively stable whereas the CPC remained the site of main fumarolic activity until early 1986, when a long-term decrease in lake level commenced (Fig. 2.11).

During the first half of year 1987, fumarole temperatures averaged 540°C at the top of the CPC and 800°C on its W side. However, fumaroles were less vigorous than in the previous year. Crater lake temperature increased from 58°C in January 1987 to 70°C in June 1987. Since January 1987, the lake level continued to fall markedly (Fig. 2.11), exposing three terraces of grey, water-saturated sediment. Concentric fractures developed along the lakeshore, particularly on the E and NE sides. Rockslides occurred on the eastern inner wall of the crater and on the CPC.

A swarm of A-Type earthquakes, representing either a small episode of renewed magma ascent or another, less extensive hydrofracturing event that increased heat transfer to the lake, occurred between February and May, 1986 (Rymer and Brown, 1989; Rowe *et al.*, 1992b), marking the onset of *Stage*



→ *Figure 2.11.* Time-series trends of lake pH, temperature and volume, together with fumarole temperatures (CPC and Fumarola Norte), plume height and rainfall. Note that lake data in the period between late 1988 and mid 1994 refer to a situation when the lake was reduced to a number of isolated mud pools. Rainfall is expressed as cumulative monthly totals in cycles of calendar years. Very high temperatures at the CPC in 1981–1983 correspond to observed incandescence (Fig. 2.9), and the smaller peak between mid 1986 and late 1988 is presumably related with the onset of phreatic activity that lasted until early 1994. The crater lake showed relatively high temperatures in 1978–1979 and 2005–2008, and reached maxima in 1987–1994. All data are from the OVSICORI-UNA database.

III (May 1986–August 1995) which was characterized by frequent phreatic activity and strong emission of steam and gases through the area where the lake is emplaced. This new cycle of phreatic activity started in June 1987 with a series of minor explosions that were observed throughout the following months (Fig. 2.12). Phreatic activity continued for several years with most of the phreatic eruptions occurring between mid 1987 and early 1990. Phreatic eruption columns reached elevations of 1–2 km in April 1988 as steam jets lifted lake sediments into the air that fell 0.5 km south of the crater rim. Strong phreatic explosions continued in May–June 1988, ejecting sulphur-rich sediments that fell at locations as far as 5 km SE of the crater (e.g. Poasito town which is about 4 km SE), covering vegetation and infrastructure. B-Type earthquakes increased from 12,000 per year in 1983 to over 100,000 per year in 1988 and periods of harmonic tremors reappeared.

Throughout Stage III the lake maintained a very low volume and dried out in several occasions (Rowe *et al.*, 1992a,b; Martínez *et al.*, 2000; Rymer *et al.* 2000; Venzke, *et al.*, 2002–). As the lake shrunk, lake-bottom fumaroles that were previously degassing into the water column began to degas directly into the atmosphere. In July 1988 the lake was very small with a diameter of about 20 m, and had a bright yellow colour. This condition triggered acidic rain that severely affected areas located as far as 15 km southwest of the crater in the direction of prevailing winds. In contrast, acidic deposition is typically restricted to areas 3 km or less downwind in periods when the lake is present (Barquero and Fernández, 1990; Fernández *et al.*, 1994). Because of the emission of volcanic gases and particles around the crater, tourists and the Poás Volcano National Park rangers suffered from itching of eyes and skin, respiratory discomfort, persistent headaches and stomach problems. Severe impact on vegetation and infrastructure was observed as far as 8 km SW of the active crater. These effects may have been caused by CO, CO₂, and H₂S, as suggested by some gas measurements that were carried out in September 1988 by OVSICORI personnel using Dragager gas detecting tubes. High concentrations of H₂S and water and moderate concentrations of CO₂, H₂, and HCl were measured.

By February 1989, fumarolic activity on the CPC declined, with only a few vents remaining on the top and most of them on the north side facing the acidic lake. Temperatures of the fumaroles were near boiling point, i.e. approximately 95°C. The level of the crater lake dropped drastically throughout 1988, and the lake eventually was reduced to isolated mud pools in April 1989 (Fig. 2.11). The drastic lowering in the lake level

allowed to formally document for the first time the observation in April 1989 of liquid sulphur pools at the dried bottom of the lake (Figs. 2.13A and 2.13B) (cf., Oppenheimer and Stevenson, 1989). On 1 May 1989, unusually powerful steam jets lifted lake sediments 1–2 km up into the air; these sediments later produced ash fall on populated areas 18 km southwest of the volcano. Dry ash and steam eruptions continued intermittently for several weeks with plume heights ranging between 1.5 and 2 km. The lake returned in May 1989 (at the start of rainy season) but disappeared again during the dry seasons of 1990 and 1991 (Fig. 2.14).

Between January–August 1989, 1–3 m high cones, composed of a mixture of mud and elemental sulphur and venting vapour with a mean temperature of 98°C, formed on the exposed bottom of the dried crater lake (Figs. 2.13A and 2.13B). These sulphur-mud cones, so called “Sulphur volcanoes”, ejected particles carpeting the surrounding area with bright yellow pyroclastic sulphur. Some of the sulphur cones were topped by ca. 1 m high chimney-like structures made of sulphur and sediments (Fig. 2.13B). Apart from the “Sulphur Volcanoes” there were also sporadic brilliant yellow flows of molten sulphur, up to 30 m long, a few centimetres thick, and a few metres wide that showed temperatures up to 140°C (Oppenheimer and Stevenson, 1989). A bluish haze (probably H₂SO₄ aerosols; Taran, Y., pers. comm. 2006) was observed rising from the dried lake bottom from time to time (see Fig. 2.10 for a previous example in 1985). In 1989 small boiling brine ponds and mud pots formed at the dried lake bottom during the rainy season. The water from these ponds, yellowish-green in filtered samples, consisted of meteoric water highly concentrated in sulphuric and hydrochloric acids.

In early 1989, when the dry season was at its peak, there were reports of sulphur odours and fine sulphur particles precipitating over a large area downwind of the plume. Volcanic materials reached towns on the NW, W and SW-flanks such as Toro Amarillo (7.6 km NW), San Luis (8 km SW), Trojas and San Miguel (12 km SW), San Pedro de Poás (14 km S), Cajón (14 SW), Grecia (17 km SW), Palmira (17 km W), Sarchí (18 km SW), Zarcero (19 km W), and Naranjo (20 km W), damaging and killing vegetation. Plantations of cypress, jaúl, and eucalyptus trees, as well as grassland and crops were severely damaged, whereas coffee plantations and other annual crops were the most affected, with approximate losses reaching several hundred thousands to a million US dollars for the year 1990 (Fernández, E. pers. comm., 2006). Furthermore, the enhanced emissions of gas and particles caused health problems in inhabitants of these towns who suffered from eye, skin, and throat irritation and skin allergies. As a consequence, local health clinics received an increased number of patients. During windy days particles expelled from the lake bottom travelled as far as Atenas (about 32 km SW). Some volcanic particle matter also fell around the ENE and S flanks of the volcano.

Phreatic eruptions resumed in March 1990, emptying the very shallow crater lake that had formed in the rainy season of 1989. Strong steam eruptions within the lake area, similar to those of May 1989, followed a swarm of A-Type earthquakes that occurred at Poás six hours after the 25 March 1990 subduction-zone earthquake (Mw=7.0, Protti *et al.*, 1995). This earthquake, with an epicentre offshore in the Nicoya Gulf, 170 km southwest



Figure 2.12. Colour version and full caption on page 134.

of Poás, apparently triggered the swarm of A-Type quakes. Some of these seismic events had epicentre locations aligned along various N-S and E-W lineaments on the flanks of the volcano (Rowe *et al.*, 1992a). During the second half of May and in July 1990, A-Type seismicity increased again. Low- and medium-frequency harmonic tremor of volcanic origin observed on May 28 was related to vigorous degassing. Inhabitants of Poasito (4 km SE), Fraijanes (6 km SE), and San Pedro de Poás (14 km S) felt some of the earthquakes. On March 28, 1990 reddish flames believed to represent the auto-ignition of elemental sulphur were observed at the dry bottom of the lake, suggesting that the temperature of the intensive subaerial fumaroles was at least 250°C (i.e. the approximate ignition temperature of sulphur in air). The strong activity forced the rangers of the National Park of Poás Volcano to evacuate the tourists and close the park. The Costa Rican government declared a local state of emergency. Between 1989 and 1990 fumarolic activity around the CPC, located on its top and N side, was weak with maximum temperatures of 95°C. B-type earthquakes that had peaked at >100,000 per year in 1988, continued to show similar yearly totals during 1989–1991.

Desiccation and subsequent refilling of the lake occurred during each dry season from 1989 to 1992 (Fig. 2.11), so that the lake maintained a very shallow level in these years. The maximum depth during the rainy season of 1991 and 1992 was about three metres (Fig. 2.14). It increased to ca. six metres by the end of 1993, which corresponds to a lake volume of $7.5 \times 10^4 \text{ m}^3$ (Martínez *et al.*, 2000). Lake-water temperatures during



Figure 2.14. Colour version and full caption on page 134.

the rainy months (May–December) averaged around 70°C in 1991, 1992 and 62°C in 1993. No further significant phreatic eruptions occurred until April–August 1994 (Martínez *et al.*, 2000; Rymer *et al.*, 2000).

In March 1994 the shallow crater lake experienced a rapid drop, and by April it was reduced to scattered small mud pools. Between April and early August 1994 only isolated mud pools remained on the dried bottom due to renewal of phreatic activity. On April 25 and 30, 1994, two phreatic eruptions vented from the lake sediments; fine particles travelled 1.6 km south and southwest of the crater. On June 2, 1994, a phreatic eruption produced a column that rose ca. 1.2 km above the crater floor; part of the fine non-juvenile ashes were transported about 6 km downwind from the crater. The peak of phreatic activity occurred between July 24 and 31, and on August 4, 1994 when a series of large phreatic eruptions lifted lake sediment and gas-rich water columns up to 2 km above the crater floor. The largest of these eruptions occurred on July 31, and non-juvenile ashes were distributed 12 km southwest of the summit. During the second half of July 1994, vigorous subaerial fumaroles, with estimated temperatures of 515°C, based upon measurements performed with an optical pyrometer, were issued from the dried bottom of the acid crater lake (Martínez *et al.*, 2000).

This period of strong fumarolic degassing and phreatic activity that led to the disappearance of the crater lake was also characterized by a significant increase in seismicity. Increases in the numbers of A-Type and B-Type earthquakes as well as polychromatic tremor were recorded prior to and during the



Figure 2.13a. Colour version and full caption on page 134.



Figure 2.13b. Colour version and full caption on page 134.



Figure 2.15. Colour version and full caption on page 135.



Figure 2.16. Colour version and full caption on page 135.

eruptions (Martínez *et al.*, 2000; Rymer *et al.*, 2000). Although phreatic activity ceased in early August 1994, several fumaroles, located along the northern side of the dried lake bottom, continued degassing strongly until late 1994 (Fig. 2.15). By mid-August 1994, a new lake started to emerge and filled up gradually. It showed strong convective circulation and a grey appearance due to vigorous subaqueous venting. The lake was more stable at the very end of 1994 and in early 1995. By May 1995, only very weak subaqueous fumarolic activity was left. The lake continued growing throughout 1995 and 1996 due to accumulation of meteoric water and relatively low subaqueous heat input (Fig. 2.16) (Barquero, 1998).

In April 1995 new fumaroles at boiling-point temperatures were observed for the first time in the lower part of the southern crater area where the trail ascending to the Mirador (lookout point for visitors) begins. The fumarole field spread out gradually to the S-SW along the lowest parts of inner crater wall during April 1995 – May 1996. Temperatures of the new fumaroles ranged between 57–97°C. They produced low-volume gas columns of ~50–100 m height, and sublimating sulphur was deposited around the vents. This small fumarole field remained active for almost five years until it disappeared in February 2000 (Fig. 2.20, site 2).

2.2.5 Activity between September 1995 and February 2005: Stage IV

Between September 1995 and February 2005 (*Stage IV*) subaerial fumarolic activity outside the lake developed further, although the lake itself continued receiving an important influx of volatiles and heat.

In late 1995–early 1996, moderate to strong degassing resumed at the CPC although temperatures remained around boiling point. More fumaroles appeared along the southern

crater area and at the western shore of the acid lake (Fig. 2.20, site 3, Fig. 2.17). In 1996–1999 the fumarolic field along the southern crater border extended towards the western part (see Chapter 2, Fig. 2.20 sites 2 and 3), producing alteration of the inner crater wall and generating landslides. These low-temperature fumaroles disappeared around June 2000.

These weak boiling-temperature fumaroles at the western and southern inner flanks of the crater were active until mid 2000. This enhanced fumarolic activity triggered landslides towards the lake.

By November 1997, the crater lake reached one of the highest levels since 1986, with an estimated depth of ~50 m (Martínez *et al.*, 2000). However, the lake level descended a total of about 8 metres through 1998 due to enhanced influx of heat and volatiles, as indicated by increase in lake temperature (Fig. 2.11) and concentrations of magmatic anions. These changes were accompanied by an increase in seismicity (see Chapters 3 and 4).

Between late 1998 and mid 1999, a series of concentric cracks oriented N-S, through which vapours escaped, started opening along the eastern shore of the lake and the eastern terrace. Contemporarily, a new fumarolic field started developing along the lowest part of the eastern terrace. By mid 1999, for the first time in history, springs started appearing at the inner eastern crater wall, at the contact between the eastern crater wall (eastern terrace) and the crater floor (Fig. 2.20 site 4).

Between February and April 1999, a period of enhanced fumarolic activity started around the CPC. A series of vent-opening events remain for several months (Chapter 2, Fig. 2.18). Fumarolic degassing around the CPC peaked between September and November 1999, when a large water vapour-rich plume rose 2 km above the CPC on September 28, 1999. This plume was observed from the Campus of Universidad Nacional in Heredia (~25 km SE) and the town of Chagüites (~15 km SE). Degassing around the CPC slowed down by the



Figure 2.17. Colour version and full caption on page 135.



Figure 2.18. Colour version and full caption on page 135.



Figure 2.19. Colour version and full caption on page 135.

end of 1999, but still remained fairly vigorous until July 2000 (Fig. 2.18).

This increase in the rate of degassing through the CPC was preceded by a large increment in the number of B-Type earthquakes (only 458 events were recorded in February 1999, against 5264 events in September 1999). The number of intermediate-frequency earthquakes also increased significantly between May 1999 and December 1999 (a total of 8 AB-type events registered in May, against 405 events in December 1999). This also coincided with a peak in A-type seismicity and with an increment in the total hours of recorded tremor (42.5 hours of which 0.8 hours corresponded to monochromatic tremor) between August and November 1999.

The impact of environmental acidification extended about 4.5 km downwind to the southwest of the volcano in 1999, as a result of strong subaerial degassing through the CPC. A large decrease in fumarolic activity at the cone was reported in December 1999. Nevertheless, the CPS and the fumarole field at the eastern inner crater wall have remained the main sites of fumarolic degassing within the active crater since then.

Between late December 1999 and February 2000, tremor increased, with a total of 28.75 hours recorded. Twenty-four hours of tremor were recorded on a single day in February 2000, 11 hours of which corresponded to monochromatic tremor. A fracture appeared in the eastern terrace, and new fumaroles (94°C), depositing sulphur and emitting minor amounts of vapour-gas, were noticed on the eastern crater floor and in the eastern crater wall. Vents continued to open at these locations throughout 2000 and 2001. For instance, in May 2000 a substantial increase in seismicity coincided with the appearance of new vigorous fumaroles in the eastern inner crater wall. Again in March 2001, in a matter of only 3 days, volcanic polychromatic tremor was registered during 35 hours. The enhancement in seismic activity was followed by stronger fumarolic degassing through the CPC and the appearance of more new fumaroles in the eastern crater area in May–August 2001. Furthermore, an 8-m drop of the lake level was observed in the course of 2001. In 2000 and 2001 the fumaroles and

thermal springs of the eastern crater wall had temperatures of 88°–95°C and 66°–89°C, respectively.

From October–November 2001 till today, the flux of gases released through the CPC has remained relatively low. In contrast, fumarolic activity at the eastern inner crater wall has remained vigorous. A conspicuous fumarole at the north-eastern side of the active crater (Fumarole Norte) registered a temperature of 116°C in March 2003, and 124°C in April 2005. The inner crater wall became unstable and has experienced several slumps and rock falls from 2000 till present. Like the CPC, the crater lake remained relatively quiet throughout stage IV, except for some significant heating events in June 2002–September 2003 and March 2005–September 2006 (Figs. 2.11 and 2.19).

Between mid 2002 and October 2003 vigorous upwelling and abundant floating sulphur spherules were observed. This came after a period of quiescence between November 2001 and May 2002, during which the lake had an unusual bluish colour. Upwelling activity was particularly strong in September–October 2003 when some small unusual blackish spherules, together with the more common yellow globules and pieces of molten sulphur with a ‘plastic’ texture, emerged from the lake bottom, suggesting an intensification of subaqueous fumarolic discharges (cf. Takano *et al.*, 1994a). Also between September 2002 and December 2003, a persistent emanation of corrosive fumes (HCl evaporation?), causing respiratory problems and irritation of eyes and skin near the lake edge, formed a white acid fog over the lake surface, covering all of it at times. The fog was even denser, ~5 m thick, in November 2002 (Fig. 2.19). Constant bubbling was observed at the interface between the lake and the northern slope of the CPC, and 1–5 m high water fountains were sporadically ejected here between August 2002 and September 2003. Between mid-2002 and late 2003, a large increase in B-Type seismicity was observed, which might be related to the enhanced degassing through the lake.

From late 2003 on, the lake volume increased significantly, reaching record volumes between late 2004 and early 2005. A tropical storm on the Caribbean side of Costa Rica that flooded some of the Atlantic lowlands between December 2004 and



Figure 2.20. The active crater of Poás volcano viewed from the lookout point (El Mirador) at the southern crater rim. Note the green colour of the lake. Numbers refer to main sites of subaerial fumarolic degassing within the active crater, which have shown shifts from the end of the 1970s till present. (1) CPC; (2) southern fumarolic field; (3) western fumarolic field; (4-6) eastern terrace/eastern inner crater wall fumaroles. Photograph taken by Manfred van Bergen in February 2003.

January 2005 caused strong precipitations over the central mountain range, upon which the crater lake acquired a volume of approximately 2 million cubic metres (Poás summit rainfall data of ICE; Aguilar *et al.*, 2005). Part of the eastern crater floor was flooded, leaving some subaerial fumaroles in this sector submerged for several weeks early in 2005 (Fig. 2.20, site 4; Fig. 2.21, Fig. 2.22) (Venzke *et al.*, 2002-). The lake level was the highest registered since the late 70s, and its temperature was as low as 22°C (Fig. 2.11). The volume increase was accompanied by a subtle colour change towards the end of 2003, while it turned from bluish green to light green at the end of April 2004. After decades of monitoring, this was the only time that this colour has been seen (see Chapter 4, Figs. 4.10A and 4.10B).

Throughout stage IV there were several periods of relative quiescence in the lake when temperatures were low: throughout 1995, November 2001–April 2002 and October 2003–February 2005. These quiet periods have been interpreted as a result of reduced fumarolic input. In contrast, heating events in 1998–2001, mid 2002–late 2003 and 2005–present, were marked

by sharp rises in lake temperature (Fig. 2.11) and concentrations of dissolved chemical species (see Chapter 4 Figs. 4.5 and 4.7). Fumarolic outgassing was also fairly weak at the CPC from the end of 2003 until early 2005.

By February 2005, the Fumarole Norte and other fumaroles along the eastern inner crater wall started to issue large amounts of sulphur particles. Since then, these particles have been deposited mostly on the northern–northeastern inner crater wall, giving it a yellowish colour that is visible from the lookout point (Fig. 2.21 and 2.22). Also, a few small pools and flows of molten sulphur have been observed in the eastern fumarole field (OVSICORI, open reports).

2.2.6 Activity since March 2005: Stage V

In March 2005, a new period of strong convective activity and evaporation commenced after a 10-years period of relative quiescence of the lake (**Stage V**, March 2005–to early 2008). The lake showed the first signs of more vigorous discharge from subaqueous fumaroles by conspicuous change of its



Figure 2.21. Colour version and full caption on page 136.



Figure 2.22. Colour version and full caption on page 136.



Figure 2.23. Colour version and full caption on page 136.



Figure 2.24. Colour version and full caption on page 137.

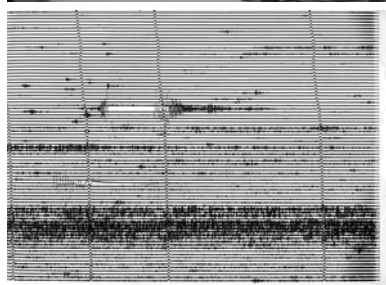
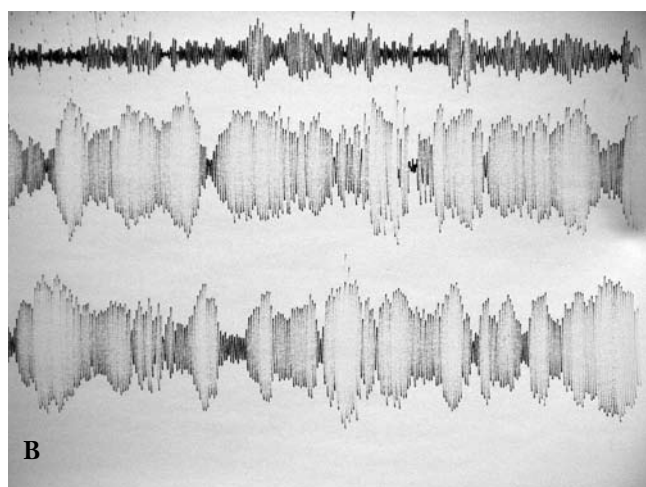
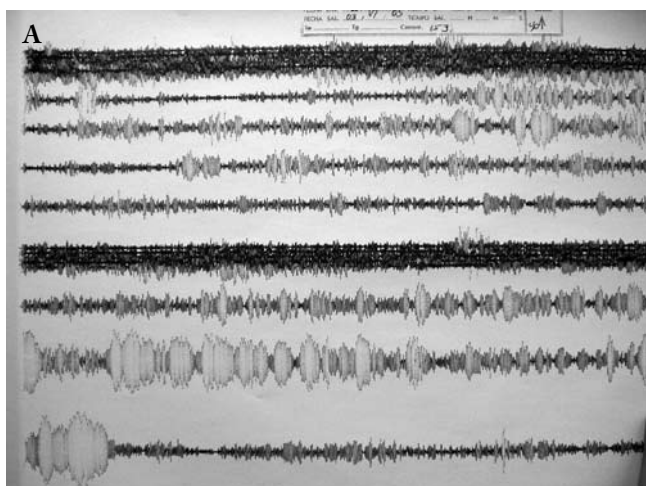


Figure 2.25. Seismograms from Poás volcano. (A) High-amplitude tremors (June 2005), some with a monochromatic character that is rarely seen at Poás; (B) Close-up of tremor signals shown in (A); (C) Monochromatic harmonic tremor with a dominant frequency of 1.5 Hz (24 March 2006). This type of volcanic tremor started on 23 March 2006 at 03:43 hrs GMT (i.e. 9:43 p.m. local time) and continued uninterruptedly until 25 March 2006 at 06:25 hrs GMT, with a total duration of 26:42 hrs (see also Fig. 2.29B); (D) High-frequency seismic event (top) and bands of polychromatic volcanic tremors (below) associated to the phreatic eruption of 25 September 2006. All of the seismograms were registered by the POA2 seismic station of OVSICORI-UNA.

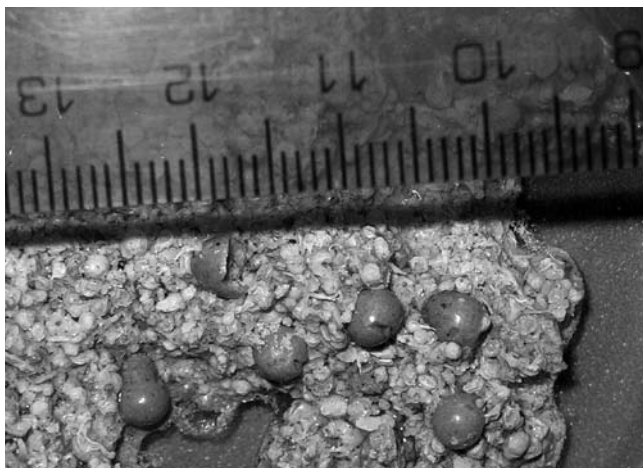


Figure 2.26. Colour version and full caption on page 137.

colour, first from greenish to milky turquoise (Figs. 2.21 and 2.22, see Chapter 4, Figs. 4.10A and 4.10B), and then to grey in May (Figs. 2.23 and 2.24). Enhanced subaqueous fumarolic discharge induced a large rise in lake temperature, conductivity and concentrations of dissolved chemical species as well as a steady drop in pH throughout 2005 (Fig. 2.11, see Chapter 4, Figs. 4.3 and 4.7).

The pH of the lake water decreased to <1.0 after April 2005 and has remained fairly low until present. Within a year (February 2005–February 2006), the pH changed from 1.25 to 0.59 and the temperature from 22°C to 51°C (Fig. 2.11). Between May and November 2005, the lake surface showed strong evaporation, upwelling and floating sulphur spherules (Figs. 2.23, 2.24, and 2.27). Between June and November 2005 yellowish sulphur spherules with “tails”, as well as large (0.5-cm diameter) hollow greyish spherules with a metallic lustre (Fig. 2.26) were observed for the very first time at Poás.

Simultaneously with the changes in the crater lake, the Fumarole Norte showed a significant increase in temperature (105°C in March 2005, rising to 203°C between May and June) and in flow rate (OVSICORI, 2006b; Chapters 2 and 4) (Fig. 5.2). The Fumarole Sur-Este showed an increase from 101°C to 113°C as well. Furthermore, fumarolic activity around the CPC has also increased since April 2005 till present. Between early 2005 and early 2006 the lake level descended by 10 metres despite an anomalously large amount of rainfall in 2005. This clearly points to an increase in the input of heat and volatiles through subaqueous fumarolic vents.

Unusually high seismic activity paralleled these drastic changes. Between January and February 2005 seismicity increased substantially. About 25 volcano-tectonic earthquakes (A-Type) were recorded within two months. Between April and October 2005 tremor reached record values (for instance, 245 hours in May, of which 34.5 hours corresponded to monochromatic tremor, and 740 hours in August, of which 168 monochromatic tremor). The last time such a level of volcanic tremor was observed at Poás was in the early 80s when magma intruded below the CPC and almost reached the crater floor (Casertano *et al.*, 1983, 1985; Fernández, 1990). In June 2005 the POA2 seismometer recorded bands of tremor signals with an amplitude higher than usual and with a predominantly monochromatic character, rarely seen at Poás and remarkably

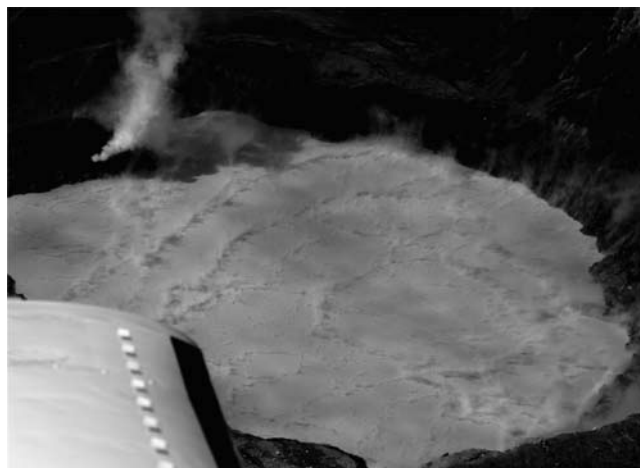


Figure 2.27. Colour version and full caption on page 137.

similar to the high-amplitude tremors commonly observed at Arenal Volcano (Barboza, V., pers. comm. 2006) (Figs. 2.25A and 2.25B). The conspicuous amount of volcanic monochromatic tremor suggests the possible intrusion of a magma body up to shallow levels beneath the crater lake. From April 2005 till present, tremor has been recorded uninterruptedly (Figs. 2.25C and 2.25D).

Between May and November 2005, AB-type seismicity also increased up to more than a thousand events per month, the highest amount ever recorded at Poás since 1986 (see Chapter 4, Fig. 4.6). The AB-type quakes are closely related to opening of fumarolic vents.

Finally, some time between the night of March 23 and early morning of March 24, 2006, phreatic activity resumed within the crater lake after a twelve year period of relative quiescence (Figs. 2.28, 2.30, and 2.31). This new episode of phreatic activity was preceded by a dramatic increase in seismicity. On March 21, 2006 (at 22:39 hrs GMT) two long lasting (8 minutes and 5 minutes) high-frequency seismic signals (up to 7.5 Hz) were recorded. This has been attributed to breaking of a sealed system, possibly the fracturing of the brittle envelope of a shallow magma body beneath the volcano (Fig. 2.29A). After this had occurred, the numbers of AB- and B-Type quakes reduced substantially. Later, on March 23, 2006 at 12:17 hrs GMT (6:17 a.m. local time), a band of monochromatic tremor that lasted for



Figure 2.28. Colour version and full caption on page 138.

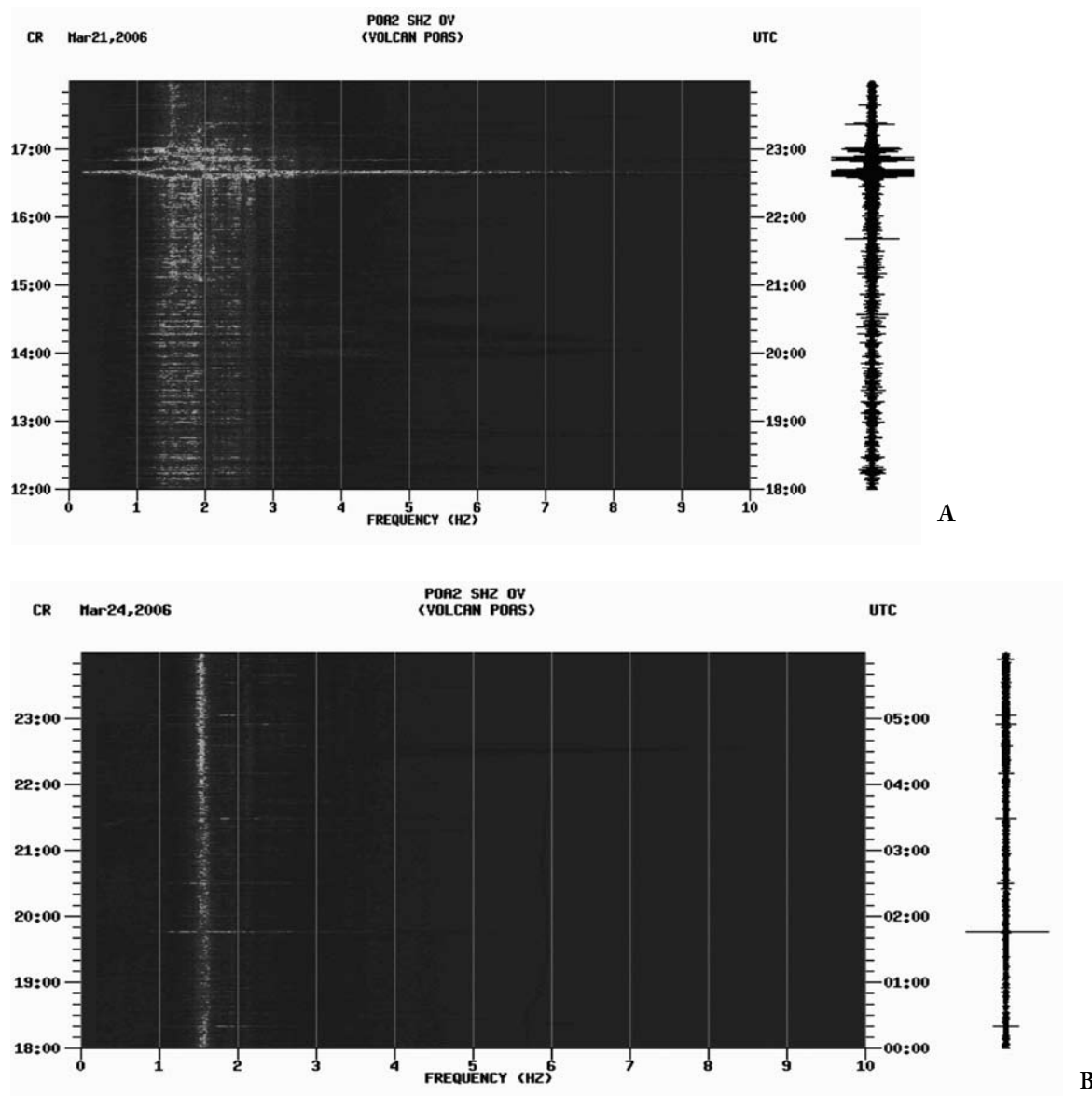


Figure 2.29. A and B. Colour version and full caption on page 139.

3.18 hours was recorded. This tremor had dominant frequencies of 1.5 Hz. A second band with similar dominant frequencies was recorded 5.14 hrs later and lasted for 4.15 hrs. Between the first and the second tremor bands 3 intermediate frequency (AB-type) events occurred with maximum frequencies of 2.8 Hz. After the second band 7 similar AB-type events were recorded. In the course of this period the AB-type earthquakes showed higher frequencies and intensity than usual, i.e. up to 3 Hz and with durations up to 50 seconds. Banded tremors were also observed at Poás between September 2002 and October 2003, and might be related to the water fountains observed at the north side of the CPC in the same period (see Chapter 4).

On March 23, 2006 at 03:43 hrs GMT (9:43 p.m. local time) monochromatic harmonic tremor started and continued uninterruptedly until March 25, 2006 at 06:25 hrs GMT, with a total duration of 26.42 hrs (Figs. 2.25C and 2.29B). The dominant frequency was 1.5 Hz. In the same period 6 AB-type events were recorded as well. This seismicity is related to the renewal of phreatic activity on March 23 and 24. A moderate

phreatic eruption, which was witnessed by park rangers and tourists from the lookout point, ejected materials that fell into the lake and on its shores around midday of March 24. Later that day, at 01:51 hrs GMT (19:51 hrs local time) a stronger phreatic eruption occurred (Fig. 2.29B). According to information provided by personnel of the Poás Volcano National Park and the Red Cross, some other minor phreatic eruptions occurred within the crater lake between the end of March and April 26. In general, muddy lake water as well as rock fragments ejected by the explosions fell within the crater area, and only the energetic nightly eruption of March 24 dispersed non-juvenile fine lake sediments as far as 5 km southwest of the volcano.

Between late March and July 2006 the seismic activity declined significantly. However, it was high again throughout the second half of 2006. A small explosion witnessed by the park rangers and some visitors on April 26 was the last of this eruptive period. A subsequent quiet interval lasted until the night of the 25-26 September. On September 25th at 21:48 hrs. local time, a high-frequency seismic signal, associated to seal

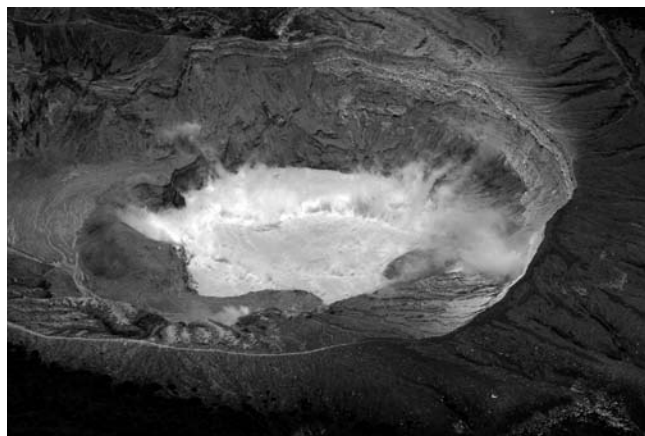


Figure 2.30. Colour version and full caption on page 138.

rupture, was recorded by the POA2 seismic station, similar to the precursory signals of March 21, a few days before the renewal of phreatic activity. This signal was followed by polychromatic tremor, related with movement of fluids through fractures or conduits, leading to the September 25 eruption (Fig. 2.25D). According to field observations carried out by personnel of the OVSICORI, it dispersed fine lake sediments as far as 12 km SW from the crater. The lake's colour changed again from milky turquoise to grey, due to strong fumarolic input. From September till December 2006, strong subaqueous discharges remained, as evidenced by a vigorous mud plume (ca. 80 m diameter) (Fig. 2.31).

A few minor phreatic explosions as well as strong convective activity were observed between September and December 2006, coinciding with a steady increase in temperature, acidity, and concentration of solutes in the lake water. For instance, in November 2006, pH, temperature, and conductivity of the lake were 0.43, 58°C, and 180 mS/cm, respectively. In December 2006, a visitor of the national park witnessed another small phreatic eruption.

No phreatic explosions were observed throughout year 2007 although strong degassing and convective activity prevailed in the lake, producing a significant lowering of its level and keeping it greyish-green and at an average temperature of ~55°C (min 48°C–max 58°C). More recently, in January 2008, at least two minor phreatic explosions in the lake were witnessed by tourists and park rangers (OVSICORI, 2008a,b). These eruptions ejected muddy water columns that rose up to about 200 metres above the lake surface and leaving rock fragments dispersed on the crater floor (OVSICORI, 2008a,b). By February 2008, lake temperature and pH were 45°C and 0.21, respectively and the lake remained greyish (see Chapter 5). Moreover, seismic stations POA2 and POA5 (the latter set up in mid 2006 at the Von Frantzius volcano, ~0.5 km N of Poás lake) recorded a large number of seismic events in 2007–2008, mainly polychromatic tremor, B and AB-type quakes. From 2005 on, the lake has been shrinking, so that in March 2008 its maximum depth was only around 26 m and its volume about $9.1 \times 10^5 \text{ m}^3$. If the current conditions in the crater lake will continue, more phreatic explosions could occur anytime in the near future.

The occurrence of over 60 registered eruptions in the last 175 years, the presence of a warm acidic crater lake and persistent subaerial fumarolic discharges with fluctuating intensity



Figure 2.31. Colour version and full caption on page 138.

highlight the active status of Poás volcano. Monitoring and study of the dynamics of the Poás crater lake–hydrothermal system provide insights of the internal volcanic/hydrothermal processes that control the physico-chemical conditions of the lake and fumaroles which is crucial for forecasting future eruptive events (see Chapters 3, 4, and 5).

2.3 Climatic conditions at Poás Volcano

The climate in Costa Rica is controlled by: (a) its geographical position, from 8°02' to 11°14' N, fairly close to the equator, (b) its narrow extension between the Caribbean Sea and the Pacific Ocean (about 300 km maximum), and (c) its topographic diversity (average 1539 m.a.s.l.) characterized by coastal plains and mountain ranges along the length of the country that are separated by a central valley. Variations in altitude and local topography result in a diversity of microclimates that sustain the magnificent ecosystems of the country.

There are two major seasons in a year: dry (from January to mid-May) and rainy (from mid-May to December). Rainfall patterns, although seasonal, vary greatly in intensity across geographical areas. A few locations in Costa Rica receive more than 9000 mm of precipitation per year (Thomas, 1990), while others receive less than 1500 mm. The winds, loaded with high amounts of water, travel from the coasts to the central part of the country. When air masses rise and get cold, water precipitates over the mountain ranges, running from the north-west to the south-east and dividing the country into a Caribbean slope and a Pacific slope. On the Caribbean slope the rainy season begins from mid to late April and continues through December and sometimes January. The wettest months are July and November, with a dry spell that occurs around August or September. Major storms, locally called “temporales del Atlántico” occasionally buffet this slope between September and February, when it rains continuously for several days, as happened in the rainy seasons of 2003 to 2005. That event was apparently due to an increase in surface temperatures of the northern and equatorial Atlantic and Pacific Ocean (data from Instituto Costarricense de Electricidad, ICE; Aguilar *et al.*, 2005). On the Pacific slope the rainy season begins in May and runs until November. This is a period in which the north-eastern trade winds (“vientos alisios”) are much reduced in intensity, so that storms often

come in from the Pacific Ocean in September and October. From December to April, the velocity of the “vientos alisios” is maximal, and this period corresponds with the dry season. Although temperatures are much colder above 2000 metres in the mountains, the average annual temperature for most of the country lies between 21.7°C (71°F) and 27°C (81°F). The coolest months are from November through January, and the warmest from March through May (Eggar, 2007).

Poás volcano, with its summit of approximately 2708 metres altitude (Fig. 2.5), is located within a cold, very humid zone of the Cordillera Volcánica Central according to Köppen’s terminology (Strahler, 1974). Here the temperature ranges from -5 to 20°C, whilst the relative humidity ranges between 80 to nearly 100% throughout the year (Calderón, 2005).

Weather conditions at Poás volcano are subject to the influence of both the Caribbean and Pacific climatic regimes. The prevailing wind direction is from the NE throughout the year, with influences of the Pacific winds coming from the west between May and January. The period with much less rainfall extends from February to April. The total average precipitation measured at the Poás Rainfall Station 84063, located at the summit of the volcano at 2564 m.a.s.l., reaches over 3000 mm annually (data from the Instituto Costarricense de Electricidad, ICE; Calderón, 2005). In fact, the total annual rainfall has shown extreme values of 2694 mm and 5095 mm in 1985 and 2003, respectively. In 2003, 2004 and 2005 the total annual precipitation at the summit was 5095, 4696, and 4884 mm, respectively. The annual rainfall registered in 2003 and 2005 was the highest since 1972 (data from ICE). The crater lake reached record levels between the end of 2004 and early 2005, which resulted in overflow and flooding of otherwise dry parts of the crater floor.

2.4 Other acidic volcanic lakes in Costa Rica

Only two of the volcanoes in Costa Rica host hyperacid lakes (pH<2): Poás and Rincón de la Vieja. The acid lake of Rincón de la Vieja is chemically similar to that of Poás. The waters of Rincón de la Vieja lake have extremely low pH (ranging from below zero to 1.2), high concentrations of dissolved elements (TDS=24,000-154,000 mg/kg; Kempton and Rowe, 2000; Tassi *et al.*, 2005; OVSICORI, unpublished data), as well as

large fluctuating concentrations of polythionates (from below detection limits to 3900 ppm; Takano, B., written comm. 2006). The chemistry of the Rincón acid lake is controlled by the input of magmatic-hydrothermal fluids and intense leaching of andesitic rock (Kempton and Rowe, 2000; Tassi *et al.*, 2006; OVSICORI unpublished data). The lake of Rincón de la Vieja is not being monitored on a regular basis as the acid lake of Poás, and only a few isolated studies of its geochemistry are available (Kempton and Rowe 2000; Tassi *et al.*, 2005), partly due to the fact that the lake is not as easily accessible. Sampling is difficult because of steep crater walls, weather conditions and a high flux of acidic volatiles within the crater. However, OVSICORI has been measuring temperature and concentrations of solutes in lake-water samples, collected as frequently as weather conditions permitted. Rincón volcano has presented at least six periods of eruptive activity over the last 150 years according to records that date back to 1851: 1854-63, 1912, 1922, 1966-70, 1983-87, 1991-98 (OVSICORI, 1995, 1998; Soto *et al.*, 2003). The most recent phreatomagmatic activity seems to have occurred in February 1983 and in March 1984, according to the reports of juvenile volcanics found among the erupted materials by Barquero and Segura (1983) and Soto *et al.* (2003).

The Botos Cone, which is part of the Poás volcanic complex, hosts the slightly acidic Botos Lake. From 1998 till present, its pH and temperature have shown ranges of 3.7-6.3 and 15°-19°C, respectively (see Chapter 5 Table 5.1). The composition of Botos Lake is influenced by meteoric input of acid gases and particles from the volcanic plume emitted by the active crater of Poás, about 1 km to the north (Figs. 2.4 and 2.5).

Finally, the lake within the currently active crater of Irazú Volcano has shown changes in chemical properties ranging from acid to slightly alkaline between 1992 and 2007. The lake waters were fairly acidic in the recent past. In June 1992 the water at the northern edge of the lake had a pH of 3.7 and a temperature of 48°C. The lake showed an earthy colour at that time. However, over the last years the lake had a greenish colour (OVSICORI, unpublished data). Between 1999 and 2007, pH and temperature of the lake ranged between 5.8-8.0 and 14-24.5°C, respectively, although temperatures at the northern edge were occasionally higher (OVSICORI, unpublished data). Geochemical data indicate that the crater lake of Irazú is fairly homogeneous.

Chemical evolution and volcanic activity of the active crater lake of Poás volcano, Costa Rica, 1993-1997¹

Summary

Concentrations of chloride and sulphate and pH in the hot crater lake (Laguna Caliente) at Poás volcano and in acid rain varied over the period 1993-1997. These parameters are related to changes in lake volume and temperature, and changes in summit seismicity and fumarole activity beneath the active crater. During this period, lake level increased from near zero to its highest level since 1953, lake temperature declined from a maximum value of 70°C to a minimum value of 25°C, and pH of the lake water increased from near zero to 1.8. In May 1993 when the lake was nearly dry, chloride and sulphate concentrations in the lake water reached 85400 and 91000 mg/L, respectively. Minimum concentrations of chloride and sulphate after the lake refilled to its maximum volume were 2630 and 4060 mg/L, respectively. Between January 1993 and May 1995, most fumarolic activity was focused through the bottom of the lake. After May 1995, fumarolic discharge through the bottom of the lake declined and reappeared outside the lake within the main crater area. The appearance of new fumaroles on the CPC coincided with a dramatic decrease in type B seismicity after January 1996. Between May 1995 and December 1997, enhanced periods of type A seismicity and episodes of harmonic tremor were associated with an increase in the number of fumaroles and the intensity of degassing on the CPC adjacent to the crater lake. Increases in summit seismic activity (type A, B and harmonic tremor) and in the height of eruption plumes through the lake bottom are associated with a period of enhanced volcanic activity during April-September 1994. At this time, visual observations and remote fumarole temperature measurements suggest an increase in the flux of heat and gases discharged through the bottom of the crater lake, possibly related to renewed magma ascent beneath the active crater. A similar period of enhanced seismic activity that occurred between August 1995 and January 1996, apparently caused fracturing of sealed fumarole conduits beneath the CPC allowing the focus of fumarolic degassing to migrate from beneath the lake back to the 1953-1955 cone. Changes in the

chemistry of summit acid rain are correlated changes in volcanic activity regardless of whether fumaroles are discharging into the lake or are discharging directly into the atmosphere.

3.1 Introduction

Crater lakes in active volcanoes are dynamic systems. They interact with cooling shallow magma bodies and/or magmatic-hydrothermal systems beneath them. Changes in heat flow and degassing rates induce variations in the chemical and physical properties of crater lakes. Changes in these properties provide the basis for volcano monitoring programs assuming that external influences (e.g. rainfall and lake-sediment interaction) can be isolated. Crater-lake geochemistry related to volcanic activity can be an important tool to predict and monitor volcanic events, especially when combined with other geophysical techniques such as seismic or deformation studies. In addition, crater lakes can be the source of increased volcanic hazards (i.e. lahars, atmospheric pollution, seepage of toxic fluids, e.g., Pasternack and Varekamp, 1997), so their activity needs to be carefully studied through volcano monitoring programs. Fortunately, reports from several well-studied crater lakes on active volcanoes are available, e.g.: Kusatsu-Shirane volcano, Japan (Takano, 1987; Takano and Watanuki, 1990; Takano *et al.*, 1994a); Ruapehu volcano, New Zealand (Takano *et al.*, 1994b); Kelut volcano, Java (Badrudin, 1994) and Laguna Caliente, Poás. The latter crater lake has been studied by Raccichini and Bennett (1977); Brantley *et al.* (1987); Brown *et al.* (1989, 1991); Rowe *et al.* (1992a,b; 1995); Rowe (1994); and Rymer *et al.* (2000).

3.2 Poás Volcano

Poás Volcano is one of the most active volcanoes of Costa Rica and is approximately 35 km northwest of San José, in the Central Cordillera of Costa Rica (10°12'00"N and 84°13'58"W, 2708 m above sea level). It is a broad well-vegetated basaltic-

¹ This chapter has been published as Martínez, M., Fernández, E., Valdés, J., Barboza, V., van der Laat, R., Duarte, E., Malavassi, E., Sandoval, L., Barquero, J., Marino, T. 2000. Chemical evolution and volcanic activity of the active crater lake of Poás volcano, Costa Rica, 1993-1997. *Journal of Volcanology and Geothermal Research* 97: 127-141.

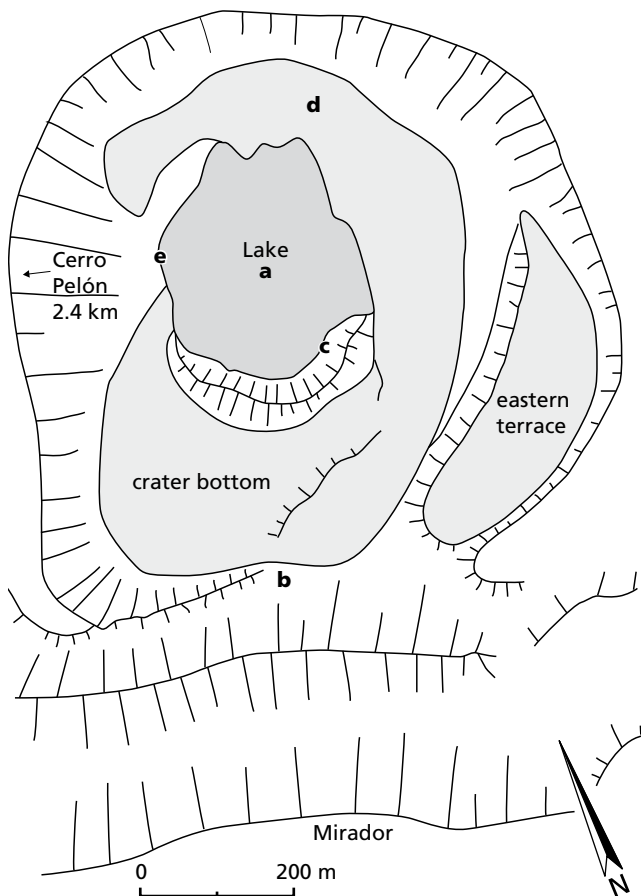


Figure 3.1. Map of the main crater of Poás Volcano, indicating the location of the areas with intense fumarolic discharge observed from 1993 to 1997: From January 1993 to May 1995, subaqueous fumarolic activity predominated at Laguna Caliente (a); then the main fumarolic activity migrated to the southern wall of the crater in May 1995 (b); finally, after January 1996, the locus of most fumarolic activity was centred on the CPC (c) formed between 1953–1955 and at the western (e). Low temperature fumaroles formed on the 80-m- long, NE-trending fracture that appeared on the northern terrace in April 1997 (d). Cerro Pelón, the acid rain sampling site, is located about 2.4 km southwest from Laguna Caliente. Map adapted from Rymer *et al.* (2000).

andesite stratovolcano, with a summit area that contains three cones and the eroded remnants of two elongate calderas (Prosser and Carr, 1987). The active cone contains a crater lake, Laguna Caliente (Fig. 3.1), which is located between the two older cones: the Von Frantzius cone to the north and the Botos cone to the south, which contains a freshwater lake at its summit (Fig. 3.6). Radiocarbon dating of pyroclastic deposits associated with the last lava flow eruption by the Botos cone gives an age of 7540 ± 100 years old (Prosser, 1985).

Laguna Caliente is a hot, extremely acidic, crater lake, filled with a concentrated chloride-sulphate brine rich in rock-forming elements, and fine native sulphur particles. According to the physico-chemical classification scheme for volcanic lakes of Pasternack and Varekamp (1997) Laguna Caliente was a hot acid hyperbrine volcanic lake from 1984 to 1990. During this period, lake temperature ranged from 38 to 96°C, pH ranged from -0.87 to 0.26 and total dissolved solids (TDS) ranged from 60 to 360 g/kg (Rowe *et al.*, 1992a). Maximum concentrations of chloride

and sulphate in samples of lake brine collected prior to the lake's initial disappearance in early 1989 were 120000 and 286000 mg/kg, respectively (Rowe *et al.*, 1992a). The temperature and extreme fluid chemistry observed in the crater lake were caused by the combined effects of subaqueous fumaroles discharging steam and magmatic gases into the bottom of the lake and intense evaporation at the surface of the hot lake.

The active crater hosts an active hydrothermal system (Casertano *et al.*, 1987) supplied with heat and volatiles by a small, shallow magma body whose upper surface is believed to be within 500 m of the crater floor (Rymer and Brown, 1989). Annual rainfall in the vicinity of the active crater is approximately 3.5 metres per year (Liao, 1997) with the dry season from January to mid-May. The volume, temperature, and water chemistry of Laguna Caliente vary considerably, responding to changes in rainfall, thermal power output, and summit seismic activity (Brown *et al.*, 1989; 1991; Rowe *et al.*, 1992a,b).

3.2.1 Summary of Historical Activity

Historical activity at Poás with reports of fumarolic activity, vapour eruptions and phreatic explosions since 1828 are summarised by Krushensky and Escalante (1967), Raccichini and Bennett (1977), Vargas (1979), Boza and Mendoza (1981), Malavassi and Barquero (1982) and Malavassi *et al.* (1993). The largest reported eruption occurred on 25 January 1910, when a large steam and ash cloud reached 4–8 km above the summit. During this eruption most of the crater lake was ejected, but the lake did not completely disappear (Calvert and Calvert, 1917).

From 1910 to 1952, the crater lake was present and nearly continuous fumarolic activity was observed in the active crater. Activity at the volcano changed markedly in 1952 when geyser-like phreatic eruptions through the crater lake returned, marking the onset of a period of phreato-magmatic activity that would continue for several years. Two vents were active at Poás' main crater during this eruption cycle: one that formed a small CPC 40 m high in the central part of the active crater, and another unnamed vent that formed about 150 m to the north of the CPC. The northern vent collapsed and later filled with water to form Laguna Caliente. By 1961, the crater lake had reformed with intermittent geyser-like phreatic eruptions, e.g. in 1977–1980, phreatic eruptions occurred with column heights from several metres to 2 km and a phreatic explosion in 1978 erupted large sulphur-encrusted blocks (Bennett and Raccichini, 1978 a,b; Bennett, 1979; Francis *et al.*, 1980).

Intense swarms of type A earthquakes were recorded beneath the active crater in July 1980. These swarms are believed to represent hydrofracturing of the chilled, brittle margin of the shallow magma body beneath the crater (Casertano *et al.*, 1987). Following the type A swarms, a very dramatic change occurred in January 1981 when high temperature fumaroles (up to 925°C) appeared on the CPC and gas columns rose up to 2 km high. At the same time, phreatic eruptions ceased to occur at Laguna Caliente (Barquero and Malavassi, 1981a,b, 1982, 1983). The temperature of fumaroles on the CPC gradually decreased from 960°C in mid-1981 to 441°C in 1987 (Barquero and Fernández, 1988) and were reduced to boiling and sub-boiling point temperatures by 1989 (Smithsonian Institution, 1989). The annual number of type B earthquakes was 12000 in

1983 (Fernández, 1990). Tremor hours were high (1250-1800 h) during 1981-1982 when high-temperature degassing was concentrated on the CPC. The CPC remained the site of obvious fumarolic activity until June 1987 when geyser-like eruptions returned to Laguna Caliente.

A swarm of type A earthquakes, representing either a small episode of renewed magma ascent or another less extensive hydrofracturing event, occurred between February and May, 1986 (Rymer and Brown, 1989; Rowe *et al.*, 1992b). Phreatic eruption columns reached 1 km in elevation on 9 April 1988 and expelled lake sediments fell 0.5 km south of the crater rim. Water temperatures of Laguna Caliente increased from 58 to 70 °C in 1988. Type B earthquakes gradually increased

from 12000 per year in 1983 to over 100 000 per year in 1988. As the lake disappeared, lake-bottom fumaroles began to degas directly into the atmosphere so that direct emissions of the acid gases SO₂, H₂S, HCl and HF began to affect large areas west and southwest of the active crater. Areas affected by acid deposition extended up to 15 km southwest of the active crater; when the lake is present, acid deposition is typically restricted to areas 3 km or less downwind of the active crater (Barquero and Fernández, 1990; Fernández *et al.*, 1994). The level of Laguna Caliente dropped drastically during 1988 and the lake disappeared completely in April 1989. After the lake disappeared, steam jets lifted lake sediments into the air and periods of harmonic tremors reappeared. On 1 May 1989,

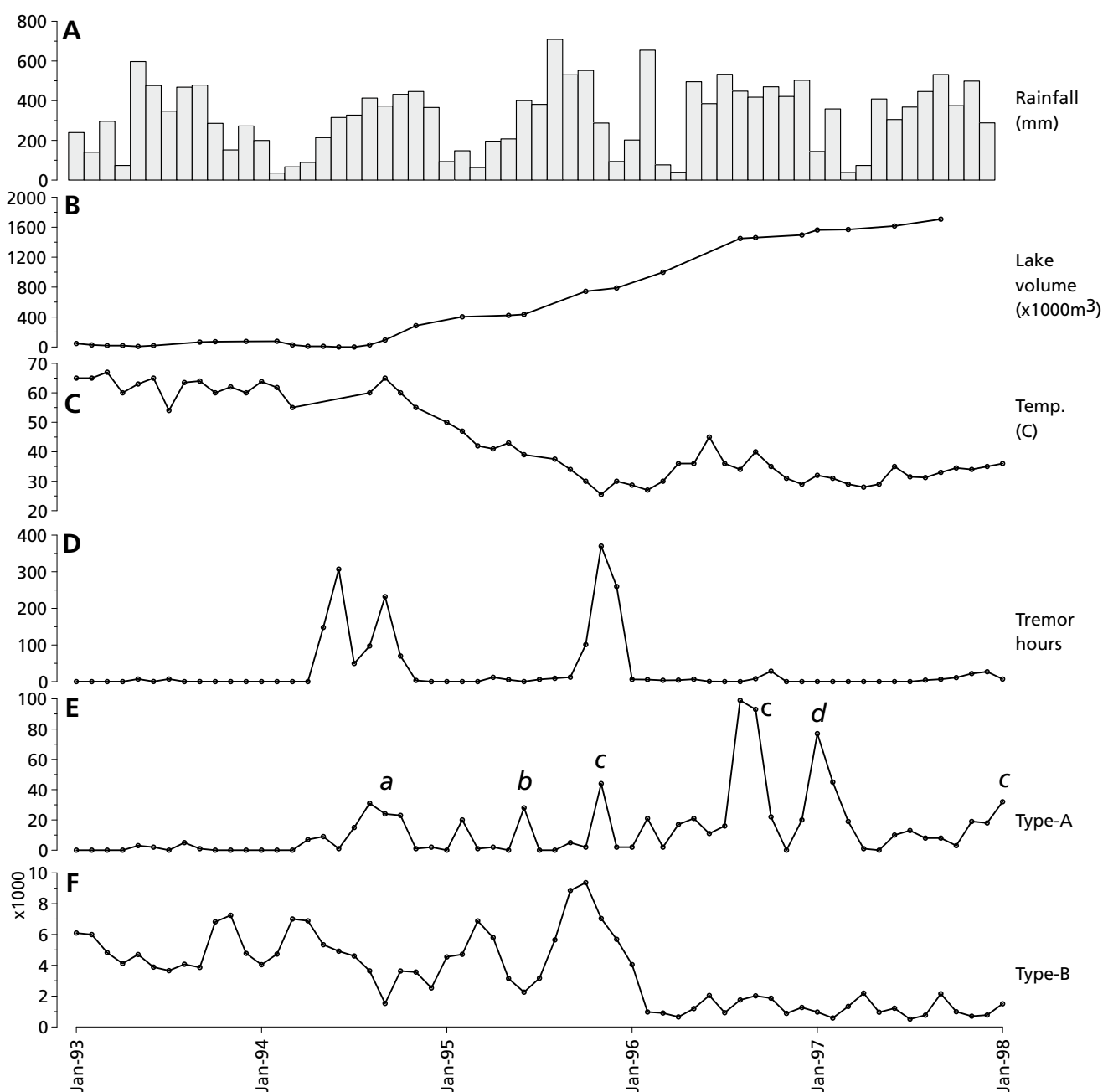


Figure 3.2. Monthly variation of physical parameters related to Laguna Caliente (1993-1997) including: (A) rainfall at the summit of Poás Volcano; (B) crater lake volume; (C) crater lake water temperature; (D,E,F) summit seismicity recorded at POA2 seismographic station: (D) tremor hours, (E) type A seismicity, and (F) Type B seismicity. On Fig. 3.2E, small letters a, b, c and d, refer to the location of fumaroles and their opening events shown in Fig. 3.1.

unusually powerful steam jets ejected lake sediments 1–2 km into the air; these sediments later fell on populated areas 18 km southwest of the volcano. Dry ash and steam eruptions continued intermittently for three weeks with plume heights ranging between 1.5–2 km (Smithsonian Institution, 1989).

Boiling brine pools, mud pots, and sulphur volcanoes up to three metres high were formed on the crater's floor. Pits filled with molten sulphur at temperatures of 140°C were also observed on the lake bottom at this time (Oppenheimer and Stevenson, 1989). Reddish flames believed to represent the combustion of native sulphur were observed around the vents of high-temperature fumaroles on the lake floor suggesting temperatures >400°C. Lake desiccation and subsequent refilling occurred during each dry season between 1989 and 1992.

Phreatic eruptions resumed in March 1990 and a strong eruption in April 1990 followed a swarm of type A earthquakes that occurred at Poás six hours after the 25 March 1990 subduction zone earthquake ($M_w = 7.0$, Protti *et al.*, 1995), with an epicentre offshore of the Nicoya Gulf, 170 km southwest of Poás volcano. Dry steam and ash eruptions, similar to those that occurred in May 1989, resumed in May 1990 when the lake again disappeared (Smithsonian Institution, 1990). Type B earthquakes that had peaked at greater than 100 000 per year in 1988, continued to show similar yearly totals during 1989–1991. Lake-water temperatures during the rainy months (May–December) varied between 63 and 71°C in 1991, and then averaged around 70°C in 1992 and 55°C in 1993. Estimated maximum depth of the lake during the rainy season of 1991 was about three metres. This depth was attained again during the rainy season of 1992 and increased to an estimated six metres in 1993 (Smithsonian Institution, 1991, 1992, 1993).

3.3 Methods

3.3.1 Lake volume and depth

Volume and depth of Laguna Caliente were calculated from 30 sets of measurements of the dry lake basin geometry made with a precision theodolite and a distance-meter between August 1994 and September 1997 (Fig. 3.2B). Prior to August 1994, the depth and volume were estimated using field documentation. Changes in the diameter and volume of the lake were calculated using consecutive differences in water level (depth) and a geometric model of the lake that assumes an inverted, flat-bottomed cone [$V = \pi h (R^2 + r^2 + Rr)/3$ where R is the large radius, r the small radius, h the differential water level]. The error introduced by the difference between the geometric model and the curved shape of the actual lake bottom is estimated to be less than 5%.

3.3.2 Seismic data

Seismic data for the summit region of Poás Volcano were recorded from the POA2 seismographic station which is about 2.8 km southwest of Laguna Caliente at an elevation of 2500 m above sea level. The POA2 station is a telemetric station equipped with a Ranger SS-1 vertical, short-period seismometer (1 Hz). Seismic activity at Poás has traditionally been classified following the categories defined by Minakami (1969): (1) type A events are high-frequency events ($f > 3.0$

Hz); (2) type B earthquakes are low-frequency events ($f < 3.0$ Hz) and (3) periods of harmonic tremor ($f = 2.0$ – 3.0 Hz). The latter are reported as the number of hours of tremor recorded per month.

3.3.3 Sampling and analytical methods

Lake temperature was measured using a thermocouple. Water samples were collected at two sites (north and south) twice a month along the lake-shore using dark high-density polyethylene bottles that were stored at room temperature. Subsequent analysis of the sample collected from the north and south sides of the lake revealed pH, chloride and sulphate concentrations that were identical within analytical error indicating that the lake was well-mixed at the time of sampling because of thermal convection (Brantley *et al.*, 1987). Lake-water samples were not filtered or diluted in the field. Data reported for the period late April to mid-August 1994 are based on samples collected from small temporal pools that formed after heavy rains on the dry lake bottom. The chemistry of these pools has been shown to be highly variable (Rowe, 1994), however, data for samples collected from these pools are included here for completeness. Rainwater samples were collected at Cerro Pelón twice a month at a site approximately 2.4 km southwest (i.e. down-wind) of the active crater (Figs. 3.1 and 3.6). Rainwater samples were collected in high-density polyethylene bottles and were stored at 5°C to minimise the growth of bacteria or algae.

All the samples were analysed for pH, chloride and sulphate. Determinations of pH were done on unfiltered samples in the laboratory using a Corning potentiometer Model 10 with a relative precision of ± 0.1 pH units. To determine the chloride and sulphate, samples were filtered with 0.2 μm pore diameter polycarbonate filters and analysed by ion chromatography on a Shimadzu HIC6A ion chromatograph that had a Shimpak ICA1 anionic exchange resin column and a Shimadzu CDD6A conductivity detector. A 2.5 mM phthalic acid and 2.4 mM Tris-(hydroxi-methyl) amino-methane (pH 4.0) solution was used as mobile phase. The chromatograph operated at 40°C with a flow-rate of 2.0 mL/min, in a range of measure of 0.1 mS/cm. Concentrations of chloride and sulphate were calculated by peak heights calibrated against a set of known standards. Analytical errors of the ion chromatography analyses are estimated to be $\pm 5\%$ for sulphate and $\pm 10\%$ for chloride.

3.4 Results

From 1993 to 1997, annual rainfall in the vicinity of the crater ranged from 3.8 to 4.6 m per year, which is 9–33% above the long-term average of 3.5 m per year (Fig. 3.2A). The only exception was during 1994 when total annual rainfall in the summit area was just below the long-term average (~ 3.4 m).

Volume of Laguna Caliente varied from an estimated 3.7×10^3 to $1.7 \times 10^6 \text{ m}^3$ between 1993 and 1997 (Fig. 3.2A). The volume decreased abruptly during the dry seasons of 1993 and 1994 but no significant volume changes were observed during the dry seasons of 1995–1997. The mild increase in the slope of the volume curve recorded from June 1995 to August 1996 (Smithsonian Institution, 1996a) is associated with a period of above-average rainfall at that time (Fig. 3.2A,B). The

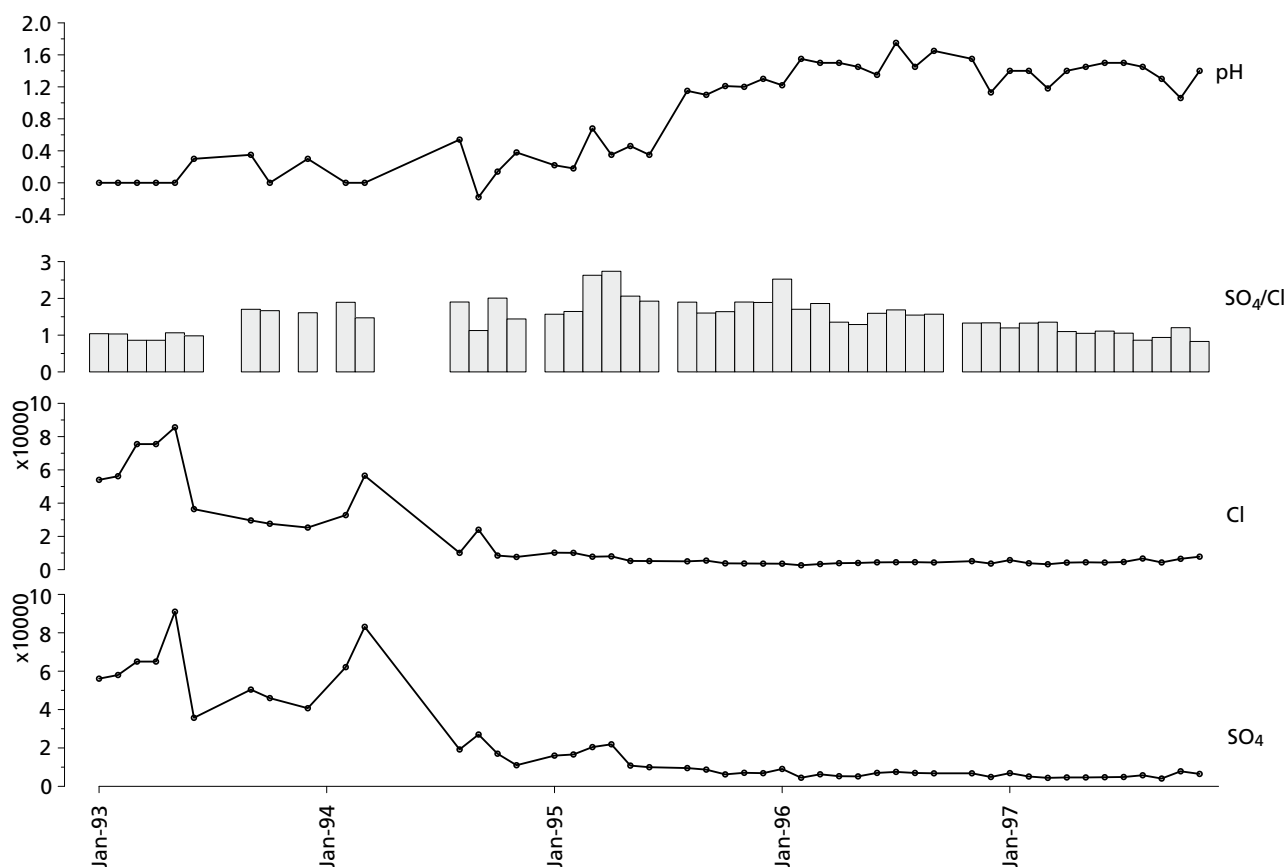


Figure 3.3. Variation of chemical parameters in water from Laguna Caliente (1993-1997) including: Lake pH; SO_4/Cl ratios; chloride and sulphate concentrations.

temperature of the crater lake ranged from 25 to 70°C between 1993 and 1997 (Fig. 3.2C).

From January 1993 to January 1996, type B seismicity was extremely high in comparison with the seismicity recorded from February 1996 to December 1997. Monthly totals of type B earthquakes ranged from 1100 to 9839 during this period. An increase in the number of type B earthquakes in March-April 1994 is related to an increase in the lake-water temperature (Fig. 3.2 C,F), with increases in the concentration of sulphate and chloride in lake water (Fig. 3.3B,C,D), and with the return of harmonic tremor and type A seismic events (Fig. 3.2D,E). Note that neither harmonic tremor nor A-type seismic events were observed at this time in 1993.

A minimum in the total number of B type earthquakes occurred in September 1994 after the enhanced period of volcanic activity and the lake began to reform (Fig. 3.2 B,F). Increases in monthly total type B events (5960-9149) and harmonic tremor hours (12-370 hours) occurred between September and December 1995. An increase in the number of type A earthquakes was also observed in November 1995 (44 events, Fig. 3.2 E). However, sulphate and chloride concentration and lake-water temperature did not change in response to the increased seismicity recorded over this time period. Similarly, increases in the frequency of type B events were noted in October-November 1993 (6360 events), and in March-April 1995 (6995 events) without any obvious changes in lake temperature, lake volume, or concentrations of chloride or sulphate.

During October-November 1993, type A and tremor earthquakes were absent, whereas in March-April 1995 only minor amounts of harmonic tremor were recorded (Fig. 3.2D,E). A dramatic decrease in the total number of type B earthquakes (range 511-2192) occurred in February 1996 (Fig. 3.2F) and continued through December 1997. This change coincided with the apparent migration of the locus of fumarolic activity from beneath the lake to the adjacent CPC (Fig. 3.1).

Plume height estimates come from field observations that were calibrated with geodetic equipment. The highest plumes were observed during the period of enhanced volcanic activity from April to September 1994. Plume heights increased steadily from 80 m to 1500 m suggesting increases in the amount of energy and gas being released by the volcano (Fig. 3.5a). On 25 and 30 April 1994, two phreatic eruptions vented grey to clear coloured ash containing old lake-floor sediments that reached 1.6 km south and southwest of the lake. On 2 June, a phreatic eruption column 1.2 km in elevation, vented dry steam and non-juvenile ash up to 1.6 km downwind from the lake. Thirteen moderate size phreatic eruptions occurred between 24-31 July and 4 August 1994. The largest eruption occurred on 31 July and non-juvenile ash was distributed up to 12 km southwest of the summit. Significant increases in the number of type A and B events were recorded prior to and during these eruptions. After the lake reformed in September 1994, the height of the steam plume was greatly reduced (e.g. 80 m, Fig. 3.5a). Similar periods of elevated plume height were observed during the dry

season of 1993 (plume heights upwards of 500 m) and from February 1996 to December 1997, when the locus of most fumarolic activity continued to shift from Laguna Caliente to the CPC south of the lake. During 1997 only small changes in plume height were recorded.

3.4.1 Trends in the chemistry of Laguna Caliente with volcanic activity

Concentrations of chloride and sulphate in Laguna Caliente ranged between 2630 and 85600 mg/L and between 4640 and 91000 mg/L, respectively for the period of 1993-1997. Lake-water pH ranged from near zero to 1.85 (Table 1, Fig. 3.3b-d). Sulphate and chloride concentrations were higher,

and lake-water pH values lower in 1993-1994, relative to the period 1995-1997 (Martínez *et al.*, 1997). Maximum sulphate and chloride concentrations were recorded near the end of the 1993 dry season. After the dry season of 1994, concentrations of chloride and sulphate declined in a more or less steady manner until mid-1997 when slight increases took place (Fig. 3.3b,c).

During the dry season of 1993, the lake ranged from small pools to a lake with a volume of nearly $4.7 \times 10^4 \text{ m}^3$ (Fig. 3.2B). Later that year, during the rainy season (May-December 1993), a minor increase in the lake-water pH was observed (~ 0.3) possibly caused by dilution associated with refilling of the lake by rainwater (Figs. 3.2a,b, 3.3d). From April 1993 to March 1994, the sulphate/chloride concentration ratio of the lake

Table 3.1. Analytical results and physical parameters of Laguna Caliente. Volcán Poás

Date of sampling	Temperature (°C)	pH (23±2°C)	Cl (mg/L)	SO ₄ (mg/L)	Lake volume (m ³)	Lake depth (m)
09-Jan-93	65	0 ^a	49100	54000	4.7×10^4	2.5
06-Feb-93	70	0 ^a	56100	58000	2.8×10^4	1.5
20-Feb-93	60	0 ^a	75900	84000	-	-
04-Mar-93	60	0 ^a	75500	65000	1.9×10^4	1
14-Apr-93	60	0 ^a	61200	55000	1.9×10^4	1
16-Apr-93	60	0 ^a	24500	47000	-	-
14-May-93	63	0 ^a	85600	91000	7.5×10^3	0.4
11-Jun-93	65	0.30	36400	35700	1.9×10^4	1
09-Sep-93	64	0.35	29600	50400	6.5×10^4	3.5
22-Oct-93	60	0.30	27600	45900	7.1×10^4	3.8
10-Dec-93	60	0.30	25300	40700	7.5×10^4	4
04-Feb-94	60	0 ^a	32800	62100	7.7×10^4	4.1
12-Mar-94	55	0 ^a	56500	83100	2.8×10^4	1.5
11-May-94	65	0 ^a	12700	19000	9.0×10^3	0.5
19-May-94	65	0 ^a	17700	17500	-	-
04-Jun-94	70	1.00	25500	19400	7.5×10^3	0.4
10-Jun-94	65	0.80	24000	9630	-	-
08-Jul-94	65	0.70	16500	24900	3.7×10^3	0.2
30-Aug-94	60	0.54	10100	19200	2.8×10^4	1.5
09-Sep-94	65	0.60	15600	15300	9.3×10^4	5
23-Sep-94	65	0.30	24000	27000	-	-
21-Oct-94	60	0.14	8470	17000	-	-
15-Nov-94	55	0.38	7640	11000	2.8×10^5	12.1
06-Jan-95	50	0.22	10200	16000	-	-
03-Feb-95	47	0.18	10100	16600	4.0×10^5	16.3
10-Mar-95	42	0.20	7780	20400	-	-
28-Apr-95	41	0.35	8000	21900	-	-
19-May-95	43	0.46	5240	10800	4.2×10^5	16.9
02-Jun-95	39	0.35	5180	9970	4.3×10^5	17.3
30-Jun-95	39	1.30	4740	9510	-	-
26-Aug-95	36	1.15	5010	9510	-	-
22-Sep-95	34	1.15	4390	8870	-	-
20-Oct-95	30	1.25	3800	6220	7.4×10^5	25.5
17-Nov-95	26	1.20	3710	7050	-	-
15-Dec-95	30	1.30	3632	6860	7.9×10^5	26.5
05-Jan-96	30	1.35	3590	9060	-	-
26-Jan-96	30	1.45	3370	7310	-	-
30-Jan-96	26	1.45	3370	6680	-	-
23-Feb-96	27	1.55	2630	4480	-	-
22-Mar-96	30	1.50	3370	6270	9.9×10^5	30.6
12-Apr-96	34	1.85	4230	5970	-	-
26-Apr-96	36	1.50	3910	5290	-	-
10-May-96	36	1.45	4010	5180	-	-
18-May-96	39	1.45	4280	5410	-	-
31-May-96	42	1.30	4330	5060	-	-

Date of sampling	Temperature (°C)	pH (23±2°C)	Cl (mg/L)	SO ₄ (mg/L)	Lake volume (m ³)	Lake depth (m)
14-Jun-96	45	1.35	4390	7000	-	-
24-Jul-96	36	1.80	4460	7520	-	-
08-Aug-96	34	1.45	4510	6970	1.4x10 ⁶	38.5
30-Aug-96	36	1.50	4370	7020	-	-
27-Sep-96	40	1.65	4320	6780	1.5x10 ⁶	38.7
05-Nov-96	35	1.50	5350	7170	-	-
28-Nov-96	31	1.55	5110	6790	-	-
18-Dec-96	29	1.50	3650	4870	1.5x10 ⁶	39.3
07-Jan-97	32	1.40	5750	6880	1.5x10 ⁶	40.4
04-Feb-97	31	1.40	3850	5110	-	-
03-Mar-97	29	1.55	3260	4410	1.5x10 ⁶	40.5
04-Apr-97	29	1.40	4330	4870	-	-
17-Apr-97	28	1.30	4230	4640	-	-
21-Apr-97	25	1.30	4570	4990	-	-
14-May-97	29	1.45	4420	4640	-	-
04-Jun-97	35	1.50	4280	4750	1.6x10 ⁶	41.3
02-Jul-97	32	1.50	4620	4870	-	-
28-Jul-97	31	1.60	4735	5120	-	-
05-Sep-97	33	1.03	5290	4640	1.7x10 ⁶	42.6
05-Sep-97	33	1.35	4330	4060	-	-
19-Sep-97	35	1.45	5750	5320	-	-
03-Oct-97	35	1.41	7580	6340	-	-
17-Oct-97	35	1.30	5980	6220	-	-
17-Oct-97	35	1.30	6520	7840	-	-
04-Nov-97	34	1.40	7800	6460	-	-
25-Nov-97	35	1.25	7660	6850	-	-
28-Nov-97	35	1.35	6900	6400	-	-

a: the analogue pH-meter indicated pH zero (it means that the pH was below or near zero).

water increased, possibly in response to a decrease in lake water chloride due to volatilisation of HCl (Rowe *et al.*, 1992a).

A sharp increase in acidity, sulphate, and chloride is noted in February-March 1994, prior to the disappearance of the lake and before the onset of the period of enhanced volcanic activity (Figs. 3.3b-d). Despite this, no significant changes in lake temperature (which remained near 60°C) were observed at this time. In April 1994, the lake volume was reduced to scattered small mud pools of highly variable temperature and composition (Smithsonian Institution, 1994a). From March to July 1994, an increase in type B seismicity was recorded at POA2 station suggesting an increased level of volcanic activity beneath the crater lake. Type A seismicity and the number of harmonic tremor hours also increased, but only after the lake had disappeared in April 1994. The numerous low-frequency events are believed to reflect shallow seismic signatures of degassing from the magma, whereas the origin of the tremors may relate to magma movement (McNutt and Harlow, 1983; Ferruci, 1995). Elevated seismic activity, low pH, and high concentrations of chloride and sulphate strongly suggest vigorous degassing of subaqueous fumaroles into the lake at this time. The cause of the intense fumarolic discharge and associated increase in seismic activity beneath the active crater could be either a hydrofracturing event or the ascent of a small volume of fresh magma. Support for the above hypotheses is provided by remote temperature measurements of the most intense fumarole vents exposed after the lake dried up completely in April 1994. Fumaroles on the dry lake bottom registered 515°C with an optical pyrometer on 21 July 1994 when plume heights were 1500 m (Fig. 3.5a).

Lake temperature, acidity, sulphate, and chloride concentrations continued to decrease steadily with some minor fluctuations through mid-1995 after the lake reformed and eruptive activity waned in August-September 1994. By mid-1995, declines in the concentration of chloride had levelled out whereas sulphate concentrations continued to decline steadily through early 1996 (Fig. 3.3b,c). Although some variation in the sulphate/chloride concentration ratio is observed after the lake reforms in September 1994, the rather narrow range of sulphate/chloride values suggests that

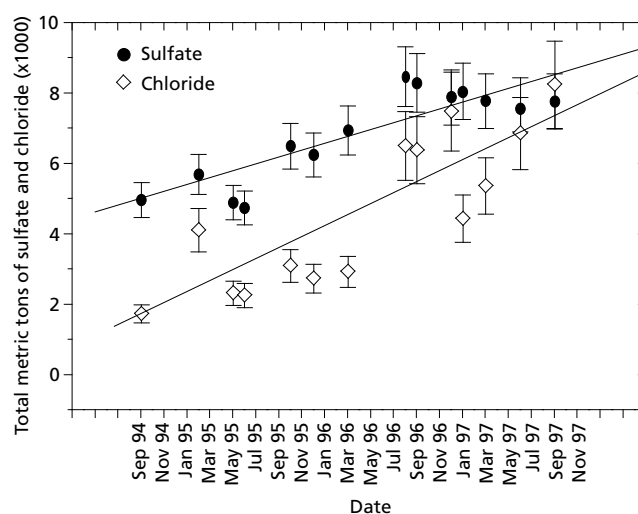


Figure 3.4. Temporal variation of the total mass of chloride and sulphate as a function of the crater lake volume (1994-1997).

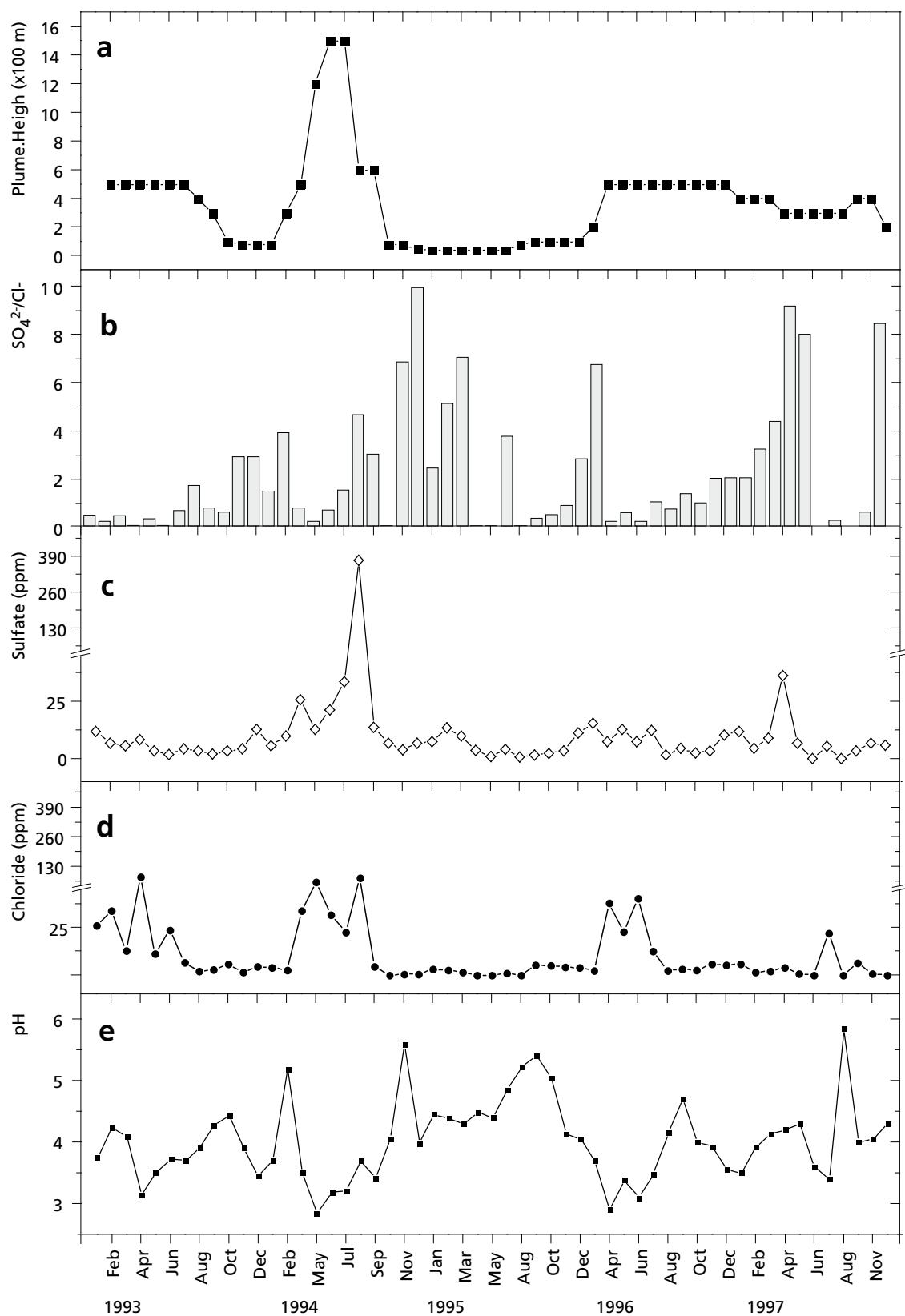


Figure 3.5. Monthly variation of rainwater chemical parameters from Cerro Pelón (2.4 km southwest of Laguna Caliente) and maximum plume heights from Poás volcano fumarolic plumes, between 1993-1997 including: (a) maximum measured plume heights; (b) SO_4/Cl ratios; (c) sulphate concentration; (d) chloride concentration; and (e) pH.

the observed declines in sulphate and chloride largely reflect a dilution trend caused by the addition of meteoric water that refilled the lake (Figs. 3.3a-c, 3.2b).

From October 1995 to January 1996, a new increase in type A, type B and tremor seismicity was recorded at Poás volcano. The number of type A events and the amount of harmonic tremor hours were slightly higher than those recorded during period of enhanced activity in mid-1994 (Fig. 3.2 D,E). Despite this period of enhanced seismicity, lake temperature declined further reaching the minimum recorded value for the period 1993-1997 (25°C) and lake volume continued to increase (Fig. 3.2 B,C). Elevated levels of seismic activity suggest changes in the subsurface hydrothermal-magmatic system that were not reflected by changes in the crater lake. Instead, field observations made during December 1995 indicate an increase in the size and relative intensity of fumarolic discharge from the CPC including renewed deposition of native sulphur at several of the newly formed fumaroles. Although not as impressive as the increase in fumarolic activity recorded after the intense seismic swarm of July 1980, these observations suggest a similar migration of fumarolic activity from beneath the crater lake back to the CPC. The migration of most fumaroles to the CPC near the end of 1995 coincides well with a gradual reduction

in lake acidity and the steady increase in lake volume that was recorded in 1996 (Smithsonian Institution, 1996b).

From March 1996 to December 1997, there were several months where more than 10 type A seismic events were recorded. Periods in which notable increases in the number of type A events were recorded include August-September 1996 and January-February 1997 when more than 50 events were recorded each month. However, periods of harmonic tremor were less common, with minor periods of harmonic tremor recorded over the period February-June 1996, October 1996, and following a year of no harmonic tremor, again in November-December 1997 (Fig. 3.2D). The peaks of type A seismicity and periods of harmonic tremor are not related to any significant changes in lake temperature or chemistry, but instead appear to coincide with new fumarole opening events within the main crater of Poás or with areal expansion of the pre-existent fumaroles (Fig. 3.1).

Finally, despite the overall dilutional trend that accompanied the refilling of the lake, estimates of the total mass of chloride and sulphate in the crater lake show overall increases in the amount of chloride and sulphate stored in the lake between 1994 and 1997. This indicates that subaqueous fumaroles continued to discharge magmatic gas-bearing steam into the crater lake. The trend for sulphate in the lake shows a general

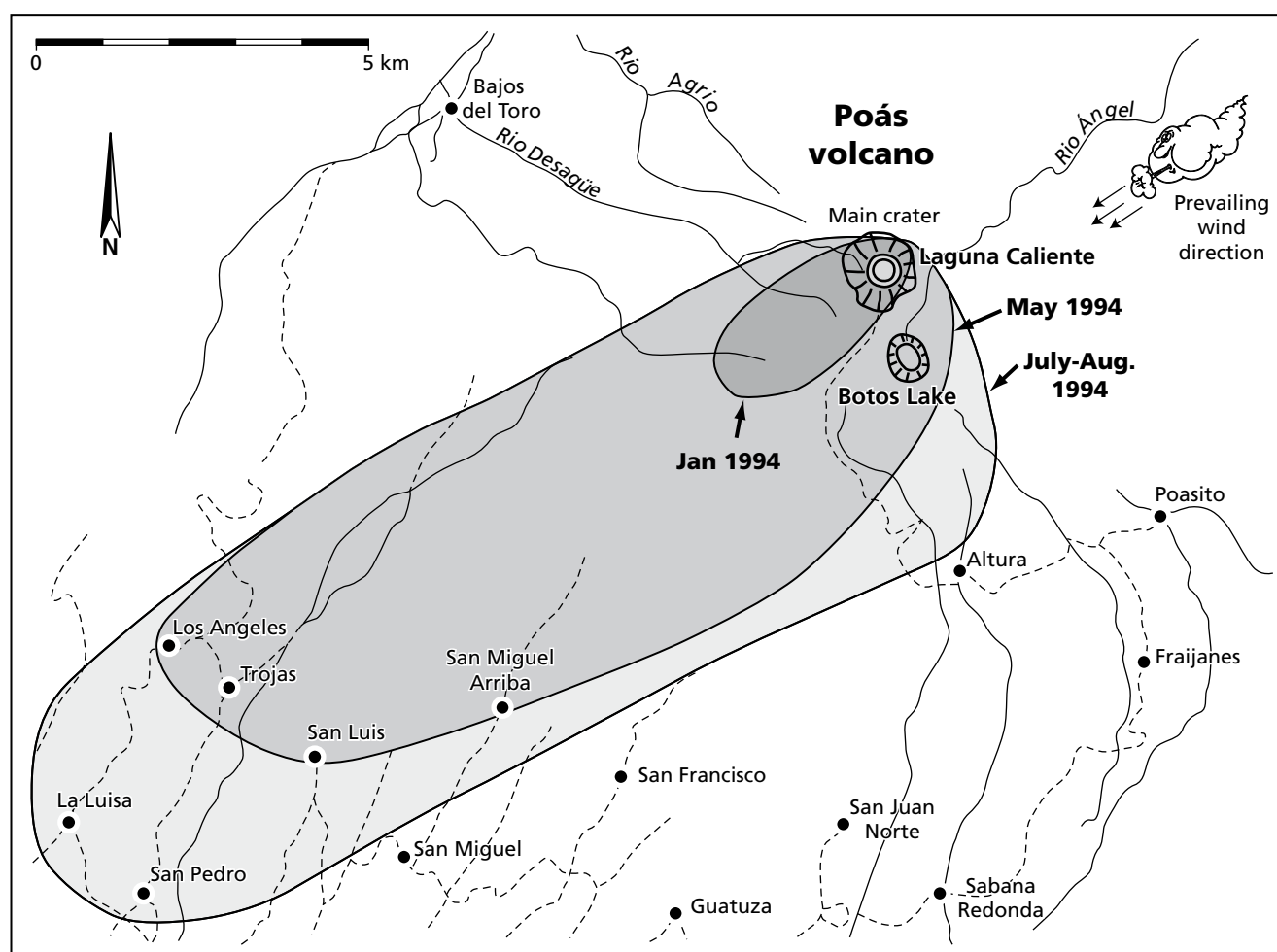


Figure 3.6. Map of Poás volcano showing areas affected by the volcanic emissions at three different dates: January 1994, May 1994 and July-August 1994, i.e. before and during the phreatic eruptions occurred between April and early-August 1994. The prevailing wind direction is shown on the figure (from northeast to southwest).

increase through mid-1996 and then it levels off and remains nearly constant through November 1997 (Fig. 3.4).

3.4.2 Trends in the chemistry of rain water with volcanic activity

The distribution of acid rain is largely controlled by the interaction of prevailing winds, that blow southwest across the summit area, with the morphology of the area near and downwind of the active crater. The chemistry of rainwater samples collected at the Cerro Pelón site, 2.4 km downwind of the active crater, is quite variable (Fig. 3.5). Composite monthly samples of both wet and dry acid deposition collected between 1993 and 1997 had pH values between 2.9 and 5.8. Sulphate and chloride concentrations in the rainwater samples range from 0.8 to 376 mg/kg sulphate and 0.6 to 85 mg/kg chloride. These values are similar to those reported by Rowe *et al.* (1995) for acid rain samples collected during the period 1988–1990 at various locations on the southwest flank of Poás (1.7–46 ppm sulphate; 3.1–49 ppm chloride).

Higher chloride concentrations were recorded in January–June 1993 (85 mg/kg), in March–August 1994 (81 mg/kg) and in April–July 1996 (41 mg/kg). The first two periods of high chloride concentration in acid rain occur within the dry season (Fig. 3.2A, Fig. 3.5d) and correlate with periods of low lake volume and elevated lake temperature, whereas the second and third periods are correlated with periods of enhanced type A and harmonic tremor activity. The latter period in April–July 1996 also was correlated with a short-lived six-degree increase in lake temperature (Fig. 3.2C). High chloride concentrations in acid rain waters may reflect enhanced volatilisation of HCl from the crater-lake surface caused by increases in lake temperature and acidity. Such episodes should be reflected by declines in the sulphate/chloride ratios of acid-rain samples (Fig. 3.5b) as observed prior to the first disappearance of the lake in early 1989 (Rowe *et al.*, 1992a). Higher sulphate concentrations in acid rain were recorded twice during the period under consideration (March–September 1994 and April 1997). Elevated sulphate concentrations appear to be related to an increase in the release of sulphate-rich particles during steam eruptions or by the release of hydrogen sulphide gas from new, low-temperature fumaroles that reappeared on the CPC in late 1995.

The area affected by volcanic emissions had elliptical shape with its major axis oriented to the southwest of the summit area (Fig. 3.6). In January 1994, the approximate area affected was a 3-km ellipse with a total area approaching 4 km². In May 1994, the area affected had increased to ca. 50 km² (ellipse axis: 12 km) and by July–August 1994, the area reached an estimated maximum of 74 km² (ellipse axis: 15 km, Fig. 3.6). On basis of the estimates made by the Costa Rican Agricultural Extension Agency, losses to crops caused by the period of enhanced acid deposition in 1994 approached 1.5 million dollars (N. Kopper, Costa Rican Agricultural Extension Agency, pers. comm., 1995). About two thirds of the economic loss came from lower productivity in coffee plantations. Other areas affected by the acid emissions included timber, crops, machinery, grazing land, native vegetation (Sandoval, 1996), livestock, housing, and human and animal health (Baxter *et al.*, 1997). Health complaints included nausea, coughing, and irritated throat, eyes and skin (Smithsonian Institution, 1994a,b).

3.5 Conclusions

The classification scheme for volcanic lakes proposed by Pasternack and Varekamp (1997) divides volcanic lakes in five categories based on physical and chemical properties of the lake. During the period 1993–1997, three of their categories can be used to describe the evolution of Laguna Caliente. Using the sum of chloride and sulphate as a proxy for TDS, the general physico-chemical evolution of Poás crater lake can be described as follows: (1) a period of peak activity from January 1993 to approximately February 1995 when lake pH was consistently near zero, lake temperature usually exceeded 45°C, and the combined concentration of chloride and sulphate ranged from 17.7% to 1.8%; (2) a short transitional period from March 1995 to September 1995 corresponding to the high activity period when the lake typically had pH values between 0.3 and 1.0, temperatures between 35 and 45°C, and chloride plus sulphate concentrations of 1.3–2.8%; and (3) a period of medium activity from October 1995 to December 1997 during which lake pH was between 1.0 and 2.0, lake temperature was generally less than 35°C and the combined concentration of chloride and sulphate was generally less than 1% (10000 mg/L).

The geochemical properties of Laguna Caliente, as well as variations in its temperature, volume and depth, reflect both climatic effects and interactions with a shallow subsurface magma body and associated magmatic-hydrothermal system. Therefore, changes in parameters normally associated with volcanic activity such as increased seismicity, plume height or fumarole temperature will tend to be related to changes in crater-lake chemistry, particularly for species derived from magmatic gases (e.g. acidity, chloride and sulphate). The relation between these parameters will be more evident when fumarolic discharge from the underlying magmatic-hydrothermal system is focused beneath the lake, as was the case between 1993 and January 1996.

During April–August 1994, plume heights (1500 m) and fumarole temperatures (515°C) recorded on the lake bottom increased dramatically suggesting a large increase in the flux of heat from the shallow magma body. Between September 1995 and January 1996 renewed magmatic-hydrothermal activity opened a new path for the ascending gases to the surface as the fumaroles beneath the lake became gradually sealed after September 1994. As a result, fumarolic activity appeared to migrate from beneath the crater lake to the CPC on the southern rim of the crater lake.

After the fumarolic activity migrated to the CPC, intensive fumarolic outgassing started to interact directly with the atmosphere decreasing the direct contribution of chemical species to the crater lake. Under the new conditions, the concentration of anions in the lake and its physical parameters (i.e. temperature) did not respond directly to changes in seismic activity. Type B events which are normally considered indicators of hydrothermal activity decreased dramatically suggesting smaller interaction of ascending gases with the volcano's hydrothermal system.

In general terms, the physico-chemical properties of Laguna Caliente evolved from those characteristic of a hot acidic hyperbrine to those of an acid-saline brine between 1993–1997. The hot acid hyperbrine corresponds to the period in which the

focus of subsurface magmatic-hydrothermal activity was beneath the crater lake whereas the acid-saline brine corresponds to the period in which the activity migrated back to the CPC (i.e. after January 1996). Migration of activity from one vent to the other has been a common feature at Poás and the return of the crater lake to a more quiescent state may mark the end of the period of lake instability that began in mid-1986 (Brown *et al.*, 1991; Rowe *et al.*, 1992a,b).

Decreases in the sulphate/chloride ratio of acid rain were caused by volatilisation of chloride from the lake as temperature, acidity and anions concentration increased as the volcano activity increased. However, the ratio observed in acid deposition samples is affected by the efficiency of HCl absorption by rainwater and also by the form in which sulphur species are emitted by the volcano. The observations presented here suggest that the crater lake has a significant role in determining the type and intensity of acid deposition, with periods of enhanced acid deposition and increased economic damage occurring when the lake declines or disappears.

Acknowledgements

Constructive reviews, helpful suggestions and discussion of this manuscript by Gary L. Rowe Jr. (U.S. Geological Survey), Johan C. Varekamp (Wesleyan University, USA), Peter Neeb (Max Planck Institut, Germany), Wendy Harrison (Colorado School of Mines, USA), and Marino Protti (OVSICORI-UNA, Costa Rica) are gratefully acknowledged. Support was provided by the DAAD (Deutscher Akademischer Austauschdienst, German Service of Academic Exchange), CEPREDENAC (Centro de Coordinación para la Prevención de los Desastres Naturales en América Central), Fondo de Incentivos para la Investigación del Ministerio de Ciencia y Tecnología-Consejo Nacional de Investigaciones Científicas y Tecnológicas de Costa Rica-MICIT-CONICIT, and the Tectonics Organized Research Unit at UCSC (University of California in Santa Cruz, California, USA).

A long-term record of polythionates in the acid crater lake of Poás volcano: Insights into the subaqueous input of fumarolic gases

4.1 Introduction

A variety of chemical constituents of volcanic crater lakes and associated fluids is classically employed to monitor volcanic activity, to assess the flow rate and nature of volcanic gases expelled from cooling magma, and to study water-rock interaction in shallow magmatic-hydrothermal systems (e.g. Giggenbach, 1974; Sigurdsson, 1977; Casadevall *et al.*, 1984b; Rowe *et al.*, 1992a,b; Christenson and Wood, 1993; Takano *et al.*, 1994b; Delmelle and Bernard, 1994; Delmelle, 1995; Pasternack and Varekamp, 1994, 1997; Armienta *et al.*, 2000; Christenson, 2000; Delmelle and Bernard, 2000; Delmelle *et al.*, 2000; Giolito, 2000; Martínez *et al.*, 2000; Sriwana *et al.*, 2000; Varekamp *et al.*, 2001; Tassi *et al.*, 2003; Bernard *et al.*, 2004; Takano *et al.*, 2004).

Among the more exotic geochemical parameters with monitoring potential are the natural polymeric sulphur compounds known as polythionates, which have the general formula $(\text{O}_3\text{SS}_n\text{SO}_3)^{2-}$, where $3 \leq n \leq 20$ (Shriver and Atkins, 1999; Steudel and Holdt, 1986). They are named according to the total number of sulphur atoms: trithionate ($\text{S}_3\text{O}_6^{2-}$), tetrathionate ($\text{S}_4\text{O}_6^{2-}$), pentathionate ($\text{S}_5\text{O}_6^{2-}$), etc. Polythionates were found in waters of volcanic origin for the first time in New Zealand. Mac Laurin (1911) detected pentathionate in the crater lake of White Island Volcano, while Day and Wilson (1937) and Wilson (1941, 1953, 1959) reported the presence of various polythionates in waters from the Black Pool near Rotorua and the Black Geysir at Ketetahi thermal springs.

Polythionates can be present among the anions in acid volcanic lakes in concentrations ranging from minor or trace amounts to several hundreds or thousands of ppm. They are transient sulphur compounds formed in acid aqueous environments by reaction between SO_2 and H_2S gases (Takano and Watanuki, 1990; Takano *et al.*, 1994b). They have been detected in acid volcanic lakes (pH<3) such as the Yugama Lake at Kusatsu-Shirane in Japan (Takano, 1987; Takano and Watanuki, 1990); Ruapehu in New Zealand (Takano *et al.*, 1994b); Poás (Rowe *et al.*, 1992b; Martínez *et al.*, 2004b) and Rincón de la Vieja in Costa Rica (OVSICORI, unpublished data); Patuha in West Java (Sriwana *et al.*, 2000); Kawah Ijen in East Java (Delmelle and Bernard, 1994; Takano *et al.*, 2004); Santa Ana in El Salvador (Bernard *et al.*, 2004); Copahue in Argentina (Varekamp, J., pers. comm.

2007) and Maly Semiachik in Russia (Takano *et al.*, 1995). Tetra-, penta-, and hexathionate have been also detected in acid condensates collected from the fumaroles that were active at the eastern terrace of the active crater of Poás volcano and fumaroles sampled in 2002 and 2007 at the Central and West craters of Turrialba volcano (OVSICORI, unpublished).

Despite these reports of polythionate presence in a number of crater lakes, their long-term behaviour has been studied only in a few cases so far: Yugama Lake at Kusatsu-Shirane (Takano, 1987; Takano and Watanuki, 1990), Crater Lake at Ruapehu (Takano *et al.*, 1994b) and Laguna Caliente at Poás (Rowe *et al.*, 1992b).

Rowe *et al.* (1992b) reported the first polythionate data for Poás, covering the period 1984–early 1990 when the lake evolved from relative quiescence to an interval of high activity (for a summary of the historic activity of Poás, see Chapter 2). The authors noticed a sharp decrease in polythionate concentrations three months prior to the recurrence of phreatic eruptions in 1987 (which would persist in the following years), and suggested that rapidly changing polythionate levels could be a precursor signal of changes in the magmatic-hydrothermal system that affect subaqueous fumarolic input and trigger phreatic activity. Since then, several other periods of phreatic eruptions have occurred (the latest in 2005–2008), and frequent, sometimes drastic fluctuations in the physico-chemical properties of the crater lake have been registered (Mastin and Witter, 2000; Martínez *et al.*, 2000; Venzke *et al.*, 2002–; OVSICORI open reports). This unstable behaviour of the volcano provides a unique opportunity to evaluate the response of polythionates to marked changes in the input of magmatic volatiles and heat, and to test their value in predicting upcoming phreatic events. This chapter presents new polythionate results, which together with the previous data of Rowe *et al.*, (1992b) constitute a monitoring record of about 25 years. It will be shown that the polythionate budget in Laguna Caliente is characterized by a remarkable variability, which is directly linked to changes in the flow rate, composition and location of fumarolic emissions in the crater area. In combination with regularly monitored geochemical signatures, geophysical parameters and field observations, the findings provide new insights into the conditions of the subsurface magmatic-hydrothermal system, and in the way they control eruptive events.

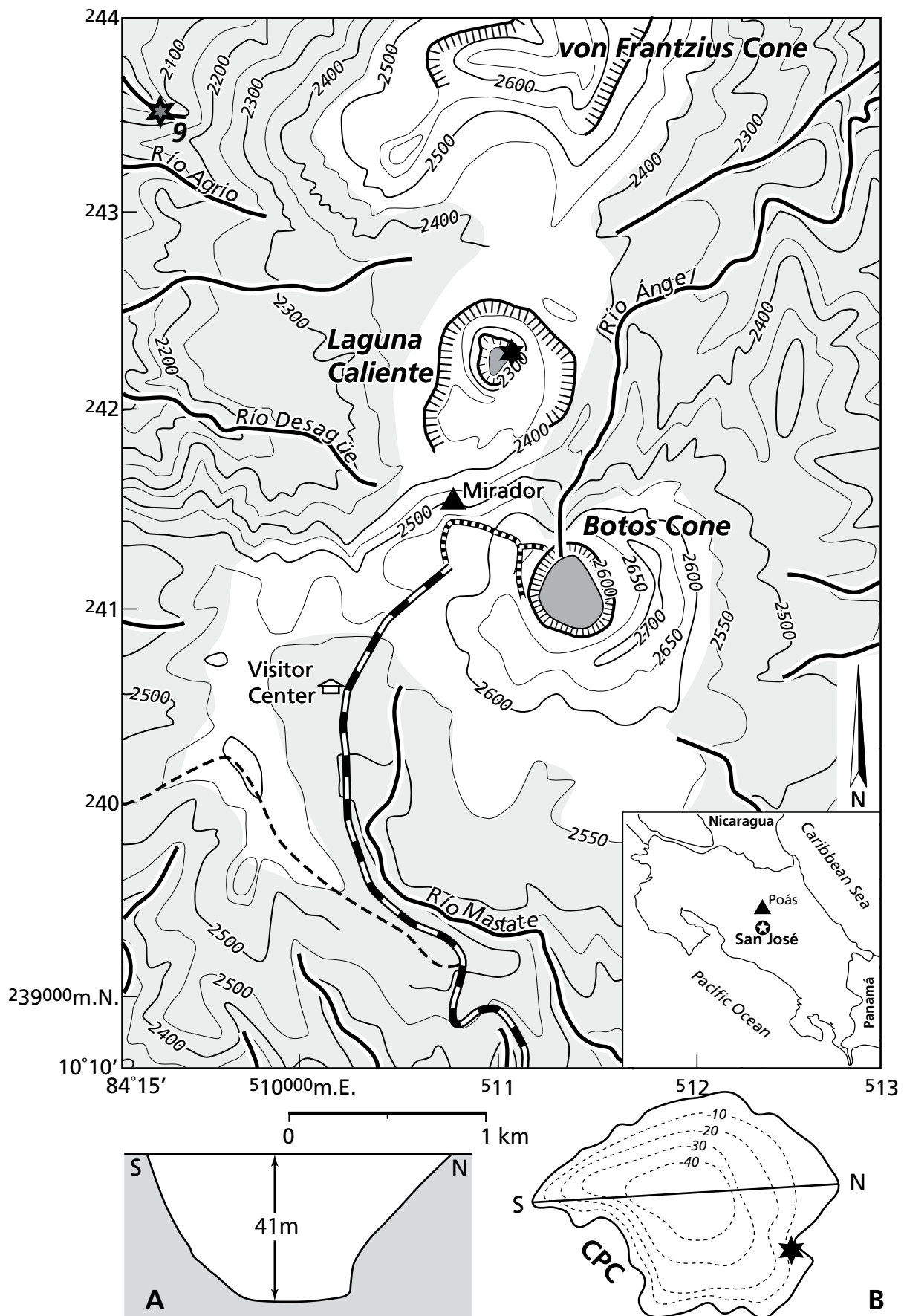


Figure 4.1. Overview of the summit area of Poás and sampling sites. Cross section (A) and bathymetric contours (B) are from a survey carried out in early 2001 (adapted from Tassi *et al.*, 2003; Duarte *et al.*, 2003c). Black star in diagram B is the location where lake waters were regularly collected. Black-grey star labelled '9' in the upper left of the map is the sampling site of the Agrio hot spring #9.

4.2 Sampling strategy and analytical procedures

4.2.1 Sampling

Samples selected for polythionate analysis were routinely collected by OVSICORI-UNA at a location on the NE side of the acidic crater lake (Fig. 4.1). Temperatures were measured at the sampling sites using thermocouple. Most of the samples were stored in dark high-density polyethylene bottles at room temperature without filtration, dilution or addition of preservatives before the polythionate analyses were conducted. From June 1990 till 1995 the average sampling intervals were 3–4 months because of the high activity of the volcano. From 1996 till November 2006, the data represent a monthly sampling frequency. A single sample from 1980 was analysed to provide the earliest polythionate signal. Previously published polythionate data (Rowe *et al.*, 1992b) cover the period from November 1984 until March 1990 and represent an approximate sampling frequency of once every two months. Collectively, the currently available polythionate record thus covers the period 1980–2006. Some samples collected in 1988–1994 that contain grey muddy material were presumably from mud pools, which formed during episodes when the lake volume was strongly reduced. As these pools had a highly variable chemistry and were largely mixtures between meteoric water and low-temperature fumarolic steam (Rowe, 1994) their results are not considered to be representative for the long-term evolution of the lake system and are not further considered here.

4.2.2 Physico-chemical data

4.2.2.1 Polythionate analysis

About 190 lake water samples were analysed for tetra-, penta-, and hexathionate ions at the Department of Chemistry of Tokyo University and at the Laboratory of Atmospheric Chemistry (LAQAT) of the Universidad Nacional in Costa Rica using similar ion-pair chromatographic techniques. This method is convenient because no sample preparation other than filtration and dilution is required.

Samples collected in October 1980, June 1990–November 1992, September 1993, September and November 1994, January and February 1995, April 1999–September 2002 were analysed at LAQAT in August–October 2002. Samples from (a) January–April and October 1993, (b) March and October 1994 and March 1995–March 1999, (c) December 2002–June 2005, and (d) July 2005–November 2006 were analysed at Tokyo University in November 1996, February 1999, February–August 2005 and April 2007, respectively. Although some samples were analysed within a few weeks after collection, the majority was stored for several years at room temperature without preservation measures.

At Tokyo University tetra-, penta-, and hexathionate ions were determined following a high-performance microbore ion-pair chromatographic separation technique with ultraviolet absorption detection, and an ion-pair chromatographic separation technique with conductivity detection (Takano, 1987; Takano and Watanuki, 1988, 1990; Table APP-4.1.1, Appendix 4.1). The first technique allows the determination of tetra-, penta-, and hexathionate in excess of 0.2 ppm, and the second that of tetra-, and pentathionate in excess of 10

ppm. Standard solutions for penta- and hexathionate were prepared from synthesized salts (Takano and Watanuki, 1988) following Goehring and Feldmann (1948). A commercially available potassium tetrathionate salt was recrystallised for the preparation of tetrathionate standard solutions.

At LAQAT separation and quantification of main polythionate species were performed using an ion-pair chromatographic technique with UV absorption detection following Miura and Kawaoi (2000) with minor modifications (Table APP-4.1.1, Appendix 4.1). A Shimadzu Model LC-10AS chromatographic system, equipped with a LC-10AS liquid delivery isocratic pump set at a flow rate of 0.6 mL/min, an automatic SIL-10A auto-injector with a 100 µl sampling loop, a SPD-10AV UV-VIS spectrophotometric detector set at 230 nm, and a SCL-10A System controller were employed. Chromatographic signals were obtained with the following settings: an Alltech/Allsphere ODS-2 analytical column 5 µm particle size (150 x 4.6 mm i.d.) coupled to a Brownlee guard column (50x3 mm i.d.); an acetonitrile–water (20:80 v/v) mobile phase [6 mM in tetrapropylammonium hydroxide, TPA, and buffered at a pH=5.0 by dropwise addition of glacial acetic acid 100%], filtered through a 0.45 µm membrane filter and degassed by vacuum. All of the reagents used for the mobile phase were analytical-grade; the acetonitrile was 99.93% HPLC grade, the TPA ion pair reagent used was an aqueous solution 20% (~1M). Mobile phase, samples and standard solutions were diluted with distilled and deionised water. Samples were filtered and diluted immediately before injection into the chromatographic system. Chromatographic separations were carried out at room temperature (23±2°C). Chromatograms were displayed on a pen-recorder, and peak heights were measured by hand.

A potassium tetrathionate calibration solution was injected several times during a 6 hours sequence to monitor the response, the reproducibility of peak heights and retention times. Precision of retention times for standards and unknowns was ±0.9% within one day (n=12) and ±1% within one week (n=10) for the ion-pair UV chromatographic technique. This enabled unequivocal identification of the polythionates by retention time only. Repeated analysis (n=6) of the 21 June 2002 sample to determine the reproducibility of the procedure yielded a mean value of 190 mg/kg for tetrathionate, with a relative standard deviation (RSD) of 5%, 57 mg/kg for pentathionate (RSD=4%), and 25 mg/kg for hexathionate (RSD=4%). Reproducibility for the entire set of samples, analysed in Costa Rica within a three-month period, was tested on randomly selected samples with a range of concentrations. Results showed an average RSD of 10%, 7% and 8% for tetra-, penta-, and hexathionate, respectively. Samples were analysed in duplicate and the results were averaged. Concentration differences between duplicates were usually <5%. Detection limits were 5 mg/kg for tetra-, 1.6 mg/kg for penta-, and 0.5 mg/kg for hexathionate.

One litre of lake water (original T=32°C, pH=1.1, density=1.02 g/mL), collected on 17 March 1999, was stored at 5°C and used as a reference standard solution for polythionate calibration curves at LAQAT. This sample was periodically analysed at Tokyo University in order to determine the reliability in the use of this sample as a standard solution due to the chemical lability of polythionates (Stamm *et al.*, 1942). For instance, the analysis carried out at Tokyo University on 28

July 2002, 3 years and 4 months after collection, yielded 462 ± 8 mg/kg $\text{S}_4\text{O}_6^{2-}$, 182 ± 3 mg/kg $\text{S}_5\text{O}_6^{2-}$ and 118 ± 2 mg/kg $\text{S}_6\text{O}_6^{2-}$ (Table APP-4.1.2, Appendix 4.1). This use of natural crater-lake water as a reference has the advantage of eliminating potential problems related to matrix differences between standards and samples, and those associated with chemical instability during preparation and storage of synthetic polythionate standard salts and solutions. Polythionate concentrations in this reference sample remained at an acceptable stable level at least until August–October 2002 when analyses were run at LAQAT (Table APP-4.1.2, Appendix 4.1).

Although it has been demonstrated for natural and synthetic highly acid solutions ($\text{pH} < 2$), free from sulphur-oxidizing bacteria, that no significant decomposition of polythionates occurs at concentrations of >100 ppm over at least eight years (Takano, 1987; Takano and Watanuki, 1988, 1990; Takano *et al.*, 1994b), the stability of polythionates was verified in some lake water samples at LAQAT. As earlier analysed samples from the 1984–1990 period (Rowe *et al.*, 1992b) were not available for re-analysis, a polythionate-rich mud pool sample and the reference sample (10 June 1994, 17 March 1999), were analysed for tetrathionate on 16 October 2002 using a fresh synthetic aqueous solution of a 98% sodium tetrathionate dihydrate salt, $\text{Na}_2\text{S}_4\text{O}_6 \cdot 2\text{H}_2\text{O}$, to prepare a calibration curve. Results were even somewhat higher than data obtained in Tokyo in 1999 and 2002 (RSD = 14 and 12%), indicating that there is no evidence for significant instability of this species over a period of at least three years. On the same date, all major polythionates were also re-analysed in the 10 June 1994 sample, using the 17 March 1999 reference solution. Original and newly measured values were in reasonable agreement with 2825 and 3185 mg/kg for tetra-, 2067 and 2600 mg/kg for penta-, and 725 and 880 mg/kg for hexathionate, respectively (Table APP-4.1.2, Appendix 4.1). Repeated analyses of aliquots of the reference solution in Tokyo in 1999 and 2002 confirmed that it had maintained its quality after three years.

Comparison of concentration data obtained on aliquots of 8 samples (June 1994–September 2001) showed random differences between results from the two laboratories. Overall deviations from the mean values were better than 20% RSD (3–20% for tetra-, 2–15% for penta-, and 1–20% for hexathionate (Table APP-4.1.2, Appendix 4.1). As most analyses in Tokyo and Costa Rica were carried out with time differences of about 3 years, it is concluded that the long-term polythionate trends presented here are largely unaffected by potential interlaboratory differences or chemical instability. Re-analysis of sulphate and chloride suggests that some of the oldest samples may have experienced a certain degree of evaporation or mineral precipitation during storage. According to enrichments of both anions found, this may have raised polythionate concentrations in these cases by 15–20% at most.

4.2.2.2 Determination of major anions, dissolved gases and pH

Most of the samples collected between 1990 and June 2004 were analysed for sulphate, chloride and fluoride at the Department of Earth Sciences of Utrecht University by suppressed ion chromatography, using a fully automated Dionex Model DX-120 system (see Chapter 5). Samples were filtered

in the laboratory with $0.45 \mu\text{m}$ polycarbonate membrane filters prior to analysis. Repeated analysis ($n=14$) of a lake water sample yielded relative standard deviations better than 4% for all of the anions. Precision was about 0.1%, 0.3% and 4% for sulphate, chloride, fluoride, respectively, based on analysis of a synthetic solution. Detection limits were 0.3, 0.1 and 0.05 mg/kg, respectively. Some samples collected in 2000 were filtered with $0.45 \mu\text{m}$ polycarbonate filters and diluted in the field to prevent precipitation of gypsum. From comparison with results of samples that were untreated in the field, it was inferred that precipitation of gypsum during storage might have resulted in lowering of the measured sulphate concentrations by about 7%. Results of four untreated samples were on average 6% lower than those of filtered and diluted equivalents (Vaselli *et al.*, 2003) that had been taken on the same dates in 1998–2001. Similar effects from storage of untreated samples were also attributed to gypsum precipitation by Rowe *et al.*, 1992b.

The samples collected between July 2004 and November 2006 were analysed for sulphate, chloride and fluoride at the Laboratory of Volcano Geochemistry of OVSICORI-UNA between June and December 2006, using a fully automated microbore ion suppressed chromatographic system Dionex ICS-3000 (see Chapter 5).

The pH measurements were carried out at the Department of Geosciences of Utrecht University and the Laboratory of Volcano Geochemistry of OVSICORI-UNA on untreated samples at room temperature ($20 \pm 2^\circ\text{C}$) using a WTW-brand Multi 340i multimeter.

The combination of the data generated at Utrecht University, Tokyo University, and OVSICORI-UNA with previously available results (Casertano *et al.*, 1985; Rowe *et al.*, 1992a,b; OVSICORI, unpublished data; Nicholson *et al.*, 1992, 1993; LAQAT, Martínez *et al.*, 2000) constitutes a record for major anion concentrations, pH and temperature that covers the period 1980–2006.

Dissolved unreacted SO_2 and H_2S gases in the lake water were measured *in situ* on an irregular basis during 1999–2006, using an adapted version (Takano, B., pers. comm., 2005) of the gas detection tube method developed by Togano and Ochiai (1987). A description of the procedure is given in Appendix 4.3. Detection limits for SO_2 and H_2S are 1 and 0.2 ppm, respectively.

4.2.3 Seismic and other data

Four main types of seismic events have been distinguished at Poás, based on categories defined by Minakami (1969): (1) A-type (volcanic-tectonic), (2) B-type (long-period) quakes, (3) AB-type events (long period medium-frequency, $f=2.1$ – 3.0 Hz), and (4) T-type or volcanic tremor (cf., Martínez *et al.*, 2000). Different kinds of tremors have been registered at Poás: Low-frequency polychromatic tremor ($f < 2.0$ Hz); medium-frequency polychromatic tremor ($f=2.0$ – 3.0 Hz); high-frequency polychromatic tremor ($f > 3.0$ Hz); and spasmodic tremor ($f > 3.0$ Hz). Monochromatic tremors of different frequencies are rare (Barboza, V., pers. comm., 2005; Martínez *et al.*, 2000).

Seismic records are available for Poás since 1980. The data considered here are from two seismic stations equipped with short period (1 Hz) vertical seismometers, operated by OVSICORI since 1984 (Rowe *et al.*, 1992a; Martínez *et al.*,

2000; Rymer *et al.*, 2000; OVSICORI, unpublished data). The POA station was operational in 1984–1985 and was located at the Poasito quarry, 4.3 km SE from Poás active crater. This station was moved in 1986 to a closer location to the summit to improve its resolution of volcanic events. Subsequent data come from the POA2 station, which was installed in a site located 2.9 km SW of the active crater (10°10'63"N–84°15'05"W) and an elevation of 2500 m above sea level. Another seismic station, POA5, was installed in mid 2006 on the southern flank of the Von Frantzius cone, about 0.5 km from the northern rim of the active crater of Poás volcano (Fig. 4.1). In mid 2007, a third seismic station was also set up at the SE flank of the volcano. For the period 1980–1983, data from a station operated by the Red Sismológica Nacional of the Instituto Costarricense de Electricidad and Universidad de Costa Rica have been used (Fernández, 1990; Rowe *et al.*, 1992a; Rymer *et al.*, 2000). Between 1980 and 1985 the coverage fluctuated (37–58%), mainly due to instrumental problems (Fernández, 1990; Rowe *et al.*, 1992a), whereas the records available from 1986 on represent a nearly continuous coverage (>90%).

The T-type quakes of 1980–1983 were originally reported as annual number of individual events (Fernández, 1990; Rowe *et al.*, 1992a; Rymer *et al.*, 2000). Because OVSICORI reports data on T-type quakes in hours per day or month, it is difficult to include this early period in a complete time series. In March 1981 an extremely large number of tremors were recorded by the station of the Red Sismológica Nacional (Fernández, 1990). In view of the accompanying strong release of hot gases through the composite pyroclastic cone (CPC) in 1981–1983 (Fig. 4.6, see also Chapter 2 Fig. 2.9), the total duration of these tremors was probably much longer than during any later interval, including the peak activity in 2005–present (Stage V). To visualize this anomalous record in the time series plots, an arbitrary total of 1000 hours of tremor was adopted for March 1981, and the recorded declined through 1984 was taken into account (Fig. 4.6). The discontinuous 1980–1983 record of A- and B-type data was converted to monthly events by recalculating annual numbers of events (Fernández, 1990; Rowe *et al.*, 1992a) to 100% coverage and dividing the result over equal monthly intervals. Because the number of A-type events during a series of swarms registered in a two-week period in mid July 1980 presumably numbered in the thousands (Casertano *et al.*, 1983, 1985), and counting from the seismogram was disabled, this peak activity is indicated with an arrow in plots (Fig. 4.6). AB-type seismic data are not available for Stage I and for most of Stage II because the Red Sismológica Nacional did not distinguish between A- and AB-type seismicity. Thus, AB-type data are only available from March 1984, when a country-wide seismographic network started operating as a joint project between the University of California at Santa Cruz and OVSICORI-UNA.

All field-related data (lake volume, temperature, etc.) are from the database of OVSICORI (Venzke *et al.*, 2002–; OVSICORI, unpublished, see Chapter 5). Monthly rainfall data were provided by the Centro de Servicios y Estudios Básicos de Ingeniería of the Instituto Costarricense de Electricidad (ICE). Most of the rainfall data come from the summit rain gauge located a few meters from the Visitor's Centre of Poás Volcano National Park, which is operated and maintained by ICE through collaboration with the park rangers of Poás Volcano

National Park (gauge identification: ICE Hydromet station 084063 Grande Tárcoles watershed, latitude 10°11'N longitude 84°14'W, at 2564 m.a.s.l.). The data for 1981–1983, December 1985 and September 2000 were taken from an ICE rain-gauge station located at Vara Blanca, 8 km SE of the summit gauge (gauge identification: ICE Hydromet station 69505, at 1804 m.a.s.l.). Comparison of rainfall recorded at both ICE stations over the period 1977–2004 (ICE, written comm., 2004) indicates that monthly trends are reasonably consistent.

4.3 Results and discussion

4.3.1 Polythionate results

Analytical results of tetra-, penta-, and hexathionate are given in Table 4.1, together with concentration data for sulphate, chloride and fluoride and other relevant parameters. For completeness, published data of Rowe *et al.* (1992b) have been included, so that Table 4.1 lists a polythionate record for the period October 1980–November 2006.

The results show that polythionates formed a significant part of the anion budget during the transitional period between Stages II and III, and between the end of Stage III and most part of Stages IV and V. Polythionate concentrations were generally as high as several hundreds or thousands of milligrams per kilogram. Corresponding peak areas in chromatograms show a decrease with increasing number of sulphur atoms per molecule, indicating diminishing concentrations in that order (Fig. 4.2). By and large, the most abundant polythionate species observed are, in decreasing order of concentration, tetra-, penta-, and hexathionate (Table 4.1; Figs. 4.5, 4.6, 4.7). Nonetheless, during Stage II and during the first fourteen months of Stage III the polythionates were present in a different order: $S_5O_6^{2-} > S_4O_6^{2-} > S_6O_6^{2-}$ (Rowe *et al.*, 1992b). This particular distribution has been also observed in some briefs periods of relative quiescence in the lake: mid 1991–early 1992, mid 1995–January 1996, the first four months of 2002 and May–July 2006, when the concentrations of polythionates tend to be rather low (Table 4.1).

Many of the chromatograms showed two or three additional peaks that were eluted after the hexathionate ion, corresponding to several higher homologues of polythionates such as heptathionate ($S_7O_6^{2-}$), octathionate ($S_8O_6^{2-}$) and nonathionate ($S_9O_6^{2-}$) (Fig. 4.2, Fig. APP-4.1A and Fig. APP-4.1B in Appendix 4.1) (cf., Steudel and Holdt, 1986). Qualitative inspection of all of the chromatograms suggests that these larger polythionates are present in the lake water during periods when the shorter polythionate homologues are abundant (e.g., from late 1994 to late 1998, and sporadically in 1999, 2001, 2002, and 2005–2006), and that they were undetectable during periods when the latter were present in low amounts or were not detected at all (e.g., 1987–1994, mid 1995–early 1996, late 2001–early 2002, late 2003 to March 2005, and late 2006). Higher polythionates, including nona- and decathionate, have also been detected in the acid crater lakes of Ruapehu (Takano *et al.*, 1994b) and Kusatsu-Shirane (Takano, 1987) volcanoes. Because long chain polythionates are more susceptible to thermal and sulphitolytic breakdown than the shorter polythionates (Fujiwara *et al.*, 1988; Takano *et al.*, 2001;

Table 4.1. Polythionate and major anion concentrations (mg/kg) of Poás crater lake for the period 1980–2006.

Date	Temp. (°C)	pH _{lab} 24±2°C	S ₄ O ₆	S ₅ O ₆	S ₆ O ₆	Total S _x O ₆	S ₄ O ₆ / S ₅ O ₆	S ₄ O ₆ / S ₆ O ₆	SO ₄	Cl	F	PT _{lab}
Stage II												
31-Oct-80	45	0.11	190	270	130	590	0.7	1.5	65500	26900	1320	(1)
28-Nov-84	48	0.07	83	410	100	593	0.2	0.9	57700	23700	1500	(2)*
24-Jan-85	44	0.14	1190	2120	770	4080	0.6	1.5	49500	25400	1660	(2)*
20-Mar-85	44	0.13	1120	1760	510	3390	0.6	2.2	48200	24700	1560	(2)*
06-May-85	44	0.14	450	1180	360	1990	0.4	1.3	55000	22000	1400	(2)*
22-Aug-85	45	0.17	970	1740	520	3230	0.6	1.8	54200	21100	1280	(2)*
09-Oct-85	45	0.18	600	1270	460	2330	0.5	1.3	52900	20700	1260	(2)*
04-Feb-86	39	0.26	1160	1420	520	3100	0.8	2.2	36900	16500	1010	(2)*
Stage III												
02-May-86	38	0.20	1730	1810	630	4170	1.0	2.7	40100	16500	970	(2)*
23-Aug-86	52	0.20	1700	1700	520	3920	1.0	3.3	41200	18900	1020	(2)*
31-Oct-86	54	0.14	1040	1310	420	2770	0.8	2.5	52000	23200	1240	(2)*
10-Jan-87	58	-0.01	1560	1370	620	3550	1.1	2.5	64400	30400	1590	(2)*
27-Feb-87	62	-0.03	170	630	120	920	0.3	1.4	78600	33700	1750	(2)*
19-Mar-87	62	0.00	53	70	b.d.l.	123	0.8	n.a.	82900	35900	1820	(2)*
27-Jul-87	68	-0.27	2	6	b.d.l.	8	0.3	n.a.	103000	44900	2110	(2)*
10-Sep-87	65	-0.23	b.d.l.	b.d.l.	b.d.l.	n.a.	n.a.	n.a.	108000	43400	2060	(2)*
27-Nov-87	60	-0.24	b.d.l.	b.d.l.	b.d.l.	n.a.	n.a.	n.a.	101000	48000	1910	(2)*
16-Jan-88	64	-0.37	b.d.l.	b.d.l.	b.d.l.	n.a.	n.a.	n.a.	127000	59300	2250	(2)*
02-Mar-88	60	-0.31	b.d.l.	b.d.l.	b.d.l.	n.a.	n.a.	n.a.	118000	51300	2100	(2)*
24-Jun-88	65	-0.61	b.d.l.	b.d.l.	b.d.l.	n.a.	n.a.	n.a.	175000	73100	2970	(2)*
02-Sep-88	65	-0.53	b.d.l.	b.d.l.	b.d.l.	n.a.	n.a.	n.a.	196000	44200	3810	(2)*
26-Oct-88	65	-0.43	b.d.l.	b.d.l.	b.d.l.	n.a.	n.a.	n.a.	192000	47400	4220	(2)*
07-Feb-89	75	-0.87	b.d.l.	b.d.l.	b.d.l.	n.a.	n.a.	n.a.	286000	28000	10400	(2)*
03-Mar-89	82	-0.55	b.d.l.	b.d.l.	b.d.l.	n.a.	n.a.	n.a.	233000	27200	6310	(2)*
31-May-89	85	-0.09	110	6	b.d.l.	116	18	n.a.	124000	25100	6150	(2)*
22-Jun-89	80	-0.44	b.d.l.	b.d.l.	b.d.l.	n.a.	n.a.	n.a.	175000	40600	8420	(2)*
26-Jul-89	82	-0.55	250	90	25	365	2.9	10	175000	46500	8600	(2)*
17-Aug-89	87	-0.36	b.d.l.	b.d.l.	b.d.l.	n.a.	n.a.	n.a.	99300	39200	7230	(2)*
24-Oct-89	85	-0.56	b.d.l.	b.d.l.	b.d.l.	n.a.	n.a.	n.a.	154000	64100	7910	(2)*
26-Jan-90	78	-0.29	22	20	b.d.l.	42	1.2	n.a.	109000	52000	6400	(2)*
21-Feb-90	85	-0.56	16	10	b.d.l.	26	1.5	n.a.	103000	95200	8460	(2)*
17-Mar-90	75	-0.60	b.d.l.	b.d.l.	b.d.l.	n.a.	n.a.	n.a.	165000	63100	8730	(2)*
01-Jun-90	83	-0.46	b.d.l.	b.d.l.	b.d.l.	n.a.	n.a.	n.a.	67800	36600	9440	(1)
10-Jul-90	94	-0.44	b.d.l.	b.d.l.	b.d.l.	n.a.	n.a.	n.a.	85600	79600	15400	(1)
13-Sep-90	88	-0.70	b.d.l.	b.d.l.	b.d.l.	n.a.	n.a.	n.a.	90300	114000	25400	(1)
08-Dec-90	73	n.d.	b.d.l.	b.d.l.	b.d.l.	n.a.	n.a.	n.a.	34800	40800	4860	(1)
08-Feb-91	65	-0.40	b.d.l.	b.d.l.	b.d.l.	n.a.	n.a.	n.a.	32000	52400	5930	(1)
19-Apr-91	78	-0.42	b.d.l.	b.d.l.	b.d.l.	n.a.	n.a.	n.a.	43600	50700	5610	(1)
26-Jul-91	63	-0.38	90	110	20	220	0.8	4.5	51300	47900	4310	(1)
24-Sep-91	71	-0.44	b.d.l.	b.d.l.	b.d.l.	n.a.	n.a.	n.a.	67800	55800	6320	(1)
21-Oct-91	74	n.d.	8	16	9	33	0.5	0.9	70000	58500	6560	(1)
01-Nov-91	70	-0.50	9	b.d.l.	b.d.l.	9	n.a.	n.a.	72100	61100	6790	(1)
12-Dec-91	64	-0.30	105	130	73	308	0.8	1.4	40700	35800	4690	(1)
17-Jan-92	67	-0.50	b.d.l.	b.d.l.	b.d.l.	n.a.	n.a.	n.a.	75000	58700	5750	(1)
07-Feb-92	67	-0.60	75	100	37	212	0.8	2.1	41600	32900	3700	(1)
13-Mar-92	65	-0.70	b.d.l.	b.d.l.	b.d.l.	n.a.	n.a.	n.a.	119000	87400	8800	(1)
03-Apr-92	75	-0.80	b.d.l.	b.d.l.	b.d.l.	n.a.	n.a.	n.a.	147000	102000	11000	(1)
24-Jul-92	70	-0.60	12	b.d.l.	b.d.l.	12	n.a.	n.a.	94200	67800	8260	(1)
21-Aug-92	75	-0.60	b.d.l.	b.d.l.	b.d.l.	n.a.	n.a.	n.a.	78900	63300	6870	(1)
18-Sep-92	70	-0.60	b.d.l.	b.d.l.	b.d.l.	n.a.	n.a.	n.a.	93100	74400	8390	(1)
07-Oct-92	75	-0.50	30	24	20	74	1.1	1.2	52400	71600	5060	(1)
19-Nov-92	80	-0.50	b.d.l.	b.d.l.	b.d.l.	n.a.	n.a.	n.a.	38400	73000	5720	(1)
23-Jan-93	65	0.00	b.d.l.	b.d.l.	b.d.l.	n.a.	n.a.	n.a.	56100	54000	4510	(2)
25-Feb-93	65	0.00	160	196	110	466	0.8	1.4	58000	56200	n.d.	(2)
02-Apr-93	60	0.00	b.d.l.	b.d.l.	b.d.l.	n.a.	n.a.	n.a.	65000	75500	7550	(2)
09-Sep-93	64	0.35	b.d.l.	b.d.l.	b.d.l.	n.a.	n.a.	n.a.	50400	29600	5840	(1)
22-Oct-93	60	0.00	b.d.l.	b.d.l.	b.d.l.	n.a.	n.a.	n.a.	46000	27600	5330	(2)
12-Mar-94	55	0.00	b.d.l.	b.d.l.	b.d.l.	n.a.	n.a.	n.a.	83100	56500	7780	(2)
23-Sep-94	65	-0.18	1020	530	850	2400	1.9	1.2	27000	24000	2660	(1)
21-Oct-94	60	0.14	3700	2660	990	7350	1.4	3.7	17000	8470	1220	(2)

Date	Temp. (°C)	pH _{lab} 24±2°C	S ₄ O ₆	S ₅ O ₆	S ₆ O ₆	Total S _x O ₆	S ₄ O ₆ / S ₅ O ₆	S ₄ O ₆ / S ₆ O ₆	SO ₄	Cl	F	PT _{lab}
15-Nov-94	55	0.38	b.d.l.	b.d.l.	b.d.l.	n.a.	n.a.	n.a.	11000	7640	n.d.	(1)
06-Jan-95	50	0.22	2700	1530	900	5130	1.7	3.0	16000	10200	1060	(1)
03-Feb-95	47	0.18	2340	1420	880	4640	1.6	2.7	16600	10100	990	(1)
10-Mar-95	42	0.68	1800	1230	500	3530	1.5	3.6	20500	7780	950	(2)
Stage IV												
08-Sep-95	34	1.10	294	290	140	724	1.0	2.2	8710	5440	530	(2)
20-Oct-95	30	1.21	b.d.l.	b.d.l.	b.d.l.	n.a.	n.a.	n.a.	6230	3800	190	(2)
05-Jan-96	29	1.22	40	80	36	156	0.5	1.0	9060	3590	200	(2)
23-Feb-96	26	1.55	244	75	40	359	3.3	6.4	4480	2630	140	(2)
22-Mar-96	30	1.50	290	130	66	486	2.3	4.3	6270	3370	200	(2)
26-Apr-96	36	1.50	315	110	80	505	2.9	3.9	5290	3910	200	(2)
10-May-96	42	1.45	450	170	84	704	2.7	5.4	5180	4020	330	(2)
14-Jun-96	45	1.35	690	330	170	1190	2.1	4.0	7000	4390	330	(2)
24-Jul-96	36	1.75	520	290	110	920	1.8	4.6	7520	4460	270	(2)
08-Aug-96	35	1.45	240	180	90	510	1.3	2.8	6970	4510	360	(2)
27-Sep-96	40	1.65	580	270	120	970	2.2	4.7	6780	4320	220	(2)
28-Nov-96	31	1.55	580	310	96	986	1.9	6.0	6790	5110	300	(2)
18-Dec-96	29	1.13	310	170	80	560	1.8	3.8	4870	3650	260	(2)
07-Jan-97	32	1.40	490	240	100	830	2.0	4.8	6880	5750	290	(2)
04-Feb-97	31	1.40	360	170	100	630	2.1	3.5	5110	3850	310	(2)
03-Mar-97	29	1.18	230	130	90	450	1.8	2.6	4410	3260	170	(2)
17-Apr-97	27	1.40	270	150	80	500	1.7	3.3	4640	4230	230	(2)
14-May-97	29	1.45	510	200	70	780	2.5	7.2	4640	4420	310	(2)
04-Jun-97	32	1.50	610	250	60	920	2.5	10	4750	4280	230	(2)
02-Jul-97	32	1.50	500	200	75	775	2.5	6.7	4870	4620	210	(2)
22-Aug-97	31	1.45	700	270	60	1030	2.6	12	5770	6690	200	(2)
05-Sep-97	35	1.30	590	260	50	900	2.3	12	4060	4330	170	(2)
17-Oct-97	34	1.06	790	280	56	1126	2.9	14	7840	6520	360	(2)
04-Nov-97	35	1.40	810	280	64	1154	2.9	13	6460	7800	280	(2)
06-Feb-98	38	0.90	840	420	115	1375	2.0	7.3	7910	7920	420	(2)
25-Mar-98	37	0.79	990	430	110	1530	2.3	9.1	9120	9440	490	(2)
17-Apr-98	37	0.68	b.d.l.	b.d.l.	b.d.l.	n.a.	n.a.	n.a.	10900	8870	460	(2)
15-May-98	36	0.64	810	370	120	1300	2.2	6.8	11500	12400	620	(2)
25-Jun-98	36	0.99	260	170	35	465	1.6	7.4	7500	6490	500	(2)
30-Jul-98	35	0.73	890	490	160	1540	1.8	5.7	10800	11800	600	(2)
26-Aug-98	35	0.73	890	420	120	1430	2.1	7.3	7970	8410	390	(2)
21-Sep-98	35	0.74	850	400	110	1360	2.1	7.6	9850	10800	550	(2)
04-Nov-98	35	0.85	350	190	110	650	1.9	3.3	8140	8740	480	(2)
23-Dec-98	27	0.90	330	170	80	580	1.9	4.0	7650	7840	600	(2)
13-Jan-99	32	0.77	430	210	130	770	2.1	3.4	9110	9890	640	(2)
25-Feb-99	33	0.68	470	220	110	800	2.1	4.2	10600	11700	660	(2)
17-Mar-99	32	0.81	460	180	120	760	2.5	3.9	9760	10900	720	(2)
21-Apr-99	32	0.72	380	200	150	730	1.9	2.6	10400	11300	800	(1)
07-May-99	34	0.71	360	200	150	710	1.8	2.4	10700	11600	810	(1)
18-Jun-99	34	0.68	330	130	90	550	2.6	3.7	8550	7510	480	(1)
07-Jul-99	32	0.68	300	170	140	610	1.7	2.1	11100	12200	720	(1)
19-Aug-99	35	0.81	290	150	110	550	2.0	2.6	10200	11200	720	(1)
08-Sep-99	39	0.62	290	130	90	510	2.2	3.2	8220	8120	660	(1)
22-Oct-99	38	0.61	290	190	140	620	1.5	2.1	12100	13300	920	(1)
05-Nov-99	39	0.80	380	140	100	620	2.7	3.7	9250	9130	730	(1)
27-Dec-99	34	0.72	300	200	140	640	1.5	2.1	10400	11400	790	(1)
21-Jan-00	38	0.76	240	100	62	402	2.3	3.9	9270	9850	740	(1)
10-Feb-00	44	0.69	210	100	60	370	2.0	3.5	10200	10800	830	(1)
13-Mar-00	36	0.71	120	65	50	235	1.9	2.5	9270	9620	700	(1)
11-Apr-00	32	0.74	230	110	66	406	2.0	3.4	9780	10400	830	(1)
05-May-00	31	0.67	200	100	53	353	2.0	3.8	8330	8280	810	(1)
09-Jun-00	31	0.77	210	97	87	394	2.1	2.4	9260	11900	710	(1)
17-Jul-00	33	0.74	110	52	30	192	2.1	3.7	7230	9050	510	(1)
24-Aug-00	31	0.60	150	90	57	297	1.6	2.6	9240	13300	700	(1)
12-Sep-00	35	0.60	190	87	62	339	2.2	3.1	9410	12700	620	(1)
10-Oct-00	35	0.70	180	84	52	316	2.2	3.5	8900	11700	580	(1)
21-Nov-00	34	0.71	160	76	40	276	2.0	4.0	8930	11900	670	(1)
01-Dec-00	34	0.90	160	72	50	282	2.2	3.3	8320	10900	610	(1)
12-Jan-01	31	0.86	120	80	78	278	1.6	1.6	8700	11400	680	(1)
23-Feb-01	31	0.83	120	80	97	297	1.6	1.3	7870	9670	540	(1)

Date	Temp. (°C)	pH _{lab} 24±2°C	S ₄ O ₆	S ₅ O ₆	S ₆ O ₆	Total S _x O ₆	S ₄ O ₆ / S ₅ O ₆	S ₄ O ₆ / S ₆ O ₆	SO ₄	Cl	F	PT _{lab}
08-Mar-01	32	0.65	130	79	38	247	1.7	3.5	9080	11600	710	(1)
26-Apr-01	35	0.75	120	66	25	211	1.8	4.7	9400	11700	660	(1)
08-May-01	34	0.70	160	80	80	320	2.0	2.0	9080	12200	690	(1)
13-Jun-01	35	0.67	150	74	84	308	2.0	1.8	9100	11700	560	(1)
19-Jul-01	28	0.70	190	70	34	294	2.7	5.5	7270	8400	460	(1)
03-Aug-01	24	0.85	160	74	72	306	2.2	2.2	8090	9760	510	(1)
07-Sep-01	27	0.39	360	110	80	550	3.3	4.6	8510	9590	540	(1)
18-Oct-01	28	0.85	360	160	105	625	2.2	3.4	7800	8280	380	(1)
27-Nov-01	30	1.07	b.d.l.	b.d.l.	b.d.l.	n.a.	n.a.	n.a.	3450	2720	82	(1)
07-Dec-01	30	1.43	b.d.l.	b.d.l.	b.d.l.	n.a.	n.a.	n.a.	3310	2830	67	(1)
31-Jan-02	30	1.51	6	10	9	25	n.a.	n.a.	3590	2540	52	(1)
27-Feb-02	23	1.17	9	14	12	35	0.6	0.7	6050	4670	160	(1)
13-Mar-02	26	1.06	33	50	7	90	0.6	4.7	6390	5760	190	(1)
03-Apr-02	25	1.04	53	80	14	147	0.7	3.8	6830	6420	380	(1)
16-May-02	29	1.08	b.d.l.	b.d.l.	b.d.l.	n.a.	n.a.	n.a.	6060	6260	230	(1)
11-Jun-02	29	0.90	67	50	37	154	1.3	1.8	5060	5780	130	(1)
30-Jul-02	32	0.99	140	52	30	222	2.7	4.8	6800	7620	320	(1)
04-Sep-02	38	0.90	580	220	70	870	2.7	8.4	7660	8720	300	(1)
11-Dec-02	39	0.84	620	280	63	963	2.2	9.9	8510	10700	430	(2)
17-Jan-03	34	0.83	460	300	138	898	1.5	3.3	8780	10500	480	(2)
28-Feb-03	36	0.77	600	380	143	1123	1.6	4.2	8870	10900	520	(2)
31-Mar-03	39	0.70	940	460	143	1543	2.1	6.6	9360	15000	580	(2)
30-Apr-03	41	0.67	910	560	170	1640	1.6	5.3	10500	16100	620	(2)
20-May-03	41	0.70	810	470	180	1460	1.7	4.5	11000	16200	620	(2)
17-Jul-03	35	0.64	400	380	184	964	1.1	2.2	11800	17100	650	(2)
12-Aug-03	33	0.61	720	450	148	1318	1.6	4.9	8860	18200	720	(2)
30-Sep-03	33	0.62	280	240	112	632	1.2	2.5	13800	15300	560	(2)
28-Oct-03	28	0.80	6	4	b.d.l.	10	1.5	n.a.	9290	12700	320	(2)
05-Dec-03	24	0.93	b.d.l.	b.d.l.	b.d.l.	n.a.	n.a.	n.a.	6100	8310	240	(2)
20-Jan-04	24	1.17	b.d.l.	b.d.l.	b.d.l.	n.a.	n.a.	n.a.	5260	6670	180	(2)
03-Feb-04	29	1.11	b.d.l.	b.d.l.	b.d.l.	n.a.	n.a.	n.a.	4550	5880	190	(2)
23-Mar-04	25	1.05	b.d.l.	b.d.l.	b.d.l.	n.a.	n.a.	n.a.	5290	6530	180	(2)
27-Apr-04	28	1.12	b.d.l.	b.d.l.	b.d.l.	n.a.	n.a.	n.a.	5300	6330	160	(2)
25-May-04	28	1.31	b.d.l.	b.d.l.	b.d.l.	n.a.	n.a.	n.a.	3940	5380	26	(2)
11-Jun-04	29	1.20	b.d.l.	b.d.l.	b.d.l.	n.a.	n.a.	n.a.	4540	6480	65	(2)
01-Jul-04	26	1.24	b.d.l.	b.d.l.	b.d.l.	n.a.	n.a.	n.a.	5680	5320	n.d.	(2)
12-Aug-04	25	1.10	b.d.l.	b.d.l.	b.d.l.	n.a.	n.a.	n.a.	7690	6320	170	(2)
22-Sep-04	29	1.16	b.d.l.	b.d.l.	b.d.l.	n.a.	n.a.	n.a.	7170	5860	140	(2)
22-Oct-04	27	1.08	b.d.l.	b.d.l.	b.d.l.	n.a.	n.a.	n.a.	7940	6920	160	(2)
2-Dec-04	23	1.17	b.d.l.	b.d.l.	b.d.l.	n.a.	n.a.	n.a.	7750	5930	130	(2)
22-Feb-05	22	1.25	b.d.l.	b.d.l.	b.d.l.	n.a.	n.a.	n.a.	3780	3680	92	(2)
Stage V												
21-Mar-05	32	1.22	b.d.l.	b.d.l.	b.d.l.	n.a.	n.a.	n.a.	4670	5330	130	(2)
12-Apr-05	34	0.97	190	110	10	310	1.6	21	7340	6570	220	(2)
4-May-05	41	1.02	470	120	30	620	3.9	15	8120	6900	260	(2)
24-Jun-05	50	0.92	1160	360	70	1590	3.3	16	9310	8380	470	(2)
14-Jul-05	50	0.79	540	250	110	900	2.2	4.8	9900	8800	530	(2)
24-Aug-05	51	0.75	860	470	172	1502	1.9	5.0	11400	10200	690	(2)
20-Sep-05	52	0.70	1100	820	270	2190	1.3	4.1	12800	11100	750	(2)
30-Nov-05	54	0.64	1850	1390	410	3650	1.3	4.5	13600	11600	920	(2)
31-Jan-06	51	0.65	1620	1310	500	3430	1.2	3.2	15700	12000	870	(2)
28-Feb-06	51	0.59	760	670	280	1710	1.1	2.8	17700	13400	990	(2)
1-Apr-06	54	0.63	710	500	275	1485	1.4	2.6	17200	15700	1050	(2)
25-May-06	47	0.72	90	100	48	238	0.9	1.8	19500	15900	1130	(2)
22-Jun-06	46	0.59	110	100	50	260	1.1	2.3	23100	16300	1090	(2)
20-Jul-06	43	0.62	70	70	30	170	0.9	2.2	21300	13400	890	(2)
11-Aug-06	43	0.52	120	95	58	273	1.2	2.0	25400	16100	1100	(2)
05-Sep-06	41	0.47	280	240	100	620	1.2	2.8	27500	17100	1100	(2)
28-Oct-06	53	0.50	100	50	22	172	1.9	4.4	29000	16300	1170	(2)
10-Nov-06	57	0.43	85	40	25	150	2.1	3.4	29100	13200	950	(2)

PT lab refers to laboratory where polythionates were separated and analyzed: (1) LAQAT-Universidad Nacional. Heredia; (2) Tokyo University.

*: data from Rowe et al. (1992b); b.d.l.: below detection limit; n.d.: not determined; n.a.: not applicable.

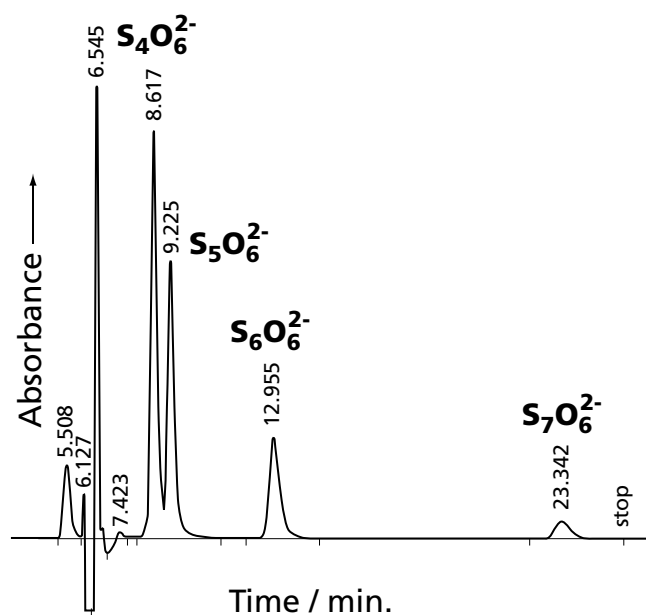


Figure 4.2. Example of a chromatogram for a lake-water sample (collected on 21 August 1999) obtained at LAQAT, where separation and quantification of the thionates were performed following Miura and Kawaoi (2000) (see procedure B in Table APP-4.1.1, Appendix 4.1). The sample was diluted 25 times. Peaks of tetrathionate, pentathionate, hexathionate and heptathionate are labelled. The peaks that eluted before the tetrathionate are due to unknown impurities in the sample.

Takano *et al.*, 2004), and because they are much less abundant and difficult to quantify, only the concentrations of the tetra-, penta-, and hexathionate are reported here. Throughout this paper “total polythionates” refers to the sum of concentrations of these three anions.

Figures 4.3, 4.5, 4.6, and 4.7 portray polythionate trends observed during the successive stages of activity of the volcano. To eliminate potential dilution or evaporation effects in the lake waters, we preferred to normalize polythionate concentrations against fluoride rather than on chloride, because the latter anion may be influenced by significant volatilisation of HCl from the lake water during increased fumarolic activity within the crater lake, as it was observed between mid 1988 and early 1989 (Fig. 4.5; Rowe *et al.*, 1992b).

4.3.2 Behaviour of polythionates in the crater lake of Poás

As mention before, five successive main stages of volcanic activity can be distinguished at Poás volcano since the late 1970's until the present day, based upon the profiles of a set of geochemical and geophysical parameters regularly monitored by OVSICORI (Figs. 4.3, 4.5, 4.6, 4.7). Nevertheless, since polythionate data are available for the period late 80's till 2006, this chapter starts the discussion on their behaviour from the arbitrarily defined Stage II.

4.3.2.1 Stage II (September 1980-April 1986): Period with high polythionate concentrations, moderate convective activity but no phreatic eruptions

During Stage II the concentrations of polythionate species were distributed in the following order: $S_5O_6^{2-} > S_4O_6^{2-} > S_6O_6^{2-}$ (Rowe *et al.*, 1992b). Single data points for October 1980

and November 1984 suggest that polythionates were initially present in relatively low amounts (together about 600 mg/kg). However, from early 1985 on, an irregularly increasing trend was observed that culminated in a maximum of about 4350 mg/kg in May 1986 (Table 4.1; Figs. 4.5, 4.6, 4.7). This strong rise coincided with swarms of A-type seismic activity (peaking in June-August), and also marked the start in May of a period of elevated B-type seismicity (Fernández, 1990; Rowe *et al.*, 1992a), which continued throughout Stage III (Fig. 4.6). The observed lowering of the lake volume after 1985 was probably partly due to relatively low rainfall in 1985, 1986, and 1987 (Fig. 4.3), but increased heat input must have significantly contributed to a rapid decline in early-mid 1986 (Rowe *et al.*, 1992a). A marked increase in lake temperature was not observed until June 1986 when 48°C was measured, which was 10°C higher than in the previous month (Fig. 4.3).

Trends of individual polythionate species were not entirely parallel. A conspicuous change in relative abundances was found in February and May 1986 when, compared to the other species, tetrathionate apparently had formed at much higher rates than previously. Pentathionate remained predominant throughout, but tetrathionate was present in almost equal amount at the peak levels of May 1986 (Figs. 4.5, 4.6). As discussed in Rowe *et al.* (1992b), fluctuations in polythionate speciation and their stability in the lake reflected changes in the SO_2/H_2S ratio of subaqueous fumaroles. The observed distribution of $S_5O_6^{2-} > S_4O_6^{2-} > S_6O_6^{2-}$ points to the predominance of H_2S -enriched subaqueous fumaroles with a molar SO_2/H_2S ratio of <0.07 , which would favour the formation of pentathionate over tetrathionate (Fig. 4.8) (Takano *et al.*, 1994b).

Despite the termination of phreatic eruptions by the end of 1980, several thousands of A-type seismic events were recorded between April and August 1980, which preceded an interval of strongly increased well-defined volcanic tremors between September 1980 and 1984 (Casertano *et al.*, 1985; Fernández, 1990). This enhanced seismicity coincided with a very high flux of high-temperatures gases (800–1020°C, Fig. 4.6) from the CPC in January 1981–September 1983, producing a strong sulphurous odour (Malavassi and Barquero, 1982; Barquero and Malavassi, 1983). COSPEC measurements recorded SO_2 fluxes of about 800 tons/day in February 1982 (Barquero and Fernández, 1983; Casadevall *et al.*, 1984a).

This dramatic release of hot SO_2 -rich gas from the CPC may be associated with the emplacement of a small magma body below it. If so, both the intrusion and the channelling of the expelled volatiles must have been confined to the small area below the CPC, because the properties of the lake were only modestly affected, as for example shown by the distribution of polythionate species pointing to an input of H_2S rather than SO_2 -rich gas.

Casertano *et al.*, (1987) suggested that, during maximum heating of the CPC in 1981–1983, the lake was still in continuous hydraulic connection with the rising hot fluids, consistent with the steady increase in lake temperature in these years (see Fig. 4.3). The lake had temperatures around 50°C, a greyish-turquoise colour, and showed strong evaporation and streaks of floating sulphur globules. By the end of October 1983 the water level has descended about 10 meters (Fig. 4.3). The detected increase in the $S_4O_6^{2-}/S_5O_6^{2-}$ and $S_4O_6^{2-}/S_6O_6^{2-}$ ratios

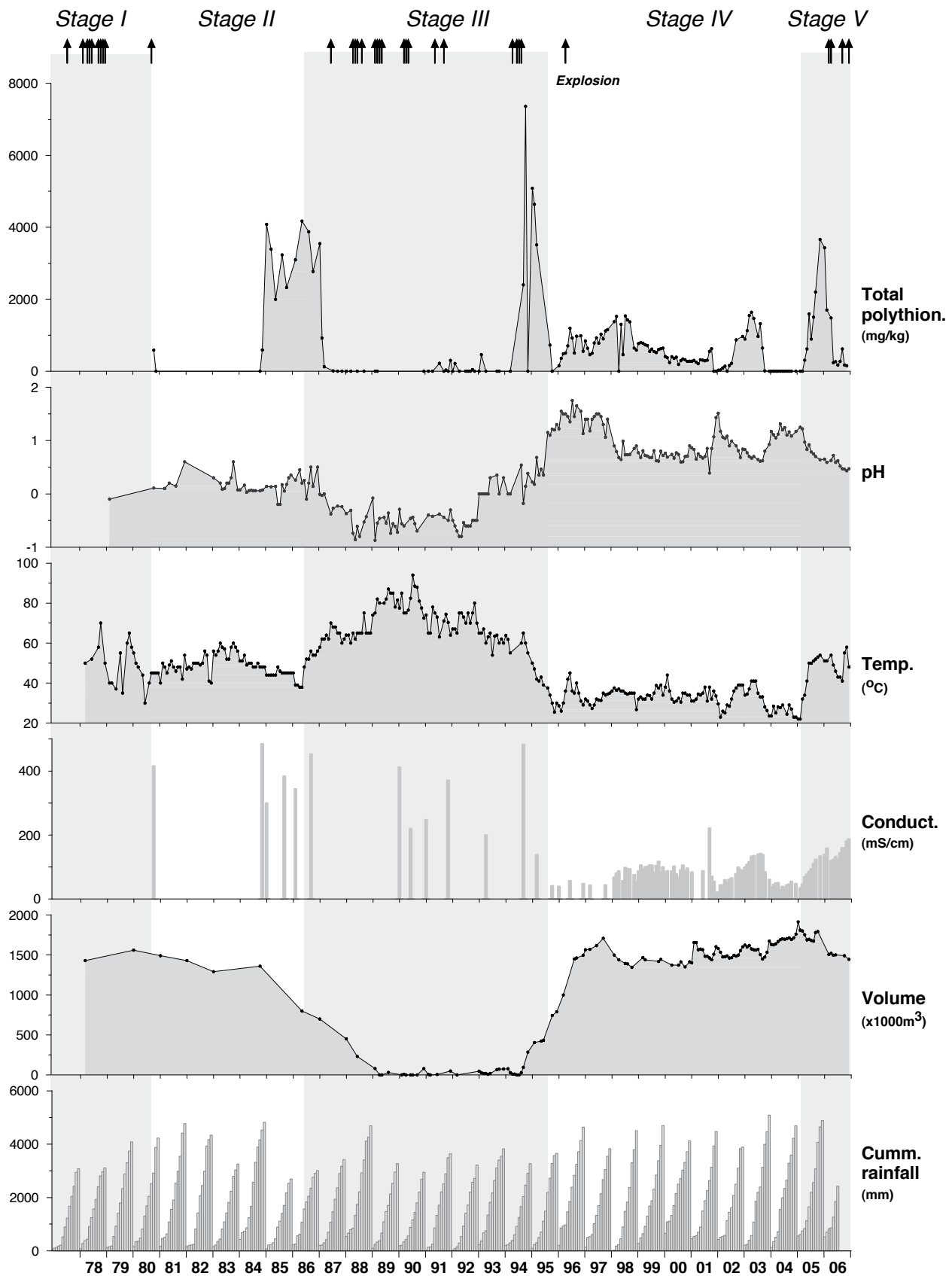


Figure 4.3. Time series of total polythionate concentrations (sum of tetra-, hexa- and pentathionate), pH, temperature, conductivity and volume of the crater lake between 1978 and 2006. Rainfall registered at the summit of Poás (ICE pluviometer) is expressed as cumulative monthly totals in cycles of calendar years. Arrows on top of the graph indicate phreatic eruptions and a minor hydrothermal explosion at the northern side of the CPC that occurred on 8 April 1996, presumably as a result of unclogging of fumarolic vents.

in 1985–mid 1986 can thus be explained by an increase in the $\text{SO}_2/\text{H}_2\text{S}$ ratio of subaqueous fumaroles after October 1985 (Fig. 4.5). This change probably occurred in early 1986 when swarms of A-Type earthquakes and elevated B-type seismicity were recorded, possibly induced by hydrofracturing of the magmatic carapace and subsequent release of magmatic volatiles (Rowe *et al.*, 1992 a,b). Some episodes of harmonic tremor of short duration (<1 min) and low amplitude (<1mm), which are rare at Poás and are not well understood, were also recorded in early 1986 (Fernández, 1990). This author suggested that this particular type of tremor could represent either intruding magma or strong degassing through rigid zones according to the model proposed by Aki *et al.* (1977) for Kilauea volcano. Shallow intrusion of fresh magma batches as source of the enhanced SO_2 output is also envisaged from micro-gravity increases in the southern part of the crater observed between 1986 and 1989 (Fig. 4.6) (Rymer *et al.*, 2000, 2004, 2005).

4.3.2.2 Stage III (May 1986–August 1995): Period with little or no polythionates, frequent phreatic eruptions and intense fumarolic discharge

After the peak levels of May 1986 polythionate concentrations showed a strong steady decrease concomitant with an increase in lake temperature, a decrease in pH and a reduction in lake volume (Fig. 4.3). By mid 1987 the lake temperature had risen above 60°C, the pH had dropped to negative values, and the polythionate concentrations were below the detection limits. These effects roughly coincided with the first geyser-like phreatic eruptions from the lake in June 1987 (see Chapter 2, Fig. 2.12) (Venzke *et al.*, 2002–; Rowe *et al.*, 1992a). Since then, polythionates remained undetected for most of Stage III; only occasionally minor amounts were measured (Fig. 4.3). By the end of Stage III, after cessation of phreatic eruptions in early August 1994, a new lake started to rise, the temperature dropped, the pH increased, and a significant amount of polythionates were formed, as observed for the first time in September 1994. The initial recovery of the lake was characterised by high polythionate concentrations ($\Sigma \text{S}_x\text{O}_6^{2-}$ up to 7360 mg/kg in October 1994), similar to those observed in May 1986. Irregular activity variations in the lake must have occurred in view of their temporary disappearance in November 1994 (Figs. 4.3, 4.5, 4.6, 4.7).

If the occasional presence of polythionates in the course of Stage III is taken into account, a generalised pattern in the species distribution can be discerned. Available data between 1989 and early 1990 show a strong dominance of tetrathionate over the other species at very low overall concentrations. In contrast, pentathionate was overall the most abundant species in samples between mid 1991 and early 1993, whereas the distribution changed in favour of tetrathionate again at the high $\Sigma \text{S}_x\text{O}_6^{2-}$ concentrations towards the end of Stage III (Table 4.1; Figs. 4.5, 4.7).

The breakdown of polythionates at the beginning of Stage III was accompanied by an increase in $\text{SO}_4^{2-}/\text{F}^-$ ratios of lake samples till mid 1988 (Fig. 4.5). Although polythionate breakdown by thermal effects or otherwise will generally produce sulphate (Takano and Watanuki, 1990; Takano *et al.*, 2001), this process alone cannot account for the rise in SO_4^{2-} concentrations and $\text{SO}_4^{2-}/\text{F}^-$ observed between May and July

1986. Moreover, the trend of increasing $\text{SO}_4^{2-}/\text{F}^-$ ratios in lake samples probably started already in early 1985 (see also Chapter 5). Hence, increased input of hot SO_2 -rich volatiles must have been responsible for most of the sulphate production, consistent with an increase in the $\text{SO}_2/\text{H}_2\text{S}$ ratio of subaqueous fumaroles, as inferred from the change in the distribution of polythionate species since August 1986 (Figs. 4.5, 4.6) (albeit with temporary reversals in some of the late 1986 and early 1987 samples). The enhanced SO_2 input in August 1986 produced maximum $\text{S}_4\text{O}_6^{2-}/\text{S}_{5,6}\text{O}_6^{2-}$ ratios at low $\Sigma \text{S}_x\text{O}_6^{2-}$ concentrations in the first half of Stage III as a result of thermal breakdown and sulphitolytic reactions (Takano and Watanuki, 1990; Takano *et al.*, 2001), although for most part of Stage III the polythionates were absent (Figs. 4.3, 4.5, 4.6). A plot of polythionate concentrations versus lake temperature shows that polythionates reached maximum concentrations when the temperature ranged between 38°C and 65°C, and that they were not stable at >65°C (Fig. 4.4). In Ruapehu Crater Lake complete degradation of polythionates occurred at temperatures above 47°C (Takano *et al.*, 1994b). Thus, both thermal and sulfitolitic decomposition was probably responsible for the disappearance of polythionates during Stage III.

Accompanied by a notable increase in B-type seismicity (Fig. 4.6), these changes in the lake geochemistry culminated in frequent, moderate to strong geyser-like phreatic explosions, and strong subaqueous fumarolic discharges within the lake area, starting in June 1987 and continuing till the beginning of 1988 (see Chapter 2, Fig. 2.12). Phreatic activity intensified in early 1988 and continued until early 1989 when the lake disappeared, enabling for the first time the direct observation of large pools of molten sulphur and sulphur cones on the dried lake bottom (See Chapter 2, Figs. 2.13A and 2.13B) (Oppenheimer and Stevenson, 1989). Since then, a series of strong phreatic

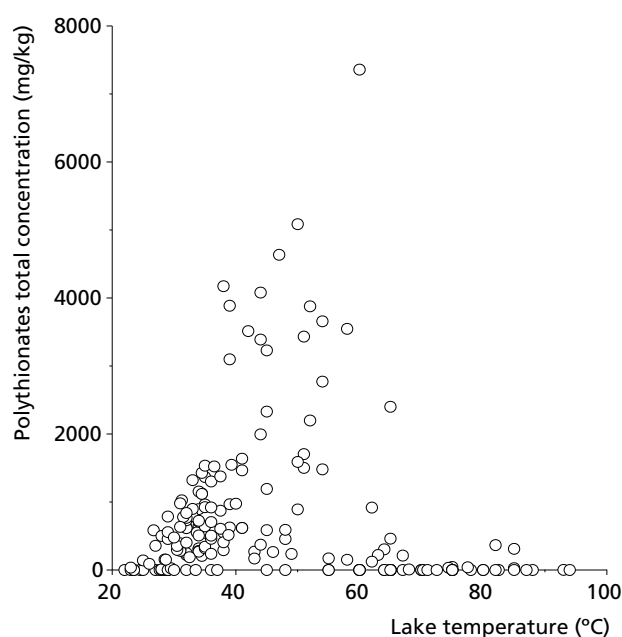


Figure 4.4. Total polythionate concentrations versus lake temperature for the period October 1980–November 2006. Maximum concentrations were observed at temperatures between 38°C and 65°C, whereas higher temperatures result in the breakdown of polythionates.

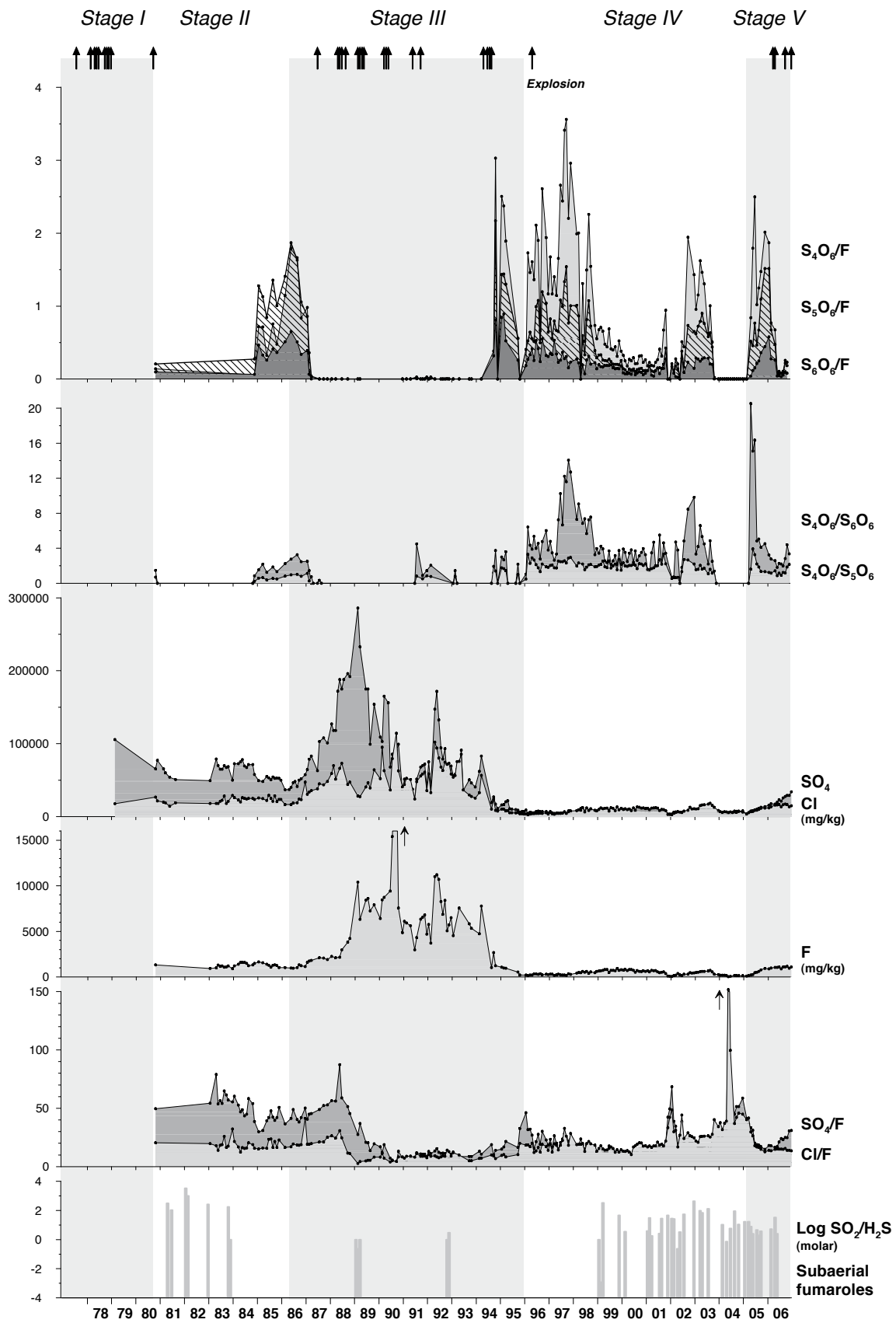


Figure 4.5. Time series of polythionate concentrations normalised to fluorine, S_4O_6/S_5O_6 and S_4O_6/S_6O_6 ratios, concentrations (mg/kg) and ratios of major anions, as well as molar SO_2/H_2S ratios of subaerial fumaroles. Except for the latter, all ratios are wt./wt. Arrows on top of the graph indicate phreatic eruptions. Arrows in the F and Cl/F panels indicate values that are out of scale.

explosions that ejected mud, sulphur, and lake sediments (some up to heights of ~2 km) occurred throughout 1989 and early 1991 (Venzke *et al.*, 2002-; Rowe *et al.*, 1989), coinciding with periods of significant T-type seismic activity and A-type seismic swarms (A-type seismic signals were recorded together with T-type events in 1989 and 1990 but not in 1991) (Fig. 4.6). The strong phreatic activity and intense release of gases and steam reduced the lake to scattered mud pools during the dry seasons (April 1989, April 1990 and March 1991), and prevented it from reaching normal levels during rainy seasons. In addition, the yearly rainfall between 1989 and early 1991 (2950–3600 mm) was somewhat less than the average of ~4 m year⁻¹ (Fig. 4.3).

The subsequent shift towards a polythionate distribution of $S_5O_6^{2-} > S_4O_6^{2-} > S_6O_6^{2-}$ (in cases when they were detected) and the inferred concomitant decrease in the SO_2/H_2S ratio of subaqueous fumaroles marked a period of noticeable lower activity in the lake area. Conditions of only moderate fumarolic degassing and absence of phreatic eruptions (Venzke *et al.*, 2002-; Barquero, 1998) prevailed from mid-1991 throughout 1992 and 1993. The lake level rose to a maximum of several meters, especially during the rainy seasons of 1991 and 1993 when rainfall was relatively heavy (Fig. 4.3). Although the lake remained shallow, recorded water levels were higher than in the previous years (depths were ~5 m and 4 m in December 1991 and December 1993, respectively) (Barquero, 1998; Venzke *et al.*, 2002-), while temperature and concentrations of dissolved species were generally lower than in 1986–1989 (Figs. 4.5, 4.6). Between mid 1991 and 1993 seismic activity was relatively low, with A-type and T-type seismicity being virtually absent, and a slight decrease in the predominant B-type seismic events (Fig. 4.6). COSPEC measurements carried out in February 1991 showed an average flux of 91 tons of SO_2 per day (Andres *et al.*, 1992).

As a prelude to renewed activity, the shallow lake evaporated at a rapid rate in early 1994, and was reduced once again to mud pools by March. This desiccation was preceded by an increase in AB-type seismicity in November 1993, and was accompanied by increases in A-type, AB-type, and B-type seismicity. Between June and early August 1994 numerous strong phreatic explosions and strong discharges of gas and steam occurred within the lake area. Occasionally, a large water-rich plume rose to heights of more than 2000 meters above the crater floor. The largest phreatic explosions were registered in the second half of July (Venzke *et al.*, 2002-; Martínez *et al.*, 2000). Swarms of A-type, AB-type, and numerous T-type seismic events preceded or accompanied this explosive activity (Fig. 4.6), which was further marked by sulphur combustion (suggesting temperatures $\geq 248^\circ\text{C}$ which is the auto-ignition temperature of elemental sulphur) and high-temperature fumaroles (up to about 700°C) at the dried lake bottom (Barquero, 1998; Venzke *et al.*, 2002-).

The increase in seismicity as well as heat and volatile fluxes that triggered the mid-1994 phreatic activity is possibly related to (hydro)fracturing rather than to a magmatic intrusion. If a fresh magmatic intrusion was emplaced, it must have occurred within a restricted zone underneath the lake area (Martínez *et al.*, 2000), since no notable increases in temperatures have been observed around the CPC since late 1988 (Fig. 4.6).

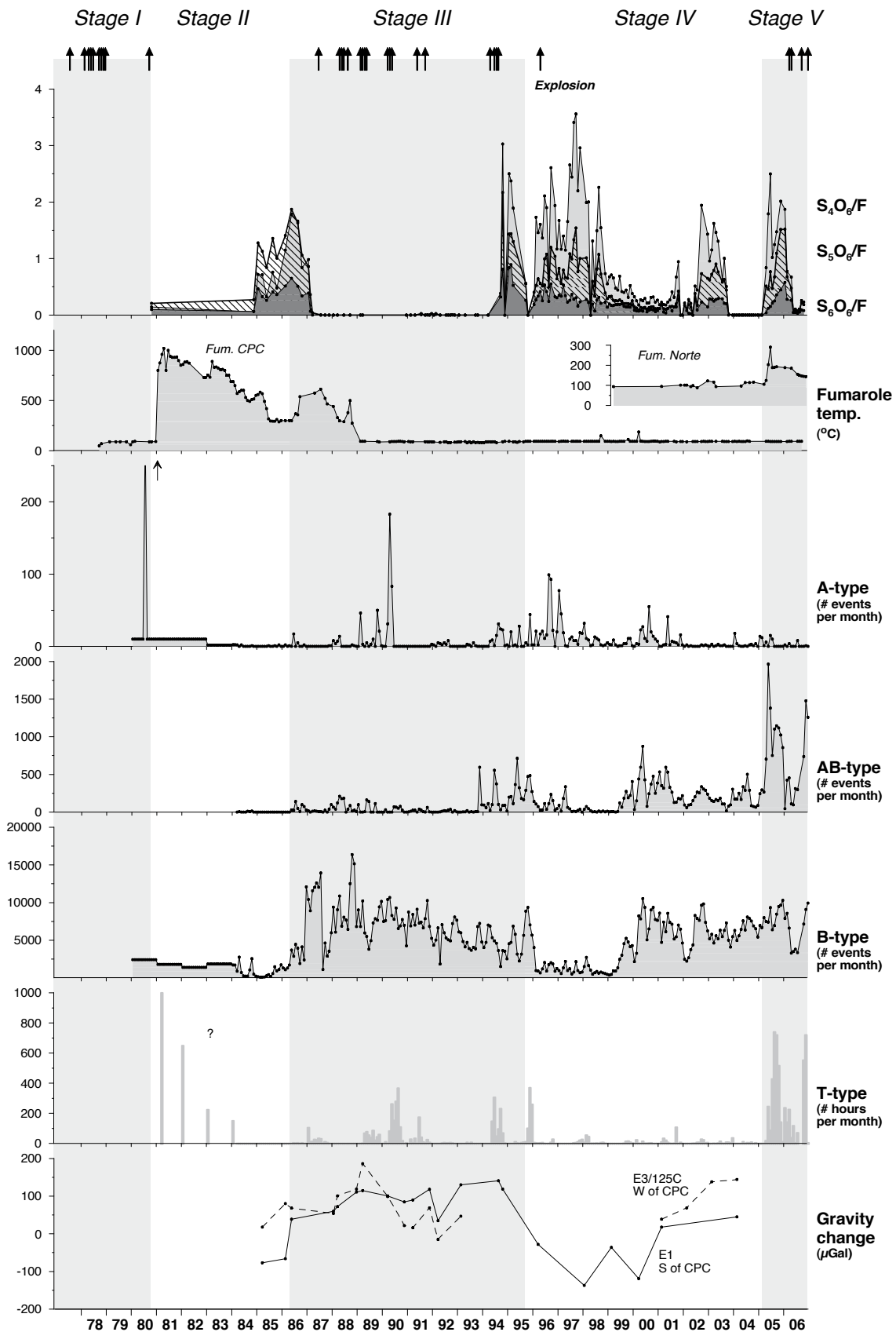
A new lake started to form in mid August–September 1994 when the peak of the rainy season was near, but it remained shallow and grey due to the vigour of subaqueous discharges (Fig. 4.3) despite the relatively heavy rainfall and the lowering of fumarolic discharge and temperature (92°C , Barquero, 1998; Venzke *et al.*, 2002-). Between October 1994 and January 1995 the lake depth approached ~15–20 meters, and in April 1995 it appeared quiet with its typical milky turquoise colour (Barquero, 1998; Martínez *et al.*, 2000; Venzke *et al.*, 2002-).

The limited data available for 1994–1995 shows that polythionates returned in significant amounts, apparently due to considerable input of volatiles. Large fluctuations in their concentrations reflect strong variations in gas fluxes. The high polythionate concentrations, particularly between September 1994 and March 1995 (except for November 1994 when they were not detected), were marked by a dominance of the tetrathionate ion: $S_4O_6^{2-} > S_5O_6^{2-} > S_6O_6^{2-}$ (Table 4.1, Figs. 4.5, 4.6, 4.7). These observations suggest that the SO_2/H_2S ratio of the subaqueous discharge still remained relatively high. After March 1995 and around the transition between Stage III and Stage IV, input of volatiles and heat seems to have reduced substantially, as indicated by the sharp decrease in polythionates, which coincides with decreasing temperature, acidity, and anion concentrations.

Water samples collected from mud pools during the recession of the crater lake show a variable chemical composition since they are mixtures of brine left during evaporation of the lake, fumarolic steam condensing at the bottom of the pools, and rainwater (Rowe, 1994). Some pools contained unusual high concentrations of polythionates (e.g. $\Sigma S_xO_6^{2-}$ 6740 mg/kg in the sample from 10 June 1994 analysed by Bokuichiro Takano). However because of their isolated and transient nature the mud pools will be ignored in the evaluation of long-term chemical trends of the lake.

4.3.2.3 Stage IV (September 1995–February 2005): Period of relative quiescence in the crater lake, significant fluctuations in polythionate concentrations and in the input of volatiles and heat

The three main polythionates were present in the lake throughout most of Stage IV, but concentrations were variable (Fig. 4.7, Table 4.1). Totals ranged between zero and 1640 ppm, suggesting drastic changes in the subaqueous fumarolic input. Despite this variability, overall trends shown by the individual species were largely parallel. Their distribution was dominated by the tetrathionate ion ($S_4O_6^{2-} > S_5O_6^{2-} > S_6O_6^{2-}$), except for some brief intervals when pentathionate prevailed ($S_5O_6^{2-} > S_4O_6^{2-} > S_6O_6^{2-}$) and total polythionate concentrations dropped, like in January 1996 and January–April 2002. An unusual distribution of hexathionate dominance ($S_5O_6^{2-} > S_6O_6^{2-} > S_4O_6^{2-}$) in a few samples collected in November 1984 and January–February 2002 might be due to analytical error or to degradation, since these samples originally contained low amounts of polythionates (cf., Takano and Watanuki, 1988). The general predominance of the tetrathionate ion throughout Stage IV suggests that the subaqueous fumaroles were relatively rich in SO_2 , with a SO_2/H_2S ratio of >0.07 during most of the time (Fig. 4.8).



During Stage IV the total influx of heat and volatiles into the crater lake was lower than in Stages I–III and V, although in early 2005 strong subaqueous fumarolic activity within the lake turned it into a convective grey and hotter lake. Sites of fumarolic degassing included more subaerial vents outside

the lake area, extending from the CPC to the crater floor and inner crater walls (see Chapter 2, Figs. 2.21 and 2.22). These conditions may explain the general relative quiescence of the lake observed during most of this stage, but field observations and the lake's chemical and physical properties reveal that it

→ *Figure 4.6.* Time series of F-normalised polythionate concentrations compared with fumarole temperatures, seismicity and microgravity changes monitored at Poás volcano. Seismicity is distinguished according to A, AB, B and tremor(T)-type characteristics, and is expressed as numbers of monthly events, except for T-type seismicity, which is given in hours per month. Arrow in the A-type panel refers to July 1980 when recorded quakes numbered in the thousands within a two-week period (Casertano *et al.*, 1985). Peaks in volcanic tremor were registered between March 1981 and 1983 but exact numbers of monthly hours are unknown (question mark in T-type panel). They coincided with very high temperatures of the CPC fumaroles (700–1020°C), which produced an SO₂ flux of about 800 tons per day (Casadevall *et al.*, 1984; Fernández, 1990). Microgravity data (Rymer *et al.*, 2005) are shown for two stations near the CPC and reflect changes relative to a base station 7 km from the crater, normalised to the difference observed in 1987. Arrows on top of the graph indicate phreatic eruptions.

continued to receive a significant input of heat and volatiles during most part of Stage IV (see Chapter 5). The marked fluctuations in polythionate patterns apparently reflect dynamic changes in activity of subaqueous vents throughout this period. Based on the mode of these variations in polythionates and in other monitored parameters, five substages can be distinguished (Fig. 4.7), the most salient features of which are described in the following sections.

4.3.2.3.1 Substage IVA (September 1995 – July 1997)

Following the last months of Stage III when polythionates concentrations were high, the transition towards this sub-stage showed first a rapid decline to values near or below detection limits. A concomitant decrease in temperature from 42 to 26°C, increase in pH from ~0.7 to 1.6 (Fig. 4.7), and shifts towards lower S₄O₆²⁻/S₅O₆²⁻ and S₄O₆²⁻/S₆O₆²⁻ ratios (Figs. 4.5 and 4.7) argue against thermal breakdown or sulphitolysis of polythionates in response to increased subaqueous input of heat and volatiles (cf. Takano *et al.*, 1994b). Instead, these observations are consistent with a weakening of the injection rate and lower SO₂/H₂S ratios of fumarolic gases, which is further supported by decreasing sulphate, chloride, and fluoride concentrations (Fig. 4.7).

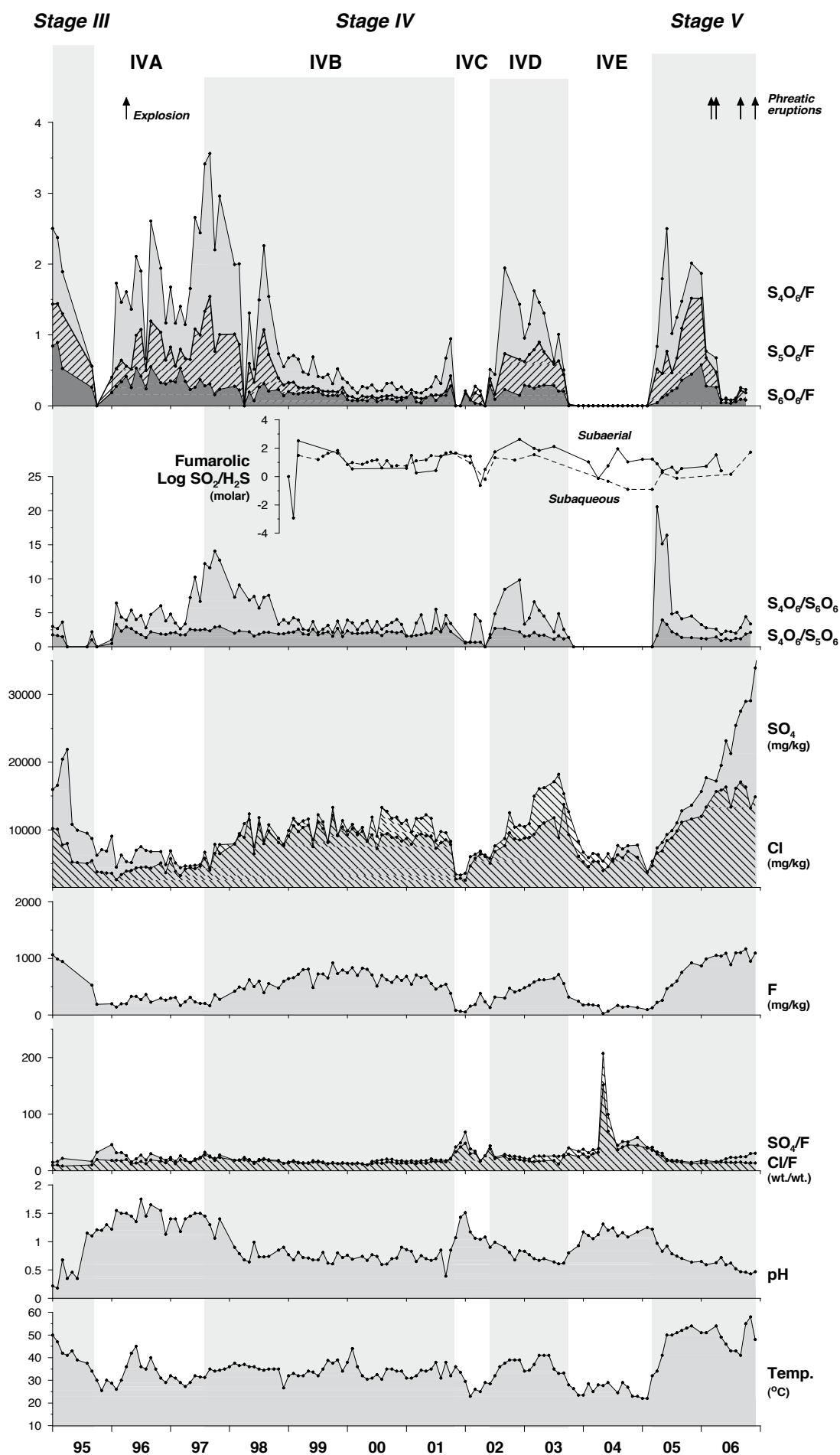
Field observations confirm this interpretation. After the new lake had started to form in mid August – September 1994, the filling rate was initially slow and the colour grey despite heavy seasonal rainfall (Fig. 4.3), due to still persistent vigorous fumarolic degassing in the lake area (Barquero, 1998; Venzke *et al.*, 2002–). However, after the lake had approached ~20 meters depth between October 1994 and January 1995, subaqueous fumarolic activity had been weak around April 1995 when the lake was fairly quiet with a typical milky turquoise colour (Barquero, 1998; OVSICORI, unpublished data). This quiescence resulted in a rapid and steady increase of the lake volume from May 1995 until 1996, which continued to grow until reaching a record level in November 1997 (Fig. 4.3). All these features strongly suggest that the decline in polythionate levels was caused by a substantial decrease in the input of heat and volatiles that might be caused by temporal partial blockage of subaqueous vents.

Polythionates reappeared in January 1996, after which significant amounts were produced in the course of this sub-

stage. Tetrathionate was the predominant species except during the initial build-up when pentathionate briefly prevailed, possibly due to relatively low SO₂/H₂S ratios of subaqueous fumaroles. The rise of concentrations in early 1996 points to renewal of fumarolic input, and the large production of polythionates towards the end of substage IVA suggests a sustained influx of gases with moderately high SO₂/H₂S ratios (Fig. 4.7) (cf. Takano, 1987; Takano and Watanuki, 1990). Although concentrations of the major anions, pH and lake temperature responded to the initial increase in gas flux, a clear correlation was obscured by dilution effects from the steady increase of the lake volume throughout 1995–1997, partly due to above-average rainfall in 1995–1997 (Fig. 4.3). In September–December 1997 reached a record level of more than 1.7×10⁶ m³ and a depth of about 45 m (Martínez *et al.*, 2000).

The renewed polythionate production coincided with the enhanced fumarolic activity at the CPC and other on-shore locations (see Chapter 2, Fig. 2.20), and with visible upwelling in the lake. More vigorous discharge around the CPC had started in September 1995, marking the beginning of Stage IV after a 7-years period of only very weak fumarolic activity around the CPC. Fumaroles with temperatures of ~93°C escaped from old and new fractures located mostly on its northern face above the lake's surface, increasing the plume height from about 100 m to an average of ~500 m until May 1996. Other accompanying features observed at the CPC were small flows of molten sulphur, indicating minimum temperatures of 113–119°C (Shriver and Atkins, 1999), minor landslides towards the lake and a constant bubbling below the lake's surface near the CPC, which would persist until the end of 2001. A small phreatic explosion at the northern face of the CPC on 8 April 1996, registered by the POA2 seismometer of OVSICORI and witnessed by park rangers and visitors, turned the colour of the lake from turquoise to greyish for almost six weeks. Strong irritating sulphur smells were noticed in the crater area around this time. Intermittently throughout the entire substage, sulphur odours also reached villages some 6 km southwest and west of the active crater (Fernández, E., pers. comm., 2007). The explosive event possibly marked the clearance of fumarolic vents, which might have been clogged by sediments and solidified sulphur that had accumulated since the previous phreatic activity in 1994. Moreover, an increase in the relative concentration of CO₂ from 0.01 to 2.1% and a shifting in the values of δ¹³C from -21.1 to -6.2‰ values measured at the CPC by Williams-Jones *et al.* (2000) indicate a greater permeability around the CPC consistent with the increase in vigour in the fumarolic degassing and the occurrence of minor landslides around the CPC. The CPC has remained one of the main sites of fumarolic degassing till present although degassing rates have been variable throughout Stages IV and V.

Elsewhere near the lake shores, initially in the southern sector, later also in the western and north-western sectors (see Chapter 2, Fig. 2.20 sites 2 and 3), new subaerial fumaroles giving off minor columns of gases (plume heights <100 m, temperatures < 97°C), started manifesting as well (the first subaerial fumaroles opened by April 1995). This opening of subaerial vents coincided with enhanced A-, AB- and B-type seismicity in 1995 (Fig. 4.6). H₂S smells from these fumaroles were frequently perceived at the lookout point and at the



→ *Figure 4.7.* Detailed time series of polythionate concentrations (normalised to fluorine) and ratios of other major anions (wt/wt) for part of Stage III, the Stage IV and the first years of Stage V, together with other crater-lake parameters and molar $\text{SO}_2/\text{H}_2\text{S}$ ratios of subaerial (measured) and subaqueous (inferred, see text) fumaroles. Note the (near) absence of polythionates in the beginning of substage IVA and in substages IVC and IVE, periods of relative quiescence in the lake, whereas the low concentrations of polythionates after 2006 is rather related to enhanced fumarolic outgassing through the lake. Concentrations of anions are given in mg/kg.

Visitor's Building of the National Park. They remained active for about 5 years until they ceased completely in June 2000 (Venzke *et al.*, 2002-; Mora *et al.*, 2004).

During the months immediately before the reappearance of the polythionates a remarkable increase in volcanic tremor had been registered (on the order of several hundreds of hours per month in October–December 1995), as well as a significant increase in AB and B-type seismicity. A peak number of A-type seismic events was recorded in November 1995 (Fig. 4.6). This upsurge in seismic activity can be interpreted as being related to build up of pressure in the magmatic/hydrothermal system, opening of cracks or conduits and movement of fluids (McNutt, 2000). Another notable observation is the sharp ~75% drop in B-type seismic events to a level similar to that observed before 1985–1986 (Fernández, 1990), after the re-appearance of strong fumarolic activity on the CPC in late 1995 – early 1996. Substage IV A is marked by a low number of B-type events, which is thought to reflect a lower degree of interaction between the subsurface heat source and the shallow aquifer beneath the crater (Barboza, V., pers. comm., 2005). This agrees with the decrease of the lake temperature and anion concentrations, and with the rise in pH and lake volume between late 1995 and early 1996.

4.3.2.3.2 Substage IVB (August 1997 – October 2001)

From mid 1997 on, polythionate concentrations first increased until reaching peak levels in early 1998, and then showed sharp drops in April (below detection limits) and June 1998 (Table 4.1, Fig. 4.7). This brief interval of low concentrations ended with a rise to values similar to those observed before April. It occurred right after maxima in the $\text{S}_4\text{O}_6^{2-}/\text{S}_5\text{O}_6^{2-}$ and $\text{S}_4\text{O}_6^{2-}/\text{S}_6\text{O}_6^{2-}$ ratios (Fig. 4.7), which can be attributed to influx of volatiles with increased $\text{SO}_2/\text{H}_2\text{S}$ ratios or higher discharge rates (Takano and Watanuki, 1990). The combined trends can be interpreted to result from the continuous injection of gas carrying increasing amounts of SO_2 . First a $\text{SO}_2/\text{H}_2\text{S}$ ratio was reached that favoured an optimum production of total polythionates, then further increased ratios resulted in a more efficient production of tetrathionate compared to the longer polythionates (cf., Fujiwara *et al.*, 1988; Fujiwara, 1989 and Maekawa, 1991, cited in Takano *et al.*, 1994b; Takano *et al.*, 2001), while an excess of SO_2 finally caused a temporary breakdown of polythionates due to sulfitolysis. A shift back to lower $\text{SO}_2/\text{H}_2\text{S}$ values then allowed their formation again (Figs. 4.7 and 4.8). The inferred increasing volatile input at the beginning of Sub-stage IVB is supported by the increasing trend of SO_4 , Cl and F concentrations in the lake (Fig. 4.7), accompanied by a drop in pH, while relatively high levels of these anions confirm that it

received a significant influx throughout this sub-stage. Hence, the brief disappearance of polythionates in April 1998 was the result of their breakdown by sulfitolysis. It is of importance to note that this absence was not followed by phreatic activity, unlike what was observed in March–June 1987.

From November 1998 to October 2001 the polythionate concentrations showed a steady decline, coinciding with a period when many new fumarolic vents opened, especially along the southern, western and eastern inner crater walls. A brief sharp increase in the concentrations of polythionates, $\text{S}_4\text{O}_6^{2-}/\text{S}_5\text{O}_6^{2-}$ and $\text{S}_4\text{O}_6^{2-}/\text{S}_6\text{O}_6^{2-}$ ratios, major anions, and temperature in September–October 2001, just before the polythionates dropped to below detection limits in November, pointed to a sudden short-lived influx of SO_2 -rich fumarolic gases into the lake. This is consistent with a peak in unreacted dissolved SO_2 which had been detected within a range of 20–255 ppm between 1999 and October 2001 (Fig. 4.7, Table APP-4.2.2, Appendix 4.2).

From August 1997 on, when the lake composition started showing a remarkable change, the concentration of chloride had been practically always higher than that of sulphate, except for the interval November 2001–April 2002, whereas between July 2004 and October 2006 the lake waters switched again to a composition richer in sulphate than in chloride which is the typical distribution (Table 4.1, Fig. 4.7). The lake level dropped by about 8 meters during the first half of 1998, and remained more or less constant throughout the next two and a half years, despite the significant amount of rainfall in 1999 and 2000, which ultimately led to a lake-level rise in the first months of 2001 (Fig. 4.3).

Field observations and geophysical data provide evidence for a relationship between volatile output and lake chemistry and polythionate behaviour:

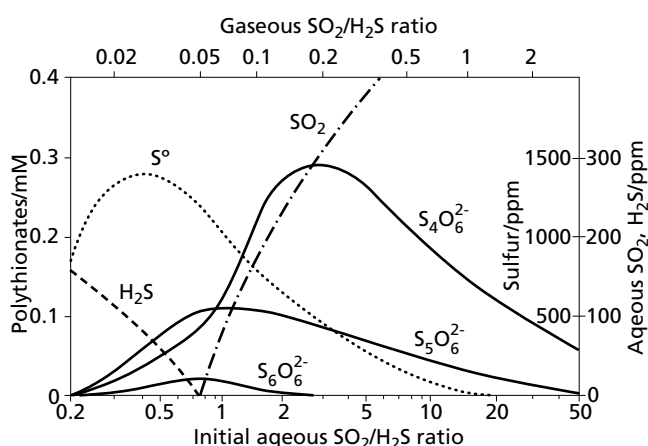


Figure 4.8. Predicted distributions of polythionates, elemental sulphur, SO_2 and H_2S in an aqueous solution. The $\text{SO}_2/\text{H}_2\text{S}$ ratio of entering fumarolic gas (upper horizontal axis) controls the initial aqueous $\text{SO}_2/\text{H}_2\text{S}$ ratio in solution (lower horizontal axis), which determines the distribution of polythionate species, elemental sulphur, and concentrations of any excess H_2S or SO_2 that remains in solution after polythionates and elemental sulphur have formed (from Takano *et al.*, 1994b).

4.3.2.3.2.1 Microgravity

Microgravity surveys detected a remarkable increase from 1996 to 2001 at stations near the N and NE lake shores, possibly signalling a magma intrusion, which must have been small and localized since most of the other stations showed continuous decreases (Rymer *et al.*, 2005). Gas release from such a supposed intrusion might be associated first with the re-appearance of polythionates in the lake, and later with their sulfitolysis-induced disappearance.

4.3.2.3.2.2 Seismicity

Numerous swarms of A-type earthquakes and an intensification of AB-type seismicity between the end of 1996 and the first months of 1997 had preceded the initial increase in volatile concentrations, whereas remarkably sustained volcanic tremors between October 1997 and March 1998 preceded the disappearance of polythionates in April 1998. In addition, a short-lived increase in A and B-type seismicity was observed (Fig. 4.6). Whereas at Poás tremors generally occur in short discontinuous events, a single episode on 21 February 1998 carried on for 2.5 hours, and 55 hours of tremor were recorded during the whole month. This incidence of sustained tremor could be related to continuous rise of magmatic/hydrothermal fluids in conduits that on one hand reached the lake bottom and led to more input of volatiles and heat, and on the other fuelled the new fumaroles around the lake.

The enhancement of hydrothermal activity in the crater area between 1999 and October 2001 coincided with increased levels of B- and AB-type seismicity after two and a half years of relative quiescence (Fig. 4.6), suggesting a stronger interaction between the subsurface heat source and the shallow aquifer beneath the crater. Tremor, which was rare in 1999, took place for less than 30 minutes per day in September–November 1999 when the plume from the CPC reached maximum altitudes (Fig. 4.9). Several unusual low-frequency earthquakes with periods of 40–175 seconds were recorded in this period as well (Barboza, V., pers. comm. 2005). An exceptional increase in tremor (a total of 108 hours were recorded only in September 2001, of which 7% corresponded to monochromatic tremor) coincided with the peak in polythionate concentrations observed in September–October.

4.3.2.3.2.3 Upwelling

The lake showed upwelling activity during most part of substages IVA and IVB, specifically in its central part and near the CPC, with sulphur globules emerging from the subaqueous vents. During September 1997–July 1998 convection was more intense and many more sulphur globules appeared. In contrast, in September–November 1998 upwelling activity and evaporation were weak, although more vigorous fumaroles continued appearing on the eastern side of the CPC. Throughout 2000 and 2001, the lake was entirely covered by an acidic whitish fog (HCl?). In August–September 2001 large bubbles (diameter of ca. 3m) were observed in the central part of the lake.

4.3.2.3.2.4 Fumarole activity

From December 1997 and throughout 1998 when the polythionates reached maximum concentrations the plume reached altitudes of nearly 600 m above the CPC. Between

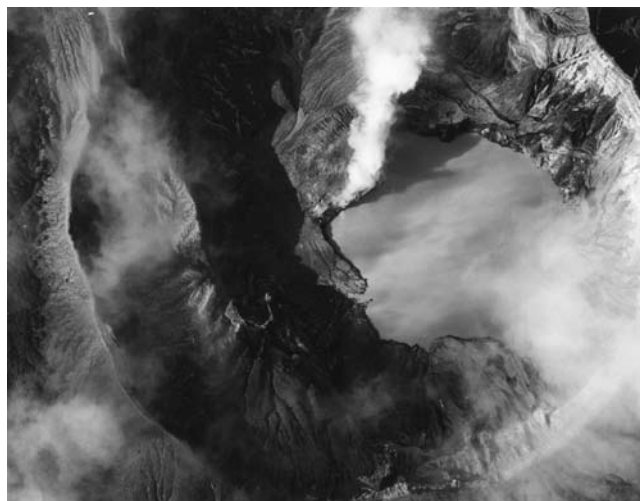


Figure 4.9. Colour version and full caption on page 140.

February 1999 and June 2000 an unusually strong plume rose 0.7–2 km above the northern fractured side of the CPC (the plume was ~2 km height in September 1999) (Fig. 4.9), and was seen in San José at 35 km southeast of the crater.

In April 1999 the first appearance of weak low-temperature fumaroles (40–95°C) was observed in the eastern sector of the crater (see Chapter 2, Fig. 2.20 site 4). In July, long concentric cracks and some springs (15–95°C) appeared here as well, coinciding with a magnitude 3.2 earthquake (Richter scale) that was felt at the summit of the volcano on 18 July 1999. More fumaroles and springs continued appearing in this area in 2000 and 2001 (Duarte *et al.*, 2003a), and most have existed till today. The widening of cracks have produced instability and collapses. On the other hand, the fumaroles in the SW sector of the crater (see Chapter 2 Fig. 2.20 sites 2 and 3) became more vigorous during the second half of 1999 when outgassing at the CPC increased. In early 2000 these fumaroles weakened and eventually disappeared in June 2000 (Venzke *et al.*, 2002–; Mora *et al.*, 2004) at the same time when degassing through the CPC diminished and the gas-vapour plume returned to altitudes of 100–500m. Gas condensates from the CPC, collected in late 1999–early 2000, showed a significant increase in sulphate, chloride and fluoride concentrations, as did the fumarole temperature (188°C in March 2000 at a poorly accessible spot on the north side of the CPC) (Fig. 4.6) (Vaselli *et al.*, 2003; Fernández *et al.*, 2003a).

4.3.2.3.2.5 Gas fluxes

Infrequent remote-sensing measurements carried out in substage IVB suggest that the SO₂ flux was of the same order of magnitude as the average of 90 tons per day measured in February 1991 by Andres *et al.*, (1992): in February 2001 the minimum average flux of SO₂ was about 40 tons per day (Fournier *et al.*, 2001, 2002), and in March 2002 the flux averaged 61 tons per day (Galle, 2002). Between the second half of 1999 and the first part of 2000 a rise in radon emission through the crater floor has been observed (García *et al.*, 2003). Significant increases in soil temperature and diffuse H₂ and CO₂ emissions in the eastern sector of the crater (see Chapter 2, Fig. 2.20 sites 4, 5, and 6), recorded in 2000–2002, have been considered as possible precursor of pending volcanic unrest

(Melián *et al.*, 2001, 2003, 2004). Alternatively, the invasion of deep hot permeable zones by meteoric water becoming enriched in volatiles and undergoing redox reactions may explain the strong fumarolic activity around the CPC, the opening of the new field in the eastern sector and the H_2 anomalies (Vaselli *et al.*, 2003, see Chapter 5). Fracturing and subsequent increase in permeability of the volcanic edifice could have been triggered by ground deformation due to the presence of a dense already crystallised magma body beneath the southern side of the lake (Fournier *et al.*, 2001) or by local tectonic earthquakes (Mora *et al.*, 2004).

4.3.2.3.2.6 Impact of gas emissions

Residents of villages located 6 km southwest and west of the active crater reported occasional strong sulphurous odours, especially during the dry months of 1998 (January–May) (Venzke *et al.*, 2002–). Between November 1999 and June 2000, a strong release of gases around the CPC and a dense fog over the lake caused severe irritation of the respiratory system, eyes and skin of OVSICORI personnel working on the crater floor.

The stronger release of toxic volcanic gases within the active crater and their apparent accumulation in the Botos Lake depression in September–December 1998 seems the most probable cause of death of a number of wild birds found at the N-NE sector of this lake (Fig. 4.1), which contains slightly acidic (pH~3.7–6.3) (OVSICORI, unpublished) $Ca-SO_4$ waters that are influenced by meteoric input of acid gases and particles from the nearby volcanic plume at the active crater of Poás that is about 1 km to the north (Figs. 2.4 and 2.5) as a result of local wind patterns.

From mid 1999 till mid 2000, fumarolic degassing caused severe acidification of the immediate surroundings with impacts on vegetation, infrastructure, quality of air and water resources, as well as human and animal health (Duarte *et al.*, 2003b; Fernández *et al.*, 2003b; OVSICORI, unpublished data). Strong sulphurous odours were reported by inhabitants of the towns of Grecia and Naranjo at about 20 km SW from the crater, and in the village of Poasito about 4 km SE from the crater.

4.3.2.3.3 Substage IVC (November 2001–May 2002)

A sharp decline in polythionates concentrations to below detection limits characterized this short interval when the lake activity was relatively calm and visible upwelling had stopped. Only very low amounts of polythionates were sporadically detected in November 2001–May 2002, with a distribution that was dominated by the pentathionate ion. The $S_4O_6^{2-}/S_5O_6^{2-}$ and $S_4O_6^{2-}/S_6O_6^{2-}$ ratios were lower than in the previous years (Fig. 4.7), suggesting that during the end of this substage the subaqueous fumaroles were significantly depleted in SO_2 . Thus the SO_2/H_2S ratios composition of the subaqueous fumarolic discharges shifted from SO_2 -excess (>0.07) to H_2S -excess (Fig. 4.8) (Fujiwara 1989; Maekawa, 1991, both cited in Takano *et al.*, 1994b).

The drop in the polythionate concentrations coincides with a sharp decrease in the concentrations of other major anions, a significant increase in pH and gradual cooling of the lake water (Fig. 4.7). Free dissolved SO_2 or H_2S gases were not detected. In addition, the lake colour changed from milky turquoise to unusual milky bluish, suggesting the presence of less

suspended particulate matter in the water column and much less subaqueous fumarolic activity (see Chapter 5).

Because the lake level volume also decreased by about 8% between January–June 2002 (Fig. 4.3), it is clear that these drastic changes were not due to dilution of the lake waters alone, but primarily signalled a substantial decrease in heat and volatile supply, presumably because of temporary blockage of the subaqueous fumarolic vents. Hence, the gas discharge within the lake area was too weak to produce appreciable amounts of polythionates.

At the same time, fumarolic activity around the CPC decreased so much that only a very weak plume of ~50 m or less was observed, although vigorous activity continued in the fumarolic field on the eastern side of the crater (see Chapter 2 Fig. 2.20 sites 4 and 5). Noticeable decreases in B and AB-type seismic events and absence of high-frequency earthquakes and volcanic tremor were recorded as well (Fig. 4.6). All these observations point to a significant decrease in the influx of volatiles and heat into the lake.

4.3.2.3.4 Substage IVD (June 2002–September 2003)

This substage is marked by renewed heating of the lake and the reappearance of polythionates in such amounts that concentrations similar to those observed in 1997–1998 were reached. Overall increasing trends of polythionate concentrations as well as $S_4O_6^{2-}/S_5O_6^{2-}$ and $S_4O_6^{2-}/S_6O_6^{2-}$ ratios coincided with substantial increases in lake–water temperatures (from 29 to 41°C) and SO_4 -Cl-F concentrations, and with a concomitant decrease of pH (Fig. 4.7). It is noteworthy that temperature and polythionate concentrations showed parallel trends with peaks around September 2002 and June 2003, whereas the SO_4 , Cl and F ions continued to accumulate until July–September 2003. Most of the cations showed a similar behaviour (see Chapter 5). This period of high polythionate concentrations was terminated by a sudden decline to below detection limits in October 2003.

Dominance of the tetrathionate ion throughout the substage and presence of unreacted dissolved SO_2 in the lake water point to relatively high SO_2/H_2S ratios of subaqueous fumarolic discharges. Yet, the patterns of the individual polythionates fluctuated and were not always parallel, especially during the second half of this period (Fig. 4.7), suggesting variations in the injection rates and proportions of SO_2 and H_2S .

It is of interest to note that during this substage the polythionate concentrations do not follow the steadily increasing trends of SO_4 , Cl and F, but show peaks that rather tend to correspond with peaks in the lake temperature (Fig. 4.7). The decrease of polythionate concentrations when major anions still continued to rise may be the result of sulphitolytic breakdown or reflect an influx of (recycled?) brine water into the lake. The latter alternative would be supported by the corresponding early decrease of the temperature and by a gradual increase in Cl/F and Cl/ SO_4 ratios in the lake observed in the second half of this substage. This might also fit into an overall pattern of increasing importance of Cl relative to the other anions observed throughout Stage IV in the lake, thermal springs, and fumarole condensates (Chapter 5).

Simultaneous with the return of polythionates, the visible appearance of the lake changed significantly. In late May–early June 2002, it recovered its typical milky sky-blue colour after

the previous months when it was clear dark blue due to the small load of suspended particles. In late July 2002 the lake had turned dark greenish due to convective circulation that transported abundant sulphur globules and bottom sediment to the surface at a spot close to its centre. Convection and floating sulphur globules were observed practically throughout the whole substage, but the activity was particularly strong in September–October 2003 when some small unusual blackish globules appeared together with the commonly observed yellow sulphur globules and pieces of molten sulphur with a ‘plastic’ texture emerged from the bottom of the lake, suggesting an intensification of subaqueous fumarolic discharges (cf. Takano *et al.*, 1994a). At the same time, especially between September 2002 and December 2003, a persistent emanation of acidic fumes (HCl evaporation?), causing respiratory problems and irritation of eyes and skin near the lake edge, formed a white acidic fog that floated over the lake surface and covered all of it at times. This fog was even denser, ~5 m thick, in November 2002 (see Chapter 2 Fig. 2.19, and Chapter 5). Constant bubbling was observed at the interface between the lake and the north face of the CPC, and water “spurts” of about 1–5 m length were sporadically ejected from the same location between August 2002 and September 2003. In spite of the large and relatively constant volume ($\sim 1.5 \times 10^6 \text{ m}^3$) the lake level showed some fluctuations, possibly the result of lower yearly rainfall in 2002 (Fig. 4.3) in combination with stronger evaporation in 2002–2003 due to increased input of heat.

Throughout this substage, the fumarolic emissions from the CPC remained modest and fairly constant, producing a plume of less than 400 m high, except for a short-lived increase up to 600 m in February 2003. New thermal springs, fumaroles and cracks continued to appear in the eastern sector, and their plumes reached altitudes between 50–300 m similar to the previous substage. In December 2002 the temperature of the Fumarola Norte (Fig. 4.6 and Table APP-4.2.1, Appendix 4.2) rose from boiling point to 122°C. Bright reddish-orange and white hydro-sulphosalts were observed along the Norte and Quebrada Roja streams (Bandy, 1938). An OVSICORI field survey in early January 2003 provided indications that a minor hydrothermal explosion had occurred somewhere in this area (see Chapter 2, Fig. 2.20 site 4) in the preceding month. The concentric cracks that had appeared in July 1999 became wider, and crater wall collapses were observed. All these manifestations thus indicate that during this period fumarolic discharges were centred in an area comprising the CPC, the lake and the eastern inner crater wall.

During this substage, B-type and AB-type seismic activity increased, reaching maximum intensity between September–October 2002. This followed a substantial drop in the number of events recorded near the end of the previous substage. The increase in seismicity accompanied the appearance of new fumaroles on the CPC and in the eastern sector of the crater. At the end of the substage, AB-type seismicity decreased dramatically, whereas B-type earthquakes continued to be recorded in large quantities.

Rare types of short-duration monochromatic tremors, which are distinct from the continuous long-duration tremors typically recorded at Poás, as well as “banded” tremors (a rarity for this volcano) and “intrusive” signals were registered by the

OVSICORI POA2 seismic station between mid-2002 and the end of 2003. For instance, eight hours of unusual volcanic tremors with monochromatic characteristics were recorded in August 2002, and were followed later that month by several “intrusive” earthquakes, consisting of a continuous two-phase signal (an initial event, usually of the AB-type, that preceded several minutes of monochromatic tremor), which could be indications of hydrofracturing or intrusive processes. Short-duration (<1 minute) monochromatic tremors and “intrusive” signals were also recorded at Poás in 1986 before renewal of geyser-like phreatic activity in the crater lake, and have been related to the ascent of minor magmatic intrusions (Fernández, 1990; Rowe *et al.*, 1992a).

During September 2002, thirty hours of polychromatic tremor were registered, as well as eleven hours of intermittent or “banded” tremor with periodic bursts separated by quiescent periods of ~3 hours. The “intrusive” signals continued sporadically between October 2002 and October 2003, together with polychromatic tremors. The “banded” tremor was again registered in October 2003 but lasted then only four hours and were alternated with periods of quiescence of ~2 hours. McNutt (1991, 1996, 2000) hypothesised that “banded” tremor, in the case of hydrothermal processes, may be caused by sequential refilling of cavities and boiling off, as occurs during geyser activity, whereas in magmatic cases it may signal flow into a shallow reservoir. At Nevado del Ruiz volcano this phenomenon has been related to prolonged intermittent venting of gas through conduits (Martinelli, 1990). The banded tremors observed at Poás between September 2002 and October 2003 may be related with “water spurts” observed at the north face of the CPC in the same period.

Microgravity surveys showed a rise in sub-surface mass in stations to the west and south of the CPC between 2000 and 2008, which has been attributed to a highly localized dendritic intrusion beneath the crater (Rymer *et al.*, 2005; Rymer, H., pers. comm. 2008), similar to other inferred events associated with microgravity rises over the last 20 years (cf., Fig. 4.6). The enhanced input of heat and SO_2 -rich volatiles into the lake system, in combination with the accompanying manifestations, might suggest that a minor intrusion of magma has occurred during substage IVD, but without triggering phreatic explosions at that time.

4.3.2.3.5 Substage IVE (October 2003–February 2005)

A sharp decline in polythionate concentrations to below detection limits in October–November 2003, comparable to that observed in substage IVC, was the start of this period of quiescence, which was marked by much less input of heat and volatiles into the lake. Polythionates were monitored and remained undetected until April 2005. In a few determinations conducted during this period only traces of dissolved SO_2 and no H_2S were detected between June 2004 and March 2005.

The lake temperature, which had decreased gradually from a maximum of 41°C in April–June 2003, ranged between 35 and 23°C during the second half of 2003 and throughout 2004. Anion concentrations decreased substantially, with fluoride showing the lowest values ever measured at Poás, hence the high SO_4/F and Cl/F ratios observed in May–June 2004. The pH increased by about 0.7 units.



Figure 4.10. A and B. Colour version and full caption on page 140.

From late 2003 on, the lake volume increased significantly and continued growing until at least 1.9 million m³ between late 2004 and early 2005 reaching the highest volume recorded since the late 70s and culminating in the flooding of part of the eastern crater floor (see chapter 2 Figs. 2.21 and 2.22). Subaerial fumaroles in this sector remained underwater for several weeks (Mora and Ramírez, 2004). This expansion of the lake was caused by extremely heavy rainfall in 2003 and 2004 (Fig. 4.3), which were the rainiest years recorded at the summit of Poás volcano in the last 15 years (ICE, 2006; Aguilar *et al.*, 2005). The volume increase was accompanied first by a subtle colour change towards the end of 2003, but at the end of April 2004 it turned from bluish green to light green. After decades of monitoring, this was the only time that such a colour has been seen (Fig. 4.10). A similar colour has also been observed in other acid crater lakes during periods of reduced gas emission (e.g., White Island, Venzke *et al.*, 2002-).

A conspicuous reduction in the vigour of fumarolic outgassing was observed around the CPC, which had been one of the main sites with persistent strong gas emission since late 1995. The plume that typically reached an altitude of 500 meters or more remained particularly low (<200m) throughout most of 2004, occasionally allowing views of some of the vents. Temperatures remained rather constant around boiling point (93–95°C). In contrast, vigorous subaerial fumarole discharges (<120°C) continued in the eastern fumarolic field. The Fumarole Norte (Fig. 4.11, Table APP-4.2.1 Appendix 4.2) showed a temperature rise up to 116°C, and some new fumaroles opened, which is consistent with the recorded high number of B and AB-type earthquakes during this substage (Fig. 4.6). During the peak of the dry season of 2005 (March–April), deposition of bright yellow-orange and white water-soluble hydroxysulfates was again observed along the Norte-Este and Este acid sulphate-springs. Landslides continued to accompany the vigorous fumarolic activity in this sector.

The large decrease in the flux of fumarolic gases and heat within the area comprising the lake and the CPC might be the consequence of a structural change which led to a localized blockage of the gas conduits beneath the lake, without affecting the fumarolic field in the eastern region that started forming in late 1998 and 1999.



4.3.2.4 Stage V (March 2005–Present): Period characterized by the reappearance of polythionates, renewal of intense subaqueous fumarolic discharge and occurrence of phreatic explosions

This period is marked by peak activity, culminating in phreatic explosions in March, April, September and December 2006, and includes the most recent polythionate data available for this study. After their absence for more than a year, the polythionates reappeared in April–May 2005, after which their abundance increased sharply until reaching maximum concentrations of about 3500 ppm between November 2005 and January 2006 (Figs. 4.3 and 4.7). Subsequently, before the onset of phreatic activity, a steep decrease was observed down to values of 150–620 ppm recorded since then (Table 4.1; Figs. 4.3 and 4.7). Excess dissolved SO₂ was detected between May 2005 and late 2006, and the order of species abundance was virtually always found to be S₄O₆ > S₅O₆ > S₆O₆, indicating that the injected gas was again characterized by a relatively high SO₂/H₂S ratio. An exception was observed in May–July 2006 when pentathionate was dominant, coinciding with the presence of 2 mg/L of dissolved H₂S in July, the first time that this species was detected since 1999. The S₄O₆/S₆O₆ ratios at the start of Stage V were the highest recorded in 25 years, while the S₄O₆/S₅O₆ ratios were close to stage IV values (Figs. 4.5 and 4.7). Tetra- and pentathionate showed fluctuating but parallel trends, whereas hexathionate was initially produced in very small amounts and gradually increased in the course of 2005–early 2006. The strong decrease of polythionates that started in late 2005–early 2006 and their low concentrations in 2006 are apparently due to sulphitolytic (and thermal?) breakdown caused by a sustained influx of SO₂-rich gases, since the decline occurred during a period of steadily increasing SO₄-Cl-F concentrations and temperature as well as decreasing pH (Fig. 4.7). Starting from 22°C in February 2005, the lake temperature rose sharply in the next months until reaching peaks of 50–54°C in the second half of 2005 (Fig. 4.7), similar to temperatures registered during the latest period of phreatic eruptions in 1994.

The intensification of activity was accompanied by marked changes in the appearance of the lake. It turned from a quiet green reservoir in 2004 (Fig. 4.10) to a grey fuming lake in early 2005 (Fig. 4.11), showing several convective cells that brought up abundant sulphur globules (see Chapter 2 Fig. 2.26). The

lake level lowered several meters throughout 2005 despite of heavy rainfall at the summit of the volcano in 2004 and 2005 (Fig. 4.3). Strong evaporation of irritating acidic fumes affected the wellbeing of volcanologists working near the lake. The sparse vegetation within the crater died rapidly due to the impact of gases and aerosols.

All these observations pointed to a significant new influx of condensing magmatic gases and heat that affected the entire lake system. From early 2005 on, the combined changes in geochemical and seismic behaviour could be interpreted as warning signals for pending phreatic outbreaks, possibly associated with new gas releases provoked by fracturing of the brittle envelope of a cooling magma body or by the intrusion of a fresh magma batch. The latter alternative would be supported by increases in micro-gravity in the south-western part of the crater floor since 2001 (Rymer *et al.*, 2004, 2005, Rymer, H., pers. comm. 2008), which would imply that magma emplacement at shallow levels must have started already about halfway Stage IV (Fig. 4.6).

In early 2006, further changes in monitored signals, pointing to a continued increase in the input of hot gases into the lake and conduits of subaerial fumaroles, were the prelude of phreatic eruptions that took place in March, after a period of almost 12 years of relative quiescence. Several mild phreatic eruptions from the lake were observed in March–April 2006. Later that year at least two small phreatic eruptions occurred on 25–26 September and another (about 30–50 m high) on 16 December was reported by a visitor of Poás Volcano National Park.

It is conceivable that deep penetration of large amounts of meteoric groundwater into the magmatic/hydrothermal system played a role in triggering the phreatic activity, given the high record of rainfall registered in 2003–early 2005, the flooding of the eastern crater floor and the rate of degassing, fracturing and wall collapses in the eastern sector (cf., Vaselli *et al.*, 2003 and Section on Substage IVB for a similar mechanism to explain the upcoming fumarolic activity in 1998–2000). However, the strong rise in all magmatic volatiles, particularly SO_2 and HF argues for new releases from a magma source as main controlling factor. A possible relationship between subaqueous and subaerial fumarolic degassing will be discussed in sections 4.5.3 and 4.5.4.



Figure 4.11. Colour version and full caption on page 138.

During Stage V, fumarolic degassing has been centred within the lake area and the fumarolic field in the eastern sector. The Fumarola Norte at the NE inner crater wall (Fig. 4.11) showed sudden changes in temperature (from 105°C in March 2005 to 200°C in May 2005), as well as changes in gas composition, especially between May 2005 and early 2006 (OVSICORI, unpublished data) (Table APP-4.2.1 in Appendix 4.2). It released large amounts of sulphur crystals that were deposited over a large area of the north-eastern inner crater wall, and molten sulphur ponds formed in the vents (OVSICORI, 2006a). Emissions from the CPC remained moderately low at <95°C, similar to the previous stage (Fig. 4.6).

In April 2006, shortly after the climax of phreatic activity, an average SO_2 flux of 84 tons/day was recorded by Mini-DOAS (OVSICORI, 2006c). This flux did not reach the Stage-II levels of 500–800 tons/day measured in 1981–1982 (Casadevall *et al.*, 1984a) but was higher than the 29 tons/day in March 2003 and similar to the 90 tons/day values in early 1991 (Andres *et al.*, 1992).

The onset of increased activity in the lake coincided with a strong increase in seismicity between April and November 2005, particularly AB-Type events and polychromatic as well as monochromatic tremors (Fig. 4.6). This was only the second time that such an intensity of volcanic tremor was recorded at Poás since the period of peak heating in 1981–1983 (Stage II), which was presumably due to a magmatic intrusion beneath the CPC (Brown *et al.*, 1991) where fumaroles reached temperatures of more than 1000°C (Fig. 4.6). It was the first time for AB-Type events, but it is unknown if they were similarly abundant in Stage II because they were not classified as such before 1984. Clear increases in AB-Type quakes and polychromatic tremor were preceded and accompanied the different intervals when phreatic eruptions occurred in 2006 (Fig. 4.6). Swarms of A-type quakes were registered in January–February, April and June–July 2005, but their number remained relatively modest compared to other periods with increased seismicity of this type.

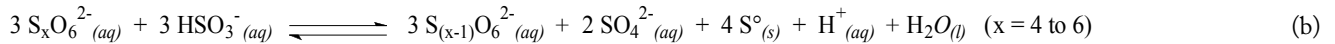
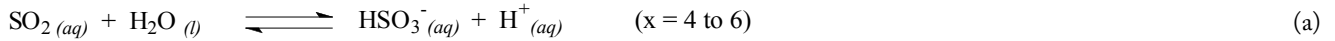
By the end of 2006, dissolved volatiles in the lake reached the highest levels of Stage V. Highest temperatures were recorded in November (58°C) after a minor dip in the previous months. The lake has retained its grey colour and continued to show strong convective activity. A few minor phreatic explosions, “mud plumes” and molten sulphur floating on the surface further characterized its behaviour. OVSICORI’s seismic stations POA2 and POA5 continued recording high levels of seismicity, particularly AB-Type quakes and tremor (Fig. 4.6).

The lake has shown strong convective activity and the seismic stations POA2 and POA5 continued recording a high number of seismic events, mainly polychromatic tremor and AB-type quakes throughout 2007. Temperature of the acid crater lake registered 57°C in July 2007 and its colour has remained virtually greyish. If the current conditions in the acid crater lake continue prevailing, then more phreatic explosions could be expected to occur anytime in the near future (see Chapter 5).

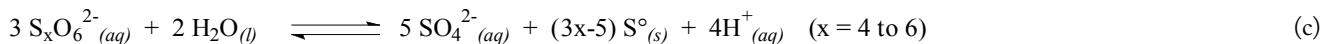
4.3.3 Polythionate – sulphate relationships

Reactions between SO_2 and H_2S that occur when subaqueous fumaroles enter the lake system usually produce a variety of sulphur species, including sulphate (mainly as bisulphate), polythionates and other aqueous species, as well as native sulphur,

depending on the $\text{SO}_2/\text{H}_2\text{S}$ ratios of the fumarolic discharges, redox conditions and flow rate. Polythionates are formed at relatively high $\text{SO}_2/\text{H}_2\text{S}$ (Goehring, 1952), reach maximum concentrations when this ratio is around 0.13 (Fujiwara, 1989; Mackawa, 1991), but are decomposed via sulphitolysis at higher ratios, yielding elemental sulphur and sulphate as main products (Takano *et al.*, 2001) according to:



Decomposition will also occur as a result of increasing temperature:



Hence, SO_2 -induced or thermal decomposition of polythionates will contribute to an (extra) increase in the total sulphate concentration of an acidic crater lake. For example, significant increases in the concentration of SO_4 in Yugama crater lake were accompanied by breakdown of polythionates during periods of phreatic activity (Takano and Watanuki, 1990).

Polythionate concentrations in the Poás lake have rapidly declined several times over the 1980–2006 period: May 1986–July 1987 (beginning of Stage III), October–November 1994 (end of Stage III), January–October 1995 (Stage III–IV transition), March–April 1998, October–November 2001, September–October 2003 (Stage IV) and November 2005–May 2006 (Stage V). These events are not obviously related to corresponding increases in sulphate concentrations (Figs. 4.5 and 4.7) because it can be inferred that several different mechanisms associated to either increased or decreased activity have played a role.

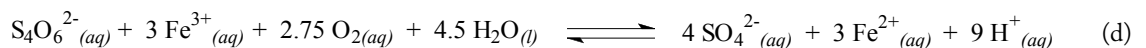
The polythionate decrease at the start of the active Stage III was accompanied by an increase in the SO_4 concentrations, pointing to sulphitolysis and/or thermal breakdown. Still, this can only account for about 16% of the increase in sulphate observed between May and July 1986 (Fig. 4.5). Hence, increased input of hot SO_2 -rich volatiles must have been responsible for most of the sulphate production, consistent with an increase in the $\text{SO}_2/\text{H}_2\text{S}$ ratio of subaqueous fumaroles, as inferred from the change in the distribution of polythionate species since August 1986 (Figs. 4.5 and 4.6) (albeit with temporary reversals in some of the late 1986 and early 1987 samples).

On the other hand, polythionate decay alone may account for the sulphate increase of March–April 1998 (Substage IVB), and November 2005–May 2006 (Stage V). It is of interest to note that precipitation of gypsum and other sulphates may obscure the inverse relation between dissolved sulphate ions and polythionate decomposition, since the lake water is usually saturated with these minerals (Chapter 5).

The three other periods in Stage IV with a temporary decline in polythionates (Fig. 4.7) require a different explanation.

Decreased SO_4 , Cl, F and dissolved SO_2 concentrations, increased pH and a drop in temperature during these periods point to a reduction or complete stop of subaqueous fumarolic venting. Marked peaks in SO_4/F and Cl/F ratios reflect a stronger decline of F relative to the other anions, which is consistent with less magmatic input, given the preferential reaction of HF with wall-rocks at relative low temperatures of volcanic gases (c.f., Symonds *et al.*, 1990; Stimac *et al.*, 2003). The observations thus provide evidence for temporary clogging of subaqueous fumarolic vents and a decrease in the temperature of the discharges. A parallel short-lived decrease in $\text{SO}_2/\text{H}_2\text{S}$ ratios of subaqueous and subaerial fumaroles during Substage IVC suggests that this blockage affected large parts of the subsurface system feeding the entire crater area. During Substage IVE, however, lower $\text{SO}_2/\text{H}_2\text{S}$ ratios were only observed in the lake water, while subaerial fumaroles showed little change.

Furthermore, the cessation of convective activity would promote the development of stratification in the water column, including an aerated shallow layer. According to experiments on Yugama lake water, polythionate concentrations are relatively insensitive to aeration (Takano and Watanuki, 1990), but the combination of oxygen and Fe^{3+} at low pH will oxidize polythionates to sulphate an order of magnitude faster than oxygen alone (Druschel *et al.*, 2003). A representative reaction describing this oxidative decomposition (cf., Takano and Watanuki, 1988; Takano *et al.*, 2001; Druschel *et al.*, 2003) could be:



Because an influx of oxygen-rich fresh rainwater into the lake will readily lead to the oxidation of Fe^{2+} into Fe^{3+} , and because low $\text{Fe}^{2+}/\text{Fe}_{\text{Total}}$ ratios (~ 0.01) were indeed measured in samples of surface water during periods with stagnant fumarolic input, it is conceivable that this mechanism has further enhanced the polythionate breakdown.

Finally, microbial decomposition of polythionates may have also contributed to their disappearance at the start of Substage IVA and during Substages IVC and IVE when

bacterial activity could have been boosted by relatively high pH conditions, as was also observed in the ultra acid crater lake of Maly Semiachik volcano (Takano *et al.*, 1995, 1997). So far, the presence of *Acidithiobacillus sp.* in the lake water of Poás and some unidentified rod-shaped and spherical acidophilic bacteria in the bottom sediments has been reported (Sugimori *et al.*, 1995, 2001), but the potential effect of micro-organisms on the polythionate budgets remains to be assessed.

4.3.4 $\text{SO}_2/\text{H}_2\text{S}$ ratios of subaqueous and subaerial fumarolic discharges

The molar $\text{SO}_2/\text{H}_2\text{S}$ ratios of subaqueous fumarolic discharges were estimated from the concentrations of dissolved unreacted SO_2 and H_2S gases measured *in situ* between 1999 and 2006, following an adapted version of the method of Togano and Ochiai (1987) (see protocol in Appendix 4.3). Since SO_2 is more soluble in water than H_2S , the $\text{SO}_2/\text{H}_2\text{S}$ ratio of gas species dissolved in the lake water will be larger than that of the injected fumarolic gases (e.g., at 20°C, SO_2 is about 15 times more soluble than H_2S in pure water, Takano *et al.*, 1994b; IUPAC 1983, 1988). The calculated $\text{SO}_2/\text{H}_2\text{S}$ ratios of subaqueous fumaroles are based on the solubilities of both gas species in pure water at 1 atmosphere for the lake temperatures measured (IUPAC 1983, 1988; Xia *et al.*, 1999, 2000), assuming that these solubilities are also valid for the acid lake waters of Poás. To estimate $\text{SO}_2/\text{H}_2\text{S}$ ratios of the subaqueous fumarolic discharges a H_2S concentration of 0.2 ppm (its detection limit) was adopted, because this species was only once detected (about 2 ppm in July 2006) over the period when dissolved gases were monitored (it was either completely consumed through chemical reactions or was present at concentrations below the detection limit). Hence, the calculated ratios reported here (Fig. 4.7) are minima. Dissolved unreacted SO_2 was always detected in significant amounts, except in November–December 2001 and June 2004–March 2005, when traces were measured at most (Table APP-4.2.2, Appendix 4.2).

The inferred $\text{SO}_2/\text{H}_2\text{S}$ ratios of subaqueous and subaerial fumaroles are similar in magnitude and, with the exception of Substage IVE, show parallel behaviour in the time series since 1999 (Fig. 4.7; see Table APP-4.2.2, Appendix 4.2 for a compilation of gas data used), which indicates that the gas that enters at the lake bottom has largely the same origin as that emitted from the on-shore vents. The disappearance of polythionates coincided with a parallel decrease in the $\text{SO}_2/\text{H}_2\text{S}$ ratios during Substage IVC, whereas in Substage IVE a decrease was only seen in the subaqueous fumaroles, suggesting a decoupling with the pathways to the subaerial vents during this period. This may imply that in Substage IVE (partial) blockage of rising gases was confined to relatively shallow levels below the lake.

Common feeding controls and gas source for subaerial and subaqueous fumaroles are further suggested by field observations. A simultaneous increase in vigour of vapour and gas release from the lake surface, the CPC fumaroles and Fumarola Norte was seen in March 2006 (Fig. 4.11), and both the lake water and the Fumarola Norte showed a simultaneous conspicuous temperature rise in 2005 (Fig. 4.6). These observations suggest, as already pointed out by Fournier *et al.*, (2004) that the

fumarolic field at the eastern terrace are the result of fractures going deep below the crater floor (see Chapter 5).

4.3.5 Relationship between polythionates and seismic activity

Seismic activity at Poás is complex, due to the dynamics of the magmatic and hydrothermal systems, their interactions and the possible combination with tectonic processes (Fernández, 1990; Rowe *et al.*, 1992a; Martínez *et al.*, 2000; Rymer *et al.*, 2000). Predominant seismic signals are the B-type or low-frequency earthquakes and the AB-type or intermediate-frequency quakes (Fig. 4.6). The B-type earthquakes are presumably generated within a few hundred metres from the surface, are concentrated below the crater floor, and may reflect interaction of liquid-gas phases within fracture conduits or bubble formation/collapse in the hydrothermal system. The AB-type quakes have been attributed mostly to fumarole-opening events. The A-type or high-frequency earthquakes (volcano-tectonic quakes) and the T-type or volcanic tremor are not as frequently observed as the B- and AB-type quakes, confirming the shallow character of most of Poás' seismic activity. The A-type quakes at Poás have been related to tectonic readjustments within the local fault system that may or may not be triggered by regional subduction-related earthquakes (Fernández, 1990). They have also been associated to fracturing of the brittle carapace of a shallow magma body underlying the hydrothermal system (Casertano *et al.*, 1987), or to mechanical fracturing of country rock, suggesting pressure build up in the system. The T-type seismicity has been interpreted as a result of continuous movement of fluids or magma through a rigid medium (Aki *et al.*, 1977; Fernández, 1990).

Relationships between seismicity and polythionates are difficult to evaluate for Stage II because of the scarcity of data. Despite high seismic activity and a high discharge rate of SO_2 from CPC fumaroles in the early 1980s, the lake was probably characterized by low polythionate concentrations with a dominance of pentathionate (Fig. 4.6), indicative of H_2S -enriched gaseous input and relatively modest activity. This illustrates a particular feature at Poás, namely that the location of major fumarolic discharge may distort a straightforward relationship between the nature of volcanic degassing and the behaviour of the lake.

The strong rise in polythionate concentrations and the shift from pentathionate to tetrathionate dominance in early 1986 were associated with an initial increase in A-, AB- and B-type earthquakes as well as short-duration harmonic tremors after a relatively quiet period. The sharp drop in polythionate concentrations to below detection limits in early 1987, approximately 3 months before renewal of phreatic activity (Rowe *et al.*, 1992b), coincided with a more conspicuous increase in seismicity, in particular B-type earthquakes. High levels of B-type seismicity remained throughout Stage III when the locus of fumarolic activity was centred within the lake area, and polythionates remained virtually below detection limits (Fig. 4.6). The enhanced heat and volatile output could have been the result of an ascending magma beneath the lake, sometime between 1985 and 1986, and subsurface hydrofracturing (Fernández, 1990; Rowe *et al.*, 1992a,b; Rymer *et al.*, 2005). Peaks in A-type seismicity and tremor in 1990 and 1991 have

been interpreted in terms of this hydrofracturing, which did promote degassing but without the intrusion of new magma at that time (Fernández, 1990; Rymer *et al.*, 2000).

Some of the swarms of A-type quakes in 1994 coincided with large peaks in tremor (Fig. 4.6), strong degassing and the occurrence of phreatic explosions that may have been associated with renewed magma ascent (Martínez *et al.*, 2000) or fracturing of the brittle envelope of the cooling magma present. Subsequent large variations in polythionates contents in the returning lake were accompanied by fluctuations in seismicity.

Changes in the contents and distribution of polythionates during Stage IV, reflecting changes in the flow rate and/or in the $\text{SO}_2/\text{H}_2\text{S}$ ratios of subaqueous fumaroles, coincided with periods of either high or low levels of seismicity. Most conspicuous is that the transition from relatively low to much higher B- and AB-type activity around 1999 roughly coincided with the sulphitolytic decline of polythionates. The enhanced input of SO_2 -rich volatiles may thus have been driven by stronger interaction between the magmatic and lake-hydrothermal systems. Following the brief quiet interval of Substage IVC, the sudden rise of polythionates, apparently prompted by an increase in volatile input, was accompanied by an increase in AB- and B-type seismicity and by uncommon tremors (Fig. 4.6). Some of these had also been recorded in 1980 when magma was intruding, but in this case, given the lack of A-type earthquakes, the tremors have been interpreted as an indication of fluid movement through pre-existent fractures (Barboza, V., 2005, pers. comm.).

The reappearance of polythionates in April 2005, their subsequent sulphitolytic or thermal breakdown and the renewal of phreatic explosions all point to the injection of hot SO_2 -rich gas promoted by the opening of conduits and the rise of fluids, as signalled by swarms of A-type events and by a dramatic increase in AB-type seismicity that preceded and accompanied the large numbers of volcanic tremors registered throughout Stage V (Fig. 4.6). The monochromatic character of some of these tremors is usually related to movement of magma or magmatic/hydrothermal fluids at depth.

In summary, changes in the concentrations and speciation of the polythionates in response to fluctuations in the rate and composition gas/volatile input are often accompanied by changes in the activity or type of seismic signals. Increases in seismicity often come together with enhanced input into the lake, leading either to the production of polythionates or to their breakdown when the flow rate of volatile and heat release reaches maximum levels. In other cases, the disappearance of polythionates can be caused by weakening or shutdown of subaqueous fumarolic discharge as supported by decrease of seismic activity as clearly observed over substage IVC.

4.3.6 Agrio River springs: seepage water from the crater lake?

A number of highly acidic chloride-sulphate springs, located 2-5 km northwest from the crater, form one of the main sources of the Agrio River (see Chapter 6). Since the end of the 19th century it has been speculated that a direct connection exists with the crater lake, and that the springs represent seepage points. Rowe (1994) and Rowe *et al.* (1995) argued that the springs represent lake brines which are diluted by meteoric ground water during flow through the NW crater wall, based

on geographical, hydro-geologic features, chemical and stable-isotope data (Craig, 1961) on the lake, the springs and the river for the period 1987-1989, as well as heat and mass-balance considerations. However, temperature, discharge rate as well as physico-chemical properties of the Agrio River have shown a long-term stability compared to the fluctuating lake properties, which may indicate that there is no direct hydraulic connection.

Over the period 1987-2002 the Agrio main spring showed constant properties ($\text{pH}=1.1-1.5$, $T=51-56^\circ\text{C}$, $\text{SO}_4=12000-17000$ ppm, $\text{Cl}=5900-6300$ ppm, $F=135-180$ ppm), whereas considerable fluctuations were seen in the crater lake over the same period (e.g., temperature ranging between 22°C and 94°C). The other springs ($\text{pH}<2.4$, $T=15-30^\circ\text{C}$) have remained fairly stable as well. Furthermore, the discharge of the Agrio springs has remained virtually unchanged (Martínez *et al.*, 2004a; see Chapter 6), even during the almost 9-year peak activity in the crater lake (mid-1986 till late-1995, Stage III), when the lake completely dried up several times. If a hydraulic connection exists, this would imply that lake water needs more than 9 years to reach the seepage springs. Although Rowe *et al.* (1995) and Sanford *et al.* (1995) estimated a travel time of 1-30 years, the above observations do not provide unequivocal evidence in favour or against the hypothesis of a direct connection.

The O-H isotopic compositions of the Agrio springs plot on the meteoric water line, except for spring-9, which is shifted towards the isotopic composition of the lake. This would be consistent with the involvement of a seeping lake-brine component (Rowe, 1994). In terms of major anion proportions the Agrio-9 spring water plots close to the trend defined by the lake water prior to 1989 (Stage II and first years of Stage III) (Fig. 4.12). The relative enrichment in F seen in the lake water since then has not propagated into the spring waters, at least not until April 2002 when the latest sample was taken. This implies that, if the spring water were largely diluted lake water, the travel time should be at least 13 years.

The frequent presence of abundant polythionates in the lake may provide further clues as to question if lake water is lost through seepage (cf. Takano *et al.*, 2004). Samples collected in 1994 and 1998-2002 were analysed but polythionates were not detected in any of the Agrio springs, which might argue against seepage. However, a similar situation has been described at Copahue volcano in Argentina where the acid crater lake contained significant amounts of polythionates, while they were absent in seepage springs emerging at a distance of not more than 150 m from the lake (Varekamp *et al.*, 2001). At Ijen volcano in Indonesia, highly acid seepage springs, issued only 0.2 km from its lake and having almost the same temperature and chemical composition, contain a concentration of total polythionates that is only 36% of that in the lake. Takano *et al.* (2004) derived a subsurface flow rate of 0.077 km/year based on the kinetics of thermal degradation of polythionates. According to groundwater transport modelling and tritium chronology the flow rate at Poás would be 0.13-1.3 km/year (Sanford *et al.*, 1995).

These examples serve to illustrate that absence of polythionates in the Agrio springs provides no conclusive evidence against a subsurface connection with the lake. A compilation of data

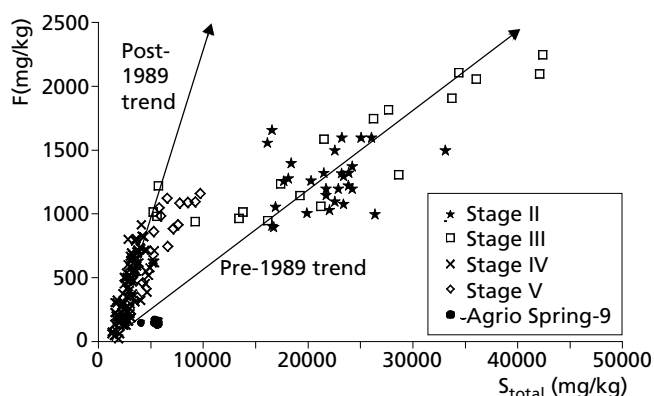


Figure 4.12. Total sulphur versus fluorine concentrations in Agrio hot spring-9 and lake samples collected throughout the five stages of activity. Agrio spring waters sampled in June 1987 and between July 1999 and April 2002 plot close to the pre-1989 trend line for the lake. Strongly enriched lake samples of Stage III are not shown.

from the lake suggests that thermal decay of polythionates occurs above about 65°C (Fig. 4.4), similar to decomposition temperatures of 55°C–60°C observed at Ruapehu crater lake (Takano *et al.*, 1994b). Given the relatively high temperature (>50°C) of the main spring despite the apparent dilution with meteoric water, thermal decomposition is a conceivable option to explain the absence of polythionates. Also, enrichment in SO₂ or bacterial activity in the aquifer cannot be ruled out. Nevertheless, the chemical signatures are no unequivocal evidence of lake seepage, since the Agrio spring waters could tap from a high-temperature, volatile-rich hydrothermal subsurface reservoir that also feeds the lake system.

4.4 Conclusions

Polythionates (tetra-, penta-, and hexathionate), together with other sulphur-bearing species, are commonly present despite the wide range of temperature, chemical composition and volume shown by the lake. They usually constitute a significant part of the total sulphur budget of the crater lake. However, polythionates are only detected as long as the lake temperature does not exceed the 60–65°C and the rate of injection of SO₂ gas into the lake is not excessive. In general, large amounts (up to 7400 mg/L) have been present during the stages in which the strongest fumarolic discharge occurred subaerially and was centred mainly outside the lake area (i.e. Stages II and IV). In contrast, polythionates have been virtually absent when strong fumarolic activity was predominantly located within the lake

area (i.e. Stage III and part of Stage V), leading to thermal and sulphitolytic breakdown. Polythionates have also been absent during quiescent periods when subaqueous fumarolic discharge was very weak, presumably due to partial sealing of feeding conduits (i.e. beginning of substage IVA, and substages IVC and IVE).

The prevailing distribution of polythionates is S₄O₆>S₅O₆>S₆O₆. This order is predominantly observed in periods when polythionate concentrations are highest, reflecting substantial influx of gas into the lake with relatively high SO₂/H₂S ratios, as was the case during large parts of Stages III, IV, and V. Relatively modest concentrations of polythionates are usually associated with the sequence S₅O₆>S₄O₆>S₆O₆, which is associated to weakened discharge rate and/or decreased SO₂/H₂S ratios of gases entering the lake, as observed during Stage II and some brief intervals later.

The observed strong fluctuations in the concentrations and speciation of polythionates over the last decades reflect the dynamic character of the magmatic-hydrothermal system of Poás. Processes that control the responsible changes in volatile input include shallow intrusions of fresh magma, fracturing of the brittle envelope of cooling magma volumes, and opening, closure or spatial shifts of conduits and fractures that determine the degree to which the volatiles are intercepted by the lake.

Polythionates provide strong signals of renewed input of SO₂-rich gas into the lake that may be followed by phreatic eruptions. An increase in polythionate concentrations, a change in their speciation from penta- to tetrathionate dominance, possibly followed by a sharp concentration drop due to sulphitolytic breakdown are typical features that are likely to precede eruptive events. It should be noted, however, that a sequence of rising polythionates followed by a drop may also occur without a subsequent phreatic eruption.

The release of sulphur-bearing gas from the magmatic-hydrothermal system can be monitored reliably through the time-series analysis of polythionate species in the lake. This approach is at least complementary to traditional gas monitoring at subaerial fumarolic vents, and has practical advantages in terms of sampling and analytical techniques.

Changes in the flux of volatiles into the lake inferred from monitoring polythionates and common anions are often also reflected by changes in the level and/or nature of seismic activity.

Absence of polythionates in the acid springs that feed Agrio River is inadequate as argument against or in favour of the hypothesis that the springs issue seepage water that is directly derived from the lake. If the acid seepage carries a lake component, then the travelling time to the NW flank should be at least 15 years.

Long-term geochemical evolution of the lake, springs and fumaroles in the active crater of Poás volcano

5.1 Introduction

This chapter presents a comprehensive overview of the evolution of Laguna Caliente during about three decades (1978–2008), integrating an extensive set of new geochemical data with published results. Data on thermal springs at the eastern crater wall as well as on fumarolic emissions are included in the discussion. Chief objective is to identify processes that regulate the properties of the lake system and the hydrothermal manifestations observed in the crater area. Temporal changes in chemical parameters are used to deduce the behaviour of the underlying magmatic/hydrothermal system.

5.2 Geological background of Poás volcano

Poás is located in central Costa Rica ($10^{\circ}12'00''\text{N}$ and $84^{\circ}13'58''\text{W}$) on the border of the Valle Central where about 60% of the population lives. Its summit elevation is 2708 m a.s.l. It is part of a Quaternary volcanic range known as the Cordillera Volcánica Central, which extends from NW to SE and includes Platanar-Porvenir, Poás, Barva, Irazú and Turrialba volcanoes (Carr *et al.*, 2007). Volcanic activity in this region is a result of the northeastward subduction of the Cocos Plate beneath the Caribbean plate (see Chapter 2 Fig. 2.1).

Starting about 1 million years ago (according to a radiometric age of an ignimbrite at its base), the eruptive activity of Poás has built a complex stratovolcano that currently rises about 1300 m from its base and encompasses a volume of about 100 km^3 (Prosser and Carr, 1987). Its rounded relatively flat shape with gentle slopes is probably the result of several caldera forming events. Two nested calderas, one about 6 km in diameter, the other elliptical with a N–S longest axis of 4 km, are important structural features in the summit area.

The currently active crater is about 1120 m in diameter along its N–S axis and is 252 m deep (Van der Laat, pers. comm. 2006). It lies at an elevation of about 2325 m.a.s.l. between two extinct volcanic centres, the Von Frantzius cone to the north and the Botos cone to the southeast. All of these structures are situated within the smaller of the nested calderas, which probably formed more than 40,000 years ago. According to geologic studies of the active crater that included old lake sediments and sulphur

deposits in pyroclastic sequences, degassing through a shallow hydrothermal system has occurred periodically over the last 10,000 years (Prosser and Carr, 1987). The Botos Cone hosts a cold and slightly acidic crater lake of about 400 m in diameter at an elevation of about 2600 m (Fig. 5.1). Radiocarbon dating of pyroclastic deposits associated with the last lava eruption from the Botos cone has yielded an age of 7540 ± 100 years (Prosser and Carr, 1987).

The strongest historic eruption (vulcanian or phreato-magmatic?) occurred in 1910 (Calvert and Calvert, 1917). During a period of moderate phreatic and phreatomagmatic eruptions in 1952–1955, the lake in the currently active summit crater disappeared and a composite pyroclastic cone (CPC), a minor lava flow and a pit crater formed. The CPC, often referred to as the “dome” (Fig. 5.1; see also Figs. 2.9 and 2.20 in Chapter 2), probably grew taller (~ 40 m) than the present 25–27 m, as about a third of it collapsed on its northern side into the pit crater, the location of the current lake (Krushensky and Escalante, 1967; Bennett and Raccichini, 1978a,b).

Prosser and Carr (1987) recognized three felsic-to-mafic sequences in the lavas and pyroclastics emplaced in a 10,000–20,000 period of the recent eruptive history that had started with caldera formation. The lavas are calc-alkaline basalts and andesites, with minor compositional differences depending on their geographic position (Prosser and Carr, 1987; Malavassi, 1991). Products from a summit group, probably the most relevant in terms of interaction with the acid lake-hydrothermal system, have SiO_2 contents ranging between 51 and 67 wt% and MgO contents between 1 and 6 wt%. All rock types carry abundant plagioclase phenocrysts, whereas basalts contain additional augite and magnetite, and andesites two pyroxenes and magnetite.

5.3 The crater-lake area

The active crater currently shows several types of surface hydrothermal manifestations: the hyper-acid crater lake that is fed by subaqueous fumaroles, subaerial fumaroles and small acid thermal springs that drained into the acid lake until they virtually disappeared in January 2007. Acid seepage springs on the NW flank of the volcano contribute to the headwaters of

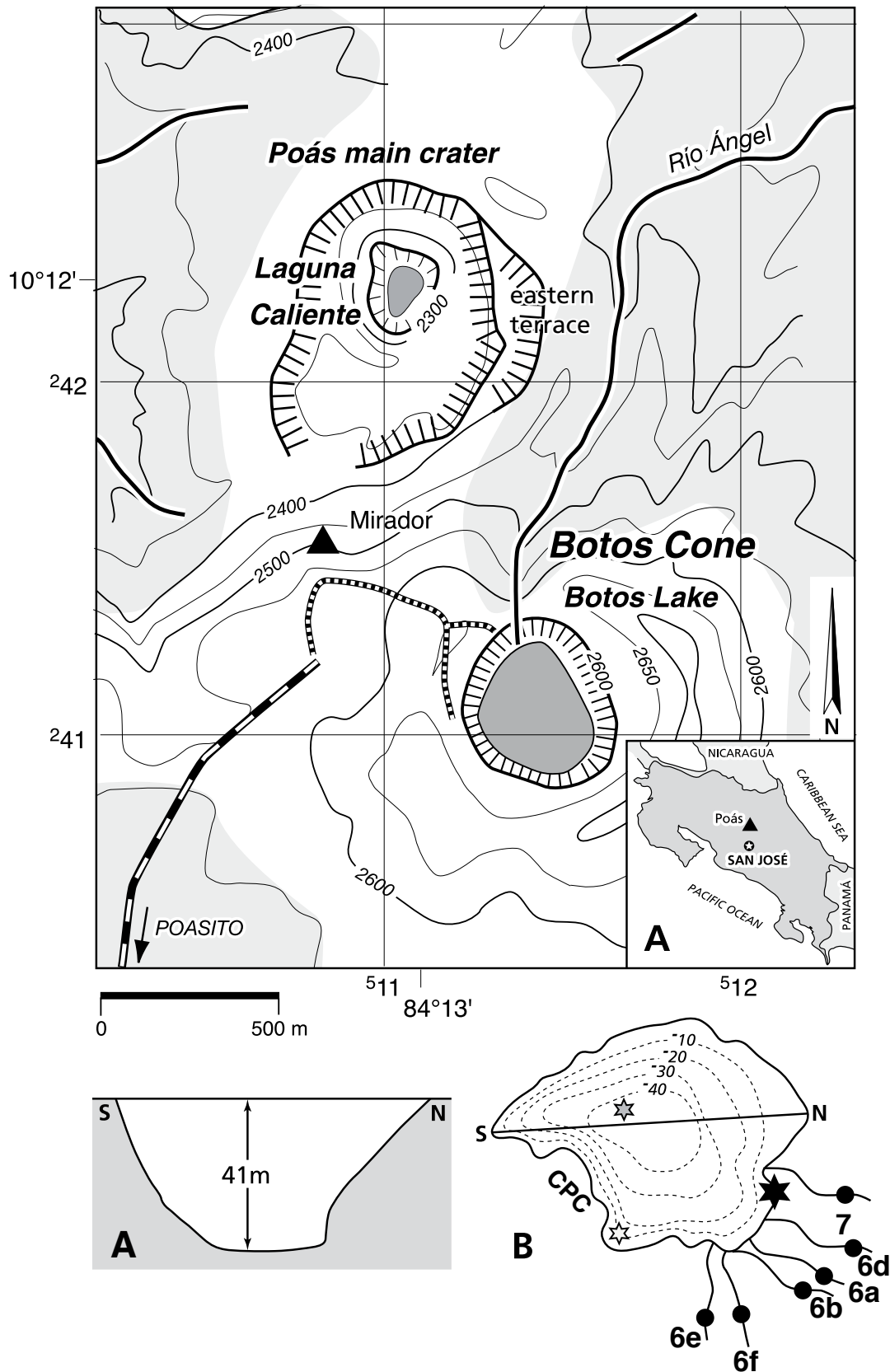


Figure 5.1. Overview of the summit area of Poás and sampling sites. Cross section (A) and bathymetric contours (B) are from a survey carried out in early 2001 (adapted from Tassi *et al.*, 2003; Duarte *et al.*, 2003c). Black star in diagram B shows the regular sampling site; grey star refers a location where samples were taken along a vertical profile during the 2001 survey; white star indicates a site near the CPC where some samples were taken in 1998 and 2001; numbered black dots on the right side of diagram B represent thermal springs at the foot of the eastern terrace that drain into the lake: 6a, 6b, and 6d – Este springs (6d is also known as Quebrada de Hierro spring); 6e – Algas Blancas Spring; 6f – Algas Verdes Spring; 7 – Norte-Este spring (cf., Vaselli *et al.*, 2003).

the Agrio River. Details of the hydrologic structure of Poás, including locations and properties of active-crater and other flank springs, are given in Rowe *et al.* (1989), Rowe *et al.* (1995), Vaselli *et al.* (2003), and Chapter 6.

The hyper-acid lake, locally known as Laguna Caliente, lies at an average elevation of 2325 m.a.s.l. When full, it has approached a diameter of approximately 320 m and depths between 45 and 55 m (Van der Laat, pers. comm. 2006). Bathymetric contours and maximum depth, based on a survey in early 2001 (Tassi *et al.*, 2006) are given in Fig. 5.1. The lake has been the site of frequent phreatic and rare phreatomagmatic eruptions. More than 60 subaqueous eruptions have been documented since the first historical eruption reported in 1828 (Martínez *et al.*, 2000; Mastin and Witter, 2000; see Chapters 2, 3, and 4). The most recent periods of phreatic explosions have been observed in 1994 and 2006–2008.

5.4 Sampling, analytical procedures and data sources

5.4.1 The acid crater lake

Compositional data for the crater-lake waters and time series presented here are compiled from new results (this work) and various published and unpublished sources. The great majority of all samples were collected on a monthly basis by a team of OVSICORI, at a designated location on the northeastern shore (Fig. 5.1). A few samples were taken near the CPC or at various depths near the centre of the lake (Vaselli *et al.*, 2003), primarily to test the chemical homogeneity of the lake. Usually, samples were stored in high-density dark polyethylene bottles without any preservation (see Martínez *et al.*, 2000; Chapters 3 and 4). The lake temperature was routinely measured *in-situ* using conventional thermocouples.

Two samples provide the earliest geochemical data on the acid crater lake of Poás volcano known so far. The oldest one included in this study was collected in February 1979 and analysed for some of the major ionic species by the Instituto Costarricense de Electricidad (ICE), using unspecified techniques (ICE, unpublished report). The other, collected on 31 October 1980 by OVSICORI, was only recently analysed (November 2002) at the Department of Earth Sciences of Utrecht University.

Other early data (November 1980 – August 1981) were reported by Casertano *et al.* (1985). Concentrations of major chemical species, determined by unknown analytical techniques, are comparable with those of the October–1980 sample. No compositional data are available for 1982, but lake temperatures were regularly measured by OVSICORI volcanologists (Venzke *et al.*, 2002–; unpublished data OVSICORI). A set of unpublished OVSICORI data covers the period January 1983–October 1984. Analyses for major anionic species were performed at the laboratory of OVSICORI within a few days or weeks after sampling, with the use of ion-selective electrodes, complexometric titration and turbidimetric techniques (Giggenbach, 1975; Martínez *et al.*, 1993).

The period November 1984–January 1991 is covered by extensive sets of major-element and other relevant geochemical data documented in Rowe (1991) and Rowe *et al.* (1992b). These samples were analysed in the late 1980s and early 1990s

by IC and ICP-AES. Data reported by Nicholson *et al.* (1992, 1993) cover the next interval (April 1991 – January 1993). These samples were analysed within a few weeks after collection by a combination of IC, classic wet-chemical techniques and ICP-AES. Both sets of results are complemented by data obtained by OVSICORI. Major anions for the period February 1993–November 1997 were generated through a joint project on volcanic emissions of OVSICORI and LAQAT (Universidad Nacional). The analyses were run at LAQAT within few days after collection of samples, using non-suppressed ion chromatography (Martínez *et al.*, 2000). Major and trace-metal concentrations in the same samples were determined at the Department of Earth Sciences (Utrecht University), as described below. It should be noted that some of the samples collected between 1988 and 1994 were presumably taken at mud pools when the lake volume was significantly reduced, since storage bottles contained considerable amounts of muddy material. As these mud pools have a highly variable composition and are largely mixtures of meteoric water and low-temperature fumarolic steam (Rowe, 1994), their results are not considered representative for the long-term evolution of the lake system, and will be mostly ignored.

All of the concentration data on dissolved anionic and cationic species for the period February 1998–November 2006 were determined at Utrecht University (2002–2007). Lake waters collected from December 2006 till March 2008 were analysed for major anions at the Laboratory of Volcano Geochemistry of OVSICORI in Costa Rica. Procedures used at both laboratories are described below.

5.4.2 Thermal springs

Thermal springs issuing acidic water at various locations on the eastern terrace from 1999 till 2006 (see Fig. 5.1), were repeatedly sampled at irregular time intervals. Geochemical data reported in Vaselli *et al.* (2003) cover the period 2000–2003. Other data are from OVSICORI (unpublished) and this work. A single average for the period 1988–1990, given in Rowe *et al.* (1995), is available for comparison with earlier spring activity within the crater.

Temperature measurements were carried out with a conventional mercury thermometer or thermocouple. Filtration was performed directly in the field by passing the waters through 0.45- μ m nylon filter membranes. Several fractions of filtered water were stored in different bottles. One was acidified with bi-distilled nitric acid for ICP-AES and ICP-MS analyses. Another was not acidified and kept for IC analysis of chloride and fluoride. A third aliquot for the analysis of Ca, Si and sulphate was immediately diluted with ultrapure water to prevent precipitation of gypsum or silica.

5.4.3 Fumarole condensates

Fumarole condensates were sampled at the CPC and on the eastern terrace between 1981 and 2003 (Fig. 2.20, sites 1 and 4 in Chapter 2). Compositions of condensate samples collected at the CPC fumarole in the 1980s come from Gemmell (1987), Prosser, (1983) and Rowe *et al.*, (1992a). Subsequent CPC data (1997–2003) and those on the eastern terrace are from Vaselli *et al.* (2003), OVSICORI (unpublished data) and this work. The latter were analysed at the laboratories of OVSICORI and

the Department of Earth Sciences (Utrecht University), using the same procedures as applied on the crater lake samples (see below). The condensate samples were filtered in the laboratory prior to analysis.

5.4.4 Analytical procedures for water samples

Physico-chemical parameters in all of the aqueous samples were determined as follows. Conductivity and pH measurements were usually performed at room temperature ($20\text{--}24\pm 2^\circ\text{C}$) with a WTW multi-parameter analyser, model Multi 340i (see Chapter 4). A large number of samples were analysed for fluoride, chloride and sulphate at the laboratories of the Department of Earth Sciences (Utrecht University) by suppressed ion chromatography (Weiss, 1986), using a fully automated Dionex chromatographic system (Model DX-120) equipped with a liquid delivery pump, a Dionex DS4-1 autosuppressor-conductivity detector with a thermally controlled conductivity cell, a Midas Spark auto-sampler, and a system controller. An anionic exchange resin Dionex IonPac analytical column (AS14, 9- μm particle size, 4x250mm), protected with a Dionex guard column (AG14, 4x50mm), was used. Running conditions were: 35°C , a 3.5 mM Na_2CO_3 /1.0 mM NaHCO_3 (pH=10.60) mobile phase, and a flow rate of 1.2 ml/min (pressure of 1632 psi).

The IC analyses conducted at the Laboratory of Volcano Geochemistry of OVSICORI-UNA were run with a fully automated Dionex microbore chromatographic system (Model ICS-3000), equipped with a quaternary liquid delivery pump, a Dionex electrolytic autosuppressor (ASRS ULTRA II), coupled to a conductivity detector with a thermally controlled conductivity cell, a Dionex AS auto-sampler, and a system controller. A Dionex IonPac anionic high-capacity analytical column (AS9-HC, 9 μm particle size, 2x250mm), protected with a Dionex guard column (AG9-HC, 2x50mm), was used. Running conditions were as follows: A 9-mM carbonate solution with a pH of 10.88, prepared on the basis of sodium carbonate was used as mobile phase. Each sample was run for 26 minutes with a flow rate of 0.250 ml/min (pressure of 1300 psi) at a temperature of 30°C . The used sample volume was 10 μl , and the flush volume between samples was 400 μl .

Reagents used for the mobile phases were analytical-grade. The aqueous samples that had not been filtered in the field were filtered in the laboratory immediately before the IC analyses, using a Sartorius polycarbonate filter-holder receiver with 0.45- μm pore-size polycarbonate membrane filters coupled to vacuum pump. The highly saline acid-lake, spring-water, and condensate samples were diluted (by weight), in order to obtain concentrations fitting within calibration lines. If necessary, samples were diluted at least twice (usually 50 and 400 times), because of disparate concentrations of analytes (relatively low concentrations of fluoride compared to sulphate and chloride). All solutions and dilutions were done with ultrapure water (18.2 megaohms). The anions were identified and quantified by comparison to certified commercial solution standards. Detector response signals were integrated using chromatography management systems (Dionex PeakNet 5.1 and Dionex Chromeleon 6.70SP2a). Standard solutions were run 5 times, and a certified synthetic solution (Dionex 7 anion certified standard solution) was injected 10 times, alternating

between batches of 20 samples during sequences of 12-hours of continuous analysis, for quality control and to monitor the response and reproducibility of peak areas and retention times (see also Chapter 4).

Since the complete set of chemical data has been generated at different laboratories with various analytical techniques over a long time span, and since long-term storage may have affected sample quality (e.g., by evaporation or precipitation of solid phases), some of the still available lake-water samples that had been analysed previously (Rowe *et al.*, 1992b; Nicholson *et al.*, 1993; OVSICORI-LAQAT laboratories) were re-analysed at Utrecht University in 2004. Comparison of anion concentrations in crater-lake samples (July 1985–November 1996) showed only random differences with the earlier results. Overall absolute deviations were on average $\sim 10\%$ (ranging from 1% to 15%) (Table APP-5.1.1, Appendix 5.1).

ICP-AES and ICP-MS analyses were performed at the Department of Earth Sciences (Utrecht University) on a group of selected samples. Concentrations of major and trace elements were determined following standardised analytical procedures. Samples were filtered in the laboratory prior to analysis, and were diluted (by weight) down to a convenient TDS range to minimise spectral interferences and blockage of instrumental components. Dilutions for ICP-AES analyses were made with a 5% v/v HNO_3 solution, prepared from a commercial solution (65% ultrapure HNO_3), and for ICP-MS analyses with a 2% v/v bi-distilled HNO_3 solution.

Certified multi-element stock solutions were used to prepare standard solutions for ICP-AES analysis. Certified solutions (matrix 5% HNO_3 , containing about 100 mg/L of each of the analytes of interest) were used for quality control. Standard solutions for ICP-MS analysis were prepared from certified multi-element stock solutions with a 5% HNO_3 matrix, so that analyte concentrations fell within the calibration range (100 ppt – 100 ppb). Standards for the ICP-AES and ICP-MS analyses were matrix matched to minimize the effects of spectral interferences.

Generally the relative standard deviation of the ICP-AES analytical determinations was within 3%, and for the ICP-MS the precision was better than 10%. In comparison, the rare earth element (REE) concentrations we measured in the Poás acid lake waters were better than $\sim 20\%$ respect to the concentrations reported earlier in a few common samples by Rowe *et al.* (1992b) and Nicholson *et al.* (1993), despite of being stored for about 20 years. The differences can be due to several factors like errors inherent to the techniques used for the analytical determinations, large dilution of samples, precipitation of mineral phases or evaporation of the samples during storage, and so on. However, according to these estimates we consider acceptable to combine the chemical data on major and minor aqueous solutes measured by the different authors with our own data sets.

5.4.5 Crater-lake volume

Crater-lake volumes have been estimated by different approaches. The data set encompasses the entire period 1978–March 2008, the years since 1995 being covered in detail. For 1978–1986, Rowe *et al.* (1992a) reported lake volumes from shore profiles using a detailed geological map of Prosser

(1983), and from estimated lake-surface areas and depths given by other workers (Barquero, 1980; Neshyba *et al.*, 1988). For 1987–1990, surface areas from oblique photographs were compared with measured or estimated lake diameters and depths (Brantley *et al.*, 1987; Venzke *et al.*, 2002–). Volumes for 1991–1993 were estimated from differences in lake levels, as measured periodically by OVSICORI personnel (OVSICORI, unpublished data). Finally, the volumes for 1994–2008 were determined from measurements of the dry lake basin geometry, made with a precision theodolite and a distance-metre, and using shore profiles and lake-level changes relative to a fixed reference point. A geometric model assumed the lake as a ~45 m deep flat-bottomed cone with a constant slope (Martínez *et al.*, 2000). A bathymetric survey carried out in February 2001 yielded a maximum depth of 41 m and a volume of about 1.2×10^6 ($\pm 10\%$) m³ (Duarte *et al.*, 2003c; Vaselli *et al.*, 2003). The most recent survey (March 2008) found a maximum depth of 26 m and a volume of 9.1×10^5 ($\pm 25\%$) m³ (Duarte *et al.*, 2008), consistent with a gradual decline since 2005. Since shores, walls and bottom surface of the lake are irregular and its morphology may not have been constant in time, it is estimated that errors in some of the reported volumes can be as high as 25%.

5.5 Results and discussion

5.5.1 Lake chemistry

Available compositional data on the acid crater lake of Poás volcano cover the period from the late 1970s till early 2008. Major-element concentrations, pH, temperatures, other relevant parameters and data sources are listed in Table 5.1 and trace-element contents in Table 5.2. Time series trends of major anions, pH, temperature, and volume of the acid lake from 1978 to 2008 are shown in Figure 5.2, along with temperatures of the subaerial fumaroles of the composite pyroclastic cone (CPC) and the Fumarole Norte at the eastern terrace, the most prominent venting sites in the crater area over long periods of time. Figure 5.3 shows time series plots of concentrations of major cations present in the acid lake. Throughout this chapter, S_T in waters or condensates refers to total sulphur measured by ICP-AES (without any oxidative treatment of the sample), whereas SO_4 refers to free sulphate present in the original solution measured by IC.

5.5.1.1 Homogeneity of the lake

The lake has been regularly sampled and monitored at a fixed site at its northeastern edge because of easy access. Virtually all of the data discussed here come from this location (Fig. 5.1). Available data from other locations and from a depth profile allow for testing to what extent measured parameters are laterally and vertically homogeneous. For this purpose, in December 1998 and February 2001 additional samples were taken at the southeastern edge of the lake, near the CPC (Fig. 5.1, diagram B).

The samples collected in the vicinity of the CPC showed generally higher concentrations of anions (Table 5.3). Differences in temperature, acidity and concentrations of solutes between the two sites were particularly large in December 1998. In contrast, differences were only modest in February 2001,

although anion concentrations were still somewhat higher near the CPC. These results are consistent with the differences in levels of fumarolic degassing observed in 1998 and 2001. The CPC showed enhanced fumarolic discharge between September 1998 and early 2000 (Venzke *et al.*, 2002–; see Chapters 2 and 4), whereas its fumarolic activity had weakened substantially between February and April 2001. Accompanying subaqueous fumarolic input near the CPC may thus have been stronger in December 1998, producing locally a more conspicuous chemical and temperature anomaly in the lake.

Neshyba *et al.* (1988) documented horizontal and vertical temperature distributions obtained in 1984, using a radio-controlled catamaran raft with air-screw propulsion. They reported a surface temperature of 48°C at the northern shore, and an increasing tendency towards the centre of the lake by about 1.4°C. Three vertical profiles yielded temperature maxima of 0.2–0.3°C warmer than surface and bottom temperatures, situated at variable depths (near surface, 14 and 20 m). Sediment temperatures were up to 2.2°C higher than temperatures of overlying bottom water. The authors interpret their findings by either a single convecting cell occupying the entire lake (upwelling near the south shore because of evident boiling, advection of the hot fluid in a surface layer to the opposite shore, downwelling of cooled fluid and return along the bottom), or a cell of torroidal shape (upwelling along the crater walls, downwelling near the centre).

In January 1987, about five months before phreatic activity in the lake resumed, Brantley *et al.* (1987) investigated its homogeneity at eight sites, using a sampling raft. They found temperatures between 58 and 64°C and densities (measured at 60°C on unfiltered samples) of 1.0575 ± 0.0015 g/cm³. Compositions were largely homogeneous, although temperatures were 1.2°C warmer at mid-depths in the centre of the lake. Slightly lower densities and temperatures along the eastern shore were tentatively attributed to input of groundwater associated with an ephemeral stream.

Vaselli *et al.* (2003) collected five samples along a vertical profile, down to 41 m depth, near the centre of the crater lake (Fig. 5.1, diagram B) during a bathymetric survey on 31 January 2001. Analytical results indicate that concentrations of major rock-forming elements and most trace elements, as well as temperature and pH were constant (Tables 5.1 and 5.2). Nonetheless, SO_4 and Cl showed an anomalous vertical distribution, while F concentrations only slightly increased toward the lake bottom.

In general, solute abundances and temperatures are fairly homogeneously distributed, promoted by convective action. Some local inhomogeneity may occur, however, depending on the vigour of convection, proximity of subaqueous discharge points of gas and thermal waters, or efficiency of mixing with meteoric water. Inhomogeneity of major volatile species will be strongest near the discharge vents.

5.5.1.2 Chemical evolution of the acid lake

The geochemistry of the crater lake has shown remarkable changes throughout the last three decades that should be seen as surface manifestation of a highly dynamic magmatic-hydrothermal system. The evolution of the lake has been divided into five main stages, a detailed description of which is given in

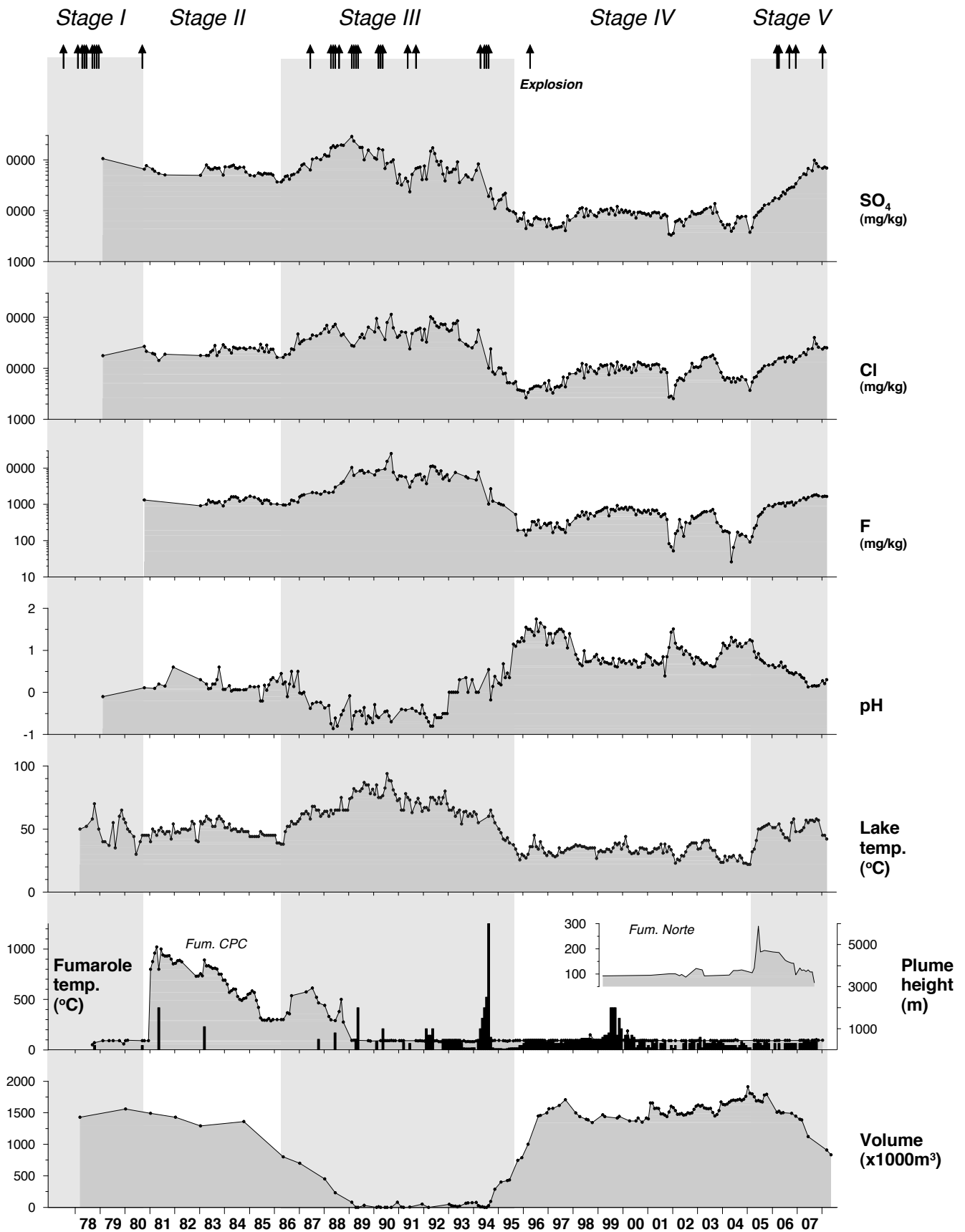


Figure 5.2. Time series plots (1978 – early 2008) of major anion concentrations (as measured by IC), pH, temperature and volume of the acid lake of Poás volcano showing variations between the five main stages distinguished. Fumarole temperatures (CPC and Fumarola Norte) and plume height (m. above the crater floor) are shown as well. Arrows on top of the figure indicate phreatic eruption events. Explosion in April 1996 may be due to a sudden unclogging of vents at the CPC, which showed only weak degassing in the previous 7 years.

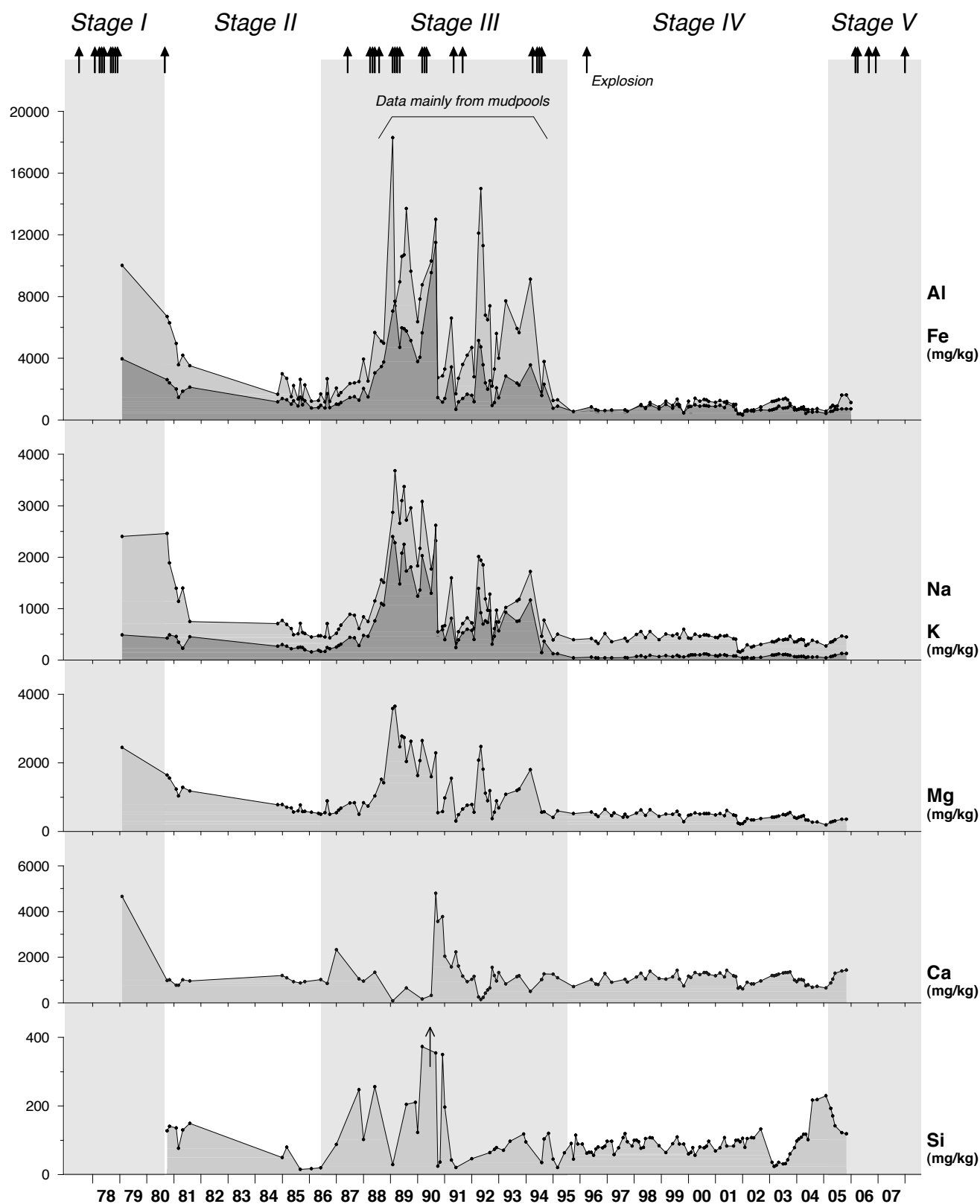


Figure 5.3. Time series plots (1979 – 2005) of major cation concentrations in the acid lake of Poás volcano for the five main stages distinguished. Arrows on top of the figure indicate phreatic eruption events and a small explosion at the CPC. Arrow in the silicon time series (Stage III) indicates concentrations higher than 300 ppm. Some of the samples collected in Stage III were presumably taken at mud pools.

Date	Temp. (°C)	pH _{lab} 24±2°C	Cond. mS/cm (24±2°C)	SO ₄	S _{total}	Cl	F	Al	Fe	Ca	Mg	Na	K	Si	Mn	P	TDS	SO ₄ /Cl	F/Cl	Mg/Cl	Data source
Stage I																					
Mar-78	50	n.d.	n.d.	n.d.	n.d.	n.d.	n.d.	n.d.	n.d.	n.d.	n.d.	n.d.	n.d.	n.d.	n.d.	n.d.	n.d.	n.d.	n.d.	n.d.	(1)
Jun-78	52	n.d.	n.d.	n.d.	n.d.	n.d.	n.d.	n.d.	n.d.	n.d.	n.d.	n.d.	n.d.	n.d.	n.d.	n.d.	n.d.	n.d.	n.d.	n.d.	(1)
Sep-78	58	n.d.	n.d.	n.d.	n.d.	n.d.	n.d.	n.d.	n.d.	n.d.	n.d.	n.d.	n.d.	n.d.	n.d.	n.d.	n.d.	n.d.	n.d.	n.d.	(1)
Oct-78	70	n.d.	n.d.	n.d.	n.d.	n.d.	n.d.	n.d.	n.d.	n.d.	n.d.	n.d.	n.d.	n.d.	n.d.	n.d.	n.d.	n.d.	n.d.	n.d.	(1)
Dec-78	50	n.d.	n.d.	n.d.	n.d.	n.d.	n.d.	n.d.	n.d.	n.d.	n.d.	n.d.	n.d.	n.d.	n.d.	n.d.	n.d.	n.d.	n.d.	n.d.	(1)
Feb-79	40	-0.10	n.d.	106000	n.d.	17700	n.d.	10000	3970	4660	2450	2400	490	n.d.	95	n.d.	147000	6.0	n.d.	0.14	(2)
Mar-79	40	n.d.	n.d.	n.d.	n.d.	n.d.	n.d.	n.d.	n.d.	n.d.	n.d.	n.d.	n.d.	n.d.	n.d.	n.d.	n.d.	n.d.	n.d.	n.d.	(1)
May-79	37	n.d.	n.d.	n.d.	n.d.	n.d.	n.d.	n.d.	n.d.	n.d.	n.d.	n.d.	n.d.	n.d.	n.d.	n.d.	n.d.	n.d.	n.d.	n.d.	(1)
Jul-79	55	n.d.	n.d.	n.d.	n.d.	n.d.	n.d.	n.d.	n.d.	n.d.	n.d.	n.d.	n.d.	n.d.	n.d.	n.d.	n.d.	n.d.	n.d.	n.d.	(1)
Aug-79	35	n.d.	n.d.	n.d.	n.d.	n.d.	n.d.	n.d.	n.d.	n.d.	n.d.	n.d.	n.d.	n.d.	n.d.	n.d.	n.d.	n.d.	n.d.	n.d.	(1)
Oct-79	60	n.d.	n.d.	n.d.	n.d.	n.d.	n.d.	n.d.	n.d.	n.d.	n.d.	n.d.	n.d.	n.d.	n.d.	n.d.	n.d.	n.d.	n.d.	n.d.	(1)
Nov-79	65	n.d.	n.d.	n.d.	n.d.	n.d.	n.d.	n.d.	n.d.	n.d.	n.d.	n.d.	n.d.	n.d.	n.d.	n.d.	n.d.	n.d.	n.d.	n.d.	(1)
Dec-79	58	n.d.	n.d.	n.d.	n.d.	n.d.	n.d.	n.d.	n.d.	n.d.	n.d.	n.d.	n.d.	n.d.	n.d.	n.d.	n.d.	n.d.	n.d.	n.d.	(1)
Jan-80	55	n.d.	n.d.	n.d.	n.d.	n.d.	n.d.	n.d.	n.d.	n.d.	n.d.	n.d.	n.d.	n.d.	n.d.	n.d.	n.d.	n.d.	n.d.	n.d.	(1)
Feb-80	50	n.d.	n.d.	n.d.	n.d.	n.d.	n.d.	n.d.	n.d.	n.d.	n.d.	n.d.	n.d.	n.d.	n.d.	n.d.	n.d.	n.d.	n.d.	n.d.	(1)
Mar-80	48	n.d.	n.d.	n.d.	n.d.	n.d.	n.d.	n.d.	n.d.	n.d.	n.d.	n.d.	n.d.	n.d.	n.d.	n.d.	n.d.	n.d.	n.d.	n.d.	(1)
May-80	44	n.d.	n.d.	n.d.	n.d.	n.d.	n.d.	n.d.	n.d.	n.d.	n.d.	n.d.	n.d.	n.d.	n.d.	n.d.	n.d.	n.d.	n.d.	n.d.	(1)
Jun-80	30	n.d.	n.d.	n.d.	n.d.	n.d.	n.d.	n.d.	n.d.	n.d.	n.d.	n.d.	n.d.	n.d.	n.d.	n.d.	n.d.	n.d.	n.d.	n.d.	(1)
Aug-80	40	n.d.	n.d.	n.d.	n.d.	n.d.	n.d.	n.d.	n.d.	n.d.	n.d.	n.d.	n.d.	n.d.	n.d.	n.d.	n.d.	n.d.	n.d.	n.d.	(1)
Stage II																					
Sep-80	45	n.d.	n.d.	n.d.	n.d.	n.d.	n.d.	n.d.	n.d.	n.d.	n.d.	n.d.	n.d.	n.d.	n.d.	n.d.	n.d.	n.d.	n.d.	n.d.	(1)
31-Oct-80	45	0.11	416	65500	23200	26900	1320	6700	2610	980	1650	2460	430	130	30	15	109000	2.4	0.05	0.06	(3)
Nov-80	45	n.d.	n.d.	77100	n.d.	21400	n.d	6300	2410	1020	1560	1890	490	140	65	n.d.	112000	3.6	n.d.	0.07	(1,4)
Dec-80	45	n.d.	n.d.	n.d.	n.d.	n.d.	n.d.	n.d.	n.d.	n.d.	n.d.	n.d.	n.d.	n.d.	n.d.	n.d.	n.d.	n.d.	n.d.	n.d.	(1)
Jan-81	40	n.d.	n.d.	n.d.	n.d.	n.d.	n.d.	n.d.	n.d.	n.d.	n.d.	n.d.	n.d.	n.d.	n.d.	n.d.	n.d.	n.d.	n.d.	n.d.	(1)
Feb-81	50	n.d.	n.d.	65700	n.d.	19600	n.d	4970	2010	780	1240	1400	460	140	60	n.d.	96000	3.4	n.d.	0.06	(1,4)
Mar-81	48	0.10	n.d.	60000	n.d.	18900	n.d	3580	1470	770	1030	1140	350	80	60	n.d.	87000	3.2	n.d.	0.05	(1,4)
Apr-81	45	n																			

Date	Temp. (°C)	pH _{lab} 24±2°C	Cond. mS/cm (24±2°C)	SO ₄	S _{total}	Cl	F	Al	Fe	Ca	Mg	Na	K	Si	Mn	P	TDS	SO ₄ /Cl	F/Cl	Mg/Cl	Data source
May-82	50	n.d.	n.d.	n.d.	n.d.	n.d.	n.d.	n.d.	n.d.	n.d.	n.d.	n.d.	n.d.	n.d.	n.d.	n.d.	n.d.	n.d.	n.d.	n.d.	(1)
Jun-82	50	n.d.	n.d.	n.d.	n.d.	n.d.	n.d.	n.d.	n.d.	n.d.	n.d.	n.d.	n.d.	n.d.	n.d.	n.d.	n.d.	n.d.	n.d.	n.d.	(1)
Jul-82	49	n.d.	n.d.	n.d.	n.d.	n.d.	n.d.	n.d.	n.d.	n.d.	n.d.	n.d.	n.d.	n.d.	n.d.	n.d.	n.d.	n.d.	n.d.	n.d.	(1)
Aug-82	50	n.d.	n.d.	n.d.	n.d.	n.d.	n.d.	n.d.	n.d.	n.d.	n.d.	n.d.	n.d.	n.d.	n.d.	n.d.	n.d.	n.d.	n.d.	n.d.	(1)
Sep-82	56	n.d.	n.d.	n.d.	n.d.	n.d.	n.d.	n.d.	n.d.	n.d.	n.d.	n.d.	n.d.	n.d.	n.d.	n.d.	n.d.	n.d.	n.d.	n.d.	(1)
Oct-82	54	n.d.	n.d.	n.d.	n.d.	n.d.	n.d.	n.d.	n.d.	n.d.	n.d.	n.d.	n.d.	n.d.	n.d.	n.d.	n.d.	n.d.	n.d.	n.d.	(1)
Nov-82	41	n.d.	n.d.	n.d.	n.d.	n.d.	n.d.	n.d.	n.d.	n.d.	n.d.	n.d.	n.d.	n.d.	n.d.	n.d.	n.d.	n.d.	n.d.	n.d.	(1)
Dec-82	40	n.d.	n.d.	n.d.	n.d.	n.d.	n.d.	n.d.	n.d.	n.d.	n.d.	n.d.	n.d.	n.d.	n.d.	n.d.	n.d.	n.d.	n.d.	n.d.	(1)
Jan-83	56	0.30	n.d.	49500	n.d.	18000	n.d.	n.d.	n.d.	n.d.	n.d.	n.d.	n.d.	n.d.	n.d.	n.d.	n.d.	2.8	0.05	n.d.	(1)
Feb-83	54	n.d.	n.d.	n.d.	n.d.	n.d.	n.d.	n.d.	n.d.	n.d.	n.d.	n.d.	n.d.	n.d.	n.d.	n.d.	n.d.	n.d.	n.d.	n.d.	(1)
Mar-83	56	n.d.	n.d.	n.d.	n.d.	n.d.	n.d.	n.d.	n.d.	n.d.	n.d.	n.d.	n.d.	n.d.	n.d.	n.d.	n.d.	n.d.	n.d.	n.d.	(1)
Apr-83	60	0.20	n.d.	79000	n.d.	18000	1000	n.d.	n.d.	n.d.	n.d.	n.d.	n.d.	n.d.	n.d.	n.d.	n.d.	4.4	0.06	n.d.	(1)
May-83	58	0.09	n.d.	70000	n.d.	18000	1300	n.d.	n.d.	n.d.	n.d.	n.d.	n.d.	n.d.	n.d.	n.d.	n.d.	3.9	0.07	n.d.	(1)
Jun-83	57	0.10	n.d.	65000	n.d.	21000	1150	n.d.	n.d.	n.d.	n.d.	n.d.	n.d.	n.d.	n.d.	n.d.	n.d.	3.1	0.05	n.d.	(1)
Jul-83	52	0.20	n.d.	65000	n.d.	22500	1200	n.d.	n.d.	n.d.	n.d.	n.d.	n.d.	n.d.	n.d.	n.d.	n.d.	2.9	0.05	n.d.	(1)
Aug-83	52	0.20	n.d.	70000	n.d.	28000	1080	n.d.	n.d.	n.d.	n.d.	n.d.	n.d.	n.d.	n.d.	n.d.	n.d.	2.5	0.04	n.d.	(1)
Sep-83	58	0.30	n.d.	67500	n.d.	18000	1100	n.d.	n.d.	n.d.	n.d.	n.d.	n.d.	n.d.	n.d.	n.d.	n.d.	3.8	0.06	n.d.	(1)
Oct-83	60	0.60	n.d.	68500	n.d.	21000	1200	n.d.	n.d.	n.d.	n.d.	n.d.	n.d.	n.d.	n.d.	n.d.	n.d.	3.3	0.06	n.d.	(1)
Nov-83	58	n.d.	n.d.	n.d.	n.d.	n.d.	n.d.	n.d.	n.d.	n.d.	n.d.	n.d.	n.d.	n.d.	n.d.	n.d.	n.d.	n.d.	n.d.	n.d.	(1)
Dec-83	56	0.07	n.d.	50000	n.d.	29000	900	n.d.	n.d.	n.d.	n.d.	n.d.	n.d.	n.d.	n.d.	n.d.	n.d.	1.7	0.03	n.d.	(1)
Jan-84	51	0.07	n.d.	72500	n.d.	26000	1200	n.d.	n.d.	n.d.	n.d.	n.d.	n.d.	n.d.	n.d.	n.d.	n.d.	2.8	0.05	n.d.	(1)
Feb-84	51	n.d.	n.d.	n.d.	n.d.	n.d.	n.d.	n.d.	n.d.	n.d.	n.d.	n.d.	n.d.	n.d.	n.d.	n.d.	n.d.	n.d.	n.d.	n.d.	(1)
Mar-84	54	0.16	n.d.	72500	n.d.	23000	1380	n.d.	n.d.	n.d.	n.d.	n.d.	n.d.	n.d.	n.d.	n.d.	n.d.	3.2	0.06	n.d.	(1)
Apr-84	49	0.03	n.d.	75000	n.d.	20000	1600	n.d.	n.d.	n.d.	n.d.	n.d.	n.d.	n.d.	n.d.	n.d.	n.d.	3.8	0.08	n.d.	(1)
May-84	50	0.06	n.d.	78000	n.d.	26000	1600	n.d.	n.d.	n.d.	n.d.	n.d.	n.d.	n.d.	n.d.	n.d.	n.d.	3.0	0.06	n.d.	(1)
Jun-84	50	0.06	n.d.	69500	n.d.	25000	1600	n.d.	n.d.	n.d.	n.d.	n.d.	n.d.	n.d.	n.d.	n.d.	n.d.	2.8	0.06	n.d.	(1)
Jul-84	48	0.06	n.d.	67500	n.d.	24000	1500	n.d.	n.d.	n.d.	n.d.	n.d.	n.d.	n.d.	n.d.	n.d.	n.d.	2.8	0.06	n.d.	(1)
Aug-84	48	0.06	n.d.	71400	n.d.	25000	1230	n.d.	n.d.	n.d.	n.d.	n.d.	n.d.	n.d.	n.d.	n.d.	n.d.	2.9	0.05	n.d.	(1)
Sep-84	50	n.d.	n.d.	n.d.	n.d.	n.d.	n.d.	n.d.	n.d.	n.d.	n.d.	n.d.	n.d.	n.d.	n.d.	n.d.	n.d.	n.d.	n.d.	n.d.	(1)
Oct-84	48	0.06	n.d.	71500	n.d.	25000	1330	n.d.	n.d.	n.d.	n.d.	n.d.	n.d.	n.d.	n.d.	n.d.	n.d.	2.9	0.05	n.d.	(1)
28-Nov-84	48	0.07	485	57700	33000	23700	1500	1670	1180	n.d.	780	710	270	n.d.	65	30	88200	2.4	0.06	0.03	(1,5)
Dec-84	48	0.22	n.d.	n.d.	n.d.	n.d.	n.d.	n.d.	n.d.	n.d.	n.d.	n.d.	n.d.	n.d.	n.d.	n.d.	n.d.	n.d.	n.d.	n.d.	(3)
24-Jan-85	44	0.14	300	49500	n.d.	25400	1660	3000	1400	1200	790	770	300	50	40	n.d.	88200	1.9	0.07	0.03	(1,5)
Feb-85	44	n.d.	n.d.	n.d.	n.d.	n.d.	1560	2700	1300	n.d.	n.d.	n.d.	n.d.	n.d.	n.d.	n.d.	n.d.	n.d.	n.d.	n.d.	(3)
20-Mar-85	44	0.13	n.d.	48200	n.d.	24700	1560	n.d.	n.d.	1100	710	690	270	80	35	n.d.	84800	2.0	0.06	0.03	(1,5)
Apr-85	44	n.d.	n.d.	n.d.	n.d.	n.d.	n.d.	n.d.	n.d.	n.d.	n.d.	n.d.	n.d.	n.d.	n.d.	n.d.	n.d.	n.d.	n.d.	n.d.	(3)
06-May-85	44	0.14	n.d.	55000	n.d.	22000	1400	1510	1030	n.d.	690	610	220	n.d.	n.d.	n.d.	84500	2.5	0.06	0.03	(1,5)
Jun-85	48	-0.20	n.d.	53000	20200	29500	1260	2240	1250	930	570	490	n.d.	n.d.	30	n.d.	88000	1.8	0.04	0.02	(3)
Jul-85	46	-0.20	n.d.	50500	n.d.	25000	1060	n.d.	n.d.	n.d.	n.d.	n.d.	n.d.	n.d.	n.d.	n.d.	n.d.	2.0	0.04	n.d.	(3)
22-Aug-85	45	0.17	n.d.	54200	n.d.	21100	1280	1350	910	n.d.	600	510	240	n.d.	n.d.	n.d.	87500	2.6	0.06	0.03	(1,5)
Sep-85	45	0.05	384	52500	21400	28500	1320	2620	1480	880	780	710	250	15	35	15	89100	1.8	0.05	0.03	(3)
09-Oct-85	45	0.18	n.d.	52900	n.d.	20700	1260	1350	980	n.d.	580	540	240	n.d.	n.d.	n.d.	84200	2.6	0.06	0.03	(1,5)
Nov-85	45	0.30	n.d.	52500	22000	23500	1030	2280	1250	930	590	520	200	n.d.	30	14	82800	2.2	0.04	0.03	(3)
Dec-85	45	0.35	n.d.	50000	n.d.	23500	n.d.	n.d.	n.d.	n.d.	n.d.	n.d.	n.d.	n.d.	n.d.	n.d.	n.d.	2.1	n.d.	n.d.	(1)

Date	Temp. (°C)	pH _{lab} 24±2°C	Cond. mS/cm (24±2°C)	SO ₄	S _{total}	Cl	F	Al	Fe	Ca	Mg	Na	K	Si	Mn	P	TDS	SO ₄ /Cl	F/Cl	Mg/Cl	Data source
Jan-86	45	n.d.	n.d.	n.d.	n.d.	n.d.	n.d.	n.d.	n.d.	n.d.	n.d.	n.d.	n.d.	n.d.	n.d.	n.d.	n.d.	n.d.	n.d.	n.d.	(3)
04-Feb-86	39	0.26	344	36900	19800	16500	1010	1210	780	n.d.	560	450	160	17	35	14	64700	2.2	0.06	0.03	(1,5)
Mar-86	39	n.d.	n.d.	n.d.	n.d.	n.d.	n.d.	n.d.	n.d.	n.d.	n.d.	n.d.	n.d.	n.d.	n.d.	n.d.	n.d.	n.d.	n.d.	n.d.	(3)
Apr-86	38	0.45	n.d.	37000	n.d.	n.d.	n.d.	n.d.	n.d.	n.d.	n.d.	n.d.	n.d.	n.d.	n.d.	n.d.	n.d.	n.d.	n.d.	n.d.	(1)
Stage III																					
02-May-86	38	0.20	n.d.	40100	n.d.	16500	970	1250	800	n.d.	530	470	190	n.d.	n.d.	n.d.	70100	2.4	0.06	0.03	(1,5)
Jun-86	48	0.25	n.d.	46500	16100	18400	950	1690	960	1030	500	470	170	20	25	n.d.	70700	2.5	0.05	0.03	(3)
Jul-86	52	-0.10	n.d.	48000	n.d.	n.d.	n.d.	n.d.	n.d.	n.d.	n.d.	n.d.	n.d.	n.d.	n.d.	n.d.	n.d.	n.d.	n.d.	n.d.	(1)
23-Aug-86	52	0.20	n.d.	41200	n.d.	18900	1020	1170	780	n.d.	550	450	170	n.d.	n.d.	n.d.	73000	2.2	0.05	0.03	(1,5)
Sep-86	56	0.50	453	50000	28600	24000	1310	2670	1700	850	890	700	240	n.d.	45	18	82400	2.1	0.05	0.04	(3)
31-Oct-86	54	0.14	n.d.	52000	n.d.	23200	1240	1200	810	n.d.	500	430	220	n.d.	n.d.	n.d.	86200	2.2	0.05	0.02	(1,5)
Nov-86	54	n.d.	n.d.	n.d.	n.d.	n.d.	n.d.	n.d.	n.d.	n.d.	n.d.	n.d.	n.d.	n.d.	n.d.	n.d.	n.d.	n.d.	n.d.	n.d.	(1)
Dec-86	56	0.50	n.d.	57500	n.d.	47500	1150	n.d.	n.d.	n.d.	n.d.	n.d.	n.d.	n.d.	n.d.	n.d.	n.d.	1.2	0.02	n.d.	(1)
10-Jan-87	58	-0.01	n.d.	64400	n.d.	30400	1590	2070	1020	2340	550	520	250	88	25	n.d.	107000	2.1	0.05	0.02	(1,5)
27-Feb-87	62	-0.03	n.d.	78600	n.d.	33700	1750	1600	1010	n.d.	620	600	280	n.d.	n.d.	n.d.	121000	2.3	0.05	0.02	(1,5)
19-Mar-87	62	0.00	n.d.	82900	n.d.	35900	1820	1780	1130	n.d.	680	680	310	n.d.	n.d.	n.d.	126000	2.3	0.05	0.02	(1,5)
Jun-87	58	-0.38	n.d.	63000	n.d.	38000	n.d.	n.d.	n.d.	n.d.	n.d.	n.d.	n.d.	n.d.	n.d.	n.d.	n.d.	1.7	n.d.	n.d.	(1)
27-Jul-87	68	-0.27	n.d.	103000	n.d.	44900	2110	2370	1460	n.d.	830	890	440	n.d.	45	28	157000	2.3	0.05	0.02	(1,5)
10-Sep-87	65	-0.23	n.d.	108000	n.d.	43400	2060	2400	1510	n.d.	840	870	430	n.d.	n.d.	n.d.	160000	2.5	0.05	0.02	(1,5)
27-Nov-87	60	-0.24	n.d.	101000	n.d.	48000	1910	2500	1290	1060	500	610	280	250	35	n.d.	157000	2.1	0.04	0.01	(1,5)
16-Jan-88	64	-0.37	n.d.	127000	n.d.	59300	2250	3940	2040	950	840	840	480	100	55	n.d.	198000	2.1	0.04	0.01	(1,5)
Feb-88	n.d.	n.d.	n.d.	118000	n.d.	70000	n.d.	n.d.	n.d.	n.d.	n.d.	n.d.	n.d.	n.d.	n.d.	n.d.	n.d.	1.7	n.d.	n.d.	(1)
02-Mar-88	60	-0.31	n.d.	118000	42000	51300	2100	2520	1500	n.d.	740	750	460	n.d.	40	30	178000	2.3	0.04	0.01	(1,5)
Apr-88	n.d.	n.d.	n.d.	172000	n.d.	n.d.	n.d.	n.d.	n.d.	n.d.	n.d.	n.d.	n.d.	n.d.	n.d.	n.d.	n.d.	n.d.	n.d.	n.d.	(1)
24-Jun-88	65	-0.61	n.d.	175000	26200	73100	2970	5670	3040	1340	1040	1150	760	260	70	n.d.	264000	2.4	0.04	0.01	(1,5)
Jul-88	n.d.	n.d.	n.d.	188000	n.d.	n.d.	n.d.	n.d.	n.d.	n.d.	n.d.	n.d.	n.d.	n.d.	n.d.	n.d.	n.d.	n.d.	n.d.	n.d.	(1)
02-Sep-88	65	-0.53	n.d.	196000	n.d.	44200	3810	5100	3450	n.d.	1520	1560	1100	n.d.	n.d.	n.d.	258000	4.4	0.09	0.03	(1,5)
07-Feb-89	75	-0.87	n.d.	286000	n.d.	28000	10400	18300	7060	90	3590	2870	2400	30	130	n.d.	359000	10	0.37	0.13	(1,5)
03-Mar-89	82	-0.55	n.d.	233000	n.d.	27200	6310	7400	7690	n.d.	3650	3680	2280	n.d.	n.d.	n.d.	293000	8.6	0.23	0.13	(1,5)
May-90	n.d.	n.d.	n.d.	156000	n.d.	n.d.	n.d.	n.d.	n.d.	n.d.	n.d.	n.d.	n.d.	n.d.	n.d.	n.d.	n.d.	n.d.	n.d.	n.d.	(1)
Oct-90	81	n.d.	n.d.	99300	n.d.	62600	7580	2740	1450	3570	550	450	550	24	30	n.d.	179000	1.6	0.12	0.01	(1,5)
8-Dec-90	73	n.d.	n.d.	34800	n.d.	40800	4860	2850	1160	3780	580	650	590	n.d.	40	n.d.	90000	0.85	0.12	0.01	(1,5)
Jan-91	74	n.d.	248	51400	7800	44000	6100	3300	1400	2050	980	670	400	n.d.	60	30	177000	1.2	0.14	0.02	(1,5)
08-Feb-91	65	-0.40	n.d.	32000	n.d.	52400	5930	n.d.	n.d.	n.d.	n.d.	n.d.	n.d.	n.d.	n.d.	n.d.	n.d.	0.61	0.11	n.d.	(1)
19-Apr-91	78	-0.42	n.d.	43600	n.d.	50700	5610	6600	3430	1580	1550	1600	810	43	80	70	217000	0.86	0.11	0.03	(1,6)
May-91	75	n.d.	n.d.	37500	n.d.	n.d.	n.d.	n.d.	n.d.	n.d.	n.d.	n.d.	n.d.	n.d.	n.d.	n.d.	n.d.	n.d.	n.d.	n.d.	(1)
Jun-91	73	n.d.	n.d.	23500	n.d.	24100	2970	1700	690	2230	310	330	240	21	20	20	99200	0.98	0.12	0.01	(1,6)
26-Jul-91	63	-0.38	n.d.	51300	15400	47900	4310	2700	1170	1620	490	550	390	n.d.	30	30	112000	1.1	0.09	0.01	(1,6)
24-Sep-91	71	-0.44	n.d.	67800	22100	55800	6320	3600	1390	1170	660	710	530	n.d.	43	44	213000	1.2	0.11	0.01	(1,6)
21-Oct-91	74	n.d.	n.d.	70000	n.d.	58500	6560	n.d.	n.d.	n.d.	n.d.	n.d.	n.d.	n.d.	n.d.	n.d.	n.d.	1.2	0.11	n.d.	(1,6)
01-Nov-91	70	-0.50	371	72100	n.d.	61100	6790	4200	1670	940	770	820	600	n.d.	50	57	233000	1.2	0.11	0.01	(1,6)
12-Dec-91	64	-0.30	n.d.	40700	n.d.	35800	4690	n.d.	n.d.	n.d.	n.d.	n.d.	n.d.	n.d.	n.d.	n.d.	n.d.	1.1	0.13	n.d.	(1)
17-Jan-92	67	-0.50	n.d.	75000	21700	58700	5750	4690	1600	1040	780	720	580	46	55	45	223000	1.3	0.10	0.01	(3)

Date	Temp. (°C)	pH _{lab} 24±2°C	Cond. mS/cm (24±2°C)	SO ₄	S _{total}	Cl	F	Al	Fe	Ca	Mg	Na	K	Si	Mn	P	TDS	SO ₄ /Cl	F/Cl	Mg/Cl	Data source
07-Feb-92	67	-0.60	n.d.	41600	n.d.	32900	3700	2800	1190	1160	560	610	400	n.d.	40	38	85700	1.3	0.11	0.02	(1,7)
3-Apr-92	75	-0.80	n.d.	147000	n.d.	102000	11000	12100	5140	260	2080	2010	1390	n.d.	135	170	411000	1.4	0.11	0.02	(1,7)
May-92	75	-0.80	n.d.	172000	51900	94100	11200	15000	4740	150	2480	1940	920	n.d.	155	180	393000	1.8	0.12	0.03	(1,7)
Jun-92	73	-0.54	n.d.	132000	n.d.	80300	10700	11300	3580	240	1820	1850	700	n.d.	115	150	334000	1.6	0.13	0.02	(1,7)
24-Jul-92	70	-0.60	n.d.	94200	n.d.	67800	8260	6800	2400	430	1120	1190	760	n.d.	70	89	270000	1.4	0.12	0.02	(1,7)
21-Aug-92	75	-0.60	n.d.	78900	n.d.	63300	8670	6500	1990	570	900	970	730	n.d.	60	70	249000	1.2	0.11	0.01	(1,7)
18-Sep-92	70	-0.60	n.d.	93100	27900	74400	8390	7400	2540	660	1190	1280	960	n.d.	75	81	293000	1.3	0.11	0.02	(1,7)
07-Oct-92	75	-0.50	n.d.	52400	n.d.	71600	5060	2200	930	1560	380	410	310	n.d.	25	34	136000	0.73	0.07	0.01	(1,7)
19-Nov-92	80	-0.50	n.d.	38400	13400	73000	5720	3300	1130	1200	560	610	460	74	38	45	261000	0.53	0.08	0.01	(1,7)
Dec-92	70	-0.50	n.d.	69300	n.d.	58500	6490	5600	2090	970	890	970	740	78	55	70	231000	1.2	0.11	0.02	(1,7)
23-Jan-93	65	0.00	n.d.	56100	21900	54000	4510	4000	1440	1330	690	740	570	n.d.	40	53	203000	1.0	0.08	0.01	(7,8,3)
25-Feb-93	65	0.00	n.d.	58000	n.d.	56200	n.d.	n.d.	n.d.	n.d.	n.d.	n.d.	n.d.	n.d.	n.d.	n.d.	n.d.	1.0	n.d.	n.d.	(8,1)
Mar-93	67	0.00	n.d.	65000	n.d.	75500	n.d.	n.d.	n.d.	n.d.	n.d.	n.d.	n.d.	71	n.d.	n.d.	n.d.	0.86	n.d.	n.d.	(8,1)
2-Apr-93	60	0.00	200	65000	24100	75500	7550	7710	2840	840	1080	1020	930	n.d.	80	76	163000	0.86	0.10	0.01	(8,1)
May-93	63	0.00	n.d.	91000	n.d.	85600	n.d.	n.d.	n.d.	n.d.	n.d.	n.d.	n.d.	n.d.	n.d.	n.d.	n.d.	1.1	n.d.	n.d.	(8,1)
Jun-93	65	0.30	n.d.	35700	n.d.	36400	n.d.	n.d.	n.d.	n.d.	n.d.	n.d.	n.d.	97	n.d.	n.d.	n.d.	0.98	n.d.	n.d.	(8,1)
09-Sep-93	64	0.35	n.d.	50400	18500	29600	5840	5920	2390	1150	1190	1150	750	n.d.	80	n.d.	98700	1.7	0.20	0.04	(8,1)
22-Oct-93	60	0.00	n.d.	46000	17800	27600	5330	5670	2260	1190	1240	1180	760	n.d.	78	58	91400	1.7	0.19	0.04	(8,1)
Dec-93	60	0.30	n.d.	40700	n.d.	25300	n.d.	n.d.	n.d.	n.d.	n.d.	n.d.	n.d.	118	n.d.	n.d.	n.d.	1.6	n.d.	n.d.	(8,1)
Feb-94	62	0.00	n.d.	62100	n.d.	32800	4720	n.d.	n.d.	n.d.	n.d.	n.d.	n.d.	n.d.	n.d.	n.d.	n.d.	1.9	0.14	n.d.	(8,1)
12-Mar-94	55	0.00	n.d.	83100	31300	56500	7780	9130	3560	510	1810	1720	1170	n.d.	135	99	166000	1.5	0.14	0.03	(8,1)
Aug-94	60	0.54	n.d.	19200	5200	10100	1020	1830	1570	1020	570	470	145	35	30	n.d.	36000	1.9	0.10	0.06	(8,1)
23-Sep-94	65	-0.18	483	27000	21800	24000	2660	3790	2320	1270	580	780	365	103	35	n.d.	65200	1.1	0.11	0.02	(8,1)
21-Oct-94	60	0.14	n.d.	17000	n.d.	8470	1220	n.d.	n.d.	n.d.	n.d.	n.d.	n.d.	n.d.	n.d.	n.d.	n.d.	2.0	0.14	n.d.	(8,1)
15-Nov-94	55	0.38	n.d.	11000	n.d.	7640	n.d.	n.d.	n.d.	n.d.	n.d.	n.d.	n.d.	121	n.d.	n.d.	n.d.	1.4	n.d.	n.d.	(8,1)
6-Jan-95	50	0.22	n.d.	16000	21200	10200	1060	1270	760	1260	410	390	125	45	20	n.d.	36600	1.6	0.10	0.04	(8,1)
03-Feb-95	47	0.18	n.d.	16600	n.d.	10100	990	n.d.	n.d.	n.d.	n.d.	n.d.	n.d.	n.d.	n.d.	n.d.	n.d.	1.6	0.10	n.d.	(8,1)
10-Mar-95	42	0.68	139	20500	9200	7780	950	1300	900	1100	600	500	120	20	35	10	37300	2.6	0.12	0.08	(8,1)
Apr-95	41	0.35	n.d.	21900	n.d.	8000	n.d.	n.d.	n.d.	n.d.	n.d.	n.d.	n.d.	n.d.	n.d.	n.d.	n.d.	2.7	n.d.	n.d.	(8,1)
May-95	43	0.46	n.d.	10800	n.d.	5240	n.d.	n.d.	n.d.	n.d.	n.d.	n.d.	n.d.	n.d.	n.d.	n.d.	n.d.	2.1	n.d.	n.d.	(8,1)
Jun-95	39	0.35	n.d.	9970	n.d.	5180	n.d.	n.d.	n.d.	n.d.	n.d.	n.d.	n.d.	64	n.d.	n.d.	n.d.	1.9	n.d.	n.d.	(8,1)
Aug-95	38	1.15	n.d.	9510	n.d.	5010	n.d.	n.d.	n.d.	n.d.	n.d.	n.d.	n.d.	n.d.	n.d.	n.d.	n.d.	1.9	n.d.	n.d.	(8,1)
Stage IV																					
Substage IVA																					
08-Sep-95	34	1.10	n.d.	8710	n.d.	5440	530	n.d.	n.d.	n.d.	n.d.	n.d.	n.d.	90	n.d.	n.d.	n.d.	1.6	0.10	n.d.	(8,1)
20-Oct-95	30	1.21	41	6230	3100	3800	190	490	560	710	520	400	45	45	30	3.6	13000	1.6	0.05	0.14	(8,1)
Nov-95	26	1.20	n.d.	7050	n.d.	3710	n.d.	n.d.	n.d.	n.d.	n.d.	n.d.	n.d.	115	n.d.	n.d.	n.d.	1.9	n.d.	n.d.	(8,1)
Dec-95	30	1.30	n.d.	6860	n.d.	3630	n.d.	n.d.	n.d.	n.d.	n.d.	n.d.	n.d.	89	n.d.	n.d.	n.d.	1.9	n.d.	n.d.	(8,1)
5-Jan-96	29	1.22	39	9060	n.d.	3590	200	n.d.	n.d.	n.d.	n.d.	n.d.	n.d.	n.d.	n.d.	n.d.	n.d.	2.5	0.05	n.d.	(8,1)
23-Feb-96	26	1.55	n.d.	4480	n.d.	2630	140	n.d.	n.d.	n.d.	n.d.	n.d.	n.d.	89	n.d.	n.d.	n.d.	1.7	0.05	n.d.	(8,1)
22-Mar-96	30	1.50	n.d.	6270	n.d.	3370	200	n.d.	n.d.	n.d.	n.d.	n.d.	n.d.	n.d.	n.d.	n.d.	n.d.	1.9	0.06	n.d.	(8,1)
26-Apr-96	36	1.50	n.d.	5290	n.d.	3910	200	n.d.	n.d.	n.d.	n.d.	n.d.	n.d.	63	n.d.	n.d.	n.d.	1.4	0.05	n.d.	(8,1)
10-May-96	42	1.45	n.d.	5180	n.d.	4020	330	n.d.	n.d.	n.d.	n.d.	n.d.	n.d.	65	n.d.	n.d.	n.d.	1.3	0.08	n.d.	(8,1)

Date	Temp. (°C)	pH _{lab} 24±2°C	Cond. mS/cm (24±2°C)	SO ₄	S _{total}	Cl	F	Al	Fe	Ca	Mg	Na	K	Si	Mn	P	TDS	SO ₄ /Cl	F/Cl	Mg/Cl	Data source
14-Jun-96	45	1.35	57	7000	4000	4390	330	630	850	1030	570	420	55	65	25	n.d.	15400	1.6	0.07	0.13	(8.1)
24-Jul-96	36	1.75	n.d.	7520	n.d.	4460	270	n.d.	n.d.	n.d.	n.d.	n.d.	n.d.	56	n.d.	n.d.	n.d.	1.7	0.06	n.d.	(8.1)
8-Aug-96	35	1.45	n.d.	6970	3100	4510	360	560	680	830	490	370	45	75	25	n.d.	15400	1.5	0.08	0.11	(8.1)
27-Sep-96	40	1.65	n.d.	6780	2960	4320	220	510	620	810	440	320	40	78	20	n.d.	15100	1.6	0.05	0.10	(8.1)
28-Nov-96	31	1.55	n.d.	6790	n.d.	5110	300	n.d.	n.d.	n.d.	n.d.	n.d.	n.d.	78	n.d.	n.d.	n.d.	1.3	0.06	n.d.	(8.1)
18-Dec-96	29	1.13	48	4870	2930	3650	260	550	620	1290	650	520	43	83	22	3.3	13100	1.3	0.07	0.18	(8.1)
7-Jan-97	32	1.40	n.d.	6880	n.d.	5750	290	n.d.	n.d.	n.d.	n.d.	n.d.	n.d.	97	n.d.	n.d.	n.d.	1.2	0.05	n.d.	(8.1)
04-Feb-97	31	1.40	n.d.	5110	n.d.	3850	310	n.d.	n.d.	n.d.	n.d.	n.d.	n.d.	n.d.	n.d.	n.d.	n.d.	1.3	0.08	n.d.	(8.1)
03-Mar-97	29	1.18	43	4410	2830	3260	170	540	650	910	470	360	43	97	26	3.1	11400	1.4	0.05	0.14	(8.1)
17-Apr-97	27	1.40	n.d.	4640	n.d.	4230	230	n.d.	n.d.	n.d.	550	770	n.d.	58	n.d.	n.d.	n.d.	1.1	0.05	0.13	(8.1)
14-May-97	29	1.45	n.d.	4640	n.d.	4420	310	n.d.	n.d.	n.d.	n.d.	n.d.	n.d.	n.d.	n.d.	n.d.	n.d.	1.0	0.07	n.d.	(8.1)
04-Jun-97	32	1.50	n.d.	4750	n.d.	4280	230	n.d.	n.d.	n.d.	n.d.	n.d.	n.d.	78	n.d.	n.d.	n.d.	1.1	0.05	n.d.	(8.1)
02-Jul-97	32	1.50	n.d.	4870	n.d.	4620	210	n.d.	n.d.	n.d.	n.d.	n.d.	n.d.	n.d.	n.d.	n.d.	n.d.	1.1	0.04	n.d.	(8.1)
Substage IVB																					
22-Aug-97	31	1.45	n.d.	5770	n.d.	6690	200	n.d.	n.d.	n.d.	420	610	n.d.	108	n.d.	n.d.	n.d.	0.86	0.03	0.06	(8.1)
05-Sep-97	35	1.30	n.d.	4060	2790	4330	170	500	650	1040	500	420	48	120	27	2.0	13700	0.94	0.04	0.12	(8.1)
17-Oct-97	34	1.06	44	7840	2670	6520	360	520	570	910	420	360	42	96	23	2.1	19900	1.2	0.05	0.07	(8.1)
04-Nov-97	35	1.40	n.d.	6460	n.d.	7800	280	n.d.	n.d.	n.d.	n.d.	n.d.	n.d.	n.d.	n.d.	n.d.	n.d.	0.83	0.04	n.d.	(8.1)
06-Feb-98	38	0.90	68	7910	n.d.	7920	420	n.d.	n.d.	1130	530	500	69	100	n.d.	n.d.	19900	1.0	0.05	0.07	(3)
25-Mar-98	37	0.79	81	9120	n.d.	9440	490	n.d.	n.d.	n.d.	n.d.	n.d.	n.d.	96	n.d.	n.d.	n.d.	1.0	0.05	n.d.	(3)
17-Apr-98	37	0.68	87	10900	4430	8870	460	1000	950	1300	630	560	83	77	31	3.8	24900	1.2	0.05	0.07	(3)
15-May-98	36	0.64	n.d.	11500	n.d.	12400	620	n.d.	n.d.	n.d.	n.d.	n.d.	n.d.	79	n.d.	n.d.	n.d.	0.93	0.05	n.d.	(3)
25-Jun-98	36	0.99	57	7500	3010	6490	500	810	740	1050	470	440	58	105	22	n.d.	18600	1.2	0.08	0.07	(3)
30-Jul-98	35	0.73	98	10800	n.d.	11800	600	n.d.	n.d.	n.d.	n.d.	n.d.	n.d.	n.d.	n.d.	5.9	n.d.	0.92	0.05	n.d.	(3)
26-Aug-98	35	0.73	95	7970	4580	8410	390	1130	n.d.	1390	640	550	94	108	29	n.d.	23100	0.95	0.05	0.08	(3)
21-Sep-98	35	0.74	93	9850	n.d.	10800	550	n.d.	n.d.	n.d.	n.d.	n.d.	n.d.	107	n.d.	n.d.	n.d.	0.92	0.05	n.d.	(3)
04-Nov-98	35	0.85	76	8140	n.d.	8740	480	n.d.	n.d.	n.d.	n.d.	n.d.	n.d.	n.d.	n.d.	n.d.	n.d.	0.93	0.05	n.d.	(3)
23-Dec-98	27	0.90	53	7650	2970	7840	600	850	n.d.	1080	440	400	66	84	20	2.9	20900	1.0	0.08	0.06	(3)
13-Jan-99	32	0.77	88	9110	n.d.	9890	640	n.d.	n.d.	n.d.	n.d.	n.d.	n.d.	n.d.	n.d.	n.d.	n.d.	0.92	0.06	n.d.	(3)
25-Feb-99	33	0.68	105	10600	n.d.	11700	660	n.d.	n.d.	n.d.	n.d.	n.d.	n.d.	n.d.	n.d.	n.d.	n.d.	0.90	0.06	n.d.	(3)
17-Mar-99	32	0.81	93	9760	4370	10900	720	1210	n.d.	1040	510	510	90	64	24	4.5	27400	0.90	0.07	0.05	(3)
21-Apr-99	32	0.72	101	10400	n.d.	11300	800	n.d.	n.d.	n.d.	n.d.	n.d.	n.d.	n.d.	n.d.	n.d.	n.d.	0.91	0.07	n.d.	(3)
07-May-99	34	0.71	101	10700	n.d.	11600	810	n.d.	n.d.	n.d.	n.d.	n.d.	n.d.	n.d.	n.d.	n.d.	n.d.	0.92	0.07	n.d.	(3)
18-Jun-99	34	0.68	107	8550	3320	7510	480	930	n.d.	1140	500	470	65	90	21	10	21100	1.1	0.06	0.07	(3)
07-Jul-99	32	0.68	105	11100	n.d.	12200	720	n.d.	n.d.	n.d.	n.d.	n.d.	n.d.	n.d.	n.d.	n.d.	n.d.	0.91	0.06	n.d.	(3)
19-Aug-99	35	0.81	82	10200	4550	11200	720	1350	1010	1440	590	510	95	110	28	n.d.	27800	0.91	0.06	0.05	(3)
08-Sep-99	39	0.62	104	8220	3510	8120	660	970	n.d.	1040	480	430	69	89	21	n.d.	21500	1.0	0.08	0.06	(3)
22-Oct-99	38	0.61	118	12100	n.d.	13300	920	n.d.	n.d.	n.d.	n.d.	n.d.	n.d.	n.d.	n.d.	n.d.	n.d.	0.91	0.07	n.d.	(3)
05-Nov-99	39	0.80	82	9250	4000	9130	730	450	n.d.	750	290	600	59	89	13	n.d.	22400	1.0	0.08	0.03	(3)
27-Dec-99	34	0.72	100	10400	n.d.	11400	790	n.d.	n.d.	n.d.	n.d.	n.d.	n.d.	n.d.	n.d.	n.d.	n.d.	0.92	0.07	n.d.	(3)
21-Jan-00	38	0.76	83	9270	3910	9850	740	1220	n.d.	1170	470	430	85	63	20	n.d.	24600	0.94	0.08	0.05	(3)
10-Feb-00	44	0.69	88	10200	4110	10800	830	390	880	1110	490	420	100	65	23	n.d.	25600	0.94	0.08	0.05	(3)
13-Mar-00	36	0.71	n.d.	9270	n.d.	9620	700	n.d.	n.d.	n.d.	n.d.	n.d.	100	n.d.	n.d.	n.d.	n.d.	1.0	0.07	n.d.	(3)

Date	Temp. (°C)	pH _{lab} 24±2°C	Cond. mS/cm (24±2°C)	SO ₄	S _{total}	Cl	F	Al	Fe	Ca	Mg	Na	K	Si	Mn	P	TDS	SO ₄ /Cl	F/Cl	Mg/Cl	Data source
11-Apr-00	32	0.74	87	9780	4280	10400	830	1410	n.d.	1330	550	500	100	56	23	n.d.	26300	0.94	0.08	0.05	(3)
05-May-00	31	0.67	103	8330	n.d.	8280	810	n.d.	n.d.	n.d.	n.d.	n.d.	n.d.	n.d.	n.d.	4.1	n.d.	1.0	0.10	n.d.	(3)
09-Jun-00	31	0.77	79	9260	3600	11900	710	1220	n.d.	1240	510	460	100	81	25	5.0	26800	0.78	0.06	0.04	(3)
17-Jul-00	33	0.74	66	7230	n.d.	9050	510	n.d.	n.d.	n.d.	n.d.	n.d.	n.d.	n.d.	n.d.	5.1	n.d.	0.80	0.06	n.d.	(3)
24-Aug-00	31	0.60	91	9240	3690	13300	700	1340	940	1330	520	490	120	78	19	4.6	28700	0.69	0.05	0.04	(3)
12-Sep-00	35	0.60	106	9410	3630	12700	620	1300	n.d.	1330	520	490	120	83	19	4.6	28200	0.74	0.05	0.04	(3)
10-Oct-00	35	0.70	88	8900	3420	11700	580	1200	n.d.	1260	520	470	100	97	24	5.0	26400	0.76	0.05	0.04	(3)
21-Nov-00	34	0.71	97	8930	n.d.	11900	670	n.d.	n.d.	n.d.	n.d.	n.d.	n.d.	n.d.	n.d.	n.d.	n.d.	0.75	0.06	n.d.	(3)
1-Dec-00	34	0.90	n.d.	8320	n.d.	10900	610	n.d.	n.d.	n.d.	n.d.	n.d.	n.d.	n.d.	n.d.	n.d.	n.d.	0.76	0.06	n.d.	(3)
12-Jan-01	31	0.86	84	8700	3250	11400	680	1140	880	1190	490	440	83	69	21	4.9	25700	0.76	0.06	0.04	(3)
31-Jan-01(-0.3m)*	31	0.80*	n.d.	8460	n.d.	10800	620	1130	880	1230	490	440	87	98	19	5.2	47400	0.78	0.06	0.04	(3)
31-Jan-01(-10m)*	32	0.83*	n.d.	8520	n.d.	11000	720	1150	890	1240	490	440	90	100	19	5.2	48400	0.77	0.07	0.04	(3)
31-Jan-01(-20m)*	32	0.83*	n.d.	8880	n.d.	11400	650	1230	n.d.	1280	510	460	94	98	20	5.4	48200	0.78	0.06	0.04	(3)
31-Jan-01(-30m)*	32	0.83*	n.d.	8880	n.d.	11500	740	1220	n.d.	1270	500	450	92	95	19	5.4	48500	0.77	0.06	0.04	(3)
31-Jan-01(-41m)*	33	0.83*	n.d.	8650	n.d.	11400	725	1240	n.d.	1290	510	460	94	100	20	5.4	48500	0.76	0.06	0.04	(3)
23-Feb-01	31	0.83	n.d.	7870	n.d.	9670	540	n.d.	n.d.	n.d.	n.d.	440	78	n.d.	n.d.	n.d.	n.d.	0.81	0.06	n.d.	(3)
08-Mar-01	32	0.65	n.d.	9080	3660	11600	710	1260	n.d.	1320	520	480	96	78	22	n.d.	26700	0.78	0.06	0.04	(3)
26-Apr-01	35	0.75	n.d.	9400	n.d.	11700	660	n.d.	n.d.	n.d.	n.d.	n.d.	n.d.	n.d.	n.d.	n.d.	n.d.	0.80	0.06	n.d.	(3)
08-May-01	34	0.70	n.d.	9080	3200	12200	690	1160	820	1140	460	470	100	110	19	4.7	26900	0.74	0.06	0.04	(3)
13-Jun-01	35	0.67	88	9100	3560	11700	560	1200	n.d.	1430	610	470	88	84	25	n.d.	27000	0.78	0.05	0.05	(3)
19-Jul-01	28	0.70	n.d.	7270	n.d.	8400	460	n.d.	n.d.	n.d.	n.d.	n.d.	n.d.	n.d.	n.d.	n.d.	n.d.	0.87	0.05	n.d.	(3)
3-Aug-01	24	0.85	n.d.	8090	n.d.	9760	510	n.d.	n.d.	n.d.	n.d.	n.d.	n.d.	n.d.	n.d.	n.d.	n.d.	0.83	0.05	n.d.	(3)
07-Sep-01	27	0.39	222	8510	3200	9590	540	1010	n.d.	1190	480	410	78	84	21	n.d.	23900	0.89	0.06	0.05	(3)
18-Oct-01	28	0.85	71	7800	3200	8280	380	1010	650	1160	460	400	79	100	20	n.d.	21600	0.94	0.05	0.06	(3)
Substage IVC																					
27-Nov-01	30	1.07	56	3450	1260	2720	82	310	400	650	250	170	n.d.	100	11	n.d.	8140	1.3	0.03	0.09	(3)
7-Dec-01	30	1.43	20	3310	1240	2830	67	400	400	700	220	150	n.d.	100	10	n.d.	8190	1.2	0.02	0.08	(3)
31-Jan-02	30	1.51	22	3590	1470	2540	52	360	330	620	230	190	39	110	11	n.d.	12600	1.4	0.02	0.09	(3)
27-Feb-02	23	1.17	44	6050	n.d.	4670	160	590	570	30	290	n.d.	39	79	14	2.3	12600	1.3	0.03	0.06	(3)
13-Mar-02	26	1.06	43	6390	2370	5760	190	650	570	900	380	290	46	100	20	6.7	15500	1.1	0.03	0.07	(3)
3-Apr-02	25	1.04	60	6830	n.d.	6420	380	n.d.	n.d.	n.d.	n.d.	n.d.	n.d.	n.d.	n.d.	n.d.	n.d.	1.1	0.06	n.d.	(3)
16-May-02	29	1.08	51	6060	2190	6260	230	640	590	840	340	250	38	110	14	2.6	15400	1.0	0.04	0.05	(3)
Substage IVD																					
11-Jun-02	29	0.90	61	5060	2370	5780	130	660	580	840	340	270	44	110	14	2.8	14100	0.88	0.02	0.06	(3)
30-Jul-02	32	0.99	66	6800	n.d.	7620	320	n.d.	n.d.	n.d.	n.d.	n.d.	n.d.	n.d.	n.d.	n.d.	n.d.	0.89	0.04	n.d.	(3)
04-Sep-02	38	0.90	79	7660	3010	8720	300	850	650	970	380	300	53	130	16	3.4	21800	0.88	0.03	0.04	(3)
Oct-02	39	0.81	99	9580	n.d.	12500	470	n.d.	n.d.	n.d.	n.d.	n.d.	n.d.	n.d.	16	4.3	n.d.	0.76	0.04	n.d.	(3)
Nov-02	39	0.68	92	8680	n.d.	10400	410	n.d.	n.d.	n.d.	n.d.	n.d.	n.d.	n.d.	16	4.0	n.d.	0.83	0.04	n.d.	(3)
11-Dec-02	39	0.84	89	8510	n.d.	10700	430	n.d.	n.d.	n.d.	n.d.	n.d.	n.d.	n.d.	13	3.8	n.d.	0.80	0.04	n.d.	(3)
17-Jan-03	34	0.83	98	8780	n.d.	10500	480	n.d.	630	n.d.	n.d.	n.d.	n.d.	n.d.	15	4.5	n.d.	0.84	0.05	n.d.	(3)
28-Feb-03	36	0.77	108	8870	4730	10900	520	1200	670	1200	420	360	97	36	19	3.3	26500	0.81	0.05	0.04	(3)
31-Mar-03	39	0.70	116	9360	4870	15000	580	1220	700	1190	410	350	95	24	18	3.6	32000	0.63	0.04	0.03	(3)

Date	Temp. (°C)	pH _{lab} 24±2°C	Cond. mS/cm (24±2°C)	SO ₄	S _{total}	Cl	F	Al	Fe	Ca	Mg	Na	K	Si	Mn	P	TDS	SO ₄ /Cl	F/Cl	Mg/Cl	Data source
30-Apr-03	41	0.67	134	10500	5100	16100	620	1270	750	1230	430	370	110	27	19	3.8	34700	0.65	0.04	0.03	(3)
20-May-03	41	0.70	135	11000	5310	16200	620	1320	890	1260	450	400	120	36	19	2.9	35300	0.68	0.04	0.03	(3)
17-Jul-03	35	0.64	140	11800	5150	17100	650	1360	750	1310	490	390	110	31	21	3.2	35900	0.69	0.04	0.03	(3)
12-Aug-03	33	0.61	142	8860	5290	18200	720	1410	780	1340	490	400	110	32	21	3.6	35000	0.49	0.04	0.03	(3)
30-Sep-03	33	0.62	138	13800	4470	15300	560	1320	800	1320	510	400	100	43	22	4.8	35500	0.90	0.04	0.03	(3)
Substage IVE																					
28-Oct-03	28	0.80	85	9290	3440	12700	320	1080	930	1350	560	460	93	60	27	2.9	26900	0.73	0.02	0.04	(3)
5-Dec-03	24	0.93	61	6100	2670	8310	240	820	660	1010	410	350	68	79	20	2.2	18100	0.73	0.03	0.05	(3)
20-Jan-04	24	1.17	38	5260	2370	6670	180	660	660	930	390	360	60	98	19	1.8	15300	0.79	0.03	0.06	(3)
03-Feb-04	29	1.11	45	4550	2230	5880	190	720	690	1020	420	390	65	100	21	1.9	14100	0.77	0.03	0.07	(3)
23-Mar-04	25	1.05	50	5290	2450	6530	180	800	710	1020	440	400	71	110	21	1.9	15600	0.81	0.03	0.07	(3)
27-Apr-04	28	1.12	51	5300	2450	6330	160	840	700	1000	460	390	71	120	21	1.8	15400	0.84	0.03	0.07	(3)
25-May-04	28	1.31	30	3940	1880	5380	26	680	420	750	340	280	48	120	14	1.6	12000	0.73	0.005	0.06	(3)
11-Jun-04	29	1.20	39	4540	1980	6480	65	680	550	790	330	310	61	100	15	1.9	13900	0.70	0.01	0.05	(3)
01-Jul-04	26	1.24	36	5680	n.d.	5320	n.d.	n.d.	n.d.	n.d.	n.d.	n.d.	n.d.	n.d.	n.d.	n.d.	n.d.	1.1	n.d.	n.d.	(3)
12-Aug-04	25	1.10	44	7690	1740	6320	170	680	510	690	280	380	55	220	14	3.0	17000	1.2	0.03	0.04	(3)
22-Sep-04	29	1.16	46	7170	n.d.	5860	140	n.d.	n.d.	n.d.	n.d.	n.d.	n.d.	n.d.	n.d.	n.d.	n.d.	1.2	0.02	n.d.	(3)
13-Oct-04	27	1.08	n.d.	7650	1900	6820	150	740	540	730	280	360	60	220	13	3.4	20800	1.1	0.02	0.04	(3)
22-Oct-04	27	1.08	54	7940	n.d.	6920	160	n.d.	n.d.	n.d.	n.d.	n.d.	n.d.	n.d.	n.d.	n.d.	n.d.	1.1	0.02	n.d.	(3)
2-Dec-04	23	1.17	48	7750	n.d.	5930	130	n.d.	n.d.	n.d.	n.d.	n.d.	n.d.	n.d.	n.d.	n.d.	n.d.	1.3	0.02	n.d.	(3)
Jan-05	22	n.d.	n.d.	n.d.	n.d.	n.d.	n.d.	n.d.	n.d.	n.d.	n.d.	n.d.	n.d.	n.d.	n.d.	n.d.	n.d.	n.d.	n.d.	n.d.	(3)
22-Feb-05	22	1.25	35	3780	1620	3680	92	560	420	650	200	270	45	230	10	2.7	12400	1.0	0.02	0.05	(3)
Stage V																					
21-Mar-05	32	1.22	46	4670	n.d.	5330	130	n.d.	n.d.	n.d.	n.d.	n.d.	n.d.	n.d.	n.d.	n.d.	n.d.	0.88	0.02	n.d.	(3)
12-Apr-05	34	0.97	69	7340	3010	6570	220	820	550	870	280	350	67	193	14	3.7	17400	1.1	0.03	0.04	(3)
4-May-05	41	1.02	77	8120	3660	6900	260	n.d.	n.d.	n.d.	n.d.	n.d.	n.d.	171	n.d.	n.d.	n.d.	1.2	0.04	n.d.	(3)
13-May-05	45	0.98	n.d.	8040	n.d.	7140	300	950	580	1040	290	360	74	n.d.	14	4.3	15100	1.1	0.04	0.04	(3)
16-Jun-05	50	0.92	n.d.	9090	n.d.	8230	420	1150	620	1300	310	400	93	142	15	5.1	17700	1.1	0.05	0.04	(3)
24-Jun-05	50	0.92	86	9310	4160	8380	470	870	690	n.d.	n.d.	n.d.	n.d.	n.d.	14	1.3	n.d.	1.1	0.06	n.d.	(3)
14-Jul-05	50	0.79	95	9900	n.d.	8800	530	920	700	n.d.	n.d.	n.d.	n.d.	n.d.	14	1.0	n.d.	1.1	0.06	n.d.	(3)
24-Aug-05	51	0.75	111	11400	n.d.	10200	690	n.d.	n.d.	n.d.	n.d.	n.d.	n.d.	n.d.	n.d.	n.d.	n.d.	1.1	0.06	n.d.	(3)
20-Sep-05	52	0.70	123	12800	6560	11100	750	1610	720	1400	360	470	130	122	18	7.0	31600	1.2	0.07	0.03	(3)
Oct-05	53	n.d.	n.d.	n.d.	n.d.	n.d.	n.d.	n.d.	n.d.	n.d.	n.d.	n.d.	n.d.	n.d.	n.d.	n.d.	n.d.	n.d.	n.d.	n.d.	(3)
30-Nov-05	54	0.64	134	13600	7530	11600	920	1630	670	1440	360	450	130	119	15	1.3	34000	1.2	0.07	0.03	(3)
31-Jan-06	51	0.65	140	15700	n.d.	12000	870	1120	710	n.d.	n.d.	n.d.	n.d.	n.d.	15	1.4	n.d.	1.3	0.07	n.d.	(3)
28-Feb-06	51	0.59	158	17700	n.d.	13400	990	n.d.	n.d.	n.d.	n.d.	n.d.	n.d.	n.d.	n.d.	n.d.	n.d.	1.3	0.07	n.d.	(3)
1-Apr-06	54	0.63	120	17200	n.d.	15700	1050	n.d.	n.d.	n.d.	n.d.	n.d.	n.d.	n.d.	n.d.	n.d.	n.d.	1.1	0.07	n.d.	(3)
6-Apr-06	54	0.70	104	14600	n.d.	15200	980	n.d.	n.d.	n.d.	n.d.	n.d.	n.d.	n.d.	n.d.	n.d.	n.d.	1.0	0.06	n.d.	(3)
19-Apr-06	51	0.70	102	15100	n.d.	14700	1030	n.d.	n.d.	n.d.	n.d.	n.d.	n.d.	n.d.	n.d.	n.d.	n.d.	1.0	0.07	n.d.	(3)
25-Apr-06	54	0.74	94	13800	n.d.	13000	990	n.d.	n.d.	n.d.	n.d.	n.d.	n.d.	n.d.	n.d.	n.d.	n.d.	1.1	0.08	n.d.	(3)
3-May-06	49	0.74	118	17700	n.d.	15100	1150	n.d.	n.d.	n.d.	n.d.	n.d.	n.d.	n.d.	n.d.	n.d.	n.d.	1.2	0.08	n.d.	(3)
25-May-06	47	0.72	123	19500	n.d.	15900	1130	n.d.	n.d.	n.d.	n.d.	n.d.	n.d.	n.d.	n.d.	n.d.	n.d.	1.2	0.07	n.d.	(3)

Date	Temp. (°C)	pH _{lab} 24±2°C	Cond. mS/cm (24±2°C)	SO ₄	S _{total}	Cl	F	Al	Fe	Ca	Mg	Na	K	Si	Mn	P	TDS	SO ₄ /Cl	F/Cl	Mg/Cl	Data source
22-Jun-06	46	0.59	133	23100	n.d.	16300	1090	n.d.	n.d.	n.d.	n.d.	n.d.	n.d.	n.d.	n.d.	n.d.	n.d.	1.4	0.07	n.d.	(3)
20-Jul-06	43	0.62	121	21300	n.d.	13400	890	n.d.	n.d.	n.d.	n.d.	n.d.	n.d.	n.d.	n.d.	n.d.	n.d.	1.6	0.07	n.d.	(3)
11-Aug-06	43	0.52	144	25400	n.d.	16100	1100	n.d.	n.d.	n.d.	n.d.	n.d.	n.d.	n.d.	n.d.	n.d.	n.d.	1.6	0.07	n.d.	(3)
05-Sep-06	41	0.47	160	27500	n.d.	17100	1100	n.d.	n.d.	n.d.	n.d.	n.d.	n.d.	n.d.	n.d.	n.d.	n.d.	1.6	0.06	n.d.	(3)
5-Oct-06	46	0.40	163	28400	n.d.	16700	1140	n.d.	n.d.	n.d.	n.d.	n.d.	n.d.	n.d.	n.d.	n.d.	n.d.	1.7	0.07	n.d.	(3)
12-Oct-06	55	0.46	159	29000	n.d.	16300	1170	n.d.	n.d.	n.d.	n.d.	n.d.	n.d.	n.d.	n.d.	n.d.	n.d.	1.8	0.07	n.d.	(3)
28-Oct-06	53	0.50	159	24930	n.d.	13550	740	n.d.	n.d.	n.d.	n.d.	n.d.	n.d.	n.d.	n.d.	n.d.	n.d.	1.8	0.08	n.d.	(3)
2-Nov-06	58	0.43	180	29100	n.d.	13200	950	n.d.	n.d.	n.d.	n.d.	n.d.	n.d.	n.d.	n.d.	n.d.	n.d.	2.2	0.07	n.d.	(3)
10-Nov-06	57	0.43	n.d.	34330	n.d.	13200	1030	n.d.	n.d.	n.d.	n.d.	n.d.	n.d.	n.d.	n.d.	n.d.	n.d.	2.6	0.08	n.d.	(3)
8-Dec-06	48	0.47	187	33900	n.d.	14900	1090	n.d.	n.d.	n.d.	n.d.	n.d.	n.d.	n.d.	n.d.	n.d.	n.d.	2.3	0.07	n.d.	(3)
Feb-07	48	0.42	230	44300	n.d.	17500	1290	n.d.	n.d.	n.d.	n.d.	n.d.	n.d.	n.d.	n.d.	n.d.	n.d.	2.5	0.07	n.d.	(3)
Apr-07	51	0.34	260	53000	n.d.	20400	1500	n.d.	n.d.	n.d.	n.d.	n.d.	n.d.	n.d.	n.d.	n.d.	n.d.	2.6	0.07	n.d.	(3)
May-07	57	0.25	290	50900	n.d.	18700	1360	n.d.	n.d.	n.d.	n.d.	n.d.	n.d.	n.d.	n.d.	n.d.	n.d.	2.7	0.07	n.d.	(3)
Jun-07	55	0.13	313	67300	n.d.	23900	1530	n.d.	n.d.	n.d.	n.d.	n.d.	n.d.	n.d.	n.d.	n.d.	n.d.	2.8	0.06	n.d.	(3)
Aug-07	57	0.15	353	60550	n.d.	24460	1700	n.d.	n.d.	n.d.	n.d.	n.d.	n.d.	n.d.	n.d.	n.d.	n.d.	2.5	0.07	n.d.	(3)
12-Sep-07	56	0.16	371	98300	n.d.	40300	1800	n.d.	n.d.	n.d.	n.d.	n.d.	n.d.	n.d.	n.d.	n.d.	n.d.	2.4	0.04	n.d.	(3)
26-Oct-07	58	0.15	375	84450	n.d.	30280	1840	n.d.	n.d.	n.d.	n.d.	n.d.	n.d.	n.d.	n.d.	n.d.	n.d.	2.8	0.06	n.d.	(3)
06-Nov-07	57	0.16	385	72930	n.d.	26100	1720	n.d.	n.d.	n.d.	n.d.	n.d.	n.d.	n.d.	n.d.	n.d.	n.d.	2.8	0.07	n.d.	(3)
18-Jan-08	45	0.28	313	67950	n.d.	23870	1630	n.d.	n.d.	n.d.	n.d.	n.d.	n.d.	n.d.	n.d.	n.d.	n.d.	2.8	0.07	n.d.	(3)
12-Feb-08	45	0.21	324	72000	n.d.	25540	1680	n.d.	n.d.	n.d.	n.d.	n.d.	n.d.	n.d.	n.d.	n.d.	n.d.	2.8	0.07	n.d.	(3)
11-Mar-08	42	0.30	334	68800	n.d.	25240	1640	n.d.	n.d.	n.d.	n.d.	n.d.	n.d.	n.d.	n.d.	n.d.	n.d.	2.7	0.06	n.d.	(3)

Botos Lake (1989-2003)

average (1 s.d.)	16.9 ± 1.5	4.95 ± 0.71	0.050 ± 0.032	12.2 ± 3.2	n.d.	1.9 ± 1.5	b.d.l.	b.d.l.	b.d.l.	4.9 ± 1.2	0.6 ± 0.3	0.85 ± 0.07	5.2 ± 5.4	2.8 ± 0.8	b.d.l.	b.d.l.	28	6.3	n.a.	0.32	(1,3)
range	15-19	3.76-6.25	0.029- 0.087	5.6-17		0.5-4.2				4-5.7	0.4-0.8	0.8-0.9	1.3-9.0	2-3.2							
number of samples	n=10	n=10	n=10	n=10	n=10	n=10	n=10	n=10	n=10	n=10	n=10	n=10	n=10	n=10	n=10	n=10	n=10	n=10	n=10	n=10	

Concentrations are given in mg/kg; n.d.: no data available; n.a.: not applicable; b.d.l.: below detection limit.

* Samples collected at depths between 0.3 and 41 meters during a bathymetric survey by Vaselli et al. (2003); pH was measured in the field.

Data sources: (1) OVSI-CORI; (2) Instituto Costarricense de Electricidad (ICE); (3) This work; (4) Casertano et al., 1985; (5) Rowe et al., 1992b; (6) Nicholson et al., 1992; (7) Nicholson et al., 1993; (8) Martinez et al., 2000. See text for analytical methods used.

Table 5.2 Trace-element concentrations (ICP-MS) in the acid crater lake (1980-2005) and thermal springs at the eastern terrace (2000-2002) of Poás

Date/sample	Sample code	Temp. (°C)	pH _{Lab} 24±2°C	Li	Be	B	P	Sc	Ti	V	Cr	Mn	Co	Ni	Cu	Zn
Crater Lake																
Stage II																
31-Oct-80	M-339-2	45	0.11	220	17	20400	15000	640	7670	6460	370	28500	470	220	920	3160
28-Nov-84	M-338-1	48	0.07	480	35	33400	29800	1280	16900	13500	780	64600	920	510	1020	7200
11-Jan-85	M-341-1	44	0.14	230	17	17500	13500	620	11000	6350	380	31400	440	210	500	2700
10-Sep-85	M-340-1	45	0.05	250	20	21500	15200	690	6470	7030	410	32700	500	240	790	2950
29-Nov-85	M-357	45	0.30	210	17	19100	14200	650	6620	6760	380	32100	560	280	980	3010
04-Feb-86	M-332-1	39	0.26	230	18	18700	13900	650	6420	6390	380	33200	500	240	740	2810
Stage III																
24-Sep-86	M-331-1	56	0.50	310	25	22000	17500	820	8880	8130	460	44500	600	290	1150	3940
27-Jul-87	M-360	68	-0.27	350	30	30700	27500	1130	27600	11300	630	44900	800	370	5590	6320
02-Mar-88	M-346-1	60	-0.31	320	35	33300	30600	1110	31600	11400	580	39400	890	390	6670	6600
11-Jan-91	M-336-1	74	n.d.	260	48	34400	31700	960	8260	10900	350	60700	260	120	280	9300
24-Sep-91	M-335-1	71	-0.44	230	47	52900	44100	1240	90500	11600	460	43000	540	240	2310	8530
29-Nov-91	M-337-1	70	-0.50	180	34	33500	29900	860	47700	8520	350	31700	370	190	1530	6190
19-Nov-92	M-328-1	80	-0.50	240	45	47900	44600	1190	134000	10800	440	37800	690	330	4440	7170
02-Apr-93	M-322-1	60	0.00	450	84	88900	75500	2130	63000	21200	960	79800	1100	460	4750	17200
22-Oct-93	M-324-1	60	0.00	430	69	54800	57600	1620	20700	16700	2310	78100	730	1760	2860	15700
10-Mar-95	M-315	42	0.68	180	13	9920	10200	370	2340	4080	190	34900	180	98	230	2800
Stage IV																
Substage IVA																
20-Oct-95	M-314-1	30	1.21	160	7	4550	3580	140	830	1410	75	30500	70	65	110	1510
26-Jan-96	M-305-1	29	1.22	250	9	4040	3230	160	680	1500	80	38400	90	75	80	2000
18-Dec-96	M-306-1	29	1.13	160	8	3330	3270	170	1080	1730	80	22300	90	75	110	5800
03-Mar-97	M-302-1	29	1.18	170	8	3320	3110	180	650	1790	80	25500	90	64	85	2010
Substage IVB																
05-Sep-97	M-361	33	1.30	180	7	3150	1960	140	660	1420	60	26600	70	58	80	2560
17-Oct-97	M-301-1	35	1.06	160	7	2900	2100	150	800	1490	70	23400	90	67	73	2450
17-Apr-98	M-300-1	37	0.68	210	10	5110	3810	240	1530	2510	130	30900	120	97	95	3570
13-Jul-98	M-362-1	35	0.73	250	15	6830	5420	330	1990	3440	170	39200	170	120	160	4040
01-Dec-98	M-295-1	27	0.90	110	6.0	3180	2880	170	1160	1670	85	16900	90	60	84	1920
17-Mar-99	M-269-1	32	0.81	150	10	4910	4490	280	1970	2850	150	23700	140	78	93	2560
21-Sep-99	M-312-1	39	0.62	190	13	6010	6600	380	2380	3890	200	28200	180	105	90	3200
16-Feb-00	M-271-1	44	0.69	170	11	4920	5730	330	1810	3350	170	21900	150	90	150	2630
09-Jun-00	M-#3A	31	0.77	180	11	4470	4850	300	1640	3050	150	25100	170	100	220	2600
10-Oct-00	M-270-1	35	0.70	170	11	4360	4930	300	1390	3110	150	23500	160	100	130	2560
12-Jan-01	M-277-1Lake	31	0.86	160	10	4090	4860	290	1250	2860	140	21400	140	95	160	2350
31-Jan-01 (-0.3m)*	M-525-1	31	0.80*	170	11	4650	5210	340	1330	3190	160	24100	160	84	160	2500
31-Jan-01 (-10m)*	M-526-1	32	0.83*	170	12	4780	5230	350	1330	3280	170	24200	160	86	140	2520

Date/sample	Sample code	Temp. (°C)	pH _{Lab} 24±2°C	Li	Be	B	P	Sc	Ti	V	Cr	Mn	Co	Ni	Cu	Zn
31-Jan-01 (~20m)*	M-527-1	32	0.83*	180	12	5040	5460	360	1440	3400	170	25400	170	88	140	2540
31-Jan-01 (~30m)*	M-528-1	32	0.83*	180	12	5040	5430	360	1430	3390	170	25400	170	88	140	2520
31-Jan-01 (~41m)*	M-529-1	33	0.83*	180	12	5030	5450	360	1440	3390	170	25200	170	115	140	2510
21-Sep-01	M-265-4(MCS1Poas2001)	38	0.39	220	13	8540	6550	290	1220	2920	210	24900	160	300	340	4820
05-Oct-01	M-273-1Lake	29	0.90	140	9.0	3530	3790	250	870	2330	110	18600	120	80	150	2040
24-Oct-01	M-355	32	0.85	160	9.0	3680	4160	270	940	2680	130	20300	140	80	87	1990
Substage IVC																
27-Feb-02	M-623B	23	1.17	110	6.0	1990	2310	170	480	1570	70	13600	90	57	150	1280
13-Mar-02	M-268-1	26	1.06	140	8.0	2380	6760	220	940	2370	110	19200	125	73	85	2920
16-May-02	M-359	29	1.08	120	7.0	2010	2560	190	620	1840	80	14300	95	62	180	1390
Substage IVD																
11-Jun-02	M-255-1	29	0.90	120	7.0	2300	2810	200	600	1850	90	14100	100	90	160	1340
04-Sep-02	M-358	38	0.90	130	8.0	2540	3450	250	850	2350	110	16000	125	70	130	1380
23-Oct-02	M-521A	39	0.81	130	9.0	3360	4300	270	1160	2450	130	15700	135	70	120	1670
06-Nov-02	M-520A	39	0.68	130	9.0	3120	4110	270	1110	2490	130	16100	140	80	130	1600
05-Dec-02	M-515A	39	0.82	140	9.0	2000	2900	230	880	2480	110	14500	110	61	220	1460
11-Dec-02	M-519A	39	0.84	120	8.0	2850	3830	250	1080	2180	120	13400	120	62	160	1440
27-Jan-03	M-514A	34	0.83	130	9.0	3320	4540	280	1320	2570	140	15200	140	72	180	1690
24-Feb-03	M-769	36	0.77	120	9.0	3140	4500	290	1365	2590	150	15100	140	72	190	1690
18-Mar-03	M-768	38	0.70	130	9.0	3310	4590	290	1370	2670	140	15500	150	75	190	1770
31-Mar-03	M-770	39	0.70	130	9.0	3360	4650	300	1410	2720	140	15400	150	75	210	1790
30-Apr-03	n.a.	41	0.67	100	5.6	4000	3770	720	1150	n.d.	130	12720	130	130	190	1270
20-May-03	n.a.	41	0.70	90	4.8	4000	2880	640	1020	2030	120	11490	120	74	170	1170
17-Jul-03	n.a.	35	0.64	100	5.4	5000	3250	680	1100	n.d.	150	13030	140	140	210	1280
12-Aug-03	n.a.	33	0.61	110	5.7	5000	3650	730	1110	n.d.	150	12920	140	130	240	1370
30-Sep-03	n.a.	33	0.62	150	8.0	4000	4570	860	1220	n.d.	140	16850	170	94	240	1590
Substage IVE																
28-Oct-03	n.a.	28	0.80	170	7.6	4000	2940	680	740	n.d.	110	19200	140	88	230	2490
05-Dec-03	n.a.	24	0.93	120	5.6	3000	2190	500	540	1640	68	13650	94	52	190	1690
20-Jan-04	n.a.	24	1.17	120	5.4	2000	1760	400	370	1390	53	13160	83	46	110	1680
03-Feb-04	n.a.	29	1.11	110	5.5	2000	1910	430	350	1460	60	13790	86	54	200	1920
23-Mar-04	n.a.	25	1.05	100	5.0	2000	1880	430	360	1450	57	12930	86	45	160	1540
27-Apr-04	n.a.	28	1.12	100	4.9	2000	1750	450	330	1510	64	12890	88	48	160	1320
25-May-04	n.a.	28	1.31	90	4.6	1000	1570	430	280	1350	60	10310	77	47	170	930
11-Jun-04	n.a.	29	1.20	100	4.9	2000	1870	420	310	1350	67	10910	86	69	180	1120
25-Aug-04	A	25	1.15	120	6.4	1450	3030	645	470	1615	95	12980	105	68	205	1050
13-Oct-04	B	27	1.08	120	6.6	1570	3370	680	550	1795	90	13320	110	60	225	1070
22-Feb-05	C	22	1.25	95	5.2	1170	2700	530	400	1350	80	9370	70	45	220	650
Stage V																
12-Apr-05	CH	34	0.97	125	6.8	2060	3700	720	910	1980	100	13500	110	74	187	1120

Date/sample	Sample code	Temp. (°C)	pH _{Lab} 24±2°C	Li	Be	B	P	Sc	Ti	V	Cr	Mn	Co	Ni	Cu	Zn
13-May-05	D1	45	0.98	130	7.4	2500	4300	780	960	2250	180	13900	120	105	97	1340
16-Jun-05	E	50	0.92	140	7.9	3580	5100	915	1000	2630	148	15000	140	80	100	1450
20-Sep-05	F	52	0.70	165	9.9	5300	7000	1200	1010	3540	223	17700	190	121	130	1780
02-Nov-05	G	53	0.59	155	9.8	5050	6800	1200	1010	3660	205	17200	192	115	75	1640
Crater Springs																
Este 21-Nov-00	M-811 or 6B	91	2.30	200	4.4	300	360	180	20	420	5.2	4310	30	16	210	700
White Algae 21-Sep-01	M-776-1 or 6e	52	1.55	95	4.6	110	1100	190	130	880	30	3520	35	20	140	430
Green Algae 21-Nov-00	M-822-1 or 6f	57	2.50	110	3.8	270	n.d.	138	21	400	10	2150	7.0	8.2	23	530
Norte-Este 21-Nov-00	M-810-1 or 7	91	2.60	210	6.0	240	n.d.	52	18	180	b.d.l.	4450	14	10	80	700
16-May-02	M-856 or 7	89	2.50	440	4.0	n.d.	3400	190	120	680	120	4500	85	60	420	530
Date/sample	Sample code	Ga	As	Se	Rb	Sr	Y	Zr	Nb	Mo	Ag	Cd	Sn	Sb	Cs	Ba
Crater Lake																
Stage II																
31-Oct-80	M-339-2	370	3260	100	590	19400	430	940	24	18	1.3	76	230	38	14	32
28-Nov-84	M-338-1	740	1010	200	3258	29000	620	1640	n.d.	21	3.8	130	360	17	25	n.d.
11-Jan-85	M-341-1	360	480	79	530	15700	310	780	3.2	11	0.87	65	170	6.2	12	40
10-Sep-85	M-340-1	400	770	82	590	18100	380	920	2.8	9.3	1.4	68	180	11	13	34
29-Nov-85	M-357	400	920	85	600	19500	410	960	n.d.	19	1.4	72	180	12	14	45
04-Feb-86	M-332-1	360	710	79	540	17400	390	820	3.0	22	1.3	62	160	10	12	61
Stage III																
24-Sep-86	M-331-1	440	3940	130	720	22800	550	1290	13	26	2.1	88	240	50	17	30
27-Jul-87	M-360	660	1110	140	1140	24000	630	3160	40	320	8.6	180	570	250	27	75
02-Mar-88	M-346-1	610	830	230	1140	19800	660	2870	12	420	10	170	570	250	27	n.d.
11-Jan-91	M-336-1	520	3150	200	2050	25900	800	3330	10	18	2.6	330	560	63	54	74
24-Sep-91	M-335-1	760	270	330	2840	25600	880	8120	190	85	7.6	430	1520	160	86	55
29-Nov-91	M-337-1	510	520	200	1920	18100	510	4740	83	57	5.4	280	860	97	57	53
19-Nov-92	M-328-1	660	16000	320	2510	33000	820	7540	180	700	13	290	1130	410	74	60
02-Apr-93	M-322-1	1330	750	500	5010	27000	900	11000	78	340	19	660	2310	370	160	n.d.
22-Oct-93	M-324-1	990	1340	350	3930	23000	830	6490	18	310	57	490	1440	200	120	81
10-Mar-95	M-315	240	1740	72	640	13800	360	630	n.d.	5.0	0.65	88	53	7.9	16	58
Stage IV																
Substage IVA																
20-Oct-95	M-314-1	75	300	41	390	6090	170	120	n.d.	4.0	0.54	29	4.6	0.91	9.3	52
26-Jan-96	M-305-1	65	230	28	460	6080	200	78	n.d.	15	0.36	38	1.3	0.48	11	36
18-Dec-96	M-306-1	65	470	29	270	5730	170	190	3.8	5.7	0.67	39	7.9	4.0	5.8	49
03-Mar-97	M-302-1	63	450	34	280	6040	180	38	1.7	4.5	0.32	21	n.d.	3.0	5.9	54

Date/sample	Sample code	Ga	As	Se	Rb	Sr	Y	Zr	Nb	Mo	Ag	Cd	Sn	Sb	Cs	Ba	Bi	Th	U
Substage IVB																			
05-Sep-97	M-361	56	420	22	330	5630	150	n.d.	n.d.	3.5	0.20	30	2.5	1.8	6.5	84	2.9	14	8.8
17-Oct-97	M-301-1	63	450	25	290	6220	190	n.d.	n.d.	4.6	0.20	18	3.7	1.5	5.7	62	4.8	16	7.8
17-Apr-98	M-300-1	120	1090	34	410	8490	210	42	n.d.	19	0.23	33	21	4.7	8.1	29	12	25	11
13-Jul-98	M-362-1	160	1550	54	530	11600	270	n.d.	n.d.	31	0.83	52	47	4.4	11	90	12	35	15
01-Dec-98	M-295-1	86	730	22	220	5400	120	47	n.d.	22	0.33	24	23	1.7	5.1	66	5.9	17	6.5
17-Mar-99	M-269-1	140	1250	29	350	8490	190	77	n.d.	39	0.15	41	45	3.0	8.1	68	11	27	10
21-Sep-99	M-312-1	210	1570	38	410	10600	220	110	n.d.	35	0.23	51	58	3.2	9.9	250	12	36	13
16-Feb-00	M-271-1	170	1280	31	330	9050	190	170	4.5	19	0.41	43	26	3.9	7.9	67	6.8	31	11
09-Jun-00	M-#3A	150	1160	22	310	7770	190	290	9.7	20	0.70	35	20	8.2	7.4	180	4.4	25	11
10-Oct-00	M-270-1	150	1200	30	350	8160	190	61	n.d.	18	0.35	40	24	2.0	8.2	79	11	27	11
12-Jan-01	M-277-1Lake	140	1120	27	340	7800	170	120	3.2	17	0.26	33	19	2.2	7.7	79	10	26	11
31-Jan-01(-0.3m)*	M-525-1	160	1300	32	390	8680	200	120	3.2	17	0.26	46	26	3.5	8.9	120	12	31	13
31-Jan-01(-10m)*	M-526-1	160	1320	32	390	8890	200	77	1.8	17	0.18	40	27	3.4	9.2	96	12	31	12
31-Jan-01(-20m)*	M-527-1	160	1380	34	410	9350	210	75	1.4	18	0.19	56	29	3.6	9.3	100	13	32	13
31-Jan-01(-30m)*	M-528-1	160	1370	34	400	9280	200	70	1.2	18	0.16	41	28	3.3	8.7	99	12	31	12
31-Jan-01(-41m)*	M-529-1	160	1360	33	400	9270	200	67	1.1	18	0.17	41	28	3.3	9.8	100	12	30	12
21-Sep-01	M-265-4(MCS1Poas2001)	130	1180	160	340	7710	200	n.d.	n.d.	26	6.8	33	n.d.	n.d.	7.6	232	3.5	23	13
05-Oct-01	M-273-1Lake	110	1020	26	280	6610	160	n.d.	n.d.	5.3	0.23	24	9.7	1.9	6.3	79	2.4	22	9.8
24-Oct-01	M-355	120	1110	27	300	7190	170	49	n.d.	6.1	0.12	26	12	2.8	6.8	240	2.7	28	11
Substage IVC																			
27-Feb-02	M-623B	65	630	18	190	4250	120	n.d.	n.d.	3.5	0.21	15	4.3	2.1	4.2	150	1.8	15	8.6
13-Mar-02	M-268-1	76	820	21	250	4930	140	46	1.2	4.4	0.24	17	6.5	2.2	4.3	95	2.0	16	10
16-May-02	M-359	72	630	16	180	4190	130	n.d.	n.d.	3.5	0.37	12	5.0	2.8	3.8	290	2.5	18	8.8
Substage IV																			
11-Jun-02	M-255-1	80	720	20	190	4480	130	n.d.	n.d.	4.9	0.58	13	6.8	3.4	4.0	79	3.1	17	8.8
04-Sep-02	M-358	100	920	22	220	5540	150	53	1.2	8.0	0.29	16	19	3.6	4.4	230	12	22	10
23-Oct-02	M-521A	120	1210	29	270	6420	160	58	n.d.	11	0.22	23	33	3.9	5.3	140	17	24	10
06-Nov-02	M-520A	110	1170	27	260	6110	160	69	n.d.	9.5	0.43	23	33	4.2	5.2	200	16	24	10
05-Dec-02	M-515A	83	810	22	200	4440	140	80	2.1	7.9	0.45	18	19	3.2	3.9	140	13	23	10
11-Dec-02	M-519A	100	1080	26	240	5640	150	54	n.d.	13	0.29	22	30	3.7	4.8	110	17	22	10
17-Jan-03	M-514A	130	1320	31	270	6690	170	65	n.d.	16	0.32	29	41	4.6	5.7	200	23	26	11
24-Feb-03	M-769	130	1370	28	270	6610	170	69	n.d.	20	0.98	31	47	6.2	5.8	330	27	27	11
18-Mar-03	M-768	130	1470	30	280	6880	170	75	n.d.	20	0.34	33	52	7.0	6.0	180	31	28	11
31-Mar-03	M-770	140	1520	31	290	7070	170	78	n.d.	24	0.28	34	57	8.1	6.1	140	36	28	11
30-Apr-03	n.a.	130	1230	26	270	6350	170	70	n.d.	21	n.d.	33	55	5.8	5.6	86	39	31	11
20-May-03	n.a.	130	1190	23	250	6050	170	68	0.12	21	n.d.	63	56	6.2	5.4	80	41	31	11
17-Jul-03	n.a.	130	1260	24	260	6120	180	72	0.14	20	n.d.	100	58	7.9	5.4	81	43	31	11
12-Aug-03	n.a.	130	1270	26	270	6390	180	74	0.14	20	n.d.	63	59	7.7	5.6	96	45	33	12
30-Sep-03	n.a.	140	1250	30	280	6220	200	65	0.11	16	n.d.	53	48	5.9	5.7	99	26	28	10
Substage IVE																			
28-Oct-03	n.a.	96	850	25	330	4910	170	40	b.d.l.	10	n.d.	48	26	4.2	6.6	95	17	22	10

Date/sample	Sample code	Ga	As	Se	Rb	Sr	Y	Zr	Nb	Mo	Ag	Cd	Sn	Sb	Cs	Ba	Bi	Th	U
05-Dec-03	n.a.	67	580	15	240	3580	130	28	b.d.l.	6.2	n.d.	20	15	3.0	4.7	110	8.1	17	7.7
20-Jan-04	n.a.	51	450	27	240	2930	110	17	b.d.l.	3.6	n.d.	85	6.2	2.8	4.8	100	10	14	7.6
03-Feb-04	n.a.	53	430	13	250	3100	120	24	b.d.l.	3.8	n.d.	22	7.0	3.2	5.0	57	4.6	15	8.2
23-Mar-04	n.a.	56	400	12	240	3140	120	18	b.d.l.	3.5	n.d.	17	6.9	2.7	4.7	120	4.1	17	8.8
27-Apr-04	n.a.	55	340	23	210	3070	120	15	b.d.l.	2.8	n.d.	14	5.1	2.4	4.1	90	3.0	17	8.5
25-May-04	n.a.	49	210	9.0	150	2570	89	9.1	b.d.l.	1.7	n.d.	9.1	1.9	1.7	2.8	130	1.5	13	6.1
11-Jun-04	n.a.	56	280	10	200	2830	100	13	b.d.l.	2.4	n.d.	12	2.8	2.4	3.6	100	2.2	15	7.1
25-Aug-04	A	66	265	b.q.l.	210	3390	115	19	b.q.l.	6.4	1.9	8.8	4.4	2.9	3.8	150	2.9	15	6.2
13-Oct-04	B	70	310	b.q.l.	200	3800	125	21	b.q.l.	33	4.5	10	10	3.5	4.1	165	3.1	16	6.7
22-Feb-05	C	58	215	11	145	3250	100	13	b.q.l.	18	3.4	5.5	2.7	5.7	2.6	120	1.6	13	5.6
Stage V																			
12-Apr-05	CH	88	585	b.q.l.	210	4900	140	32	b.q.l.	7.5	4.3	12	8.5	4.4	4.3	310	6.3	19	7.5
13-May-05	D1	120	1090	b.q.l.	220	6200	160	43	b.q.l.	5.8	2.1	15	11	4.0	4.6	65	14	23	8.4
16-Jun-05	E	150	1600	b.q.l.	240	8700	210	80	b.q.l.	6.0	2.7	19	17	7.5	5.3	68	25	29	11
20-Sep-05	F	222	2350	b.q.l.	290	11400	240	157	0.83	9.3	6.8	33	32	8.6	6.7	90	24	39	14
02-Nov-05	G	230	2130	35	280	11600	240	160	0.45	8.3	3.0	34	34	7.1	6.6	95	19	41	15
Crater Springs																			
Este 21-Nov-00	M-811 or 6B	1.5	360	15	47	1120	140	0.54	0.02	1.3	0.01	9.2	0.20	0.35	5.2	0.64	0.17	10	48
White Algae 21-Sep-01	M-776-1 or 6e	23	62	6.2	83	1050	94	13	b.d.l.	0.62	0.12	9.3	b.d.l.	0.47	2.8	34	0.22	17	28
Green Algae 21-Nov-00	M-822-1 or 6f	2.2	30	6.2	87	1140	68	b.d.l.	b.d.l.	b.d.l.	0.05	7.2	0.05	0.06	2.4	0.25	b.d.l.	11	43
Norte-Este 21-Nov-00	M-810-1 or 7	0.46	29	2.4	b.d.l.	190	93	b.d.l.	b.d.l.	b.d.l.	0.03	11	b.d.l.	b.d.l.	1.3	b.d.l.	0.11	0.83	17
16-May-02	M-856 or 7	120	540	n.d.	120	5470	57	76	n.d.	5.1	0.47	13	n.d.	17	1.4	150	5.1	16	3.4
Crater Lake																			
Stage II																			
31-Oct-80	M-339-2	530	800	100	430	94	30	93	14	85	17	48	45	6.8	20	29	380	1210	
28-Nov-84	M-338-1	340	680	81	340	69	25	73	13	75	13	44	38	9.8	35	31	370	1000	
11-Jan-85	M-341-1	290	570	72	290	63	21	63	9.8	59	12	34	33	5.0	17	21	320	950	
10-Sep-85	M-340-1	350	720	92	370	81	26	80	12	74	15	43	40	6.2	20	18	330	970	
29-Nov-85	M-357	380	790	99	400	89	28	87	13	80	16	46	43	6.6	21	16	350	1000	
04-Feb-86	M-332-1	340	700	89	360	80	27	81	13	76	16	43	41	6.2	18	26	290	840	
Stage III																			
24-Sep-86	M-331-1	460	930	120	500	110	37	110	18	110	22	62	58	8.8	25	62	400	1270	
27-Jul-87	M-360	420	590	60	230	48	17	72	12	86	21	66	73	12	57	97	370	3040	
02-Mar-88	M-346-1	400	710	78	290	60	20	78	13	90	21	69	77	12	63	36	440	2690	
11-Jan-91	M-336-1	500	990	120	490	110	36	130	21	130	28	84	85	13	87	77	1650	3120	
24-Sep-91	M-335-1	810	1630	200	800	170	52	180	28	170	35	98	92	15	220	150	3160	5560	
29-Nov-91	M-337-1	420	860	110	440	98	29	100	16	95	20	56	54	8.4	130	88	1820	3280	

Date/sample	Sample code	La	Ce	Pr	Nd	Sm	Eu	Gd	Tb	Dy	Ho	Er	Tm	Yb	Lu	Hf	Ta	Ti	Pb
19-Nov-92	M-328-1	950	1970	250	990	210	60	190	28	160	32	89	13	81	12	210	76	2260	3980
02-Apr-93	M-322-1	640	1190	150	580	130	40	140	23	150	32	96	15	100	16	310	95	2980	8190
22-Oct-93	M-324-1	560	1050	130	530	120	39	140	22	140	30	89	13	89	14	170	97	1520	5760
10-Mar-95	M-315	330	700	90	370	81	25	79	12	73	15	40	5.8	36	5.6	15	15	490	620
Stage IV																			
Substage IVA																			
20-Oct-95	M-314-1	140	310	40	160	37	12	37	5.9	35	7.1	20	2.8	18	2.7	2.2	8.5	120	160
26-Jan-96	M-305-1	140	300	39	160	38	12	40	6.2	38	7.8	22	3.2	20	3.2	1.2	3.9	89	120
18-Dec-96	M-306-1	120	250	33	140	32	11	34	5.3	32	6.6	19	2.7	17	2.7	2.7	21	70	160
03-Mar-97	M-302-1	120	250	34	140	34	11	35	5.5	33	6.9	20	2.8	18	2.8	0.50	10	57	110
Substage IVB																			
05-Sep-97	M-361	97	220	29	130	30	9.5	30	4.7	28	5.8	16	2.4	15	2.3	n.d.	6.0	41	75
17-Oct-97	M-301-1	120	250	34	150	36	12	38	6.0	36	7.4	21	2.9	18	2.8	n.d.	n.d.	48	83
17-Apr-98	M-300-1	140	320	42	180	40	13	41	6.4	39	8.0	23	3.3	21	3.3	0.72	11	120	230
13-Jul-98	M-362-1	190	420	56	230	53	17	54	8.5	52	11	31	4.6	29	4.6	1.7	16	190	380
01-Dec-98	M-295-1	88	190	25	100	24	7.4	23	3.6	22	4.5	13	1.9	12	1.9	0.82	4.8	88	190
17-Mar-99	M-269-1	140	310	40	170	38	12	37	5.8	35	7.2	21	2.9	19	3.0	1.4	7.4	140	350
21-Sep-99	M-312-1	180	390	50	210	46	15	45	6.9	42	8.6	25	3.6	24	3.7	2.1	9.3	180	450
16-Feb-00	M-271-1	150	320	42	170	39	13	38	5.8	35	7.1	20	3.0	19	3.1	2.2	23	150	480
09-Jun-00	M-#3A	140	310	41	170	38	12	37	6.0	35	7.3	21	3.1	20	3.2	2.5	33	110	260
10-Oct-00	M-270-1	140	300	39	160	37	12	36	5.5	34	7.0	20	2.9	19	3.0	1.1	4.4	120	270
12-Jan-01	M-277-1Lake	130	290	37	150	35	11	35	5.4	32	6.8	19	2.8	18	2.9	3.0	7.5	120	240
31-Jan-01(-0.3m)*	M-525-1	150	320	43	180	40	13	39	6.0	36	7.6	21	3.2	21	3.2	3.0	31	130	280
31-Jan-01(-10m)*	M-526-1	150	330	44	180	41	13	40	6.1	37	7.6	22	3.2	21	3.2	1.7	20	140	280
31-Jan-01(-20m)*	M-527-1	150	340	46	190	42	14	41	6.3	38	7.8	23	3.3	22	3.3	1.5	17	140	290
31-Jan-01(-30m)*	M-528-1	150	340	45	180	41	14	40	6.2	37	7.6	22	3.2	21	3.3	1.4	13	140	280
31-Jan-01(-41m)*	M-529-1	150	340	44	180	41	14	40	6.2	37	7.6	22	3.2	21	3.2	1.2	11	140	280
21-Sep-01	M-265-4(MCS1Poas2001)	140	300	40	170	37	13	40	6.3	38	7.8	23	3.3	22	3.5	n.d.	n.d.	120	210
05-Oct-01	M-273-1Lake	110	250	32	130	30	10	29	4.6	28	5.8	17	2.5	16	2.6	n.d.	n.d.	85	170
24-Oct-01	M-355	130	270	36	150	34	11	34	5.2	32	6.6	19	2.8	18	2.9	0.94	3.5	93	180
Substage IVC																			
27-Feb-02	M-623B	84	180	24	100	24	8.0	24	3.8	23	4.7	14	2.0	13	2.0	n.d.	4.2	46	96
13-Mar-02	M-268-1	91	200	27	120	27	9.2	27	4.3	26	5.3	15	2.3	15	2.4	0.60	7.9	50	1500
16-May-02	M-359	82	180	24	100	24	7.9	24	3.8	23	4.8	14	2.1	14	2.2	n.d.	6.2	39	91
Substage IVD																			
11-Jun-02	M-255-1	90	200	26	110	25	8.5	25	3.9	24	4.9	14	2.1	14	2.2	n.d.	n.d.	41	82
04-Sep-02	M-358	110	230	31	130	30	10	29	4.5	28	5.7	16	2.4	16	2.5	0.88	7.5	70	150
23-Oct-02	M-521A	120	270	35	150	33	11	31	4.9	29	6.1	17	2.5	17	2.6	1.1	5.8	97	240
06-Nov-02	M-520A	120	260	34	140	33	11	31	4.8	29	6.1	17	2.5	17	2.6	1.3	4.8	94	260
05-Dec-02	M-515A	89	200	27	120	28	9.7	28	4.4	27	5.5	16	2.4	16	2.5	1.0	13	70	190

Date/sample	Sample code	La	Ce	Pr	Nd	Sm	Eu	Gd	Tb	Dy	Ho	Er	Tm	Yb	Lu	Hf	Ta	Ti	Pb
11-Dec-02	M-519A	110	240	31	130	30	9.8	28	4.5	26	5.5	16	2.3	15	2.4	1.0	6.3	91	230
17-Jan-03	M-514A	130	280	37	150	34	11	33	5.1	31	6.2	18	2.6	17	2.7	1.2	6.8	120	320
24-Feb-03	M-769	130	290	38	160	35	12	34	5.2	31	6.5	18	2.6	18	2.7	1.4	5.9	120	320
18-Mar-03	M-768	130	290	38	160	36	12	34	5.2	32	6.5	19	2.7	18	2.7	1.4	6.5	130	330
31-Mar-03	M-770	140	300	39	160	36	12	34	5.3	32	6.6	19	2.7	18	2.7	1.5	6.2	160	400
30-Apr-03	n.a.	130	280	36	150	34	12	32	4.7	31	6.2	18	2.6	17	2.6	1.5	0.40	150	340
20-May-03	n.a.	130	270	35	140	32	11	31	4.6	30	6.0	18	2.5	17	2.5	1.6	0.44	150	350
17-Jul-03	n.a.	130	280	37	150	34	12	33	4.8	31	6.4	19	2.6	18	2.7	1.6	0.43	150	380
12-Aug-03	n.a.	140	290	38	150	35	12	34	5.0	32	6.5	19	2.7	18	2.8	1.6	0.48	160	410
30-Sep-03	n.a.	130	280	36	150	34	12	33	4.9	32	6.5	19	2.7	18	2.8	1.3	b.q.l.	120	300
Substage IVE																			
28-Oct-03	n.a.	91	210	28	120	28	9.3	28	4.2	28	5.8	17	2.4	17	2.6	0.80	b.q.l.	80	200
05-Dec-03	n.a.	69	160	21	87	20	7.0	20	3.1	20	4.2	13	1.8	12	1.9	0.44	b.q.l.	55	150
20-Jan-04	n.a.	60	140	19	79	19	6.5	19	3.0	19	4.0	12	1.7	12	1.8	0.28	0.58	40	99
03-Feb-04	n.a.	63	150	20	83	20	6.8	20	3.1	20	4.2	13	1.8	12	1.9	0.35	b.q.l.	41	100
23-Mar-04	n.a.	66	150	20	86	20	7.1	22	3.2	21	4.4	13	1.9	13	2.0	0.36	0.40	44	110
27-Apr-04	n.a.	62	150	20	85	20	7.2	20	3.2	21	4.3	13	1.9	13	2.0	0.31	b.q.l.	36	89
25-May-04	n.a.	51	120	16	69	17	6.0	17	2.5	16	3.4	10	1.5	10	1.6	0.15	b.q.l.	18	49
11-Jun-04	n.a.	59	140	19	79	19	6.5	19	2.9	18	3.8	11	1.7	11	1.7	0.23	b.q.l.	24	64
25-Aug-04	A	70	150	20	87	20	7.1	20	3.0	19	3.9	11	1.6	11	1.7	0.36	b.q.l.	22	68
13-Oct-04	B	80	170	23	98	22	7.9	22	3.3	21	4.2	13	1.8	12	1.8	0.41	b.q.l.	24	72
22-Feb-05	C	70	145	20	85	20	6.8	20	2.9	18	3.6	11	1.5	10	1.5	0.24	b.q.l.	12	38
Stage V																			
12-Apr-05	CH	98	206	26	120	24	8.9	26	3.9	24	4.8	14	2.1	13	2.0	0.59	b.q.l.	33	117
13-May-05	D1	120	224	31	143	29	11	31	4.6	29	5.7	16	2.3	15	2.3	0.77	b.q.l.	59	155
16-Jun-05	E	174	337	44	203	40	15	43	6.2	39	7.5	22	3.0	19	2.9	1.5	b.q.l.	100	277
20-Sep-05	F	225	424	56	240	51	19	54	7.8	49	9.5	27	3.8	24	3.6	2.9	2.4	196	440
02-Nov-05	G	230	430	58	246	52	19	52	8.1	46	9.8	26	4.0	25	3.8	3.3	1.4	218	468
Crater Springs																			
Este 21-Nov-00	M-811 or 6B	30	90	15	71	19	8.5	21	3.7	24	5.3	16	2.4	16	2.4	0.03	0.36	0.32	2.1
White Algae 21-Sep-01	M-776-1 or 6e	35	102	15	64	16	6.1	15	2.5	17	3.6	11	1.6	12	1.7	0.14	0.12	2.0	2.7
Green Algae 21-Nov-00	M-822-1 or 6f	25	74	12	53	13	4.6	11	1.8	12	2.5	7.2	1.1	7.3	1.1	0.01	0.50	0.79	b.d.l.
Norte-Este 21-Nov-00	M-810-1 or 7	6.4	22	4.2	23	8.1	3.5	11	2.0	14	3.2	9.5	1.4	9.4	1.4	b.d.l.	b.d.l.	b.d.l.	b.d.l.
16-May-02	M-856 or 7	86	180	22	85	17	5.9	14	2.1	12	2.3	6.5	0.93	6.2	0.96	0.94	n.d.	6.3	56

Concentrations are given in µg/kg; n.d.: no data available; n.a.: not applicable; b.d.l.: below quantification limit. All data were obtained at the Department of Earth Sciences, Utrecht University, except for 28-Nov-1984 which is from Takano et al. (2004). Samples collected at depths between 0.3 and 41 meters during a bathymetric survey by Vaselli et al. (2003); pH measured in the field.

Table 5.3. Compositional data of lake waters collected at two sampling sites the same day, the NE and SE shores of the acid lake. Concentrations are given in mg/kg.

Date	Site	Sample No.	Temp. (°C)	pH	SO ₄	Cl	F	Al	Mg	Na
1 Dec 1998	NE lake edge	1	21	1.25	5500	6300	420	850	440	400
1 Dec 1998	SE lake edge, near CPC	2	29	1.05	10800	12400	680	1300	540	500
23 Feb 2001	NE lake edge	1	31	0.83	7900	9700	540	1140	490	440
23 Feb 2001*	SE lake edge, near CPC	2	31	0.80	9300	10900	730	1000	460	440

Chapters 2 and 4. The main characteristics can be summarised as follows (cf., Fig. 5.2):

Stage I (1972–August 1980) Moderate to strong fumarolic discharge and occasional phreatic explosions within the lake.

Stage II (September 1980–April 1986) Relative quiescence in the lake, no phreatic activity despite strong discharge of high-temperature fumaroles through the CPC.

Stage III (May 1986–August 1995) Vigorous subaqueous fumarolic discharge, strong volume decrease and drying out of the lake, intense phreatic activity from the lake area.

Stage IV (September 1995–February 2005) Relative quiescence in the lake, opening of subaerial fumaroles and springs around the lake.

Stage V (March 2005–Present) Strong fumarolic discharge into the lake, from the north-eastern inner crater wall and from the CPC in 2005, renewal of phreatic activity and a steady decrease of lake volume from March 2006 on.

The stages are characterised by clear differences in the lake's properties. The lake temperature has ranged between 22°C and 94°C, consistently above the usual maximum daily ambient temperature at the summit of Poás (20°C in 1984), while pH has varied from below zero to 1.8, and TDS from 2×10^4 to 1.6×10^5 mg/kg, (i.e. 2–16wt.%). Fluctuations in many monitored parameters are observed over short time periods throughout the entire monitoring period (Figs. 5.2 and 5.3), but in general, temperature, acidity, and concentrations of dissolved solutes (TDS) were highest during the highly active Stage III, intermediate during the moderately active Stages I, II, and V, and lowest during the relatively quiescent Stage IV (cf., Rowe *et al.*, 1992b; Martínez *et al.*, 2000; see also Chapter 4). Stage I is only represented by a single sample with incomplete data and will therefore be largely ignored in the following discussion.

5.5.1.3 Major anions and relationships with activity in the crater area

Apart from the concentration trends shown in Figure 5.2, the behaviour of the major anions in the lake is further illustrated in a ternary S_T -Cl-F diagram (Fig. 5.4a,b) and in ratio diagrams (Figs. 5.5 and 5.6), which eliminate the effects of dilution or evaporation of the lake waters and visualize changes in relative abundances among these species that usually correspond to changes in the composition of input fluxes. The analysed SO₄ concentrations shown in time series diagrams tend to be lower than calculated concentrations from analysed total sulphur (S_T), given the presence of substantial amounts of polythionates

(Chapter 4). As these polymeric oxyanions account for only up to 10% of the total dissolved sulphur, the SO₄ concentration is sufficiently representative for evaluating general trends in the sulphur input.

Concentrations trends of SO₄, Cl and F are roughly parallel over the entire period, and show inverse correlations with pH. Opposite behaviour is rare and short-lived. For example, between late 1988 and early 1989 when the lake was hottest (80–94°C) and about to disappear, Cl concentrations decreased whereas SO₄ and F continued increasing (Fig. 5.2).

The S_T -Cl-F ternary diagram (Fig. 5.4a) shows that relative concentrations of the volatile elements have not remained constant. Lake samples from the distinct stages plot in different fields, consistent with systematic changes in the composition of subaqueous fumaroles (possibly accompanied with additional input of brine water of deep origin, see discussion below). Most samples of Stage III and Stage IV tend to follow a trend near the F-Cl join, indicating that highest input of volatiles and heat (Stage III) is associated with relative enrichment in F, and lowest input (Stage IV) with relative enrichment in Cl. Samples of Stage II are shifted towards the S_T apex, as are a few samples from the start of Stage III with which they overlap. A similar shift marks the transition between Stage III and Stage IV (end of Stage III – substage IVA), and is occasionally seen later during Stage IV (see Fig. 5.4b for details). Finally, the starting months of Stage V (March–November 2005) are also slightly more enriched in S_T relative to the main trend. In addition, the steady increase in volatile and heat input is accompanied by a clear gradual enrichment in F, suggesting a recent (and still ongoing) build-up towards conditions comparable to the highly active Stage III (on 3 October 2008 the lake registered pH = 0.29, 264 mS/cm, and 44°C, values similar to those at the transition between Stages II and III (see Table 5.1). Small yellow sulphur spherules with tails reappeared on the surface of the lake as well). As will be further discussed below, these changes were the prelude to the new cycle of phreatic activity that has been taken place since early 2006. S_T data are not available after 2005, but SO₄-F-Cl relationships (SO₄ concentrations based on IC data) continued to change until similar proportions as observed in Stage II and the first years of Stage III were reached after mid 2006 when phreatic activity had commenced.

5.5.1.4 Time-series trends in anion ratios

Figures 5.5 and 5.6 visualise changes in the proportions of dissolved volatile elements in time-series trends. Elements ratios show differences between the stages, more short-lived

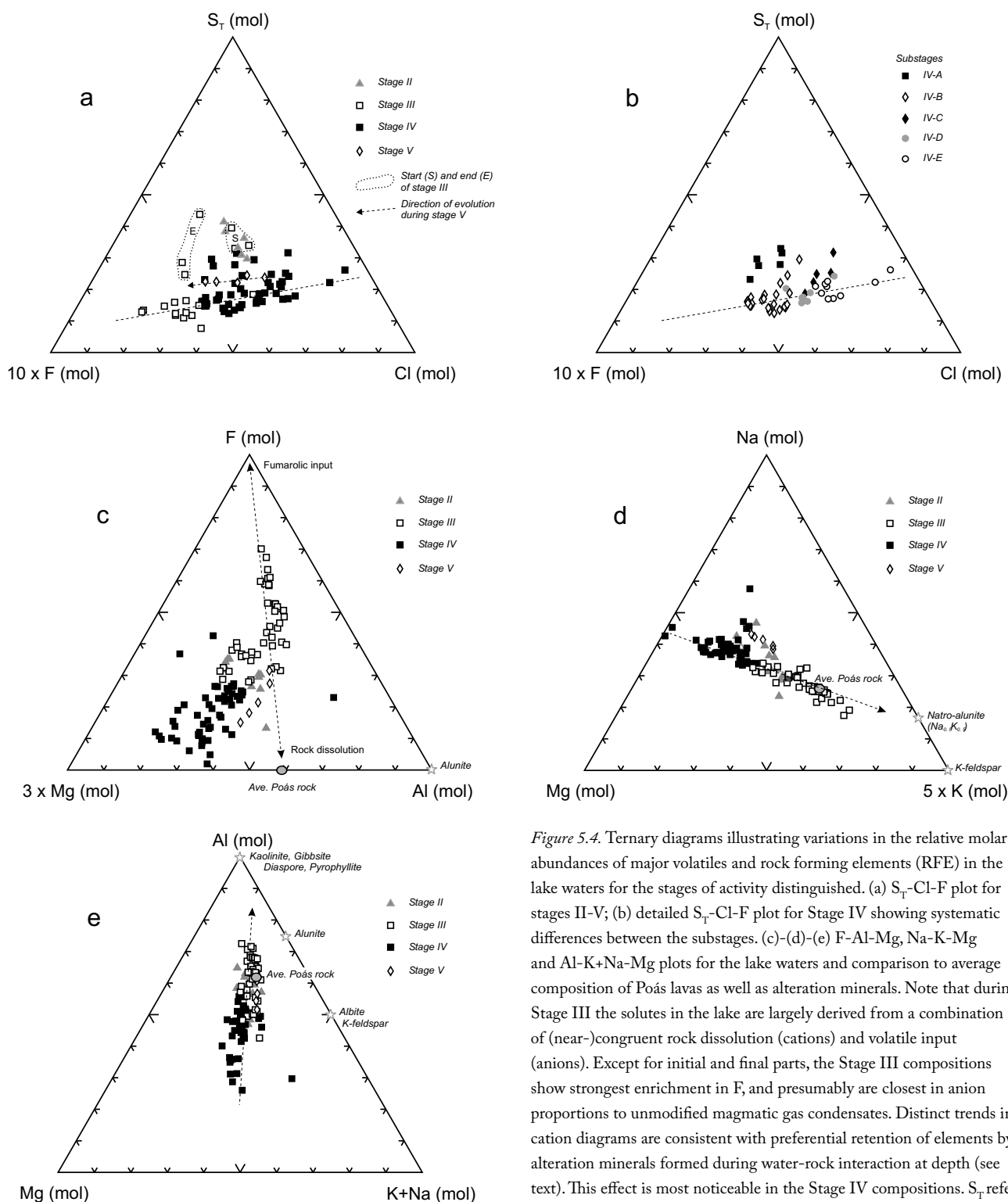


Figure 5.4. Ternary diagrams illustrating variations in the relative molar abundances of major volatiles and rock-forming elements (RFE) in the lake waters for the stages of activity distinguished. (a) S_T -Cl-F plot for stages II-V; (b) detailed S_T -Cl-F plot for Stage IV showing systematic differences between the substages. (c)-(d)-(e) F-Al-Mg, Na-K-Mg and Al-K+Na-Mg plots for the lake waters and comparison to average composition of Poás lavas as well as alteration minerals. Note that during Stage III the solutes in the lake are largely derived from a combination of (near-)congruent rock dissolution (cations) and volatile input (anions). Except for initial and final parts, the Stage III compositions show strongest enrichment in F, and presumably are closest in anion proportions to unmodified magmatic gas condensates. Distinct trends in cation diagrams are consistent with preferential retention of elements by alteration minerals formed during water-rock interaction at depth (see text). This effect is most noticeable in the Stage IV compositions. S_T refers to total sulphur measured by ICP-AES. Stage I is not represented as no complete chemical data are available.

fluctuations within stages and occasional spikes, confirming the highly dynamic nature of the lake system.

Changes in the anion ratios do not necessarily coincide with the boundaries between the main stages. Clearly, the middle part of Stage III stands out in demonstrating highest F/Cl and lowest SO_4/F ratios that coincide with peak temperatures, although it should be noted that most of these data come from mud pools since the lake had largely disappeared. Leaving

short-lived changes aside, Stage II, the first years of Stage III and the most recent years of Stage V show comparable anion ratios, indicating similarity in input and degree of activity. Stage IV, when element concentrations and temperatures were lowest, is characterised by the lowest SO_4/Cl ratios although it is of interest to notice that a first marked decrease of this ratio had already set in during the first half of Stage III (Fig. 5.5). In the course of Stage IV, the SO_4/Cl ratio further decreased to

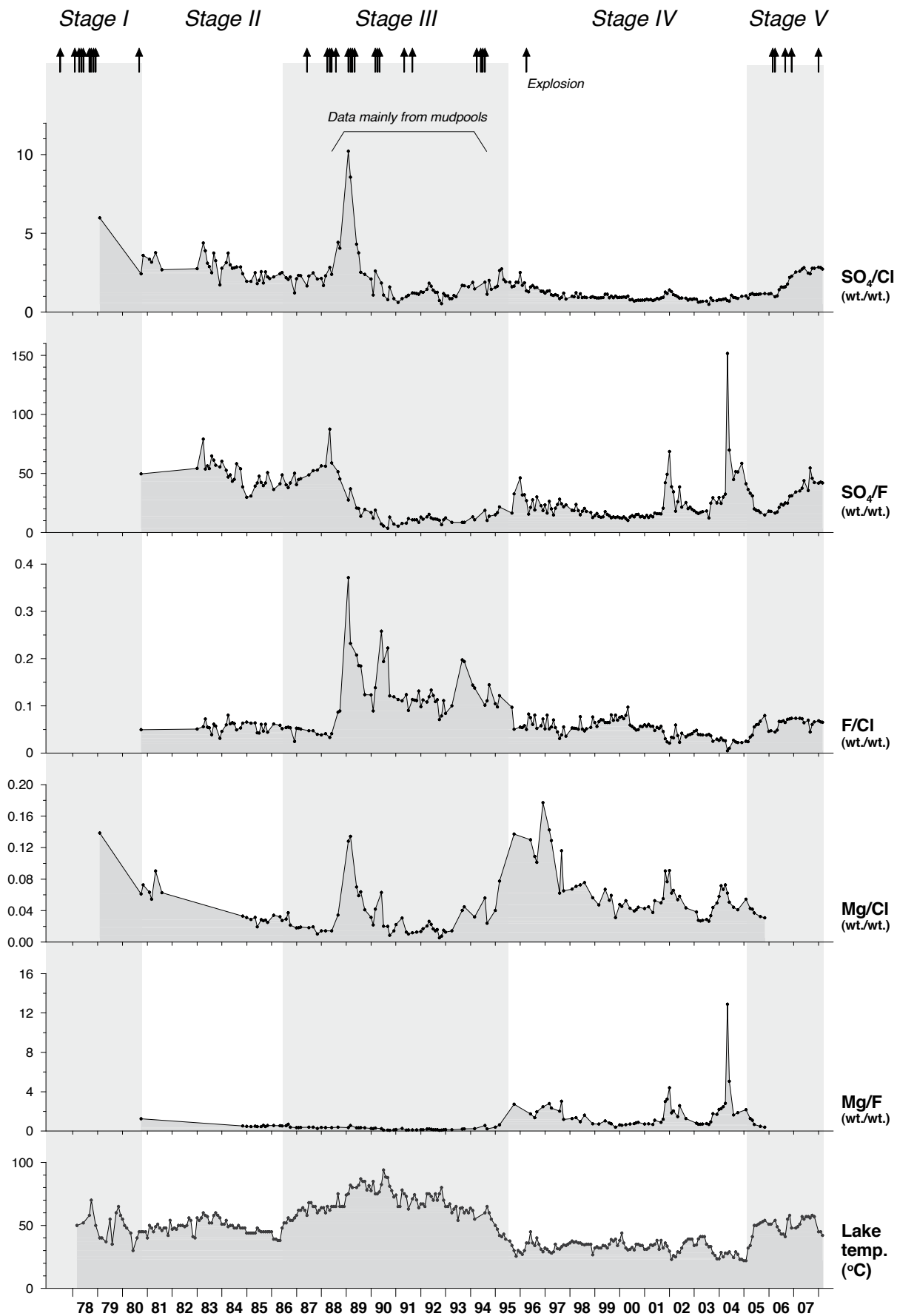
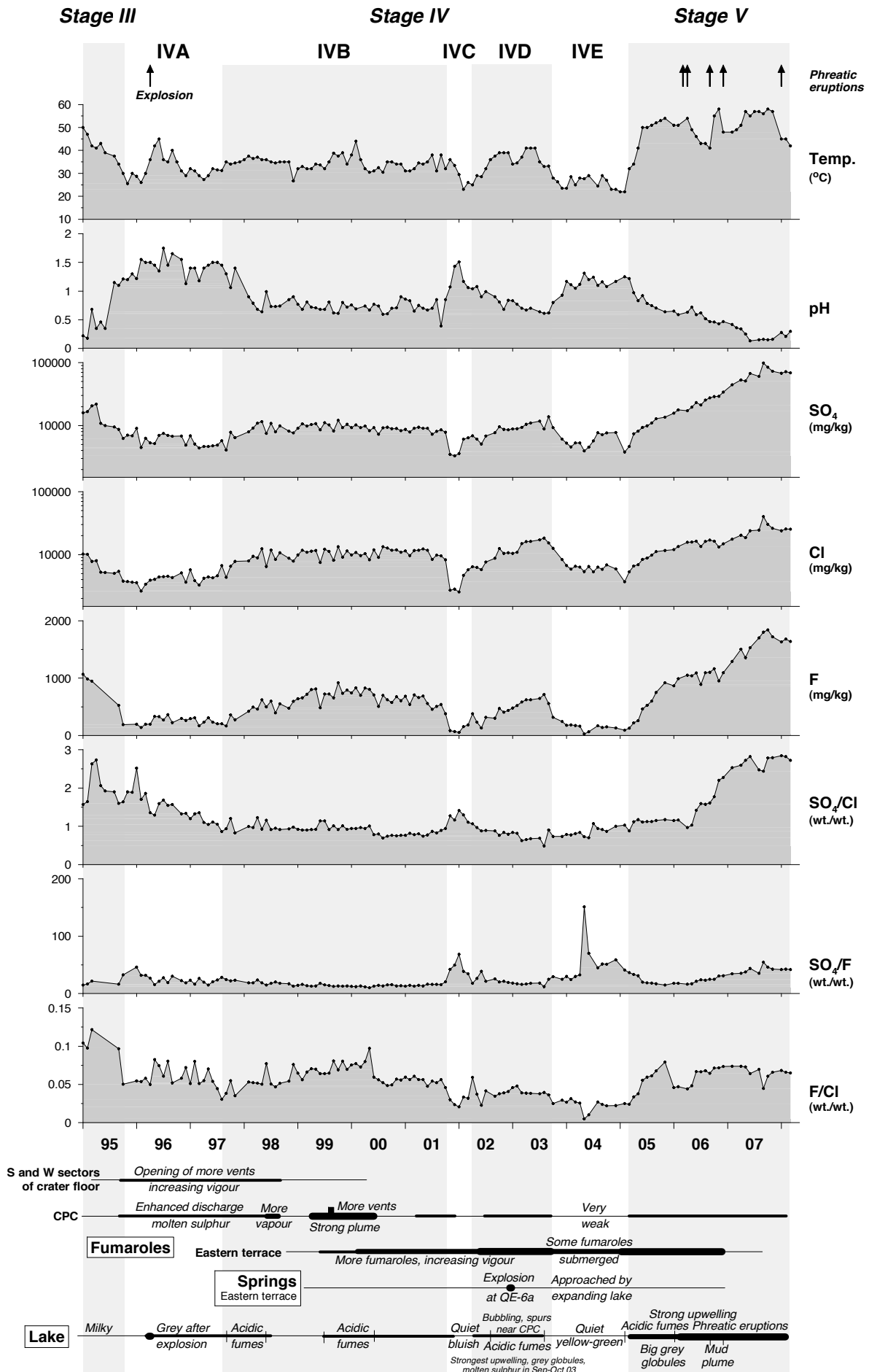


Figure 5.5. Time-series plots (1979 – early 2008) of element ratios measured in the acid lake of Poás volcano, showing noticeable differences between the five main stages, as well as superimposed fluctuations. Temperature variations are included for comparison. Some of the samples collected in Stage III were presumably taken at mud pools.



→ *Figure 5.6.* Expanded time-series plots (1995 – early 2008) of temperature, pH, concentrations of major anions and their ratios for the acid lake of Poás volcano, showing detailed variations observed during Stage IV (subdivided into substages, IVA-IVE) and Stage V. Arrows on top of the figure indicate phreatic eruption events, except for the explosion at the CPC in substage IVA. Major features for the lake, springs and fumaroles are schematically indicated. Bar thickness represents a measure of activity.

(mostly) below unity so that Cl concentrations were generally higher than SO_4 from Substage IVA on, until the ratio started to clearly rise again in Stage V. This reversal in the SO_4/Cl ratio coincided with a decrease in the F/Cl ratio over the same time period (Figs. 5.5 and 5.6), indicating conditions that favoured the input of relatively more chlorine than the other major volatile species. As will be discussed below, similar decreasing $\text{S}_\text{T}/\text{Cl}$ and F/Cl trends during Stage IV can be seen in the compositions of fumarole condensates and springs within the active crater. Collectively, these features point to subsurface changes that affected the chemistry of the entire shallow lake-hydrothermal system. Unlike the SO_4/Cl ratios, the F/Cl ratios during Stage IV were not much different from those in Stage II (Fig. 5.5).

Taking magnesium as a proxy for contributions from rock dissolution, Mg/Cl and Mg/F ratios serve to illustrate the relative importance of input of rock-forming elements versus that of volatiles. Both ratios are, on average, highest in Stage IV, lowest in Stage III and intermediate in Stage II (Fig. 5.5). Magnesium concentrations are incomplete for Stage V but there is a tendency towards a lowering of these ratios in the initial months, in line with the increasing input of volatiles and heat into the lake. Overall, cation concentrations are lowest in Stage IV (Fig. 5.3), so that the elevated Mg/Cl and Mg/F ratios reflect stronger reduction of volatile input compared to that of rock-forming elements.

5.5.1.5 Relationship between anion ratios and activity

As described by Rowe *et al.* (1992b), the start of Stage III was marked by an increase in element concentrations and temperature, and by a decrease in pH, accompanied by a reduction of the lake volume (Fig. 5.2). This might suggest that increasing anion concentrations should not necessarily be explained by a change in influx rates of volatiles, which would be supported by near-constancy of the SO_4/Cl ratio, but several observations argue for the contrary. An increase in the concentrations of Cl and SO_4 in fumarole condensates collected in 1986 on the CPC (Rowe *et al.*, 1992a) may have coincided with an increased input of both volatiles into the lake. Also, SO_4/F and F/Cl ratios show an increasing and decreasing trend in the lake waters, respectively, and are indicative of a change in the composition of subaqueous fumaroles. This might be due to some retention of F during interaction of magmatic gas with rock (Rowe *et al.*, 1992a). Since HF will react with rock more efficiently at temperatures below 300°C (Stoiber and Rose, 1970; Symonds *et al.*, 1990), it is of interest to note that in 1986 temperatures of the CPC fumaroles fluctuated around 300°C and were much lower than in 1981–1985.

Further support for changing input into the lake comes from an increase in the $\text{SO}_2/\text{H}_2\text{S}$ ratios of subaqueous fumaroles,

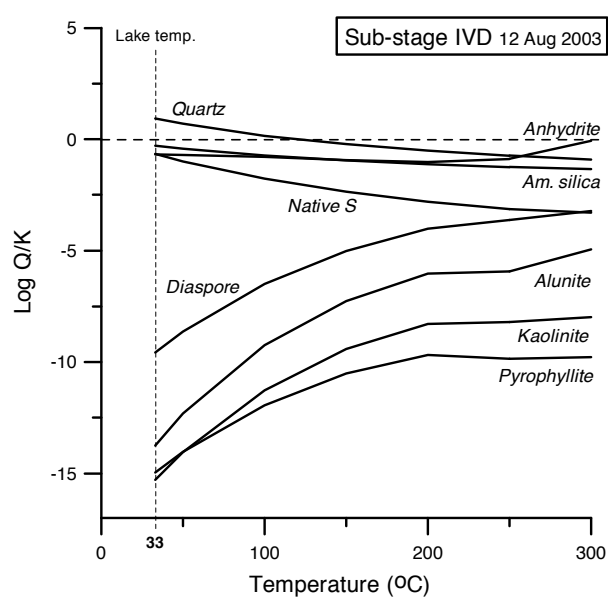
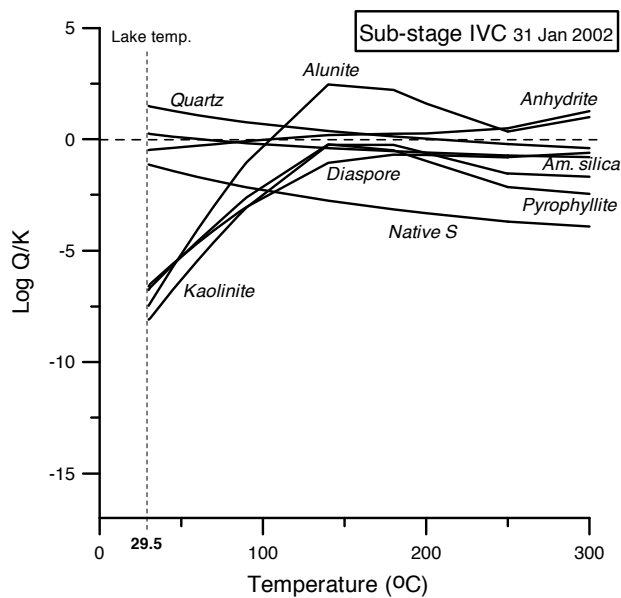
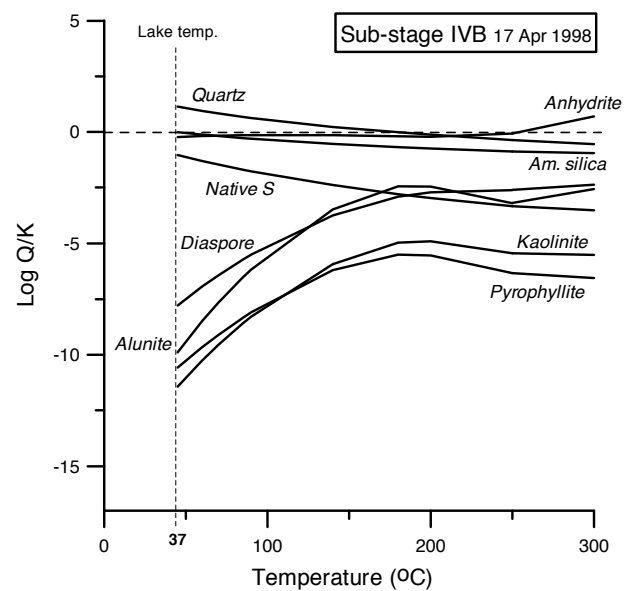
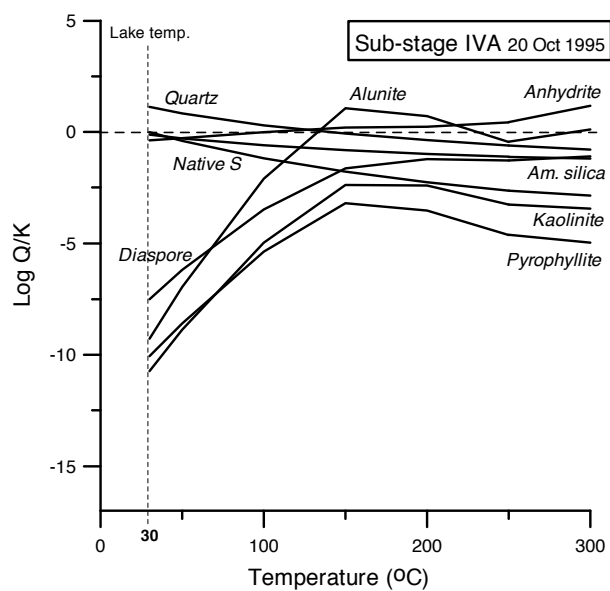
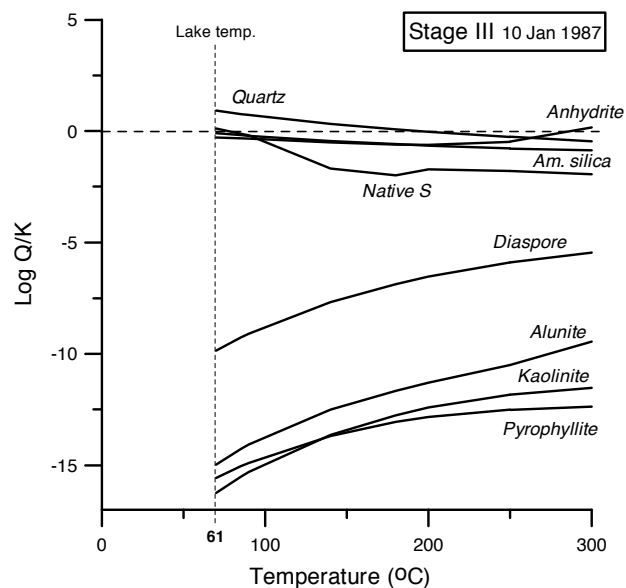
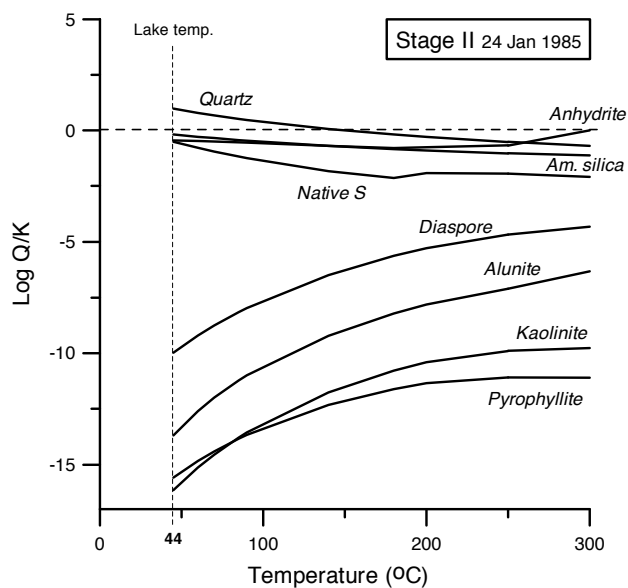
as deduced from a shift in the distribution of dominant polythionates species from penta- to tetrathionate observed in mid 1986 (Chapter 4). This was followed by a decline in the concentrations of polythionates to levels below detection limits, as a consequence of excess SO_2 injection, about three months prior to the onset of a new cycle of phreatic activity in June 1987. Some of the increase in the SO_4/F can be ascribed to this breakdown of polythionates, which is known to produce SO_4 (Takano and Watanuki, 1990; Takano *et al.*, 1994b), but it is insufficient to account for the overall increase. Hence, the combination of chemical changes indicates that an excess of SO_2 was injected into the lake (see Chapter 4). Because saturation of anhydrite/gypsum and/or native sulphur within or just below the lake is conceivable (see discussion below), it may have modulated lake's sulphate content, but not to the extent that it would obscure the increased SO_2 input.

Anomalous peaks or dips are superimposed on the long-term time-series trends of all ratios including Mg/Cl and Mg/F. The SO_4/Cl , F/Cl and Mg/Cl peaks between mid 1988 and mid 1989 (Stage III) can be attributed to a short-lived decrease in Cl concentration due to volatilisation of HCl from the acidic lake waters, rather than to further increase in the input of SO_4 , F or Mg (Fig. 5.5) (Rowe *et al.*, 1992b). This anomalous behaviour coincided with maximum temperatures and lowest pH. Substages IVA, IVC and IVE are marked by peaks in SO_4/F , Mg/Cl, Mg/F and dips in F/Cl (Figs. 5.5 and 5.6). As these intervals are further characterised by overall low anion concentrations and temperature, and by relatively high pH (Figs. 5.2 and 5.6), these features are not associated with exsolution of HCl from the lake water but reflect a temporary very low input of volatiles and heat. The influx of fluorine was reduced most, possibly again through preferential retention of F, which might be due to weakened degassing and correspondingly lower temperatures, which would enhance HF-rock interaction (see above). Overall low input is further consistent with sharp declines in polythionates, the $\text{SO}_2/\text{H}_2\text{S}$ ratios of subaqueous fumaroles, as well as the quiescence observed in the lake in substages IVA, IVC and IVE (Fig. 5.6, see also Fig. 4.7 in Chapter 4). These variations provide evidence for changes within the magmatic-hydrothermal system, which led to temporary blockage of fumarolic conduits that feed the lake region (cf., Chapter 4).

5.5.1.6 Behaviour of cations: time series and control of alteration minerals

Concentration trends of major cations (Fig. 5.3) follow the general pattern of the anions. In detail, however, minor but systematic differences among the cations can be observed. For example, Al was always more abundant than Fe during Stages I–III, whereas concentrations were similar during Stage IV. Also, K was more depleted relative to Na during Stage IV than previously. The trends of Ca and Si reflect deviations from conservative behaviour, since saturation of gypsum and amorphous silica in the lake water have influenced the concentration levels of these elements. This explains their somewhat smoother patterns compared to the other cations.

Variation among the cations are further illustrated in ternary diagrams (Fig. 5.4). Observed solute constituents are plotted together with average composition of Poás lavas and minerals in



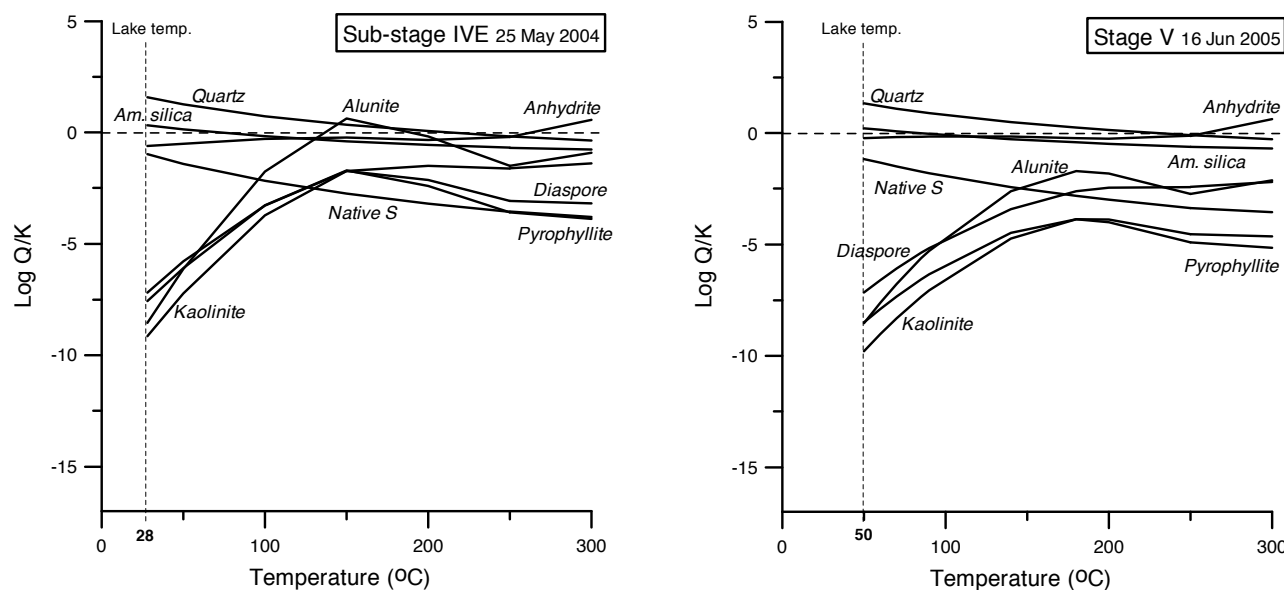


Figure 5.7. SOLVEQ-calculated saturation indices ($\log Q/K$) as a function of temperature (Reed, 1982; Reed and Spycher, 1989) for lake water samples representative of various stages and substages of the lake history between 1985 and 2005. Models were run for an adopted concentration of dissolved H_2S of 0.2 ppm. Vertical lines indicate *in-situ* measured lake temperatures. The plot for Stage III was constructed using lake chemical data from Rowe (1991).

order to explore the processes that control the lake's chemistry in the distinct stages. The Mg-Al-F diagram (Fig. 5.4c) shows that compositions during Stage III are largely governed by fumarolic input and congruent rock dissolution. Shifts away from the Al apex during the other stages point to water-rock interaction involving retention of this element. Near-congruent rock dissolution during Stage III is also suggested in the Mg-Na-K and Mg-Al-Na+K diagrams (Figs. 5.4d and 5.4e), where the lake compositions for this stage plot around average Poás lavas. In both diagrams the complete set of lake-water compositions show conspicuous linear trends, indicating that chemical signatures are controlled by secondary alteration minerals. In the Mg-Na-K triangle a phase with an approximate composition of 1:1 Na-K alunite appears to have regulated the alkali contents, demonstrating that both Na and K were not always quantitatively dissolved during water-rock interaction. Samples of Stage IV plot furthest away from the bulk rock, suggesting that alunite formation was most effective in retaining these elements in this time frame. As will be discussed below, the inferred role of alunite is consistent with mineral saturation modelling that predicts its presence in the hydrothermal system below the lake. Conversely, a group of Stage-III samples were enriched in the alkalis, presumably due to dissolution of alunite during high activity when chemical properties of the fluids were most extreme. A similar role of alunite in controlling cation concentrations has been inferred from chemical trends in the crater lake of Ruapehu volcano (Christenson and Wood, 1993).

Because Al is a major constituent of this mineral group, this element should have been retained as well. The Mg-Al-Na+K diagram (Fig. 5.4e), however, suggests an additional involvement of one or more other Al-bearing phases, since the trend is not aligned with the alunite composition. Presumably, kaolinite, pyrophyllite, diaspore and/or gibbsite formed part of the alteration assemblage as well.

5.5.1.7 Element ratios as precursor signals

Sharp increases in Mg/Cl ratios of volcanic lakes have been linked to phreatic eruptions (Kusatsu-Shirane, Ohba *et al.*, 2008), phreato-magmatic eruptions (Ruapehu, Giggenbach, 1983; Giggenbach and Glover, 1975; Christenson, 2000), dome growth (Pinatubo, Stimac *et al.*, 2003) and ash emissions (Popocatepetl, Armienta *et al.*, 2000). A high Mg/Cl ratio usually points to strong interaction between water and volcanic material at elevated temperatures, possibly due to intrusion of fresh magma (Giggenbach and Glover, 1975), or to invasion of groundwater into a region of hot rock, approaching the magma chamber (Ohba *et al.*, 2008). An increase in the ratio may thus signal pending eruptive activity.

However, at Poás the Mg/Cl ratio appears to be unsuitable as monitoring parameter for upcoming eruptive events. Apart from the above-mentioned peaks that were unrelated to eruptive activity, the Mg/Cl ratio did not show a significant increase prior to the period of phreatic activity of the late 1980's (Rowe *et al.*, 1992b). Furthermore, relatively high ratios observed near the transition between Stages I and II may also have resulted from HCl volatilisation, favoured by the extreme acidity ($pH < 0.6$) and high temperature (average $\sim 50^\circ C$) of the lake. A similar explanation might be valid for the slight increase towards the end of stage III (September 1993 – August 1994), when the highly reduced lake had a pH of 0.5 and a temperature around $60^\circ C$ (Fig. 5.5). Throughout the relatively quiet Stage IV, the observed Mg/Cl ratios were substantially higher than before the onset of eruptive activity in the late 1980's.

During 2005, prior to the phreatic eruptions of Stage V that started in March 2006, F/Cl and S_T/Cl (the latter not shown in Figs. 5.5 and 5.6) demonstrated a steady increase, pointing to an enhanced influx and condensation of SO_2 and HF-rich gas into the lake. This was not accompanied by a similar strong increase in SO_4/Cl or SO_4/F , presumably due to the sudden reappearance of polythionates in April 2005 (Chapter 4).

However, from February 2006 on, accompanied with a gradual 10-fold decline of polythionates, both ratios have shown a conspicuous increase as well. This behaviour of sulphur-bearing species is consistent with a steady enhancement of the SO_2 injected into the lake that started in early 2005. Thus, anion pairs, polythionate concentrations and lake temperature can be collectively regarded as clear precursors of the first phreatic eruptions in 2006, as they started showing changes about one year before the first event. Whether this will be applicable to predict future eruptive activity at Poás remains to be assessed, since precursor phenomena were not identical in the period preceding the activity of Stage III.

5.5.1.8 Aqueous speciation and mineral saturation modelling

The equilibrium distribution of aqueous species and the saturation state of mineral phases were explored using the SOLVEQ computer code version 1996 (Reed, 1982; Reed and Spycher, 1984), aiming to elucidate variations in the conditions in the lake water and to detect processes within the lake-hydrothermal system responsible for the compositional characteristics observed throughout stages II-V.

Calculations were performed for eight lake-water samples, considered to be representative of the lake composition during each of the stages or substages: January 1985 (Stage II, high activity), January 1987 (Stage III, peak activity), October 1995, April 1998, January 2002, August 2003 and May 2004 (Stage IV, various levels of relative quiescence), and June 2005 (Stage V, high activity) (Table 5.1, Figs. 5.2 and 5.7).

SOLVEQ was run using the H_2S - SO_4 redox buffer. Aqueous H_2S , measured infrequently during the last 10 years using a gas-tube method (Togano and Ochiai, 1987; Takano, pers. comm., 2005), remained virtually always undetected, so that the detection limit of 0.2 ppm was adopted in the calculations. Resulting saturation indices are therefore subject to some bias, but most phases discussed here are virtually insensitive to redox conditions, except for sulphides and native sulphur.

According to the SOLVEQ calculations, most of the Cl is dissociated and only a small portion is complexed as HCl . Dominant S species are HSO_4^- , as is expected at $\text{pH} < 2$, and SO_4^{2-} , while minor amounts of S are also present in the form of complexes with metals (e.g., KHSO_4 and CaSO_4). In contrast, F is mostly bonded with Al, forming AlF_2^+ and AlF_2^+ complexes. Apart from these fluorine species, much of the Al also occurs as a free ion. Most of the other major cations are predominantly present as free ions, while complexes with anionic ligands (cation-chloride and/or cation-sulphate) are significant as well. For instance, Ca is mainly present as a free ion but the CaCl^+ complex is relatively abundant. In general, the aqueous speciation calculated for the Poás lake-water samples is comparable to that inferred for the Kawah Ijen lake (Delmelle and Bernard, 1994).

Figure 5.7 illustrates the saturation state of the lake at different stages of activity for a number of relevant mineral phases. The saturation index is expressed as $\log Q/K$ values, where Q is the ion activity product and K the thermodynamic equilibrium constant at a given temperature. Values higher than, equal to or below zero indicate oversaturation, saturation, and undersaturation, respectively. Models were run for a range of temperatures between the measured lake temperature and

300°C in order to explore possible influences of the subsurface hydrothermal system on the chemical characteristics of the lake.

At the observed lake temperatures, the waters were invariably supersaturated with (crypto-)crystalline forms of silica (quartz, cristobalite and chalcedony, the latter phases not shown in Fig. 5.7). Barite (not shown) is usually saturated or oversaturated, whereas amorphous silica, gypsum/anhydrite and native sulphur are approximately saturated or slightly undersaturated. The aluminium-bearing phases alunite [$\text{KAl}_3(\text{SO}_4)_2(\text{OH})_6$], diaspore [$\text{AlO}(\text{OH})$], kaolinite [$\text{Al}_2\text{Si}_2\text{O}_5(\text{OH})_4$] and pyrophyllite [$\text{Al}_2\text{Si}_4\text{O}_{10}(\text{OH})_2$] were strongly undersaturated. At the adopted H_2S concentration of 0.2 ppm, pyrite and several other sulphides are saturated as well. Although sampled lake surface water may contain (much) less H_2S , these phases were probably stable under the more reducing conditions near the lake bottom, e.g., close to subaqueous vents (cf., Delmelle and Bernard, 1994). Preliminary SOLVEQ modelling of Poás lake water representative for the early stages yielded similar results (Rowe, 1991).

Reconnaissance analyses of suspended particles in the lake water column and of bottom sediments by powder X-Ray diffraction and electron-microprobe confirmed the presence of minerals inferred to be saturated. Amorphous silica, native sulphur, and gypsum were identified in suspended particles in a water sample collected with a 0.2- μm polycarbonate filter in September 2001. Amorphous and crystalline silica (cristobalite, trydimite?), gypsum/anhydrite, native sulphur, barite and some pyrite were found in lake sediments collected in August 2000 and September 2001. In addition, a Ti-bearing phase was found (ilmenite?). Although Ti-bearing minerals are not included in the SOLVEQ code, it is of interest to note that TiO_2 (anatase) was identified as precipitating phase in the crater lake of Kawah Ijen (Delmelle and Bernard, 1994), which is compositionally similar to the Poás lake. An alunite-jarosite mineral might also be present in the Poás sediment, although the SOLVEQ calculations indicate that alunite is not saturated at the observed lake temperatures.

Modelling the saturation status at higher temperatures (up to 300°C) explores the extent to which cation concentrations in the lake were inherited from entering brine water that had equilibrated at depth. Conversely, it also predicts which minerals would precipitate if lake water would be heated up when seeping downward through the lake bottom.

These simulations reveal strong contrasts between the active and quiet (sub-)stages (Fig. 5.7). With increasing temperatures, the lake waters from Stages II, III, substages IVB and IVD, and Stage V remain undersaturated with respect to aluminium-bearing phases (including Mg-beidellite [$\text{Mg}_{0.167}\text{Al}_{2.33}\text{Si}_{3.67}\text{O}_{10}(\text{OH})_2$], not shown), although the degree of undersaturation generally decreases. In contrast, the patterns for substages IVA, IVC, and IVE are significantly distinct, indicating saturation of alunite between 100 and 150°C. Furthermore, kaolinite and pyrophyllite tend to approach saturation as temperature increases, and are particularly close to it around 150°C for sub-stage IVC. Gypsum/anhydrite becomes usually saturated with increasing temperature as well, owing to the general increase of its saturation state.

Precipitation of alunite would lead to a relative decrease in K and Al concentrations in the lake waters. Because the SOLVEQ thermodynamic database only contains the K end member of alunite whereas the mineral is a solid solution between K and Na-endmembers, it is reasonable to suppose that Na will be retained as well. Precipitation of any of the other Al-bearing phases (kaolinite, pyrophyllite, diaspore, gibbsite) will further decrease the concentration of Al in the lake waters.

These predictions are in good agreement with the compositional trends shown in the ternary diagrams (Figs. 5.4d and Fig. 5.4e), where lake compositions appeared to be controlled by alunite (with K:Na close to 1:1) and at least one of the other Al phases. The lake waters of Stage IV plot furthest away from these minerals, particularly those of substages IVA, C and E), which is consistent with saturation of the lake waters with these minerals at elevated temperatures according to the SOLVEQ models. The role of precipitating alunite in these periods is further supported by ETR values (Fig. 5.9) and by the LREE depletion, discussed in sections 5.5.4 and 5.5.5, respectively.

5.5.2 Thermal springs in the active crater

Thermal springs along the foot of the eastern terrace (for locations see Figs. 5.1 and Fig. 2.20 Chapter 2) were a transient phenomenon within the crater area. They started appearing in March 1999 and continued to be active until drying out in January 2007 (cf., Fig. 5.6). Distribution, compositions, temperatures and flow rates varied with time. In most cases streamlets reached the lake but discharge rates were very small (maximum on the order of several litres per second).

Chemical compositions are given in Table 5.4 and variations in major anions and temperature are illustrated in Figs. 5.8a and 5.8c. These data cover the entire period of activity between Stages IV and initial part of Stage V. A limited data set reported previously by Vaselli *et al.* (2003) covers a more restricted interval (1999–2001, substage IVB).

Temperatures mostly ranged between 83 and 95°C, but were occasionally lower (not shown in Fig. 5.8a), particularly at the very start of spring activity. All of the spring waters were acid (pH=0.1–3.5) and carried a TDS load of 5300 mg/kg on average (disregarding a single anomalously high value of 14,900 mg/kg). They are clearly different from the lake water, not only because they are much more dilute but also in terms of anion proportions (Fig. 5.8c).

Chemical monitoring was infrequent and did not cover all of the discharge points, but systematic changes in compositions with time were observed in some of the most productive springs. Based on the relative amounts of S_T , Cl, and F, a sequence of roughly four distinct compositional groups can be identified in the course of Stages IV and V (Figs. 5.8a and 5.8c): (1) Practically all of the samples collected in substage IVB plot close to the S_T apex; given their enrichment in S_T over Cl and F, they can be classified as acid-sulphate waters. Quebrada Algas Blancas plotted near the S_T apex in August 2000 but was slightly more enriched in Cl in September 2001 (Fig. 5.8c). (2) Compositions of several springs showed a notable enrichment in Cl during substage IVD. This is visualised by a decrease in S_T /Cl ratios of Quebrada Este 6a and 6b springs to even lower values than observed in the lake, a shift that was accompanied by a

slight increase in temperature (Fig. 5.8a). (3) In the second half of 2004 (substage IVE), these springs were relatively enriched in S_T again, yielding S_T /Cl ratios only slightly higher than the lake water. (4) Finally, spring waters sampled during Stage V showed an enrichment in F, so that the anion proportions almost approached those of the lake waters sampled in Stages II and III (Fig. 5.8c).

The early compositions are comparable to those of crater seeps that were active in the late 1980s (Rowe *et al.*, 1995; see Table 5.4). These authors suggested that the sulphate is probably derived from oxidation of sulphur gases or weathering of native sulphur and alunite, and relatively high Ca concentrations from dissolution of gypsum. Abundant gypsum and sulphur are present in fumarolic deposits and, together with alunite, in old lake sediments or weathered tephra sequences in the crater walls. Calculated saturation indices indicated that the waters were saturated with silica, Fe-hydroxide, gypsum, potassium-jarosite and jurbanite. The seeps were actively precipitating gypsum, as was observed during Stage IV as well. Preliminary powder-XRD data point to the presence of alunite, jarosite minerals, cristobalite and tridymite near the Stage-IV springs.

5.5.3 Subaerial fumarolic gases and condensates

Over the last decades, subaerial fumarolic activity in the crater area has been characterised by marked variations in venting locations, temperatures, emission rates and compositions of gas and condensates. Fumarolic activity at the CPC has persisted almost throughout the entire period studied here, albeit with strong variations in intensity. Prior to Stage IV it was the only significant venting site, except during Stage I and the second half of Stage III when subaerial fumarolic activity was centred in the lake region. Other fumaroles, located in different areas within the active crater, only appeared in Stage IV and had a more transient existence. Modest fields in the southern and western sectors of the crater floor were active between 1995 and 2000, and more abundant and stronger fumaroles on the eastern terrace between 1998 and 2007 (see Fig. 2.20, Chapter 2). Details on lifetime and vigour of fumarolic venting activity during Stage IV are schematically given in Fig. 5.6.

Fumarolic gases and condensates have shown a rather wide range in temperatures, compositions and emission rates throughout the five-stage period. The CPC fumaroles had low temperatures (50–95°C) and low flow rates in Stage I (Fig. 5.2), but extreme temperatures (275–1020°C) and flow rates were observed in the 1980's (Stage II–first years of Stage III). Peak levels (730–1020°C) were registered in 1981–1983 (Malavassi and Barquero, 1982; Barquero and Malavassi, 1981a,b; 1983), when a strong sulphurous smell was perceived around the CPC. COSPEC measurements in February 1982 registered SO_2 fluxes around 800 tons per day (Casadevall *et al.*, 1984). From late 1988 onward, the CPC fumaroles had near boiling-point temperatures (80–95°C), except for a few occasions when temperatures were somewhat higher (e.g., 188°C in Stage IV), which was accompanied by the release of molten sulphur.

Between 1989 and 1994 (Stage III), subaerial fumaroles at the practically dry lake bottom showed temperatures from 80 to approximately 700°C, the higher temperatures being inferred by the use of an optical pyrometer, flames caused by ignition of sulphur, and a bluish fog released from the vents (Barquero,

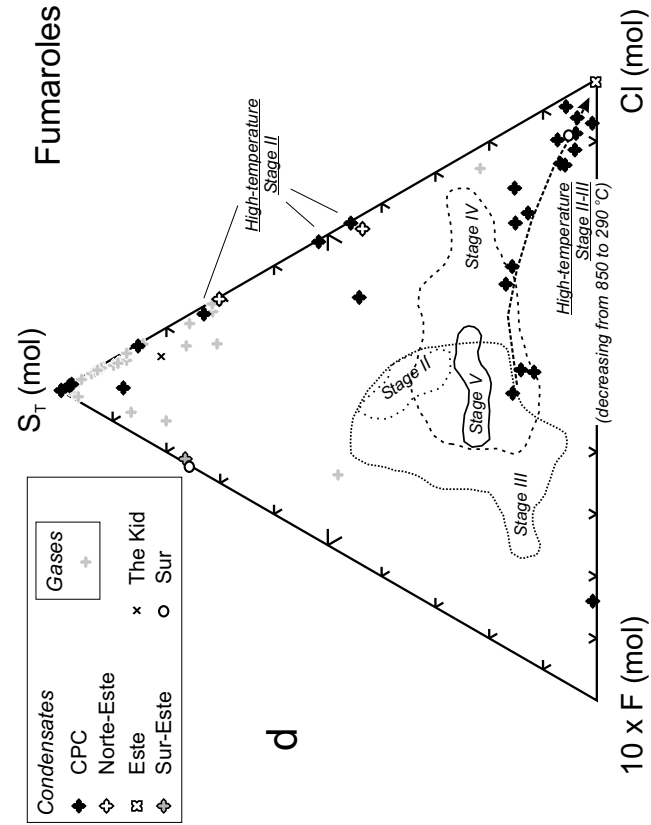
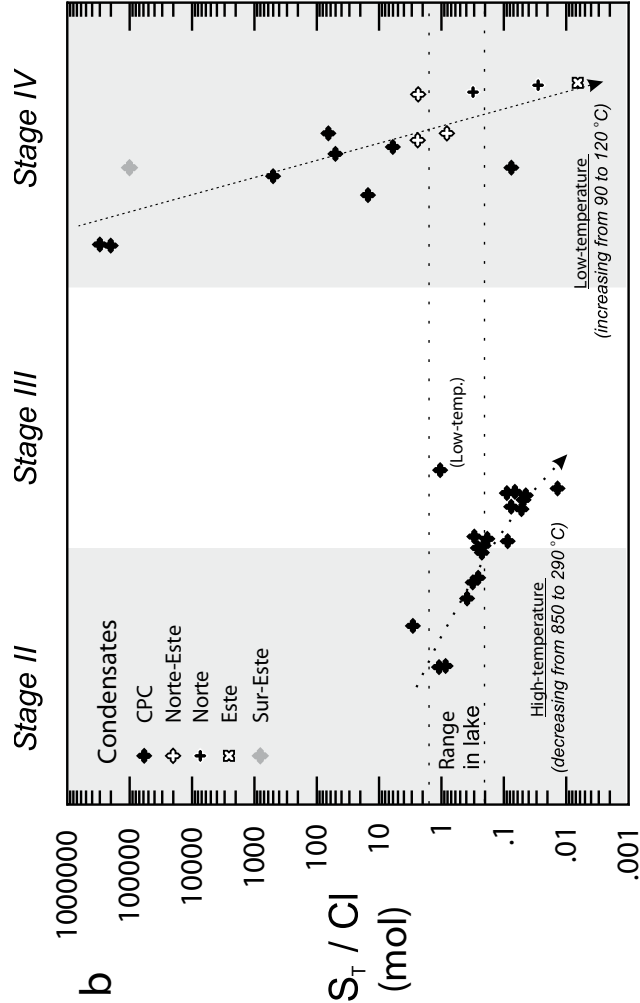
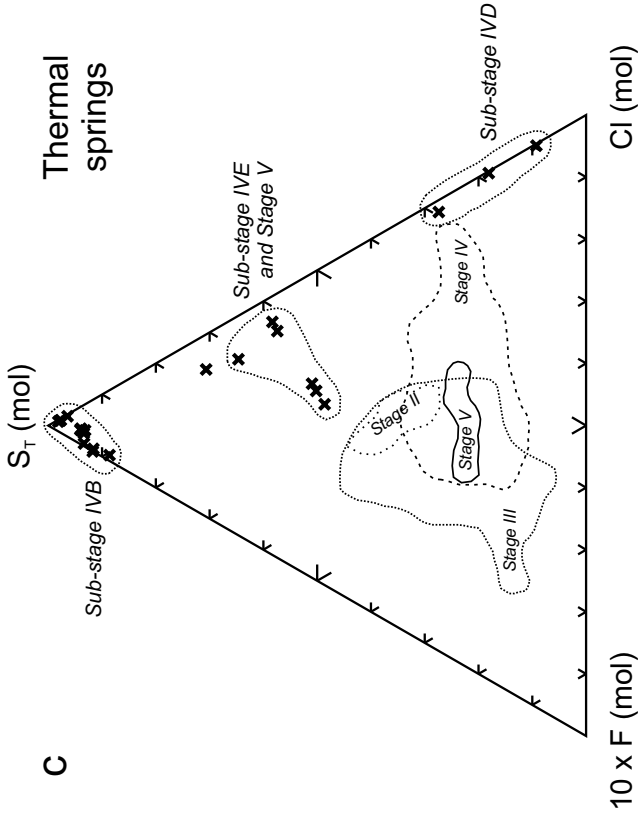
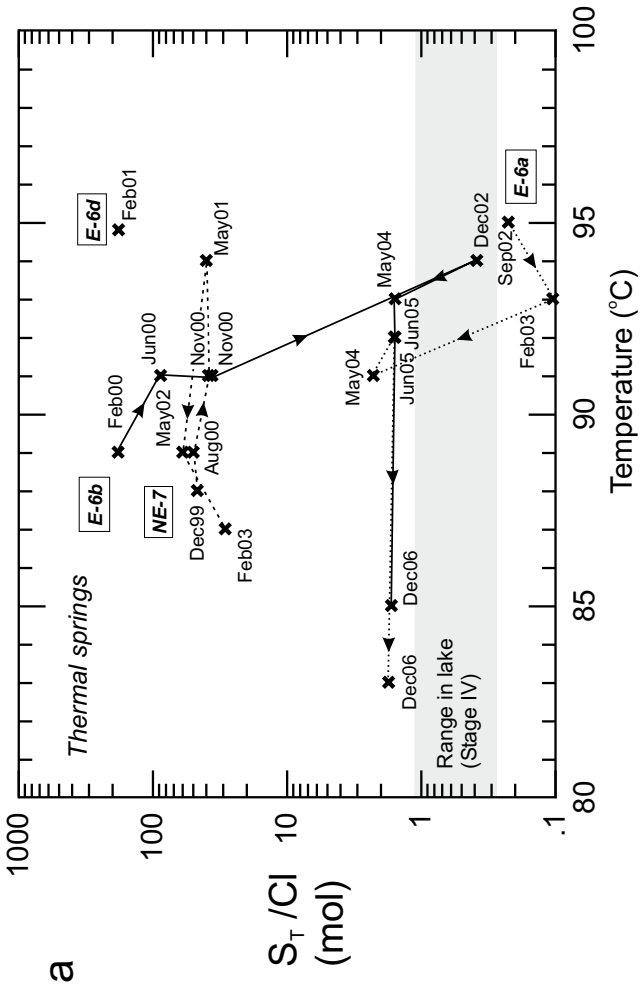
Table 5.4 Compositions of fumarole condensates and springs in the active crater of Poás Volcano.

Sample/Date	Sample code	T (°C)	pH _{Lab} (20-24±2°C)	SO ₄	Cl	F	Al	Fe	Ca	Si	Mg	Na	K	Mn	P	TDS	SO ₄ /Cl	F/Cl	Mg/Cl	Data source
Condensates																				
Norte																				
06-Nov-02	n.d.	119	1.27	4510	5350	n.d.	n.d.	n.d.	n.d.	n.d.	n.d.	n.d.	n.d.	n.d.	n.d.	n.a.	0.84	n.d.	n.d.	(1)
05-Dec-02	M-502-1	122	1.36	2050	9430	b.d.l.	15	25	20	4.6	2.0	5.3	4.1	0.35	0.46	9500	0.22	n.a.	0.0002	(2)
17-Jan-03	M-504-1	120	1.35	2210	5480	b.d.l.	2.7	6.2	4.3	0.59	b.d.l.	b.d.l.	b.d.l.	b.d.l.	b.d.l.	7700	0.40	n.a.	n.a.	(2)
28-Feb-03	n.d.	119	1.55	870	11400	n.d.	n.d.	n.d.	n.d.	n.d.	n.d.	n.d.	n.d.	n.d.	n.d.	n.a.	0.08	n.d.	n.d.	(1)
Norte-Este																				
Feb-01	7	101	n.d.	4130	640	0.50	n.d.	n.d.	n.d.	n.d.	n.d.	n.d.	n.d.	n.d.	n.d.	n.a.	6.5	0.0008	n.d.	(3)
8-May-01	FNP-1	94	1.30	2160	960	2.5	2.6	1.3	2.7	3.7	0.07	0.67	1.3	b.d.l.	b.d.l.	3130	2.2	0.003	0.0001	(2)
24-Oct-02	n.d.	93	1.96	4090	650	n.d.	n.d.	n.d.	n.d.	n.d.	n.d.	n.d.	n.d.	n.d.	n.d.	n.a.	6.3	n.d.	n.d.	(1)
Este																				
31-Mar-03	M-531	97	0.90	100	5450	b.d.l.	b.d.l.	0.26	0.57	7.2	b.d.l.	b.d.l.	b.d.l.	b.d.l.	b.d.l.	5560	0.02	n.a.	n.a.	(2)
Sur-Este																				
Feb-00	5	92	n.d.	67	0.20	0.50	n.d.	n.d.	n.d.	n.d.	n.d.	n.d.	n.d.	n.d.	n.d.	n.a.	335	2.5	n.d.	(3)
Sur																				
Feb-98	1	98	n.d.	4.0	26	0.10	n.d.	n.d.	n.d.	n.d.	n.d.	n.d.	n.d.	n.d.	n.d.	n.a.	0.15	0.004	n.d.	(3)
Feb 99	1	98	n.d.	11	<0.01	0.07	n.d.	n.d.	n.d.	n.d.	n.d.	n.d.	n.d.	n.d.	n.d.	n.a.	1100	7.0	n.d.	(3)
The Kid (La Niña)																				
Feb 01	9	95	n.d.	385	26	0.40	n.d.	n.d.	n.d.	n.d.	n.d.	n.d.	n.d.	n.d.	n.d.	n.a.	15	0.02	n.d.	(3)
CPC																				
1-Dec-81	PO-7	851	0.80	2620	880	0.70	130	17	4.5	80	10	29	79	b.d.l.	b.d.l.	3860	3.0	0.001	0.01	(4)
15-Dec-81	PO-8	852	0.80	2560	1120	0.80	10	7.2	b.d.l.	17	0.80	7.1	14	b.d.l.	b.d.l.	3740	2.3	0.001	0.001	(4)
1983	n.d.	761	n.d.	7430	950	1.4	n.d.	n.d.	n.d.	n.d.	n.d.	n.d.	n.d.	n.d.	n.d.	n.a.	7.8	0.001	n.d.	(5)
6-Jun-84	n.d.	603	n.d.	11500	11000	600	n.d.	n.d.	n.d.	n.d.	n.d.	n.d.	n.d.	n.d.	n.d.	n.a.	1.0	0.05	n.d.	(6)
11-Jan-85	n.d.	550	n.d.	10000	11700	540	n.d.	n.d.	n.d.	n.d.	n.d.	n.d.	n.d.	n.d.	n.d.	n.a.	0.85	0.05	n.d.	(6)
1-Mar-85	n.d.	584	n.d.	7640	11000	520	n.d.	n.d.	n.d.	n.d.	n.d.	n.d.	n.d.	n.d.	n.d.	n.a.	0.69	0.05	n.d.	(6)
7-Feb-86	n.d.	300	n.d.	5590	9160	110	n.d.	n.d.	n.d.	n.d.	n.d.	n.d.	n.d.	n.d.	n.d.	n.a.	0.61	0.01	n.d.	(6)
4-Apr-86	n.d.	300	n.d.	7500	10600	200	n.d.	n.d.	n.d.	n.d.	n.d.	n.d.	n.d.	n.d.	n.d.	n.a.	0.71	0.02	n.d.	(6)
2-May-86	n.d.	300	n.d.	10800	19100	130	n.d.	n.d.	n.d.	n.d.	n.d.	n.d.	n.d.	n.d.	n.d.	n.a.	0.57	0.007	n.d.	(6)
23-Jul-86	n.d.	367	n.d.	4400	18800	120	n.d.	n.d.	n.d.	n.d.	n.d.	n.d.	n.d.	n.d.	n.d.	n.a.	0.23	0.006	n.d.	(6)
23-Aug-86	n.d.	358	n.d.	7140	14300	160	n.d.	n.d.	n.d.	n.d.	n.d.	n.d.	n.d.	n.d.	n.d.	n.a.	0.50	0.01	n.d.	(6)
24-Sep-86	n.d.	538	n.d.	4820	5990	130	n.d.	n.d.	n.d.	n.d.	n.d.	n.d.	n.d.	n.d.	n.d.	n.a.	0.80	0.02	n.d.	(6)
10-Sep-87	n.d.	520	n.d.	290	2040	10	n.d.	n.d.	n.d.	n.d.	n.d.	n.d.	n.d.	n.d.	n.d.	n.a.	0.14	0.005	n.d.	(6)
30-Oct-87	n.d.	466	n.d.	270	1400	10	n.d.	n.d.	n.d.	n.d.	n.d.	n.d.	n.d.	n.d.	n.d.	n.a.	0.19	0.007	n.d.	(6)
21-Jan-88	n.d.	441	n.d.	230	1470	5.3	n.d.	n.d.	n.d.	n.d.	n.d.	n.d.	n.d.	n.d.	n.d.	n.a.	0.16	0.004	n.d.	(6)
2-Mar-88	n.d.	330	n.d.	220	1600	4.2	n.d.	n.d.	n.d.	n.d.	n.d.	n.d.	n.d.	n.d.	n.d.	n.a.	0.13	0.003	n.d.	(6)
6-Apr-88	n.d.	295	n.d.	400	1590	5.2	n.d.	n.d.	n.d.	n.d.	n.d.	n.d.	n.d.	n.d.	n.d.	n.a.	0.25	0.003	n.d.	(6)
13-Apr-88	n.d.	298	n.d.	480	2670	2.4	n.d.	n.d.	n.d.	n.d.	n.d.	n.d.	n.d.	n.d.	n.d.	n.a.	0.18	0.001	n.d.	(6)
8-Jun-88	n.d.	290	n.d.	65	2580	10	n.d.	n.d.	n.d.	n.d.	n.d.	n.d.	n.d.	n.d.	n.d.	n.a.	0.03	0.004	n.d.	(6)
22-Feb-89	n.d.	95	n.d.	690	240	3.8	n.d.	n.d.	n.d.	n.d.	n.d.	n.d.	n.d.	n.d.	n.d.	n.a.	2.9	0.02	n.d.	(6)
4-Apr-97	M-558	93	2.70	210	b.d.l.	b.d.l.	1.3	0.84	2.7	5.9	0.15	2.9	1.4	b.d.l.	b.d.l.	220	n.a.	n.a.	n.a.	(2)
17 Apr-1997	M-553	93	2.70	270	b.d.l.	b.d.l.	1.3	0.60	3.0	2.2	0.14	3.6	1.0	b.d.l.	b.d.l.	280	n.a.	n.a.	n.a.	(2)
Feb-99	2	92	n.d.	610	14	0.75	n.d.	n.d.	n.d.	n.d.	n.d.	n.d.	n.d.	n.d.	n.d.	n.a.	44	0.05	n.d.	(3)

Sample/Date	Sample code	T (°C)	pH _{lab} (20-24±2°C)	SO ₄	Cl	F	Al	Fe	Ca	Si	Mg	Na	K	Mn	P	TDS	SO ₄ /Cl	F/Cl	Mg/Cl	Data source
Nov-99	2	92	n.d.	580	1.2	0.06	n.d.	n.d.	n.d.	n.d.	n.d.	n.d.	n.d.	n.d.	n.d.	n.a.	485	0.05	n.d.	(3)
Feb-00	2	94	n.d.	96	470	140	n.d.	n.d.	n.d.	n.d.	n.d.	n.d.	n.d.	n.d.	n.d.	n.a.	0.20	0.29	n.d.	(3)
24-Aug-00	M-20	92	2.30	480	5.0	b.d.l.	b.d.l.	1.9	0.90	5.3	b.d.l.	b.d.l.	5.2	b.d.l.	b.d.l.	500	96	n.a.	n.a.	(2)
3-Nov-00	M-575	94	2.20	550	35	b.d.l.	3.4	22	17	12	1.4	3.7	3.9	0.24	b.d.l.	670	16	n.a.	0.04	(2)
24-May-01	M-18-1	94	2.60	1230	6.5	b.d.l.	6.5	8.0	3.3	7.5	b.d.l.	b.d.l.	4.8	b.d.l.	b.d.l.	1270	189	n.a.	n.a.	(2)
17-Jan-03	M-503-A	92	2.45	150	b.d.l.	b.d.l.	0.22	0.80	2.4	0.29	0.56	0.93	0.82	b.d.l.	b.d.l.	160	n.a.	n.a.	n.a.	(2)
Crater springs																				
AC seeps																				
Jun 88 - Sep 90	average ± 1σ	18.0±3.9	2.55±0.34	2760±470	366±282	34±13	146±66	97±84	587±66	55±9	56±27	50±32	7.0±31	n.d.	n.d.	4180±960	8.0	0.09	0.15	(7)
Este																				
Feb-00	6b	89	0.12*	12200	25	16	520	1000	550	n.d.	350	180	13	13	n.d.	14900	488	0.64	14	(3)
16-Jun-00	M-25 or 6b	91	2.10	3350	13	8.0	120	110	520	n.d.	28	110	3.9	1.3	n.d.	4270	258	0.62	2.1	(2)
21-Nov-00	M-811 or 6b	91	2.30	2800	29	1.4	42	350	380	n.d.	33	170	b.d.l.	4.3	0.36	3800	93	0.05	1.1	(2)
Feb-01	de Hierro or 6d	95	2.77*	3500	6.2	6.0	11	910	190	n.d.	81	130	19	5.4	n.d.	4860	565	1.0	14	(3)
20-Sep-02	6a	95	1.10	5660	9300	b.d.l.	n.d.	n.d.	n.d.	n.d.	n.d.	n.d.	n.d.	n.d.	n.d.	n.a.	0.61	n.a.	n.d.	(2)
5-Dec-02	M-506 o 6b	94	2.00	5000	4700	8.0	n.d.	n.d.	n.d.	n.d.	n.d.	n.d.	n.d.	n.d.	n.d.	n.a.	1.1	0.002	n.d.	(2)
14-Feb-03	6a	93	1.75	3900	13900	b.d.l.	n.d.	n.d.	n.d.	n.d.	n.d.	n.d.	n.d.	n.d.	n.d.	n.a.	0.28	n.a.	n.d.	(2)
25-May-04	6a	91	1.52	6440	1030	13	n.d.	n.d.	n.d.	n.d.	n.d.	n.d.	n.d.	n.d.	n.d.	n.a.	6.3	0.01	n.d.	(1)
25-May-04	6b	93	1.76	7000	1640	9.0	n.d.	n.d.	n.d.	n.d.	n.d.	n.d.	n.d.	n.d.	n.d.	n.a.	4.3	0.005	n.d.	(1)
16-Jun-05	6a	92	1.44	2170	480	16	n.d.	n.d.	n.d.	n.d.	n.d.	n.d.	n.d.	n.d.	n.d.	n.a.	4.5	0.03	n.d.	(1)
16-Jun-05	6b	92	0.99	16780	3885	33	n.d.	n.d.	n.d.	n.d.	n.d.	n.d.	n.d.	n.d.	n.d.	n.a.	4.3	0.01	n.d.	(1)
8-Dec-06	6a	83	1.85	660	144	5.8	n.d.	n.d.	n.d.	n.d.	n.d.	n.d.	n.d.	n.d.	n.d.	n.a.	4.6	0.04	n.d.	(1)
8-Dec-06	6b	85	1.92	1020	228	6.8	n.d.	n.d.	n.d.	n.d.	n.d.	n.d.	n.d.	n.d.	n.d.	n.a.	4.5	0.03	n.d.	(1)
White Algae																				
23-Aug-00	6e	42	2.47	2220	0.40	3.0	82	55	570	93	19	45	3.7	0.90	n.d.	3090	5545	7.5	48	(2)
21-Sep-01	M-776-1 or 6e	52	1.55	6680	813	10	480	570	310	220	81	130	19	3.5	1.1	9300	8.2	0.01	0.10	(2)
Algas Verdes																				
21-Nov-00	M-822 or 6f	57	2.50	2340	24	1.0	93	110	540	180	29	110	7	1.5	0.14	3400	98	0.04	1.2	(2)
Norte-Este																				
Mar-99	7	15	3.51*	2150	16	2.0	130	39	520	n.d.	36	22	2.0	0.40	n.d.	2900	134	0.13	2.3	(3)
3-Dec-99	7	88	2.7	2730	20	b.d.l.	n.d.	n.d.	n.d.	n.d.	n.d.	n.d.	n.d.	n.d.	n.d.	n.a.	136	n.a.	n.d.	(2)
23-Aug-00	7	89	2.9	2890	22	0.60	2.0	470	330	220	180	260	24	8.1	n.d.	5887	132	0.02	8.0	(2)
21-Nov-00	M-810-1 or 7	91	2.6	2600	24	1.7	12	180	410	n.d.	110	180	n.d.	5.9	n.d.	3524	108	0.07	5.0	(2)
8-May-01	FT-2 or 7	94	2.05	2700	24	2.0	2.5	450	310	210	120	220	22	6.3	n.d.	4070	113	0.08	5.0	(2)
16-May-02	M-856 or 7	89	2.50	2850	19	0.22	130	300	290	n.d.	110	410	n.d.	4.5	3.4	4130	150	0.01	5.9	(2)
14-Feb-03	7	87	1.95	2530	33	b.d.l.	n.d.	n.d.	n.d.	n.d.	n.d.	n.d.	n.d.	n.d.	n.d.	n.a.	77	n.a.	n.d.	(2)

Concentrations are given in mg/kg; n.d.: no data available; n.a.: not applicable; b.d.l.: below detection limit.

*: pH measured in situ. Data sources: (1) OVSICORI; (2) This work; (3) Vaselli et al., 2003; (4) Gemmell, 1987; (5) Prosser, 1983; (6) Rowe et al., 1992a; (7) Rowe et al., 1995



→ *Figure 5.8.* Total sulphur (S_T)-Cl-F relationships in crater springs, fumarole condensates and gas samples. (a) Temporal evolution of molar S_T /Cl ratios versus temperature of crater springs at the eastern terrace collected in Stages IV and V; (b) Time series of molar S_T /Cl ratios of fumarole condensates from different vents; (c) S_T -Cl-F plot for the thermal springs illustrating relative enrichment in S_T in substage IVB, followed by Cl enrichment in IVD, intermediate S_T /Cl ratios in IVE, and subsequent enrichment in F in Stage V; symbols as in panel a; (d) S_T -Cl-F plot for fumarolic gases and condensates from the CPC and other subaerial fumaroles collected in Stages II-IV. Fumarolic gas is relatively enriched in S_T , while condensates show a wider range of compositions; symbols as in panel b. All panels show fields for crater-lake waters for comparison. S_T (total sulphur) was calculated from free sulphate measured by IC, except for lake samples, which were analysed by ICP-AES.

1998; Martínez *et al.*, 2000; Venzke *et al.*, 2002–; Allen *et al.*, 2002; Taran, pers. comm., 2006; see also Chapters 2 and 4). SO_2 fluxes, measured in 1991, averaged around 91 tons per day (Andres *et al.*, 1992).

Virtually all subaerial fumaroles issued at the southern, western and eastern inner flanks of the active crater in Stage IV (see Fig. 2.20, sites 2–4, Chapter 2) showed temperatures around boiling point (87–95°C). However, temperatures of Fumarole Norte, active in the eastern field (Stage IV and part of Stage V, see Fig. 2.28, Chapter 2), varied between 90 and 290°C, showing a significant rise at the transition to Stage V (Fig. 5.2). Averaged SO_2 fluxes in the period February 2001–April 2006 ranged between 8 and 500 tons per day (Fournier *et al.*, 2001, 2002; Galle, 2002; Edmonds, 2003 pers. comm.; Zimmer *et al.*, 2004, OVSICORI, 2006c; Williams-Jones, 2008 pers. comm.; Hilton *et al.*, 2008) and were lower than in 1991, except for the flux determined in 2005 (see Table 6.2, Chapter 6).

Compositional data on condensate and gas samples, collected at accessible fumaroles around the CPC and at the eastern terrace are reported in Table 5.3 and Table APP-4.2.1, respectively. These tables compile the most relevant data from the following sources: Prosser (1983), Gemmell (1987), Rowe *et al.* (1992a), Venzke *et al.* (2002–), Díaz *et al.* (2002), Vaselli *et al.* (2003), Zimmer *et al.* (2004), Fischer and Taran (2004), Tassi *et al.*, unpublished, Ohba (pers. comm.), OVSICORI (unpublished) and this work.

Figures 5.8b and 5.8d illustrate the compositional evolution of gases and condensates. The discussion will be restricted here to the mutual proportions of several of the most abundant condensable gas phases (SO_2+H_2S , HCl and HF), given the emphasis on temporal changes in volcanic-hydrothermal activity and relationship with lake and spring waters. More detailed treatments of fumarole compositions can be found in the above-mentioned publications.

No complete data are available for the high-T gases emitted at the CPC during Stages II and III. Hence, the gas compositions shown in the ternary S_T -Cl-F diagram (Fig. 5.8d) are restricted to Stages IV and V, and mostly represent low-T fumaroles from the eastern crater wall. CPC gas data are a small minority and include a single data point from Stage III. Gas compositions do not show significant variations, and, except for a few outliers, all plot near the S_T apex. Molar SO_2/H_2S ratios averaged around 45, which is significantly lower than those of the high-T gases of the CPC sampled in Stage II (Table APP-4.2.1).

Condensate data displayed in Figs. 5.8b and 5.8d are mostly from the CPC and include those from the high-T gases emitted during Stages II and III. They display a much wider compositional range than the gas data, as well as systematic changes with time. The group of high-T condensates shows a general trend of decreasing molar S_T /Cl ratios with time, corresponding to a general temperature decrease from 850 to 290°C, but the earliest Stage-II samples had relatively modest anion concentrations and were depleted in F. Subsequent compositions (1984 on) were strongly enriched in F, so that proportions of sulphur and halogen species were close to those of the lake water, which is evidence for uninhibited influx of high-T gas of magmatic origin and direct condensation into the lake (cf., Brantley *et al.*, 1987; Casertano *et al.*, 1987; Rowe *et al.*, 1992b). Gradually, at the Stage II-III transition and coinciding with the first phreatic eruptions in Stage III, condensate compositions became relatively depleted in F and S_T , resulting in a shift towards the Cl corner (Fig. 5.8d) and in S_T /Cl ratios lower than those of the lake (Fig. 5.8b).

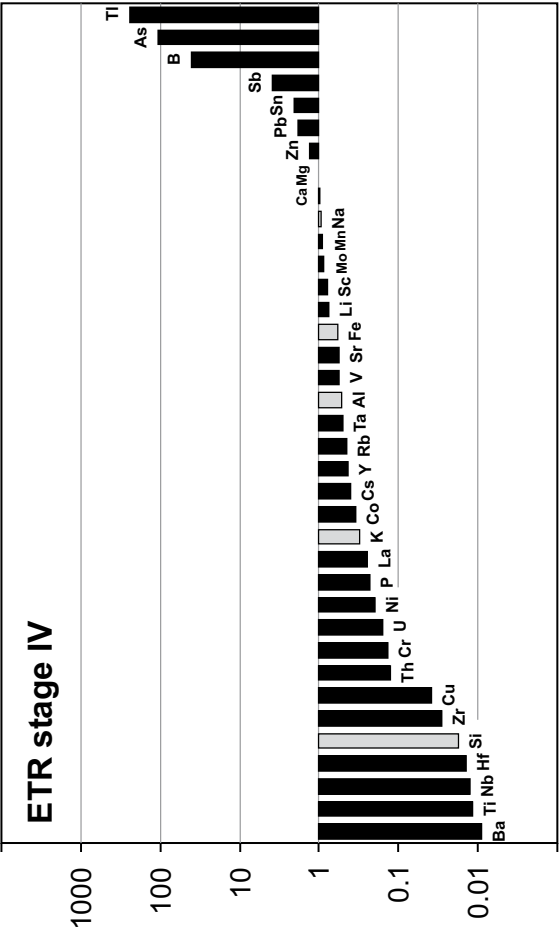
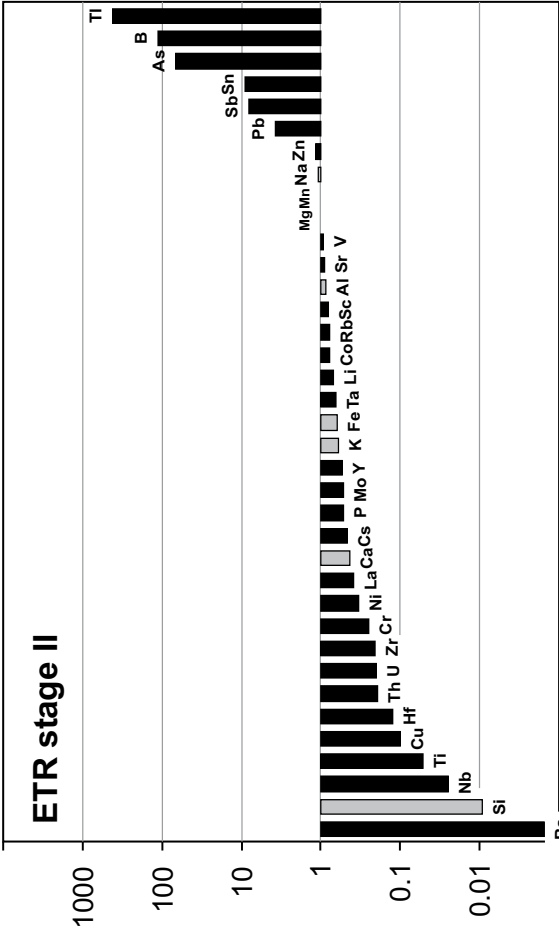
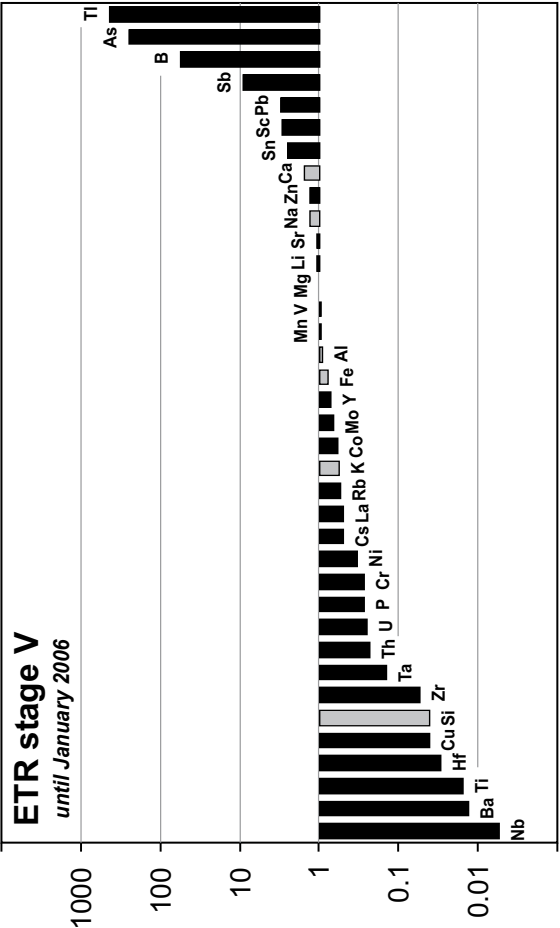
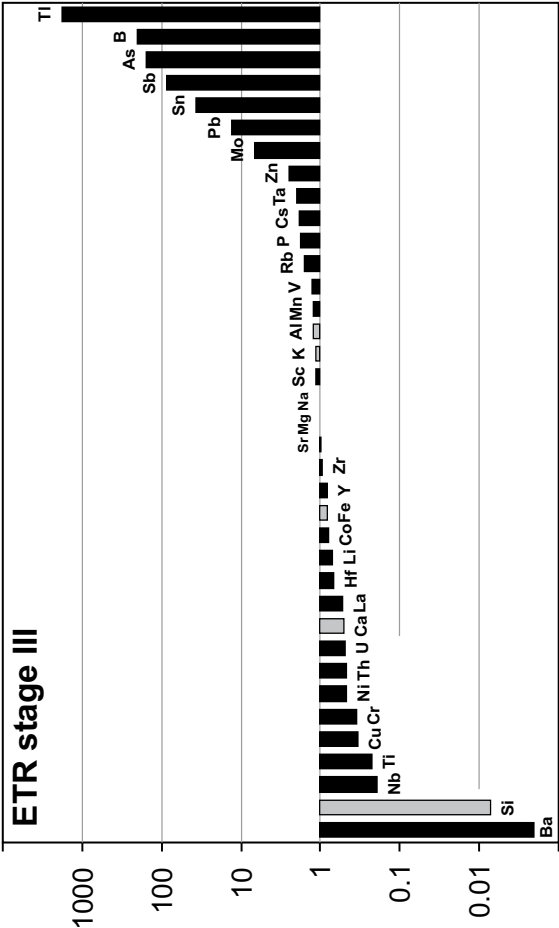
Condensates from the low-T fumaroles that were active in Stage IV had generally lower anion concentrations than the high-T condensates. Interestingly, the Norte and Norte-Este fumaroles on the eastern terrace were enriched compared to those at the CPC. With few exceptions, all condensates were relatively depleted in F, plotting near the S_T -Cl join in Fig. 5.8d. Starting with CPC compositions plotting near the S_T apex (substage IVA), they collectively show a tendency of decreasing molar S_T /Cl ratios in the course of Stage IV, reaching values lower than the lake water and coinciding with a mild increase in temperature (from 90 to 120°C) (Fig. 5.8b). This preceded a further strong temperature increase of the Norte fumarole around the Stage IV-V transition, but no data are available to detect a corresponding effect in condensate compositions.

5.5.4 Water-rock interaction: Element transfer ratios

Water-rock interaction processes that control the concentrations of dissolved elements in the lake water can be explored using the concept of element transfer ratios (ETR, Pasternack and Varekamp, 1994). Correspondence with, or deviations from congruent rock dissolution can be visualised in diagrams showing concentration ratios of elements in the fluid and in a reference rock, normalised to Mg, which is assumed to be quantitatively transferred from the rock into a fluid and to behave conservatively in lake water. ETR values greater than one indicate enrichment, and values less than one indicate depletion in the lake water relative to quantitative transfer via congruent rock dissolution.

Figure 5.9 compares ETR values in the lake water for Stages II, III, IV, and V, based on averaged element abundances for these periods. The average composition of lavas from Poás (basaltic-andesitic) was taken as reference (Malavassi, 1991; Carr *et al.*, 2003, 2007).

The ETR diagrams of the four stages are roughly similar, although there are second-order differences that can be ascribed to variations in the status of activity. In all cases the waters are relatively enriched in Zn, Pb, Sn, Sb, B, As and Tl ($ETR > 1$). Because these trace elements are highly mobile in volcanic gases (Symonds *et al.*, 1994; Churakov *et al.*, 2000), it can be assumed they were preferentially introduced into the lake water



→ *Figure 5.9.* Element transfer ratios (ETR) for lake water compositions averaged for each of the stages II–V. Positive and negative values indicate extra addition or removal of an element relative to quantitative transfer (ETR=1) during water–rock interaction (Pasternack and Varekamp, 1994). Note that most elements are depleted in the lake waters except for the Stage-III samples. Major rock-forming elements are shaded in grey. An averaged composition of Poás lavas (Malavassi, 1991; Carr *et al.*, 2003, 2007) is used as rock reference. Values were normalised against magnesium, which was assumed to dissolve congruently and behave conservatively in the lake (see text for further explanation).

largely via subaqueous fumaroles and gas condensation rather than by rock dissolution only. This is confirmed by enrichment factors (equivalent to ETR) calculated for fumarole condensates from the CPC (Fig. 5.10). The results of high-temperature (344–852°C) condensates (Gemmell, 1987), sampled in November–December 1981 (Stage II), as well as those of a low-temperature (93°C) sample, taken in April 1997 (Stage IV), indicate that strongly enriched elements in the condensates (relative to Mg and other rock-forming elements) are also enriched in the lake waters.

Several causes can be responsible for element abundances that show depletion in the lake relative to congruent rock dissolution (ETR<1): the element was (1) retained in a residue of rock dissolution, (2) incorporated in an alteration mineral that formed during rock dissolution, (3) incorporated as major constituent of a mineral that formed in the lake.

Major rock-forming elements (RFE) are depleted or have ETR's close to one. Silicon deviates most from congruent rock dissolution and is strongly depleted. Saturation and precipitation of amorphous silica in the lake environment is an obvious mechanism that can account for lowered ETR values. In addition, acid water–volcanic rock interaction will lead to silicification, implying that relatively large amounts of Si were already initially retained in alteration products. It is likely that the strongly negative ETR for Si reflects the combined effect of both processes. During Stage IV and (the initial part of) Stage V, Ca abundances were close to agreeing with quantitative transfer from volcanic rock dissolution. Relative depletion of this element during Stages II and III is consistent with saturation of gypsum when the lake was hotter and more active. In contrast, Al had an ETR<1 during the relatively quiet Stage IV, when alunite and possibly other Al-bearing phases were saturated at depth, as predicted by the SOLVEQ calculations (section 5.5.1.8). The corresponding behaviour of K (ETR<1, except for Stage III) confirms this, whereas quantitative transfer from the rocks appears to have always governed Na abundances. Iron has an ETR close to one but tends to be somewhat depleted. Saturation of pyrite, predicted by SOLVEQ calculations and observed in sulphur globules collected from the lake, might explain this. Progressive acid water–rock interaction might also lead to the formation of other Fe-bearing minerals (e.g., hematite, Delmelle and Bernard, 1994), but modelling and absence in analysed sediment samples suggest that they did not play a major role at Poás.

Among the depleted trace elements, Ba has always very low ETR values due to saturation of barite, a common phenomenon for acid crater lakes (Casadevall, *et al.*, 1984; Delmelle and Bernard, 1994; Varekamp *et al.*, 2001; Sriwana *et al.*, 2000). The

negative ETR values of titanium and other high-field-strength elements, including Th and U, can be attributed to the generally poor solubility of these elements in aqueous environments. Niobium is the least mobile of this group, while an ETR value near unity indicates that Zr was quantitatively transferred from the volcanic rocks during the highly acid conditions of Stage III. It cannot be excluded that Ti is (partly) controlled by precipitation of anatase as well (cf., Delmelle and Bernard, 1994). Lanthanum (and other REE) is moderately depleted. Its ETR value is lowest during Stage IV, consistent with the inferred saturation of alunite at depth (section 5.5.1.8). Copper shows a deviating behaviour among the chalcophile elements in being strongly depleted. This may reflect the composition of entering gases, as Cu is less abundant than Pb and Zn in condensates of high-T fumaroles of the CPC (Gemmell, 1987). In addition, Cu may have been removed by the formation of Cu-sulphide, which is readily saturated in or just below acid crater lakes where conditions are more reducing (Christenson and Wood, 1993; Delmelle and Bernard, 1994; Sriwana *et al.*, 2000).

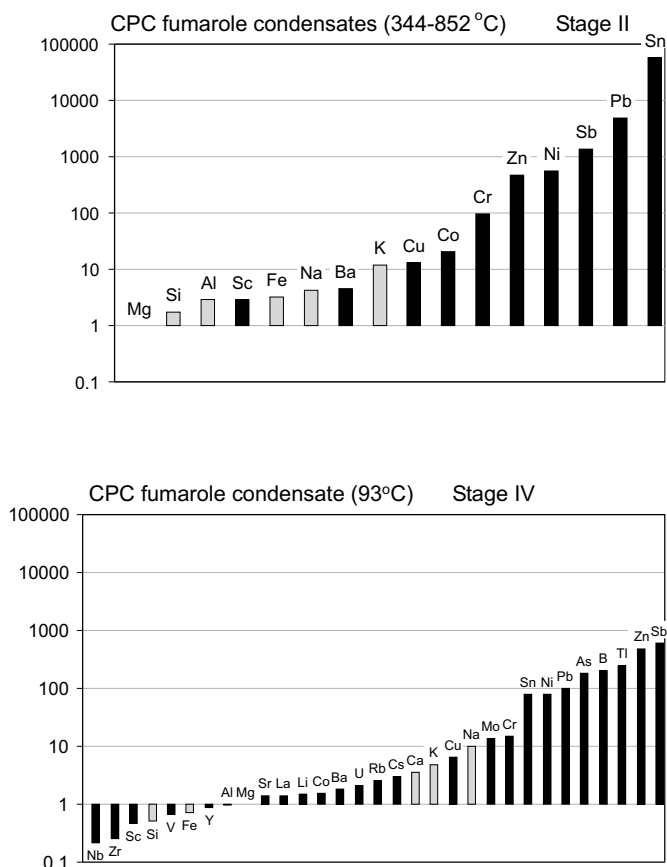


Figure 5.10. Enrichment factors for elements analysed in fumarole condensates from the CPC. Left: average of eight high-T condensates (344–852°C), sampled in November–December 1981 (Stage II) from Gemmell (1987). Right: low-T condensate (93°C) sampled on 17 April 1997 (this work). Note that enrichment of highly mobile elements relative to major rock-forming elements (shaded in grey) corresponds to ETR relationships in the lake waters, pointing to an important role of gaseous input by subaqueous fumaroles. The enrichment factors are equivalent to ETR ratios, as they were also calculated using Mg as reference element and an average composition of Poás lavas (Malavassi, 1991; Carr *et al.*, 2003, 2007) as reference rock.

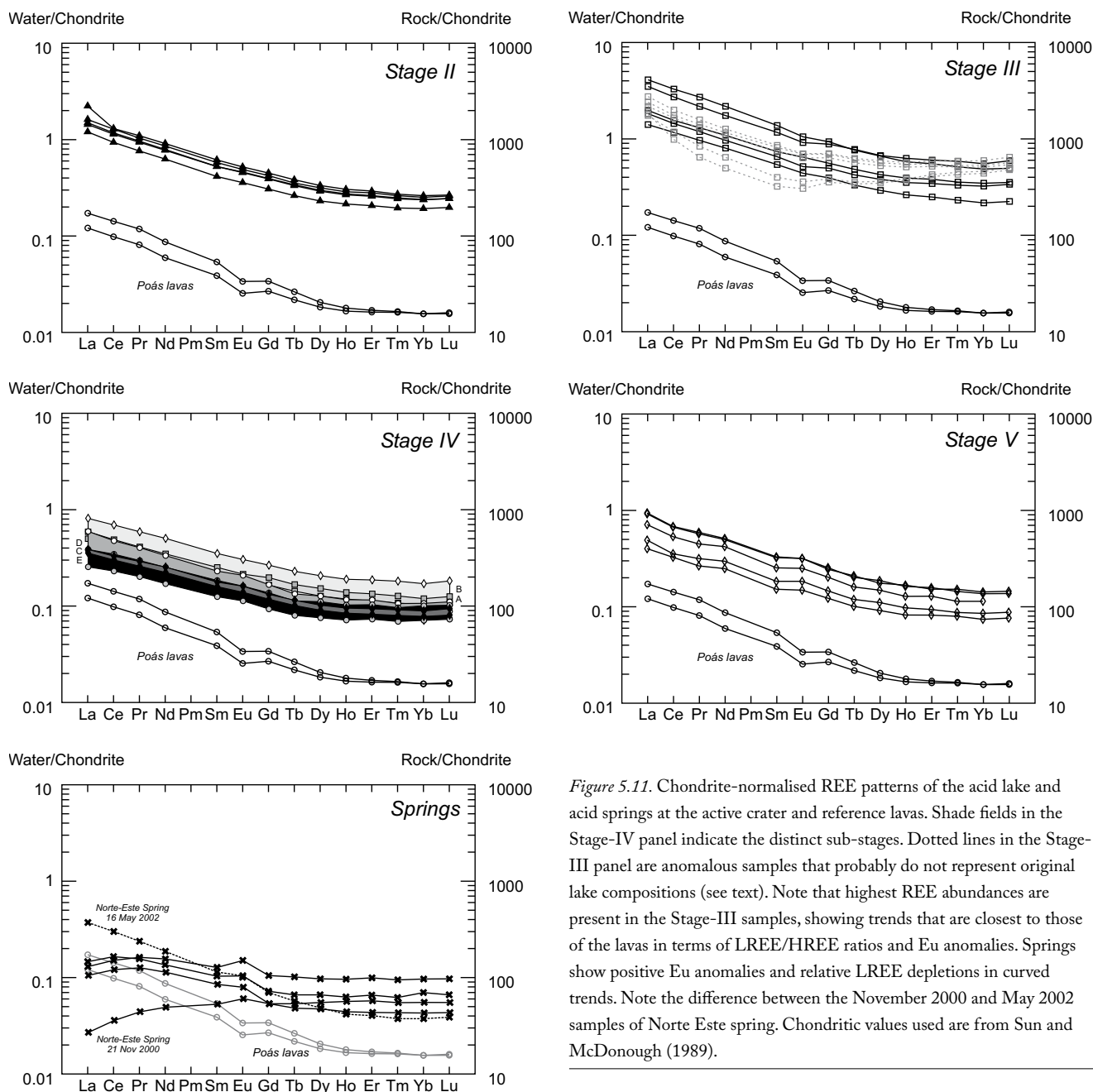


Figure 5.11. Chondrite-normalised REE patterns of the acid lake and acid springs at the active crater and reference lavas. Shade fields in the Stage-IV panel indicate the distinct sub-stages. Dotted lines in the Stage-III panel are anomalous samples that probably do not represent original lake compositions (see text). Note that highest REE abundances are present in the Stage-III samples, showing trends that are closest to those of the lavas in terms of LREE/HREE ratios and Eu anomalies. Springs show positive Eu anomalies and relative LREE depletions in curved trends. Note the difference between the November 2000 and May 2002 samples of Norte Este spring. Chondritic values used are from Sun and McDonough (1989).

The ETR relationships observed at Poás are broadly similar to those described for other crater lakes (e.g., Pasternack and Varekamp, 1994; Sriwana *et al.*, 2000; Takano *et al.*, 2004). Differences between the profiles of Stages III and IV are of interest to note (Fig. 5.9). For the highly active Stage III (peak activity, highest lake water temperatures and lowest pH), less elements show $ETR < 1$, and their values are also less negative than for Stage IV, except for elements controlled by mineral saturation in the lake (Si, Ba). This implies that congruent rock dissolution as mechanism of water-rock interaction was approached closest during Stage III. In contrast, the lake water compositions during Stage IV (relatively quiet) deviate most from quantitative transfer of RFE, and positive ETR values are only observed for trace elements that are highly mobile in the gas phase.

5.5.5 REE patterns of lake and spring waters

The crater-lake waters of Poás are characterised by total REE concentrations ranging between 340 and 5000 ppb. Together with other extremely acid crater lakes (e.g., Kawah Ijen, Copahué, Rincón de la Vieja, Keli Mutu, Ruapehu), Poás lake ranks among the most REE-enriched natural surface waters known (cf., Takano *et al.*, 2004). The REE concentrations follow the general temporal systematics in its load of dissolved elements. They are highest in Stage III, followed by Stage II. Substages IV-C and E are depleted relative to the other substages of Stage IV.

Chondrite-normalised concentrations of dissolved REE for stages II-V are displayed in Figure 5.11, together with patterns of basaltic-andesite lavas of Poás, which were constructed using high-resolution ICP-MS data of Carr *et al.* (2003). All of the lake patterns are similar, showing an enrichment of LREE over

HREE and relatively flat trends for the HREE. Some of the Stage III samples have deviating and more irregular patterns with occasional positive slopes from the middle towards the heavy REE. Because these samples are largely from mud pools, and were collected and stored unfiltered and undiluted in bottles that contained significant amounts of sediment (originally suspended in the lake water and/or newly formed gypsum), their patterns may have been influenced by precipitation and/or sorption processes, and are therefore not considered representative of pristine lake waters.

The lake-water patterns are roughly parallel to those of the lavas, suggesting that interaction with the rocks of Poás played an important role in generating the REE abundances. However, two observations are noteworthy:

Parallelism is most conspicuous for Stage III, whereas in the other stages the waters tend to be relatively enriched in the HREE compared to the lavas, with Stage IV showing the strongest difference.

Negative Eu anomalies are present in the lavas but are virtually absent in the lake waters, except for some of the Stage III samples.

In general, the shapes of REE patterns of acid crater-lake waters will be determined by the composition of the volcanic rocks and the efficiency by which individual REE have been extracted, either *in-situ* in the crater area or in the hydrothermal system below the lake (cf., Takano *et al.*, 2004).

Assuming that the reference lavas are representative of rocks with which the acid waters interacted, the REE patterns of the lake waters can be explained by (near-)congruent rock dissolution only for Stage III. In the other cases, the patterns would suggest preferential leaching of HREE or retention of LREE. Experiments simulating the alteration of andesites by acid hot-spring water have shown that LREE are easier released during initial water-rock interaction than HREE (Kikawada *et al.*, 2001). It is therefore more likely that the REE patterns of Stages II, IV and V were obtained by interaction with altered rocks that had already suffered some degree of LREE loss. Takano *et al.* (2004) also invoked exposure to intensively altered country rocks and a long history of hydrothermal alteration for acid crater lakes with LREE depletions.

Alternatively, water-rock interaction not only resulted in element leaching but was accompanied by the formation of alteration minerals that preferentially incorporate LREE. In this respect, it is conceivable that alunite-group minerals played a role, as they tend to be enriched in LREE relative to their precursor materials (Kikawada *et al.*, 2004). This latter interpretation would be consistent with a REE study of altered volcanics (latites, trachytes and rhyolites) in the active magmatic-hydrothermal system of Vulcano (Fulignati *et al.*, 1999), where the highest alteration facies (silicic alteration) are equally depleted in all REE with respect to the source rock, whereas the slightly lower, alunite-bearing facies (advanced argillic alteration), is strongly depleted only in the HREE while the LREE tend to be immobile. If the patterns of dissolved REE in the Poás lake were influenced in the same way by newly-formed alteration minerals, the water-rock interaction should have taken place in the hot sublimic environment, as

alunite does not form under the ambient lake temperatures (see section 5.5.1.8).

Similar scenarios might explain the distinct behaviour of Eu. The small negative Eu anomalies in some of the Stage III samples could be largely inherited from the lavas, in line with a close-to-congruent dissolution for this stage. Absence of Eu anomalies in the other stages is consistent with advanced degrees of rock alteration. Given the negative Eu anomaly in the parent lavas, it should have been even more pronounced in the lake waters in the case of initial alteration when Eu is expected to be released more slowly than the other REE (Kikawada *et al.*, 2001). More likely, dissolved REE distributions without obvious Eu anomalies are the result of interaction with more altered rocks (e.g., involving the breakdown of plagioclase that contains relatively much Eu), or reflect preferential removal of Eu from the host rock in a high-temperature or reducing environment where Eu^{2+} is more soluble than the trivalent REE (cf., Lewis *et al.*, 1997).

The thermal springs have lower total REE contents (120–440 ppb) than the lake, and show clearly distinct chondrite-normalised patterns (Fig. 5.11). With one exception, all samples clearly deviate from the lavas and display relatively flat HREE trends, a positive Eu anomaly and curved LREE shapes indicating progressive depletion towards the lightest REE. These distributions are reminiscent of the “gull-wing” patterns that characterise many acid-sulphate hydrothermal fluids in New Zealand and elsewhere (Wood, 2006 and references therein), except for positive (instead of negative) Eu anomalies seen here. The trend of the Norte Este sample of May 2002, the most recent spring sample available, is very different from a previous sample (November 2000) and from the other spring samples. It approaches that of the lavas, although there is a noticeable positive Eu anomaly. From a rough correspondence, the pattern might suggest some interaction with lake water, but this is not supported by a concomitant change in $\text{S}_\text{T}/\text{Cl}$ or other anion ratios in this sample (cf. Fig. 5.8a).

Collectively, the REE systematics indicate that the crater spring waters have a clearly independent history from that of the lake waters, at least until May 2002 when the last sample analysed for trace-elements was taken. The higher pH range (1.5 – 2.6) of the springs indicates that water-rock interaction occurred in a less acidic environment than below the lake, while the acid-sulphate nature of the waters points to shallow, oxidising conditions. Assuming that the local rocks were not significantly different from the reference lavas, the positive Eu anomalies suggest interaction with substantially altered rocks that had retained more Eu relative to the other REE. Depletion of the LREE can be attributed to preferential removal during earlier alteration or to retention by newly formed alteration minerals. The latter option would be consistent with the presence of alunite and jarosite minerals near the springs, as identified by XRD.

The above evidence from the lake and spring waters indicates that the behaviour of Eu is decoupled from that of the other REE, as was also observed in geothermal systems of Yellowstone (Lewis *et al.*, 1997). This is particularly well demonstrated in Ce/Yb and Eu/Eu* time-series trends for the lake waters (Fig. 5.12). Disregarding the anomalous Stage-III samples, the Ce/Yb ratios show marked fluctuations that correspond with the

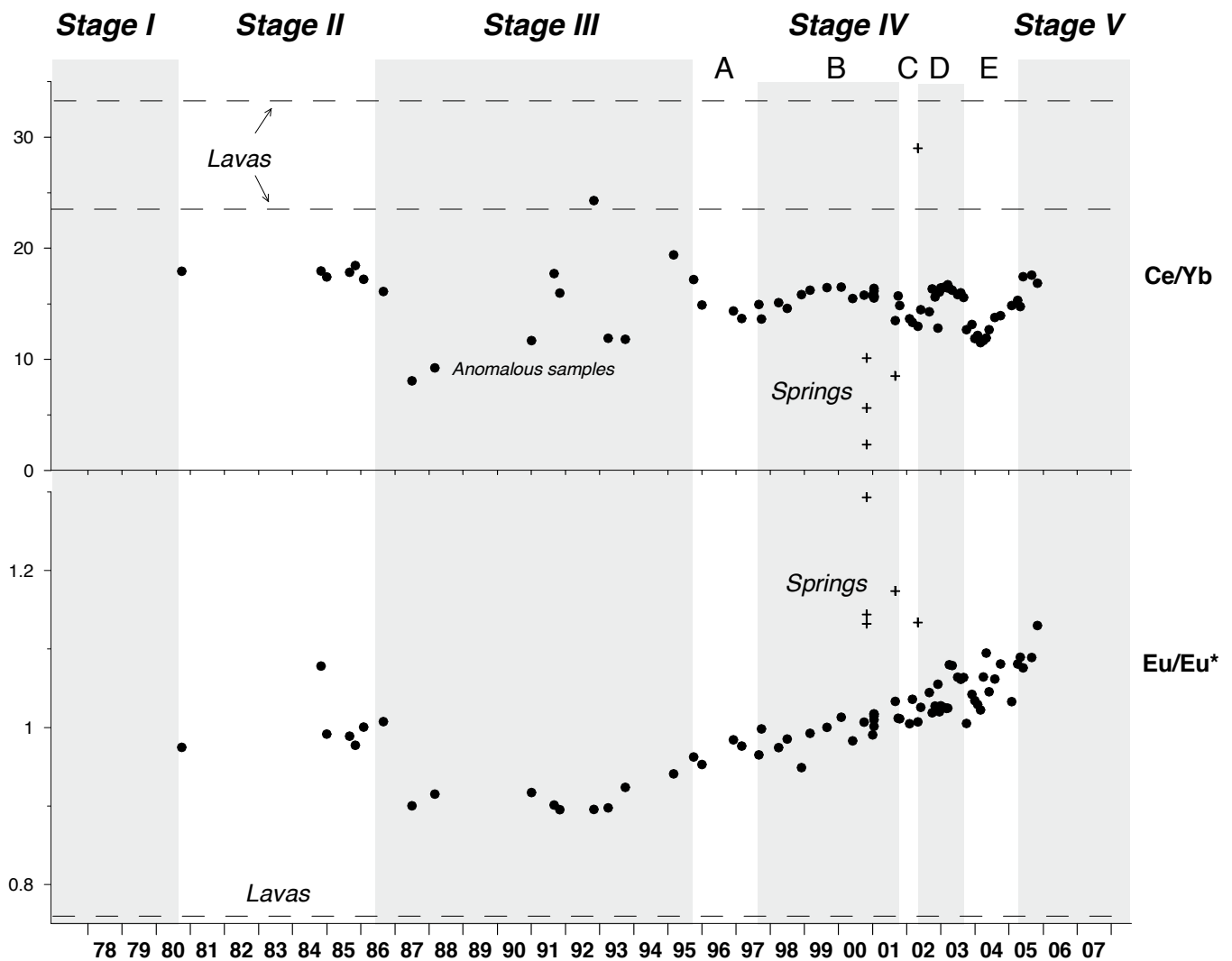


Figure 5.12. Time series of Ce/Yb and Eu anomalies [Eu/Eu^* defined as $2\text{Eu}_N/(\text{Sm}_N + \text{Gd}_N)$] for the lake water, compared with the thermal springs and the reference lavas. Subscript N refers to chondrite-normalised values (Sun and McDonough, 1989). Note the contrast between fluctuating Ce/Yb ratios and a steady increase of Eu/Eu^* from negative (<1) to positive (>1) in the course of stages III–V. Anomalous samples do probably not represent original lake compositions (see text).

stages and substages defined while they are inversely related to pH (cf. Figs. 5.2 and 5.6). Relatively high values are observed in the most active periods (Stages II–III–V and substages IVB and IVD) when pH was lowest, indicating that the degree of LREE/HREE fractionation during water-rock interaction depends on the amount of dissolved volatiles (S, Cl, F). Because the Ce/Yb ratios of virtually all of the lake samples do not overlap with those of the lavas, it can be inferred that congruent rock dissolution is not fully adequate to explain the REE signatures, although conditions of Stages II and III approached this process closest.

In contrast, the time series of Eu anomalies [Eu/Eu^* , where Eu^* is defined as $2\text{Eu}_N/(\text{Sm}_N + \text{Gd}_N)$] shows a remarkable secular increase from 1986 till 2005, independent of the (sub) stages distinguished. This trend is difficult to reconcile with increasing preferential extraction of Eu^{2+} , as there is no evidence for increasing (high) temperatures or gradually more reducing conditions. Instead, the trend can be explained by extended interaction between the acid waters and progressively more altered rocks, whereby Eu was initially removed at a slower

rate than the other REE but became more important once the residue wherein Eu had proportionally accumulated continued to be exposed to aggressive fluids. The Eu anomalies thus appear to reflect a maturation of the hydrothermal system.

The long-term Eu trend provides independent evidence that the cation load of the lake water is not primarily generated by dissolution of wall rock or run-off material from the crater walls or floor, but that it is at least partly inherited from an influx of waters that were enriched in the subsurface. Importantly, the trend starts after a sudden drop from values about one that mark Stage II, suggesting a major reorganisation of the gas-water-rock interaction regime around the onset of phreatic activity in Stage III. Because initial Eu/Eu^* values were closest to those of the reference lavas, interaction must have started with relatively pristine rocks, either from freshly intruded magma (Rymer and Brown, 1989; Brown *et al.*, 1991; Rowe *et al.*, 1992a,b; Rymer *et al.*, 2000, 2005; Fournier *et al.*, 2004) or through the opening of new fissures and cracks that probably accompanied this event.

5.5.6 Behaviour of the magmatic-hydrothermal system

The observed changes in chemical and physical properties of the lake, thermal springs and fumaroles are signals of the dynamic behaviour of the underlying magmatic-hydrothermal system.

No juvenile magmatic material was erupted during the time interval investigated here, but geophysical data have provided indirect evidence for the presence and role of magma bodies throughout this period. Static gravity data revealed a large positive anomaly in the summit area centred on the active crater and interpreted as an approximately cylindrical magma pipe with a diameter of about 1 km (Thorpe *et al.*, 1981). Presumably, its emplacement was associated with the eruptive activity of 1953–1954.

Micro-gravity surveys carried out regularly since 1985 have been interpreted in terms of magma plumbing processes with a direct impact on fumarolic degassing and behaviour of the lake (Rymer and Brown, 1987, 1989; Rymer *et al.*, 2000, 2005; Locke *et al.*, 2003; Fournier *et al.*, 2004). Time-series data from stations within the crater have shown that gravity increases and decreases are highly localised, may occur simultaneously and must have a very shallow origin. The increases have been attributed to magma rising in dendritic ('finger-like') intrusions in the upper part of the conduit system, possibly accompanied by gas-driven intrusion of mud. According to the observed anomaly patterns, the diameter of the dendrites must be 50 m at most, and the depth to their top probably not more than 50 m (Locke *et al.*, 2003). They can be seen as offshoots of the underlying magma pipe, the top of which may have been at least 500 m below the crater floor (Rymer *et al.*, 2000). The gravity decreases are supposed to reflect the withdrawal of magma. Alternating intervals of increasing and decreasing gravity have been attributed to convective recharge and drainage of the dendritic intrusions which would take up to 5 years and 7–10 years, respectively (Rymer *et al.*, 2005). Considering the integrated gravity effects over the area, the estimated mass changes in various episodes are on the order of 108–109 kg. In a long-term perspective, the overall mass in the shallow part of the conduit system remains roughly constant (Rymer *et al.*, 2005).

A high-resolution gravity survey carried out in 2002 revealed the presence of a positive Bouguer anomaly centred on the south side of the lake around the CPC, attributed to a total mass of intruded magma of at least $\sim 149 \times 10^9$ kg (Fournier *et al.*, 2004). The low-temperature nature of the CPC fumaroles (cf., Fig. 5.2) suggests that this magma was frozen, but earlier, when gas temperatures were still very high (Stage II–early years of Stage III), at least part of it must have been hot and liquid until a few meters below the surface. The total mass was inferred to represent multiple episodes of magma intrusion, since it is much larger than that associated with the 1986–89 crisis. Fournier *et al.* (2004) argued that the presence of such solidified intrusive bodies may have blocked rising magmatic gases and divert these to other areas, which would explain the fumarolic activity on the eastern side of the crater (Stage IV) where micro-gravity data do not support the presence of a shallow intrusion immediately below. If this interpretation is correct, it seems difficult to reconcile with an evolution cycle for the dendrites involving withdrawal of magma as explanation of decreasing gravity.

Energy budget modelling (Brown *et al.*, 1989, 1991; Rowe *et al.*, 1992a) has highlighted the importance of an overlying hydrothermal system (which includes the lake) in transferring heat from the magma source to the surface. This heat transport is largely achieved by multiphase convective flow. Rowe *et al.* (1992a) evaluated heat and fluid flow into and out of the lake using mass-balance calculations. In combination with chemical mass-balance considerations, they proposed a model of fluid circulation below the crater. Mass-balance arguments indicate that the lake must lose water via a seepage flux in order to sustain its hydrologic budget (Brantley *et al.*, 1987). This implies that dissolved elements will be removed as well, so that a separate influx is required to maintain the lake chemically constant. Condensation of lake-bottom fumaroles is sufficient to replenish the volatile species, but is inadequate for rock-forming elements, as their concentrations are too low in fumaroles, even at high temperatures (Table 5.4). Also, it is unlikely that dissolution of crater rock or pyroclastics compensates for daily losses, because the volume needed would be unrealistically large. Hence, mass balance for rock-forming elements must be largely maintained by influx of hot buoyant brine.

Rowe *et al.* (1992a) envisaged two zones of convection beneath the lake, an upper liquid-dominated zone and a lower vapour-dominated zone. Heat is first transferred conductively across the chilled margin of a shallow magma body (inferred to be situated at about 500 m depth) to the overlying vapour-dominated zone, and is then dissipated through condensation at the top of this zone to the upper liquid-dominated zone, of which the crater lake is the surface expression. Conversely, downward seeping brine and condensed steam is revapourised near the hot envelope of the magma. Similar conceptual models have been proposed for other crater-lake hosting magmatic-hydrothermal systems (e.g., Christenson and Wood, 1993; Delmelle *et al.*, 2000).

The dynamic changes in the active crater that characterise the investigated period can be seen as an expression of the relative importance of the vapour-dominated and liquid-dominated zone. The first obviously marks Stage III, when magmatic volatiles could reach the surface along almost dry pathways, particularly when the lake had disappeared. Close correspondence between the S–Cl–F proportions in high-T fumaroles and in the lake water is evidence for very little interference of hydrothermal groundwater. Given the high-temperature nature of the CPC fumaroles, dry pathways also existed during Stage II but were probably more confined to this location where magma almost reached the surface.

In contrast, liquid-dominated conditions prevailed during Stage IV. Subsurface invasion and expansion of a hydrothermal water body, leading to a strong modulation of volatile and heat transfer, is consistent with the chemical properties and relatively low temperature of the lake, and with the temporary appearance of thermal springs and low-T fumaroles.

During this stage, the water body was apparently efficient in scrubbing magmatic gases, a process that is promoted in periods of volcanic quiescence when water-soluble volatiles are readily absorbed in volcanic systems with high permeability and well-developed subsurface hydrothermal systems (Fisher *et al.*, 1997; Symonds *et al.*, 2001; Werner *et al.*, 2008). Such conditions pose

limits to the use of fumarole emission rates and compositions in volcano monitoring (Symonds *et al.*, 2001).

Influx of hot buoyant brine water into the lake can explain the observed change in solute concentrations. The reduction in S/Cl ratios that accompanied an overall lowering of volatile concentrations may reflect preferential input of HCl into the hydrothermal system in the waning stages of magmatic degassing. A reasonable alternative scenario is that sulphur was retained by the deposition of sulphur-rich mineral phases that are predicted to be saturated at high temperatures in the subsurface (alunite, anhydrite/gypsum). Recycling and re-incorporation of lake water (presumably mixed with fresh meteoric water) in the hydrothermal system may have enhanced the decrease in S/Cl due to the more conservative behaviour of dissolved Cl relative to SO_4 . The presence of polythionates during large parts of Stage IV (Chapter 4) suggests, however, that the flux of sulphurous gases into the lake was not entirely interrupted most of the time, despite its quiescence. Hence, a combination of these processes may be responsible for the S/Cl trend.

The cation signatures in the lake provide additional strong evidence for influx of hydrothermal water having a composition that is inconsistent with congruent rock dissolution but that must have been controlled by the formation of alteration minerals at depth, i.e. at higher temperatures than observed in the lake. The REE systematics further suggest that the inflowing hydrothermal water had interacted with progressively more altered rocks, indicating maturation of the hydrothermal system in the course of Stage IV.

An important corollary of the inferred formation of alteration minerals is the potential effect on porosity and permeability. Free movement of vapour or liquid may be slowed down or blocked, as has been envisaged in other magmatic-hydrothermal systems (e.g., Stimac *et al.*, 2003; Ohba *et al.*, 2008). Sealing was presumably effective throughout Stage IV, occasionally leading to temporary clogging of conduits, as evidenced by the composition and coloration of the lake during substages IVC and IVE when even the influx of volatiles virtually halted. The compositional changes during these intervals are short-lived, suggesting rapid recycling of the lake water, as is particularly well illustrated by the fluctuations in Ce/Yb ratios (Fig 5.12). Rowe *et al.* (1992a) inferred that fluid circulation in the liquid-dominated region is very fast, and calculated average seepage rates of ~ 450 kg/s, implying recycling of a full lake volume in half a year or less.

The rise and decline of thermal springs and low-temperature fumaroles in the eastern sector part of the crater as well as their compositional trends are entirely consistent with the pattern of upwelling hydrothermal water during Stage IV, followed by drier conditions that accompany the onset of high activity in the crater during Stage V. Their initial acid-sulphate signature may have been derived from addition of sulphur gases or locally present sulphur-bearing minerals (cf., Rowe *et al.*, 1995) to (heated) meteoric groundwater. Subsequent gradual enrichment in Cl and decreasing S/Cl ratios, accompanied by a minor increase in temperature (Figs. 5.8a and 5.8b), signalled the arrival and increasing importance of hot upwelling brine. Significantly, both the springs and the condensates reached S/Cl ratios lower than the lake, indicating that subsurface involvement of lake water

was not responsible for this compositional change. In contrast, the S/Cl increase, introduction of F and temperature decrease in the springs towards the end of their lifetime suggest mixing with lake water, presumably due to the expanding lake reservoir. The ultimate drying out of springs and fumaroles in the eastern crater sector in the beginning of Stage V marks the onset of more vigorous input of heat and magmatic gas, as testified by the steep rise in temperature and volatile concentrations in the lake, and by its decreasing volume, which continue till date. The conspicuous temperature jump in the Fumarola Norte (Fig. 5.2) fits in this pattern as well. All these phenomena are indicative of a reduction of the liquid-dominated zone and a transition towards vapour dominance. The combined features, including phreatic eruptions, point to a return to Stage III conditions.

The time-series trends of the lake properties suggest that periods with phreatic eruptions (Stages I, III and V) alternate with relatively quiet periods (Stages II and IV) in cycles of 6–10 years, which roughly correspond to vapour or liquid dominance, respectively. Several processes can be envisaged as underlying causes of changing behaviour and the triggering of phreatic eruptions:

- (1) Intrusion of magma. Evidence for the possible role of intrusion and withdrawal of dendritic intrusions largely comes from fluctuations in microgravity. Interpretations are not always unambiguous because mass variations may also be generated by changing amounts of water, vapour and mud in the subsurface below the crater, as discussed in Rymer *et al.* (2000, 2005) and Fournier *et al.* (2004). In addition, the evidence for sealing effects discussed above indicates that precipitation and dissolution of alteration minerals in pore spaces of the underlying volcanics can be a further reason of mass changes, as has also been alluded to earlier (e.g., Brown *et al.*, 1991). Similarly, subsurface deposition of native sulphur during enhanced fluxes of magmatic gases or subsequent dissolution might also account for microgravity changes (Rowe *et al.*, 1992a).

Since even small shallow intrusions will have a strong disrupting effect on the hydrothermal system, they will have a major impact on the lake, particularly in terms of input of heat and volatiles. Therefore, based on the lake chemistry, the most likely periods when intrusions have occurred are at the transitions between Stages II and III, and between Stages IV and V. It is also conceivable that minor localised intrusions were emplaced sometime before or around 1968, and at the transition between Stages I and II, given the phreatic activity observed in Stage I and the very strong temperature rise of fumaroles at the CPC and their composition of a magmatic gas in Stage II. The main power output was apparently not centred in the lake during Stage II, considering its sizable volume and intermediate chemical and thermal state.

- (2) Hydrofracturing of the brittle chilled envelope around cooling magma and release of magmatic volatiles. Rupture of this solid margin may be caused by fluid overpressure in the surroundings of the magma body, generated by volatiles exsolving from crystallizing melt. Alternatively, fracturing is promoted by cooling from downward circulating groundwater. Based on temperature, seismic and geochemical data, Rowe *et al.* (1992a) proposed that the

sudden heating events of 1981–1983 (Stage I–II transition) and 1986–1988 (Stage II–III transition) were caused by hydrofracturing, not necessarily accompanied by magma ascent.

- (3) Rupture of an impermeable layer in the rock column between the chilled margin and the lake. If circulation in the hydrothermal system is prevented by the presence of a seal that is gradually created through the filling of pore space by alteration minerals, gas may accumulate below and build up pressure until a critical threshold is reached and fracturing occurs. In view of the evidence for clogging and sealing towards the end of Stage IV, such a scenario might have played a role in triggering the recent cycle of strong upwelling and phreatic activity that started in 2005–2006. Alternating sealing and rupturing may also be responsible for the migration of fumarolic activity in the crater area. For example, the shift of the main location of volatile discharge from the CPC (Stage II) toward the lake (Stage III) could be due to precipitation of secondary minerals in the CPC, or sealing of fractures by quasi-plastic flow of rock at depth (Rowe *et al.*, 1992a).

5.6 Conclusions

- (a) The acid lake of Poás volcano has shown marked variations in chemistry, volume and temperature during decades of monitoring, indicating that magmatic-hydrothermal activity in the summit area is highly dynamic and operates on relatively short timescales. Based on unambiguous differences in physico-chemical characteristics of the lake and the location of main fumarolic outgassing, five successive stages can be distinguished in the lake's history since the late 1970s when regular data collection started. Periods with phreatic eruptions (stages I, III and V) alternate with relatively quiet intervals (stages II and IV). The observed duration of complete stages (II, III, IV) suggests that the Poás system behaves in periodical cycles of 6–10 years.
- (b) Major anions (S, Cl, F) in the lake are derived from magma degassing but variable concentrations and relative proportions are not only due to changes in the release from a magma body, but are usually also a function of multiple processes in the overlying hydrothermal system that modulate their output. Anion proportions and temperature increase indicate that uninhibited influx and condensation of high-temperature magmatic gas in the lake only occurred in the early years of Stage III, prior to its desiccation. In contrast, strongest deviations from primary magmatic gas signatures (e.g. low S/Cl ratios) and lowest concentrations point to a noticeable interference of the hydrothermal system during the quiet Stage IV.
- (c) Major cations (rock-forming elements) in the lake are mostly derived from water-rock interaction. Concentrations are variable and largely follow the anion trends, except for those that are controlled by precipitation of saturated minerals in the lake. Cation proportions do not remain constant but appear to be regulated by the degree to which rock dissolution proceeds congruently. Congruent rock dissolution was approached closest during Stage III, whereas divergence was strongest during Stage IV. Deviations follow systematic patterns and are mostly due to formation (or dissolution) of secondary alteration minerals, notably alunite and other Al-bearing mineral phases. SOLVEQ modelling indicates that their formation requires higher temperatures than observed in the lake, implying that its cation budgets are largely controlled by influx of hot brine derived from the liquid part of the underlying hydrothermal system.
- (d) Because precipitation of alteration minerals in pore spaces, fractures and channels will strongly affect porosity and permeability in the subsurface, sealing effects are inferred to be important in regulating not only the properties of the lake but also the magnitude and location of subaerial fumarolic emissions elsewhere in the crater. According to the lake chemistry, sealing was most effective during Stage IV, leading to almost complete shut-down of volatiles and heat input during brief intervals.
- (e) Rare earth elements appear to be sensitive monitors of water-rock interaction and fluid cycling. A marked secular trend in Eu anomalies from the first half of Stage III on points to extended interaction with progressively more altered rocks, reflecting maturation of the hydrothermal system and no exposure to fresh rocks since then. Short-lived fluctuations in Ce/Yb ratios during Stage IV are consistent with rapid recycling of the lake water through the underlying hydrothermal reservoir.
- (f) Thermal springs and low-temperature fumaroles in the eastern part of the crater had a transient existence throughout Stage IV until their disappearance in the beginning of Stage V. Consistent with the observed behaviour of the lake, their lifetime and gradually decreasing S/Cl ratios are a manifestation of a temporary expansion of the hydrothermal water volume in the summit area, and are not due to magmatic activity.
- (g) The successive stages of activity and quiescence in the lake area apparently coincide with alternating vapour dominance and liquid dominance in the hydrothermal system between the magma body and the crater area. Resurging input of heat and volatiles, eventually leading to eruptive activity, could be triggered by magma (fresh intrusion or fracturing of the brittle chilled margin around the cooling body) or by rupture of an impermeable seal in the overlying sequence of altered lavas and pyroclastics. Considering the trends in the lake properties alone, magma intrusion seems only conceivable at the transitions between Stages II and III, and between Stages IV and V. A local intrusion of magma may also have been responsible for a steep temperature rise of CPC fumaroles at the transition between Stages I and II. The Stage IV–V transition in the lake's properties and enhanced fumarolic degassing, which have culminated in phreatic activity from early 2005 on, followed a scenario comparable to that observed at the Stage II–III transition.
- (h) The results of this study highlight the range and complexity of processes operating in the shallow volcanic-hydrothermal system of Poás. The comprehensive sets of time-series data now available on the evolution of the lake, fumaroles and thermal springs provide a solid basis for further chemical monitoring and the prediction of future eruption events. Among the measured physico-chemical parameters of

the lake, a steep temperature rise appears to be a clear and perhaps most dependable precursor of conditions leading to phreatic eruptions. Anion trends are generally consistent but interpretation of individual species is not

always unambiguous. Reliable monitoring thus calls for a multi-parameter approach, while further robustness will be achieved through integration with geophysical data.

Volatile fluxes from Poás volcano: inferences from acid flank springs and fumarolic emissions

6.1 Introduction

Leakage of acid brines from volcano-hosted hydrothermal systems can be used to provide information on the release of volatiles from underlying crystallising magma bodies. Predominantly acid-chloride-sulphate brines that form in the subsurface hydrothermal system and circulate within the volcanic edifice of Poás are discharged from numerous springs through a confined permeable region on the northwest flank of Poás volcano, within a distance of 2 to 5 km from the currently active crater and located at elevations that range between 1290 to more than 2050 m.a.s.l. (Fig. 6.1). Collectively, the springs form the headwaters of the Agrio River, a ~7 km long acid tributary of the Rio Toro Amarillo. The acid crater lake is situated at an elevation of 2300 m.a.s.l.

In order to explore long-term systematics in volatile release from the magma body below Poás, an assessment is made of the mass flow of magmatic volatiles through riverine transport as well as through fumarolic emissions from the active crater in the periods 1987–1991 and 1992–2002. Furthermore, the chemistry of the Agrio River is compared with that of the acid crater lake to test evidence for a presumed direct connection between the acid seepage springs and the lake brines.

6.2 Background and objective

Information on the general hydrologic structure of Poás volcano, including details on the crater area and flank springs, can be found in Rowe *et al.*, 1989; Rowe (1994), Rowe *et al.* (1992a, 1995), Vaselli *et al.* (2003), and Sanford *et al.* (1995), see also Chapters 2, 4, 5. The Agrio River catchment is the only area outside the currently active crater that receives a substantial input of acid brines carrying a high load of dissolved magmatic volatiles and rock-forming elements. A connection between the acid seepage at the NW flank of the volcano and the acid brines of the crater lake was already suggested by Alexander von Frantzius in 1861 (Vargas, 1979). Water and heat-balance considerations (Brantley *et al.*, 1987), geochemical and stable-isotope signatures of the discharging acid-chloride-sulphate springs (Rowe *et al.*, 1992a,b; 1995) and groundwater transport modelling (Sanford *et al.*, 1995) have been used as evidence

for a hydraulic connection with the lake through a permeable lava-lahar sequence. Down-flow compositional effects on the brine from interaction with rock and from dilution with meteoric water, and implications for rock removal rates, mineral saturation states, dissolution rates and changes in the aquifer's permeability/porosity have been discussed by Rowe (1991), Rowe *et al.* (1992a, 1995). In spite of the evidence for a direct seepage link with the crater lake, it remains conceivable that the acid springs on the NW flank are fed by a subsurface hydrothermal reservoir hosting brine water with a similar composition to that of the lake.

This study uses new data on dissolved anion fluxes determined in a set of water samples from Agrio River collected in 1992–2002, together with previous data from Rowe *et al.*, (1992a; 1995) for the period 1987–1991 (Table 6.1). In conjunction with SO₂ fluxes measured by remote sensing techniques at the active crater (Table 6.2), an attempt is made to assess the minimum rate of volatile release from Poás in the light of the cyclical nature of activity of the magmatic-hydrothermal system (Chapter 5). The estimates are based on the assumption that the acid seepage at the NW flank and the fumarolic vents within the active crater (1) are the only locations where volatiles are emitted from the magmatic-hydrothermal system, and (2) are derived from the same common source (Rowe *et al.*, 1992a; 1995).

6.3 Methodology

During field campaigns in 1999, 2000, 2001, 2002, samples were taken and temperatures were measured at several sites along the northern branch of Agrio River (sites 9 and 5) and below the confluence of the northern and southern tributaries (sites 3a and 23). Because the seepage points are located at the head of a steep canyon, which marks the contact between Von Frantzius and pre-Von Frantzius deposits, the uppermost accessible sampling point is site 9, about 2050 m.a.s.l. A site along the southern branch, just above the confluence point of the two tributaries, was also sampled (site 4). Other acid springs and near-neutral tributaries in the upper Rio Agrio catchment (Martínez *et al.*, 2004a) are not included in this study. Approximate sampling locations are indicated in Figure 6.1.

Table 6.1 continued

Location	4	4	4	4	4	4	5	5	5	5	5	5	5	5	9c(24)	9c(24)	9c(24)	9c(24)	9c(24)	9c(24)
Sample code	M-480	M-443	M-414	M-399	M-386	M-499	M-492	M-471	M-444	M-425	M-393	M-400	M-387	M-371	-	M-451	64	M-421	M-432	M-390
Date	1998	1999	2000	2001	2002	2002	2014-Nov-96	21-Mrt-97	1998	1999	2000	17-Apr-01	25-Sep-01	29-Apr-02	15-Oct-02	1987	20-Jul-99	01-Oct-99	14-Jun-00	25-Oct-00
Elevation (m.a.s.l.)	1520	1520	1520	1520	1520	1520	1371	1371	1371	1371	1371	1371	1371	1371	1371	2050	2050	2050	2050	2050
T (°C)	19.5	20.3	18.87	20.45	20.5	17	14	16.9	17.5	16.8	16.8	17.4	17.8	18	15	56	52	52	53	51
pH	2.16	2.08	2.09	1.96	1.91	2.67	1.99	2.21	2.08	2.09	1.93	2.02	1.9	2.06	1.5	1.1	1.1	1.5	1.1	1.1
TDS (mg/L)	n.d.	n.d.	n.d.	n.d.	n.d.	n.d.	n.d.	n.d.	n.d.	n.d.	n.d.	n.d.	n.d.	n.d.	22740	27125	27215	29000	28150	28560
Cond. (mS/cm)	5.2	6.3	6.3	7.8	8.5	2.1	7.3	4.4	5.7	5.5	8.3	6.5	8.5	6.0	n.d.	47	46	n.d.	48	53
(24±2°C)																				
Salinity (g/L)	2.7	3.43	3.4	4.3	4.75	0.9	4	2.3	3.05	2.93	4.6	3.5	4.7	3.2	n.d.	31	30	n.d.	32	35
(24±2°C)																				
Flow rate (m³/s)	n.d.	n.d.	n.d.	n.d.	n.d.	n.d.	n.d.	n.d.	n.d.	n.d.	n.d.	n.d.	n.d.	n.d.	n.d.	n.d.	n.d.	n.d.	n.d.	n.d.
IC (mg/L)																				
SO ₄	1230	1570	1660	1870	2460	555	2020	1560	1660	1760	1580	1720	2415	1590	12000	15724	15882	17127	16606	17100
Cl	450	560	575	645	835	215	840	530	660	690	660	660	925	615	5930	6214	6046	6275	6297	6280
F	15	15	14	18	20	8	28	25	21	22	27	19	24	22	152	151	179	142	135	170
SO ₄ /Cl	2.7	2.8	2.9	2.9	3.0	2.6	2.4	2.9	2.5	2.6	2.4	2.6	2.6	2.6	2.0	2.5	2.6	2.7	2.6	2.7
F/F/Cl	0.03	0.03	0.02	0.03	0.02	0.04	0.03	0.05	0.03	0.03	0.04	0.01	0.03	0.04	0.026	0.024	0.030	0.023	0.021	0.027
Riverine Fluxes (tons/day)																				
S	n.d.	n.d.	n.d.	n.d.	n.d.	n.d.	n.d.	n.d.	n.d.	n.d.	n.d.	n.d.	n.d.	n.d.	n.d.	n.d.	n.d.	n.d.	n.d.	n.d.
Cl	n.d.	n.d.	n.d.	n.d.	n.d.	n.d.	n.d.	n.d.	n.d.	n.d.	n.d.	n.d.	n.d.	n.d.	n.d.	n.d.	n.d.	n.d.	n.d.	n.d.
F	n.d.	n.d.	n.d.	n.d.	n.d.	n.d.	n.d.	n.d.	n.d.	n.d.	n.d.	n.d.	n.d.	n.d.	n.d.	n.d.	n.d.	n.d.	n.d.	n.d.
Data source	(2)	(2)	(2)	(2)	(2)	(2)	(2)	(2)	(2)	(2)	(2)	(2)	(2)	(2)	(1)	(2)	(2)	(2)	(2)	(2)

23(27): site near the bridge; 3a (26): site below the confluence of the northern and southern branch; 9c (24): uppermost site along the northern branch. Location codes between brackets are from Rowe et al. (1995).

Concentration data are averages for a variable number of samples. Sources: (1) Rowe et al. (1995); (2) This work

* Volatile fluxes estimated by riverine transport in 1988-1989 by Rowe et al. (1992a).

n.d.: no data

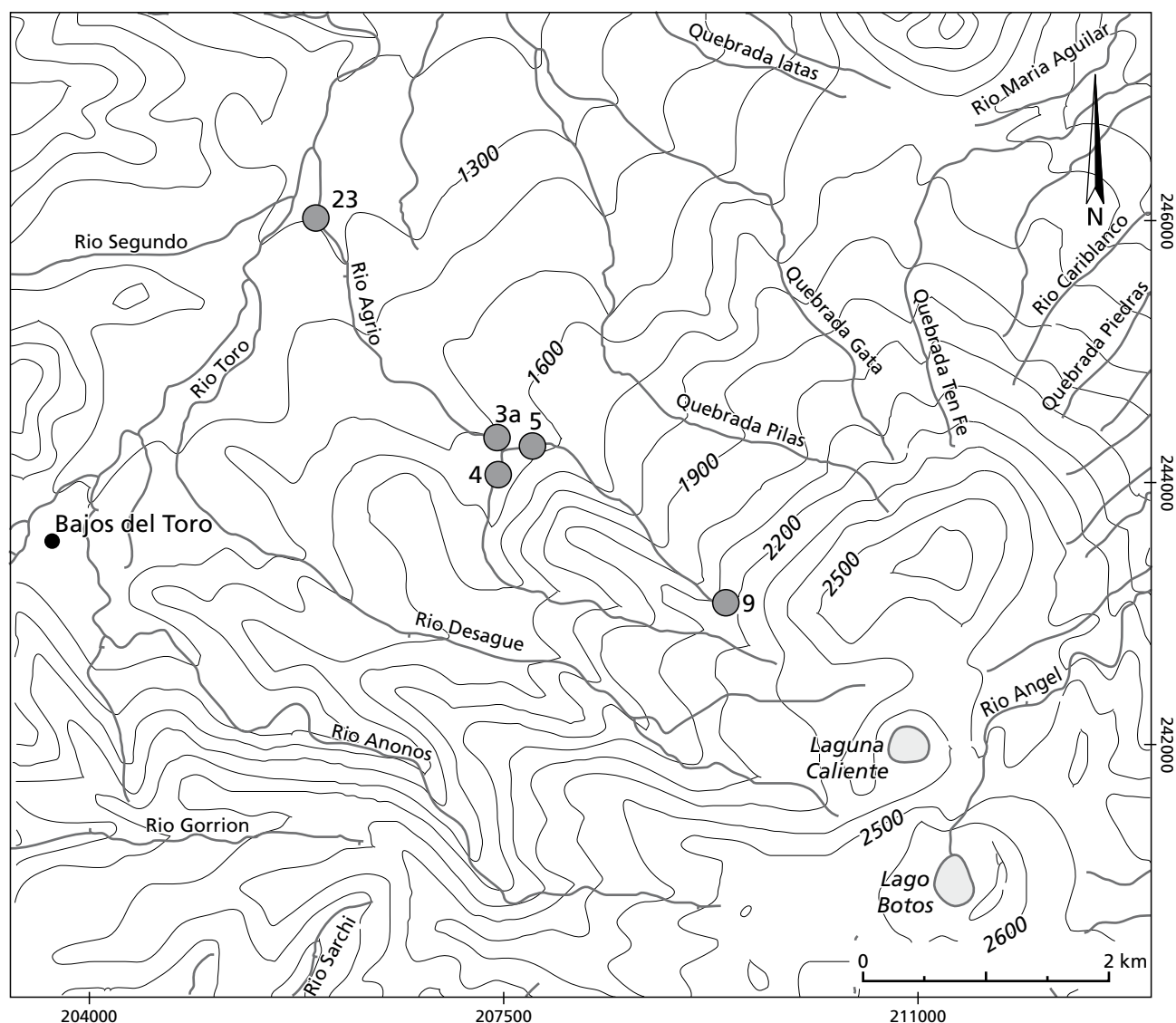


Figure 6.1. Study area and approximate location of sampling sites in the Agrio River basin, northwest of Poás volcano. Sites 9 and 5 are along the northern branch of Agrio River, site 4 along the southern branch near the confluence with the northern branch, and sites 3a and 23 below this point. Site 9 and the acid lake, Laguna Caliente, are separated by a distance of about 2 km; the difference in altitude is about 200 m.

Temperatures were measured with a conventional mercury thermometer. Conductivity, salinity, and pH were determined in the laboratory as described in Chapters 4 and 5. Elevation was determined using a handheld Garmin 55 GPS system. Water samples were collected without filtration, dilution or addition of preservatives in low-density-polyethylene bottles and stored at room temperature. Immediately before analysis, the samples were filtered through disposable Sartorius filter membranes (0.45 μm) and subsequently diluted with ultrapure water to bring F, Cl, and SO_4 concentrations within the optimum range for suppressed ion-chromatography analysis, as described in detail in Chapters 4 and 5.

Average baseflow was determined at sites 3a and 23 (Fig. 6.1), based on conventional measurements of water velocity across a narrow transect of the Agrio River and the estimated cross-sectional area, in order to assess mass-transfer rates (fluxes) of magmatic volatiles via the acid seepage (Table 6.1). The riverine mass-transfer rates for sulphur are compared with SO_2 fluxes from the crater fumaroles, measured with remote sensing

techniques (Okita, 1971; Andres and Rose, 1995; Stoiber *et al.*, 1983, Galle *et al.*, 2003) by several workers (see Table 6.2).

6.4 Results and discussion

A summary of physico-chemical data for Agrio River and estimated mass flow of volatiles through riverine transport are presented in Table 6.1, while fumarolic SO_2 fluxes from the active crater are given in Table 6.2.

6.4.1 Agrio waters: long-term stability of physico-chemical properties

The average temperature of the Agrio River is 19°C, slightly above ambient temperatures between the sampling sites. The only known high-temperature spring (average 53°C), located at site 9, forms an exception. This spring issues acid chloride-sulphate water with the lowest pH (average of 1), whereas downstream the pH fluctuates around 2 and does not change

Table 6.2. Compilation of SO₂ fluxes measured at Poás Volcano

Date	System	Type	SO ₂ flux (tons/day)	StdDev (or range)	Reference
Stage II					
Dec-81	COSPEC	Ground	600		Stoiber, R.E. pers. comm (1983), cited in Prosser and Carr (1987)
16-Feb-82	COSPEC	Air	806	416	Casadevall et al. (1984a)
Dec-82	COSPEC	Ground	500		Stoiber et al. (1986)
17-Feb-83	COSPEC	Air	710	179	Casadevall et al. (1984a)
Stage III					
13-Feb-91	COSPEC	Ground	90	30	Andres et al. (1992)
Stage IV					
3-Feb-2001	FLYSPEC	N.d.	52	(30-119)	Williams-Jones G. pers. comm. (2008)
24-Feb-2001	COSPEC	Ground (crater)	40		Fournier et al. (2001)
Mar-01	COSPEC	N.d.	8		Zimmer et al. (2004)
13-Mar-02	MiniDOAS	N.d.	61		Galle B. (2002)
31-Mar-03	MiniDOAS	N.d.	29		Edmonds M. pers. comm. (2003)
?-2003	N.d.	N.d.	80		Hilton et al. (2008)
Stage V					
?-2005	N.d.	N.d.	500		Hilton et al. (2008)
4-9 Apr-06	MiniDOAS	Ground	84		Olmos R. University of El Salvador, OVSICORI (2006c)
21-Apr-06	MiniDOAS and COSPEC	N.d.	99		Barrancos et al., 2008
24-Apr-06	MiniDOAS and COSPEC	N.d.	160		Barrancos et al., 2008
27-Apr-06	MiniDOAS and COSPEC	N.d.	86		Barrancos et al., 2008
30-Apr-06	MiniDOAS and COSPEC	N.d.	90		Barrancos et al., 2008

N.d.: no data

significantly. Similarly, conductivity and salinity are highest at site 9, and tend to decrease downstream. Its average conductivity of 49 mS/cm is close to the value registered in the acid lake during the most quiescent substages of Stage IV (Chapter 5). Anion concentrations are an order of magnitude higher than elsewhere (Table 6.1). A comparison of previous data obtained by Rowe *et al.* (1992a) and the new data presented here, shows that the geochemical properties of the site-9 spring as well as the Agrio River at each of the sampling sites have remained stable over a long period of time, at least between 1987 and 2002.

A comparison of the chemistry of the source spring of the southern branch of Agrio River (site 25, upstream from site 4, not shown in Fig. 6.1) with that of the river at site 23 (1987-1991 data in Rowe *et al.*, 1995; their location code for this site is 27), reveals a near constant composition along the trajectory down to the confluence with the Toro River, despite an eight-fold increase in flow rate. This suggests that along its entire flow path, the southern branch is fed by groundwater with a composition that closely resembles that of Agrio River downstream. It also suggests that addition of meteoric surface waters is insignificant at lower elevations. In contrast, the northern branch exhibits a 20-fold increase in flow rate with a 10-fold decrease in solute concentration between its source and the confluence with the southern branch. This implies that input of acid brines along the northern branch is largely restricted to the region where site 9 is situated (cf., Rowe *et al.*, 1995).

6.4.2 Comparison of Agrio and crater-lake waters

The long-term geochemical stability shown by the waters of the Agrio catchment contrasts with the marked variations in the properties of the acid crater lake. Lake temperature (from 22 to 94°C), pH (from below zero to 1.8), concentrations of solutes (TDS from 2×10^4 to 1.6×10^5 mg/kg), and volume (between about 2 million m³ to practically total evaporation) have all fluctuated drastically within only three decades, indicating that magmatic-hydrothermal processes controlling the overall fluxes of volatiles and heat from the summit area are highly dynamic and operate in a confined region of the volcanic edifice at relatively short timescales (Rowe *et al.*, 1992a,b; Martínez *et al.*, 2000; Vaselli *et al.*, 2003) (Chapters 2, 4, and 5).

The S_T-Cl-F ternary diagram of Fig. 6.2 reveals that the Agrio spring-9 waters are compositionally different from the acid crater-lake waters. Fields for the various stages distinguished for the lake illustrate its chemical variability, which reflects fluctuations in the input of heat and volatiles throughout the 1980-2005 period (Chapter 5). The waters of Agrio spring-9, collected between 1987 and 2002, plot as a separate group with practically constant S_T-Cl-F proportions that are different from those in the lake waters, largely due to a relative depletion in fluoride. A plausible explanation might be that dissolved fluoride behaves less conservatively than chloride and sulphate and is partly retained in the aquifer during transport.

The contrast between the long-term stability of the Agrio waters (in terms of temperature, discharge rates and physico-chemical properties) and the fluctuating nature of the acid lake,

together with the significant temperature difference between the lake and the Agrio spring-9 (the latter being at an altitude 200 m lower, Fig. 6.1) would argue against a direct hydraulic connection, or may imply a long residence time in the aquifer during subsurface transport from the lake to the seepage points.

Groundwater transport modelling pointed to a travel time varying between 1 and 30 years for the brines to cover the 2–2.5 km distance from the active crater to the seepage points (Sanford *et al.*, 1995). Estimations of the residence time based on tritium chronology yielded a range of 3–17 years, within the range of the model simulations (Rowe *et al.*, 1995). The lake volume was fairly reduced between the end of 1988 and the end of 1994, drying out in several occasions. Hence, if a hydraulic connection exists, it should take the lake brine more than 7–9 years to reach the seepage points on the NW flank (Chapter 5).

Furthermore, in terms of S_T/F ratios the Agrio spring-9 waters plot close to the trend defined by the lake waters collected prior to 1989 (Stage II and first years of Stage III, Fig. 4.12 Chapter 4). The relative enrichment in F observed in the lake since 1989 was not seen in the Agrio spring. Assuming that fluoride retention in the aquifer was not strong enough to obscure this conspicuous shift, the absence of a comparable effect in the seepage springs would imply that, if they are lake waters only diluted with meteoric water during transport, the travel time should be at least 13 years, falling within the ranges inferred by Rowe *et al.* (1995) and Sanford *et al.* (1995).

Stable-isotope and polythionate signatures might further constrain a possible subsurface connection. According to H-O isotope systematics, the seepage springs could carry a lake-brine component (Rowe, 1994). Polythionates have not been detected in the Agrio springs, whereas they have often been abundant in the lake (Chapter 4).

However, their absence does not provide conclusive evidence against a link, since polythionates in the lake are known to break down at temperatures above 65°C (Chapter 4). Given the average discharge temperature of 53°C of the Agrio spring, thermal decomposition of polythionates may occur if higher-temperature waters in the source are cooled during transport. En-route enrichment in SO_2 or bacterial activity in the aquifer could also cause the decomposition of polythionates or prevent their formation (Chapter 4) (Takano and Watanuki, 1990; Takano *et al.*, 1994b, 2001).

6.4.3 Volatile fluxes from surface waters and fumarolic emissions

Irrespective of the existence of a direct connection with the lake, the properties and long-term stability of the Agrio springs indicate that they tap from a sizeable hydrothermal reservoir residing in the summit area that is fed by magmatic volatiles, presumably derived from the same crystallising body. The composition of seeping brines can thus be used to provide information on the release rate of volatiles from the magma source. The Agrio River is the only known stream at Poás carrying large amounts of dissolved volatiles. Hence, volatile fluxes from the Agrio springs may provide quantitative insight into the degassing of Poás volcano that is more reliable than that inferred from the emission rates of fumaroles in the crater, as

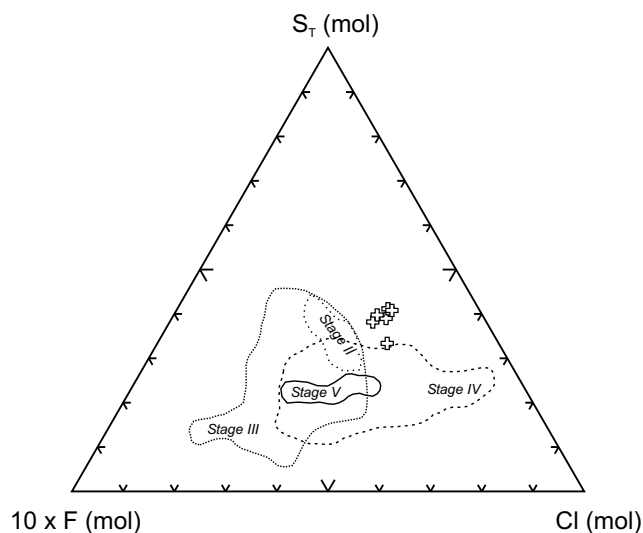


Figure 6.2. Relative abundances of S_T -Cl-F for the waters of the Agrio spring (Site 9) collected between 1987 and 2002 (open plusses), and fields for Stages II–V of the acid crater lake, covering the period between 1980 and 2005. S_T refers to total sulphur measured by ICP-AES. Note that the Agrio spring waters are somewhat depleted in F compared to the lake waters.

the latter are highly sensitive to (partly accidental) modulating effects induced by the uppermost part of the hydrothermal system (Chapter 5). Thus, a minimum volatile output from the magmatic-hydrothermal system can be assessed from the quantities of S, Cl and F discharged by the Agrio springs.

Using the data on volatile concentrations and flow rates determined in 2001–2002 (Table 6.1), flux rates were assessed and compared with results obtained for the period 1987–1991 by Rowe *et al.* (1995). According to the new data, the Poás system released on average 85 ton S (equivalent to 170 ton SO_2), 98 ton Cl and 2.7 ton F per day through riverine transport only. These fluxes are larger but of the same order of magnitude as values obtained for 1987–1991: 28 ± 8 ton S, 35 ± 9 ton Cl and 2 ± 0.5 ton F per day (Rowe *et al.*, 1995). The latter were roughly similar to losses calculated from the solidification rate of cooling magma in the high-temperature period 1981–1983: 66 ton S, 13 ton Cl and 0.5 ton F per day. However, fumarolic fluxes from the active crater have varied drastically. For instance, in February 1982 (Stages I–II transition) fluxes of 400 ton S, 60 ton Cl and 2 ton F were emitted daily from the CPC, when fumarole temperatures were around 880°C (Chapter 5, Fig. 5.2). In contrast, 1986–1989 fluxes derived from condensates of CPC fumaroles with lower temperatures (<500°C), were even lower than at the Agrio River watershed: 1 ton S, 6 ton Cl and 0.1 ton F per day (Rowe *et al.*, 1992a). These latter results are at variance with the intense fumarolic activity and phreatic explosions observed in 1987–1990 (Stage III). Volatile fluxes from the crater must have been considerably higher, but no quantitative data are available on the intense subaerial fumarolic emissions from the dried lake bottom. Instead, subsequent measurements by remote sensing techniques in February 1991, when phreatic activity was interrupted (later in Stage III), yielded an average of 90 ton SO_2 per day (Table 6.2) (Andres *et al.*, 1992). This result is similar to SO_2 fluxes measured in 2006, just after the

renewal of phreatic activity (Stage V), which ranged between 84 and 160 ton per day.

Conversely, SO₂ fluxes from the crater were relatively low in 2001–2003 (Stage IV), ranging between 8 and 80 ton per day (Table 6.2), which may be due to the inferred expansion of the fluid-dominated part of the hydrothermal system (Chapter 5), resulting in more efficient scrubbing of SO₂. Interestingly, during this interval the estimated sulphur flux through the Agrio springs was more than twice that recorded in the 1987–1991 period of phreatic activity, when almost dry pathways for magmatic gas release were established. This suggests an inverse relationship between volatile emission rates through the Agrio springs and the crater fumaroles, providing independent support for the hypothesis that these springs, the lake and other hydrothermal manifestations in the active crater belong to the same magmatic-hydrothermal system. Hence, if the inferred changes in the riverine fluxes are valid, the magmatic volatiles may directly condensate in the water body from which the Agrio springs tap, implying that this source is sensitive to variations in gaseous input.

In summary, the combined fluxes inferred for the Agrio River and the fumaroles at the active crater, yield an estimated overall SO₂ output from Poás volcano of 150 ton SO₂ per day in Stage III (active) and 250 ton per day in Stage IV (quiet). This difference seems difficult to reconcile with the respective states of activity, but it should be considered that, particularly during Stage III, large amounts of magmatic sulphurous gas are probably converted into native sulphur that is deposited in pore spaces and fractures below the lake (Rowe *et al.*, 1992a) and as liquid sulphur pools near the lake bottom (cf., Oppenheimer and Stevenson, 1989).

It is of interest to note that both the S/Cl and the F/Cl ratios in the waters of Agrio River, independent of sampling site or date, are fairly similar to the average ratios (by weight) of 2.69 and 0.055 of lake waters collected in Stage II (Chapter 5, Table 5.1), and to the average ratios of 3.4 and 0.06 of gas samples (T=960°C) collected in June 1981 (Delorme, 1983). This correspondence suggests that rising magmatic gases condensate in a reservoir that feeds the lake-hydrothermal system, the crater fumaroles as well as the Agrio River watershed.

Although metal transport is not considered here, thousands of tons of a variety of metals are transported by the Agrio and

Toro Amarillo rivers yearly. For instance, preliminary data indicate that Agrio River transports considerable amounts of potentially toxic metals (e.g., ~15 ton aluminium per day), which are discharged into Toro Amarillo River. Environmental consequences can be far reaching, as this river remains acidic (pH~4.8) down to ~50 km from its junction with the Agrio River (Fig. 6.1).

6.5 Conclusions

1. The chemical composition of acid-chloride-sulphate springs discharging into the Agrio River is relatively stable over long periods of time, in contrast to the strong variability observed in the crater lake.
2. Proportions of major anions (S-Cl-F) are consistent with the hypothesis that thermal water issued from the Agrio springs contains a component derived from the same summit hydrothermal system that also includes the lake.
3. The chemical signatures do not provide unambiguous evidence for the hypothesis that water is transported to the springs via a direct hydraulic connection with the lake. If correct, the travel time should be at least 13 years, considering that a major shift in S/F ratios that occurred around 1989 in the lake had not yet propagated to the Agrio springs by 2002. Alternatively, the subsurface hydrothermal reservoir in the summit area, rather than the lake is the source of the acid brine water.
4. Fluxes of magmatic volatiles issued by the Agrio springs are of the same order of magnitude but much more stable than those emitted from fumarole vents in the active crater. Based on data from two intervals of several years in Stages III and IV, the total SO₂ flux from both sources ranged roughly between 150 and 250 ton per day. These quantities represent a minimum total flux of sulphur from Poás volcano. The results suggest that emission rates from flank springs and crater fumaroles are inversely related. In periods when free emission of volatiles via the crater area is hampered by the underlying hydrothermal system (e.g., during volcanic quiescence), larger volatile fluxes through the Agrio springs might compensate this and thus keep overall emissions in balance.

Appendices

Appendices - CHAPTER 4

Appendix 4.1 Analytical conditions for polythionate analyses and interlaboratory comparison

Table APP-4.1.1. Analytical conditions used to separate and quantify tetra-, penta-, and hexathionate ions by ion-pair chromatography with UV detection. (A) At University of Tokyo, (B) At LAQAT-UNA, where polythionates were analysed following Miura and Kawaoi (see C), with minor adaptations.

Technique	Chromatographic analytical column	Mobil phase	pH	Detector, pump and column temp.	Loop volume	Flow rate	Quantification levels	Source
A: Microbore High-Performance Liquid Chromatography (ion-pair chromatography)	ODS-2 Spherisorb S30DS2, 100 mm X 1 mm, 3µm particle size	Acetonitrile-water 2.5/7.5 v/v containing 0.1%TBAOH v/v: 25 ml CH ₃ CN + 1 ml 0.01 M (0.1%) TBAOH + 74 ml 0.1M KH ₂ PO ₄ +H ₃ PO ₄ conc. (by dropwise addition) (total volume 100 ml)	3.5	LDC Milton Roy UV spectromonitor 0.05 abs. unit, 211 nm, LDC Milton Roy Constametric III pump, 40°C	2 µl	25 µl/min recording range 1 mV, chart speed 3.5	Trithionate in excess of 10 ppm; tetra-, penta-, and hexathionate in excess of 0.2 ppm. Samples diluted 10 times	This work (after Takano and Watanuki, 1988, 1990).
B: Ion-pair chromatography	ODS-2 Alltech Allsphere), 150 mm length X 4.6 mm I.D., 5 µm particle size	Acetonitrile-water (20:80, v/v) containing 6 mM TPAOH: 100 ml CH ₃ CN + 6.12 ml 0.49 M TPAOH + CH ₃ COOH(drops) + diluted to 500 ml with double distilled H ₂ O	5.0	UV (230 nm) 23±2°C	100 µl	0.6 ml/min	Tetra-, penta-, and hexathionate in excess of 5, 1.6, and 0.5 ppm, respectively. Samples diluted from 5 to 50 times	This work (after Miura and Kawaoi, 2000)
C: Ion-pair chromatography	Silica ODS Ultaron VX ODS, 150 mm X 4.6 mm I.D. (Shinwa Chemical Industries, Tokyo)	Idem to B	Idem to B	Idem to B	Idem to B	Idem to B	Detection limits: 20 nM S ₄ O ₆ ²⁻ , 15 nM S ₅ O ₆ ²⁻ , 18 nM S ₆ O ₆ ²⁻	Miura and Kawaoi, 2000

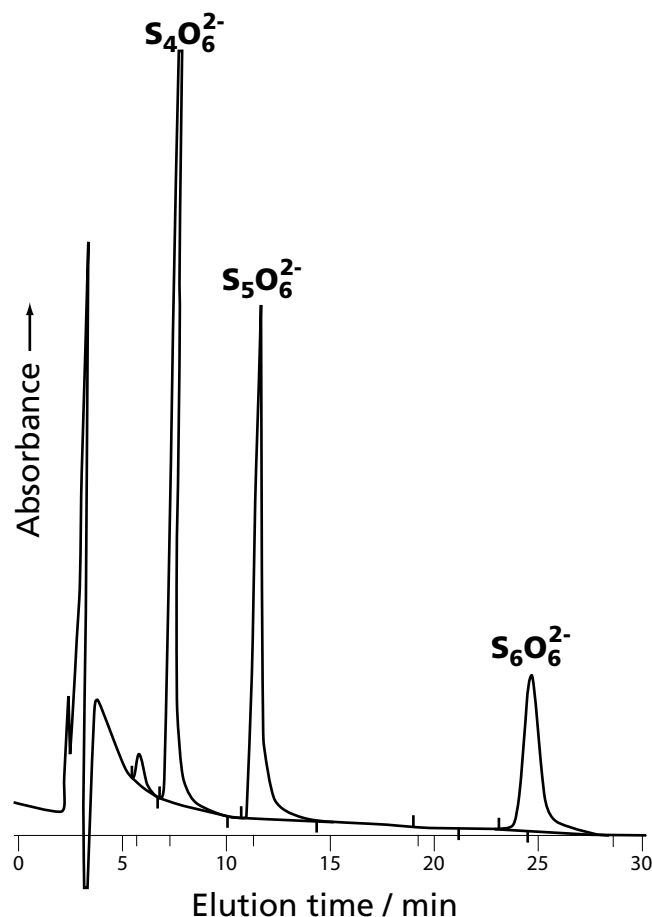


Figure APP-4.1A. Chromatogram of a lake-water sample (collected on 21 September 2001) as obtained at Tokyo University (B. Takano, pers. comm.), using microbore ion-pair chromatography with UV detection (see Table APP-4.1.1 for analytical conditions). The sample was diluted 10 times. The peaks that eluted before the tetrathionate represent unknown impurities in the lake water.

Table APP-4.1.2. Comparison of polythionate analyses carried out at LAQAT-UNA and the University of Tokyo.

Sample code	Sampling date	Analysis date	Storage time y(ears) or m(onths)	Laboratory	S ₄ O ₆ ²⁻ mg/kg	S ₅ O ₆ ²⁻ mg/kg	S ₆ O ₆ ²⁻ mg/kg	Total S _x O ₆ ²⁻ mg/kg
M-248 (mud pool)	10 Jun 1994	24 Feb 1999	4y 8m	Tokyo Univ.	2825**	2067**	725**	5617**
		18 Jan 2001	6y 7m	LAQAT	2926 ^a	2244 ^a	n.d.	n.d.
		16 Oct 2002	8y 4m	LAQAT	3185	2600	880	6930
		16 Oct 2002	8y 4m	LAQAT	3217***	n.d.	n.d.	n.d.
M-726	8 Sep 1995	23 Feb 1999	3y 5m	Tokyo Univ.	294**	294**	136**	724**
		6 Aug 2002	6y 11m	LAQAT	386	241	134	761
M-314	20 Oct 1995	23 Feb 1999	3y 4m	Tokyo Univ.	<d.l.	<d.l.	<d.l.	<d.l.
		8 Aug 2002	6y 10m	LAQAT	<d.l.	<d.l.	<d.l.	<d.l.
M-673	2 Jul 1997	9 Feb 1999	1y 7m	Tokyo Univ.	500*	204*	75*	779*
		17 Aug 2002	5y 1m	LAQAT	426	226	101	763
M-300	17 Apr 1998	10 Feb 1999	10 m	Tokyo Univ.	<d.l.	<d.l.	<d.l.	<d.l.
		7 Sep 2002	4y 5m	LAQAT	<d.l.	<d.l.	<d.l.	<d.l.
M-269	17 Mar 1999	April 1999	Few months	Tokyo Univ.	455*	213*	109*	777*
		28 July 2002	3y 4m	Tokyo Univ.	462*	182*	156*	794*
		24 Dec 2002	3y 9m	Tokyo Univ.	485*	253*	180*, ****	1069*, ****
		24 Dec 2002	3y 9m	Tokyo Univ.	587*, ****	302*, ****	n.d.	n.d.
		16 Oct 2002	3y 7m	LAQAT	509***	n.d.	122*, ****	995*, ****
		10 Mar 2005	6 y	Tokyo Univ.	548*, ****	325*, ****		
M-266	18 Jun 1999	1 Aug 2002	3y 2m	Tokyo Univ.	332*	130*	90*	552*
M-291	17 Jun 1999	12 Sep 2002	3y 3m	LAQAT	389*	105*	123*	617*
M-285	20 Sep 2001	27 Dec 2002	1y 3m	Tokyo Univ.	216*	119*	43*	378*
M-265-2	21 Sep 2001	3 Oct 2002	1y 1m	LAQAT	259	115	50	424

Results are from aliquots taken from the same sample bottle, except for the June 1999 and September 2001 samples, which were collected on two consecutive days. Note the time intervals between dates of analyses in Costa Rica and Japan. Techniques used are those described in Chapter 4 and Table APP-4.1.1, except for M-248, which was analyzed twice in Costa Rica: on 18 January 2001 by ion pair-chromatography with conductivity detection after pre-treatment with a cation-exchange resin (^a), following Takano and Watanuki (1988), and on 16 October 2002 following the Miura and Kawaoi (2000) procedure (row C in Table APP-4.1.1).

*: Calculated from mg/L data using a density of 1.02 g/ml. **: Calculated from mg/L data using a density of 1.2 g/ml. ***: Determined after calibration with synthetic tetrathionate standard solution. ****: Data from an aliquot that had been stored at LAQAT and was sent to Tokyo shortly before analysis, whereas the other M-269 aliquots analyzed at Tokyo University had always been stored there. n.d.: not determined. <d.l.: below detection limit.

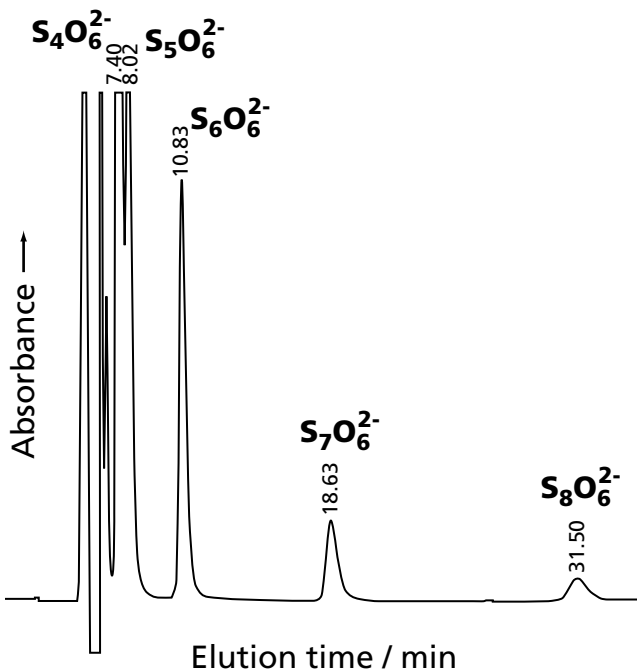


Figure APP-4.1B. Chromatogram of a lake-water sample (collected on 26 April 1996) as obtained at LAQAT-UNA (following Miura and Kawaoi, 2000; see Table APP-4.1.1 row B), showing peaks of tetra-, penta-, hexa-, hepta- and octathionate. The sample was diluted 5 times. The peaks that eluted before the tetrathionate represent unknown impurities in the lake water.

Appendix 4.2 Compositions of fumarolic gases, Poás volcano

Table APP-4.2.1 Compilation of (partial) gas compositions of fumaroles in the active crater of Poás.

Date	Sampling site	Area of main fumarolic activity	Temp. (°C)	HCl	HF	SO ₂	H ₂ S	CO ₂	H ₂ O	SO ₂ /H ₂ S	Data source
Apr-81	CPC	CPC	1020	n.d.	n.d.	61.2	0.20	23.3	(95.0)	306	(1)
Jun-81	CPC	CPC	940	n.d.	n.d.	55.8	0.52	26.6	n.d.	107	(1)
Jan-82	CPC	CPC	860	n.d.	n.d.	66.4	0.02	20.1	n.d.	3320	(1)
Feb-82	CPC	CPC	870	n.d.	n.d.	34.4	n.d.	51.0	(79.5)	n.d.	(1)
Mar-82	CPC	CPC	890	n.d.	n.d.	59.8	0	20.9	n.d.	n.d.	(2)
Dec-82	CPC	CPC	731	n.d.	n.d.	66.1	0.25	21.8	n.d.	264	(1)
Oct-83	CPC	CPC	801	n.d.	n.d.	61.9	0.35	16.4	(96.8)	175	(1)
Feb-89	CPC	Lake + CPC	95	n.d.	n.d.	4.23	18.2	77.4	(97.9)	0.23	(1)
Nov-92	CPC	Lake	118	11.3	0.26	34.2	11.6	42.4	n.d.	2.94	(2)
Feb-98	Sur	CPC+EIW	98	0.43	n.d.	n.d.	0.84	9.90	987	n.d.	(3)
Feb-99	CPC	CPC+EIW	92	1.73	0.00404	29.3	n.d.	30.1	936	n.d.	(3)
Feb-99	Sur	CPC+EIW	89	n.d.	n.d.	0.002	1.88	18.4	978	0.001	(3)
Mar-99	CPC	CPC+EIW	95	n.d.	n.d.	64.3	0.19	32.1	n.d.	330	(4)
Mar-99	Sur	CPC+EIW	94	n.d.	n.d.	0.31	47.2	52.5	n.d.	0.007	(4)
Mar-99	Norte	CPC+EIW	93	n.d.	n.d.	n.d.	1.81	98.2	n.d.	n.d.	(4)
19-Nov-99	CPC	CPC+EIW	92	1.56	0.00548	26.3	0.57	24.1	946	45.9	(3)
24-Feb-00	CPC	CPC+EIW	94	1.43	0.00678	2.95	0.86	0.739	992	3.43	(3)
Feb-00	Sur-Este	CPC+EIW	92	n.d.	n.d.	1.50	0.15	2.12	995	10.1	(3)
Feb-00	Este	CPC+EIW	89	0.27	0.05983	34.5	1.57	7.57	956	21.9	(3)
Feb-00	Quebrada Roja	CPC+EIW	84	n.d.	n.d.	n.d.	3.25	24.9	971	n.d.	(3)
Jan-01	Poás P3	CPC+EIW	76	0.32	0.010	0.82	0.21	12.0	987	3.90	(5)
Feb-01	CPC-crater lake	CPC+EIW	78	n.d.	n.d.	n.d.	n.d.	668	282	n.d.	(3)
Feb-01	Este	CPC+EIW	97	0.47	n.d.	1.14	0.26	74.2	923	4.37	(3)
Feb-01	Norte Este	CPC+EIW	101	2.29	0.00023	247	6.44	246	498	38.4	(3)
Feb-01	Norte	CPC+EIW	95	0.27	0.00013	6.82	0.22	15.9	976	30.9	(3)
Feb-01	The Kid (La Niña)	CPC+EIW	95	n.d.	n.d.	n.d.	5.39	64.7	929	n.d.	(3)
Mar-01	Poás P6	CPC+EIW	n.a.	2.40	0.010	0.46	0.25	3.30	989	1.84	(5)
Jul-01	Poás P8	CPC+EIW	108	0.99	0.010	5.72	2.17	3.37	988	2.64	(5)
Aug-01	Norte Este	CPC+EIW	101	0.67	0.000	118	4.30	82.1	794	27.5	(6)
Nov-01	Norte Este	CPC+EIW	104	0.17	0.00006	29.0	0.68	118	852	43.0	(6)
Nov-01	Norte	CPC+EIW	101	0.42	0.00021	40.6	0.74	63.3	895	54.8	(6)
29-Nov-01	Norte	CPC+EIW	101	3.49	0.02804	34.2	0.76	32.0	929	45.3	(6)
Nov-01	The Kid (La Niña)	CPC+EIW	81	0.003	0.00001	n.d.	1.25	28.9	970	n.d.	(6)
Jan-02	Norte	CPC+EIW	101	3.36	0.02697	29.0	1.03	37.3	929	28.2	(6)
Feb-02	Norte Este	CPC+EIW	103	7.94	0.03663	26.4	0.16	34.5	931	165	(6)
Feb-02	Norte	CPC+EIW	101	1.93	0.01547	17.0	0.65	28.7	952	26.1	(6)
Feb-02	The Kid (La Niña)	CPC+EIW	86	0.018	0.00011	n.d.	0.60	36.2	963	n.d.	(6)
Apr-02	The Kid (La Niña)	CPC+EIW	93	0.082	0.02399	0.25	1.08	36.2	962	0.23	(6)
Apr-02	Norte Este	CPC+EIW	98	0.55	0.00217	57.8	1.08	141	799	53.4	(6)
Apr-02	Norte	CPC+EIW	94	0.49	0.01237	31.6	0.56	62.7	901	56.3	(6)
May-02	Norte	CPC+EIW	99	1.41	0.45084	4.25	1.33	49.1	943	3.21	(6)
Jul-02	Norte	CPC+EIW	88	1.31	0.42045	36.2	0.66	53.1	908	54.5	(6)
05-Dec-02	Norte	CPC+EIW	122	n.d.	n.d.	42.8	0.10	n.d.	n.d.	428	(7)
31-Mar-03	The Kid (La Niña) (=East T3)	CPC+EIW	97	2.20	0.00024	15.8	0.16	35.1	947	96.3	(8)
31-Mar-03	Norte (T4)	CPC+EIW	116	2.22	0.00070	25.9	0.59	36.2	935	44.1	(8)
Apr-03	The Kid (La Niña)	CPC+EIW	97	1.58	0.00007	24.3	0.36	42.9	931	68.2	(6)
Apr-03	The Kid (La Niña)	CPC+EIW	97	0.30	0.00001	33.9	0.49	56.9	908	68.8	(6)
Apr-03	Norte	CPC+EIW	93	0.12	0.04616	17.1	0.75	34.7	947	22.8	(6)
Apr-03	Norte Este	CPC+EIW	118	0.91	0.00063	36.0	1.18	41.0	921	30.6	(6)
01-Jul-03	Norte Este	CPC+EIW	116	1.39	0.00012	23.1	0.18	26.3	948	128	(6)
29-Jul-03	Norte Este	CPC+EIW	116	1.90	0.00014	27.7	0.34	29.2	941	80.4	(6)
Feb-04	Este	CPC+EIW	99	0.75	0.00006	8.54	0.79	22.8	967	10.8	(6)
Apr-04	Norte Este	CPC+EIW	115	1.56	0.00013	21.5	0.18	26.4	944	121	(6)
Apr-04	Norte	CPC+EIW	97	2.37	0.00027	12.4	0.87	36.0	928	14.1	(6)
Apr-04	The Kid (La Niña)	CPC+EIW	94	0.24	0.00002	0.26	0.35	31.0	963	0.73	(6)
21-Jun-04	The Kid (La Niña) (=Poas#1 East T1)	CPC+EIW	94	0.00	n.a.	1.26	0.22	10.4	988	5.78	(9)

Date	Sampling site	Area of main fumarolic activity	Temp. (°C)	HCl	HF	SO ₂	H ₂ S	CO ₂	H ₂ O	SO ₂ /H ₂ S	Data source
21-Jun-04	Norte (=Poas#2 T2)	CPC+EIW	114	4.38	n.a.	20.5	0.39	8.99	966	53.2	(9)
25-Aug-04	Norte	CPC+EIW	114	1.70	n.a.	27.0	0.30	13.0	958	90.0	(10)
22-Oct-04	Este	CPC+EIW	94	0.10	n.a.	3.00	0.17	13.0	983	17.6	(10)
22-Oct-04	Norte	CPC+EIW	116	2.00	n.a.	23.1	2.09	14.0	958	11.1	(10)
25-Jan-05	Este	CPC+EIW	93	0.00	n.a.	5.00	0.3	12.0	983	16.7	(10)
25-Jan-05	Norte Este	CPC+EIW	99	0.30	n.a.	7.00	0.2	6.00	987	35.0	(10)
21-Mar-05	Norte	CPC+EIW+Lake	105	5.00	n.a.	17.0	1.0	12.0	966	17.0	(10)
12-Apr-05	Norte	Lake + EIW	124	2.20	n.a.	22.0	2.8	10.7	962	7.86	(10)
26-May-05	Norte	Lake + EIW	200	0.90	n.a.	2.90	1.2	0	996	2.42	(10)
16-Jun-05	Norte	Lake + EIW	200	0.90	n.a.	4.80	3.6	6.4	974	1.33	(10)
14-Jul-05	Norte	Lake + EIW	200	2.30	n.a.	28.2	6.2	11.7	949	4.55	(10)
Aug-05	Norte	Lake + EIW	190	15	n.a.	35.0	18.1	11.5	916	1.93	(10)
20-Sep-05	Norte	Lake + EIW	193	0.40	n.a.	26.1	7.1	1.00	964	3.68	(10)
28-Feb-06	Norte	Lake + EIW	188	0.02	n.a.	9.70	1.8	1.80	986	5.39	(10)
03-May-06	Norte	Lake + EIW	185	n.a.	n.a.	2.90	1.2	0.05	995	2.42	(10)

All data are in mmol/mol. except those in bold italics which are mole proportions on a dry basis (H₂O in parentheses). CPC: Composite pyroclastic cone; EIW: Eastern inner crater wall; n.a.: not analyzed. n.d.: no data. Data sources: (1) Rowe et al., 1992a; (2) Venzke et al., 2002; (3) Vaselli et al., 2003; (4) Díaz et al., 2002; (5) Zimmer et al., 2004; (6) Tassi et al., unpubl.; (7) OVSICORI-Universidad Nacional. Center for Geophysical Research CIGEFI-Universidad de Costa Rica; (8) Fischer and Taran, 2004; (9) Ohba, pers. comm. 2004-2008; (10) OVSICORI-Universidad Nacional. Ohba, pers. comm. 2004-2008

Table APP-4.2.2. Dissolved unreacted SO₂ and H₂S measured *in situ* in the acid lake of Poás. and estimated molar SO₂/H₂S ratios of subaqueous fumaroles.

Sampling date	Lake Temp. (°C)	Dissolved SO ₂ (mg/L) Measured	Dissolved H ₂ S (mg/L) Measured	Dissolved H ₂ S (mg/L) Max. estimate	SO ₂ /H ₂ S (mol/mol) Min. estimate	Log SO ₂ /H ₂ S (mol/mol)
17-Mar-99	32	150	<0.2	2.5	32	1.5
07-Jul-99	32	74	<0.2	2.5	16	1.2
19-Aug-99	35	125	<0.2	2.5	26	1.4
08-Sep-99	39	185	<0.2	2.3	43	1.6
19-Nov-99	39	300	<0.2	2.3	71	1.8
21-Jan-00	38	30	<0.2	2.3	7.1	0.85
24-Feb-00	46	40	<0.2	2.3	9.4	0.97
11-Apr-00	32	35	<0.2	2.5	7.4	0.87
24-May-00	31	50	<0.2	2.5	11	1.0
09-Jun-00	31	62	<0.2	2.5	13	1.1
21-Jul-00	33	70	<0.2	2.5	15	1.2
24-Aug-00	31	20	<0.2	2.5	4.2	0.62
12-Sep-00	35	60	<0.2	2.5	13	1.1
10-Oct-00	35	25	<0.2	2.5	5.3	0.72
21-Nov-00	34	28	<0.2	2.5	5.9	0.77
12-Jan-01	31	27	<0.2	2.5	5.7	0.76
08-Mar-01	32	60	<0.2	2.5	13	1.1
08-May-01	34	72	<0.2	2.5	15	1.2
13-Jun-01	35	143	<0.2	2.5	30	1.5
14-Aug-01	31	123	<0.2	2.5	26	1.4
10-Sep-01	38	188	<0.2	2.3	44	1.6
24-Oct-01	32	255	<0.2	2.5	54	1.7
27-Nov-01	36	<1	<0.2	2.3	-	-
07-Dec-01	34	<1	<0.2	2.5	-	-
27-Feb-02	23	48	<0.2	2.8	9.2	0.96
16-May-02	29	3.0	<0.2	2.5	0.6	-0.20
30-Jul-02	32	100	<0.2	2.5	21	1.3
06-Nov-02	37	63	<0.2	2.3	15	1.2
31-Mar-03	39	146	<0.2	2.3	34	1.5
11-Jun-04	29	2.2	<0.2	2.5	0.47	-0.33
13-Oct-04	27	0.6	<0.2	2.5	0.13	-0.90
07-Mar-05	32	0.6	<0.2	2.5	0.13	-0.90
04-May-05	41	8.0	<0.2	2.3	1.9	0.27
8-Aug-05	51	3.0	<0.2	2.1	0.75	-0.12
20-Jul-06	43	62	2	23	1.5	0.16

Sampling date	Lake Temp. (°C)	Dissolved SO ₂ (mg/L) Measured	Dissolved H ₂ S (mg/L) Measured	Dissolved H ₂ S (mg/L) Max. estimate	SO ₂ /H ₂ S (mol/mol) Min. estimate	Log SO ₂ /H ₂ S (mol/mol)
10-Nov-06	57	175	<0.2	1.8	53	1.7
13-Apr-07	51	50	<0.2	2.1	13	1.1

Molar SO₂/H₂S ratios of subaerial fumarolic input were calculated from available compositional data on subaerial gases (Table APP-4.2.1). Molar SO₂/H₂S ratios of subaqueous fumaroles were calculated based on solubilities of both gases in pure water at 1-atm partial pressure (IUPAC, 1983, 1988; Xia *et al.*, 1999, 2000) for the corresponding lake temperatures.

Appendix 4.3 Analytical procedure for in-situ measurement of aqueous unreacted SO₂ and H₂S in acid crater-lake waters using a gas-detection tube method

Togano and Ochiai (1987) developed this technique to determine dissolved gases in hot spring waters. It was later adapted by Ohsawa (1992) and Takano *et al.* (2008) for *in-situ* measurements of unreacted dissolved SO₂ and H₂S in acid crater-lake waters. For the determination of unreacted dissolved SO₂ and H₂S in the crater-lake waters of Poás, a Gastec Standard Detector Tube System was used. The system consisted of a gas sampling pump (GV 100S) and gas detector tubes (Fig. APP-4.3A).

Since March 1999 when monitoring started, detectable concentrations of dissolved SO₂ have virtually always been found in the lake water, whereas H₂S was never present (except for July 2006 when 2ppm H₂S was detected). For monitoring volcanic activity the waters should always be analysed for both species. Here, a procedure for determining dissolved SO₂ and H₂S, and for *in-situ* preparation of standard solutions will be described. Calibration of H₂S gas detection tubes in the field was done only once (7 July 1999), because of the usual absence of this species.

1. In-situ measurement of dissolved SO₂ and H₂S in acid crater lake waters

Put 10 ml of sample (the volume can be varied depending on the H₂S and SO₂ levels, see general notes below) into a 500 ml polyethylene bottle.

Add 2 ml of a 20% H₂SO₄ solution.

Close the bottle with a silicon or rubber plug (see additional notes for characteristics of the plug) to seal off the gases.

Shake the bottle gently without splashing the solution for 2 minutes.

Dissolved SO₂ and H₂S are released from the solution (Fig. APP-4.3A).

Insert the SO₂-H₂S gas detecting tubes (which are connected serially with a rubber or silicon tube in such a way that the SO₂ tube goes before the H₂S tube, as shown in Fig. APP-4.3A) into the bigger hole of the rubber or silicon plug, then suck 100 ml of the inner gases with the hand pump, and wait for 2 minutes without disconnecting the pump. For easier insertion, the tubes can be wetted with distilled water.

Colours of the detector tubes change from pink to yellow for SO₂ and from white to brown for H₂S as the gases are drawn in.

After 2 minutes, take out the tubes and read the concentrations (ppm) shown at the head of the colouration.

Concentrations of SO₂ and H₂S in the lake water sample are calculated from the calibration curves that are described below (see calculation examples).

2. Calibration for dissolved SO₂

Put 0.1000 g of NaHSO₃ (sodium hydrosulfite) into a 100-ml volumetric flask, dissolve it with distilled water, and dilute it up to the mark.

Take 1000 µl of the solution with a micropipette, put it into a 500-ml plastic bottle, add 10ml of distilled H₂O, and then add 2 ml of 20% H₂SO₄ solution.

Close the bottle with a rubber or silicon plug (see additional notes) to seal the inner gases.

Shake the bottle gently without splashing the solution for 2 minutes.

The NaHSO₃ reacts with the oxidizing agent (the acid) and gives off SO₂ (Fig. APP-4.3A).

Insert a SO₂-detecting tube (5L or 5Lb) into the bigger hole of the silicon plug, suck 100 ml of the released inner gasses with the hand pump, and wait for 2 minutes without disconnecting the pump.

The colour in the detector tube changes as the gas is drawn in. After 2 minutes take out the tube and read the concentration shown at the end of the colour-changed layer scaled in ppm units on the sensing tubes.

Repeat the same procedure using a 1200 µl of the standard solution.

Draw a calibration curve using several other SO₂ standard solutions.

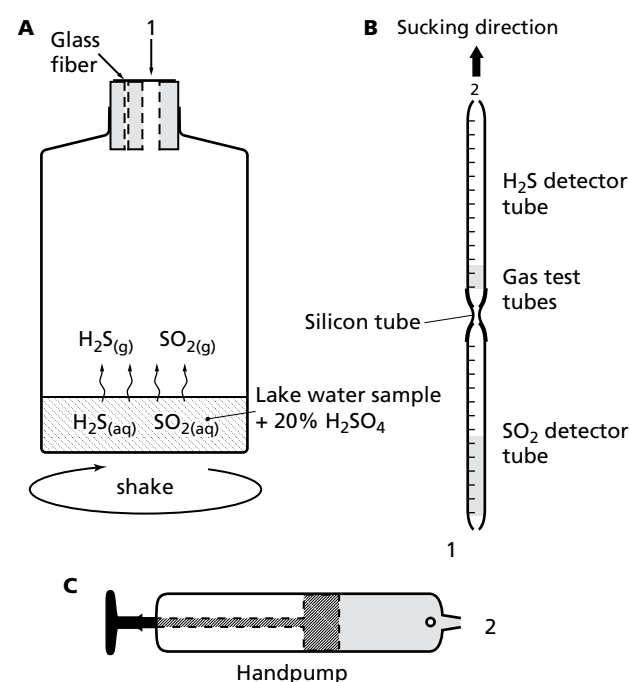


Figure APP-4.3A. Gastec system for measuring aqueous unreacted SO₂ and H₂S in acidic lake waters (modified by Takano *et al.*, 2008 after Ohsawa, 1992).

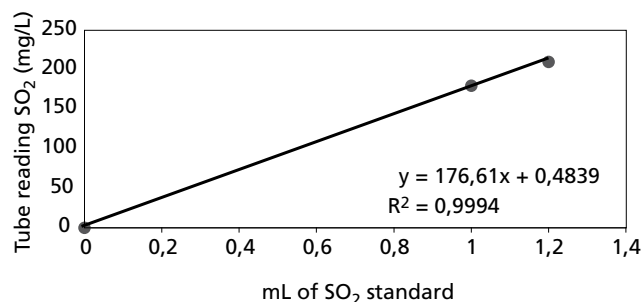


Figure APP-4.3B. Calibration curve for dissolved SO_2 gas using acidic NaHSO_3 standard solutions, prepared and measured *in situ* (on 9 June 2000 at the edge of the lake).

Plot the readings against 0, 1000, and 1200 μL (Fig. APP-4.3B).

3. Calibration for dissolved H_2S

Put 1.0000 gram of solid $\text{NaHS}\cdot\text{H}_2\text{O}$ (sodium hydrosulfide) in a 100-ml volumetric flask.

Dissolve it with distilled water, and dilute it up to the mark (solution No.1).

Transfer 1 ml of solution No. 1 into a 50-ml volumetric flask with a micropipette, and dilute it with distilled water to the mark (solution No. 2).

Then put 0.25 ml of solution No. 2 with a micropipette into a 500-ml plastic bottle, and add 10 ml of distilled water and 2 ml of a 20% H_2SO_4 solution.

Close the bottle with a rubber or silicon plug (see additional notes) to seal the inner gases.

Shake the bottle gently without splashing the solution for 2 minutes.

The dissolved H_2S is released from the solution (Fig. APP-4.3A).

Insert a H_2S gas-detecting tube into the bigger hole of the silicon plug, suck 100 ml of the inner gases with the hand pump, and wait for 2 minutes without disconnecting the pump.

The colour in the detector tube changes as the gas is drawn in.

After 2 minutes take out the tube and read the concentration at the top of the resulting colour.

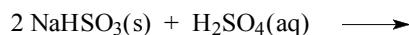
Repeat this procedure but taking 0.50 ml of the standard solution instead.

Draw a calibration curve using several other standard solutions for H_2S .

Plot the H_2S tube readings against 0, 0.25 and 0.50 ml.

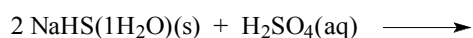
4. Calculation of concentrations of dissolved SO_2 (example)

If the sample yields a reading of 0.30 ml SO_2 from the SO_2 calibration curve, then $(300/400) \times 0.2432 \times F' \times (1000/10) = 19 \times F'$ ppm SO_2 . If $F'=1$, then the lake water sample dissolves 19 ppm SO_2 (report results with two significant digits, because readings are sufficiently accurate). In the equation "300" corresponds to the volume of SO_2 standard solution extrapolated from the SO_2 calibration curve. The NaHSO_3 standard solution 1 contains 0.10 g of the salt in 100 ml of solution. Therefore, according to the stoichiometry of the reaction below, an aliquot of 0.4 ml of the solution will generate 3.8×10^{-6} mol SO_2 (0.243 mg SO_2).



5. Calculation of concentrations of dissolved H_2S (example)

If the sample yields a reading of 0.180 ml for a 10-ml sample from the H_2S calibration curve, the concentration of H_2S should be calculated as follows: $(180/500) \times 0.046 \times F \times (1000/10) = 1.66 \times F$ ppm, where F stands for a correction factor for the purity of the $\text{NaHS}\cdot\text{H}_2\text{O}$ reagent. In this case, if $F=1$, the sample dissolves 1.66 ppm H_2S (similar comments as above). The $\text{NaHS}\cdot\text{H}_2\text{O}$ standard solution 2 contains 1×10^{-4} g of the salt in 50.00 ml of solution. Therefore, according to the stoichiometry of the reaction below, an aliquot of 0.5 ml of the standard solution 2 will generate 1.35×10^{-6} mol H_2S (0.046 mg H_2S).



6. General notes

For measuring a sample, take 10 ml of the sample without adding 10 ml of distilled water (see the procedures for SO_2 and H_2S calibration described above).

The sample volume can be changed depending on H_2S and SO_2 concentrations, but the total volume of the solution should be adjusted by adding distilled water so that it is the same as the standard solutions.

The rubber or silicon plug has two holes. A smaller hole packed with glass fiber is for letting ambient air into the bottle to compensate for the reduction of internal air when the internal air-gas mixture is pumped out. Fiberglass makes the air intake slower, and also keeps the air up in the bottle. The bigger hole is to insert the gas detecting tubes.

After sulphuric acid is added to the standard solutions or to water samples in the plastic bottle, the bottle should be closed with the rubber or silicon plug. During shaking the two holes in the plug should be covered with a piece of Scotch-tape (adhesive tape) to prevent released gases from leaking into open air. Then the tape must be removed from the bigger hole to insert the gas detecting tube, without disconnecting the plug from the 500 ml polyethylene bottle. Before inserting the tubes, care must be taken to avoid that the holes get wet from the inner solution. If not, acidic solution may enter the tubes, resulting in erroneous readings.

The inserted gas-detecting tubes should extract the gases from the lower part of the bottle. Otherwise, diluted gases will be sucked into the detecting tube.

The Scotch-tape covering the smaller hole in the rubber or silicon plug should be opened to the atmosphere just before sucking the gases out of the bottle with the hand pump.

For both SO_2 and H_2S measurements, the pump is adjusted to suck a 100-ml volume of the air contained in the polyethylene bottle.

Appendix - CHAPTER 5

Appendix 5.1 Interlaboratory comparison of analytical data.

Table APP-5.1.1. Interlaboratory comparison of analytical data on major anion concentrations in samples from the acid crater lake of Poás volcano. See experimental section for details on analytical conditions.

Date	Sample code	Temperature (°C)	pH	SO ₄	Cl	F	Data source	Analytical technique
26-Jul-85	M-766	46	n.d.	57000	21300	1100	(1)	IC
26-Jul-85		46	-0.2	50500	25000	1100	(2)	Wet chemical analysis
22-Aug-85	M-767	45	n.d.	67600	24900	1000	(1)	IC
22-Aug-85		45	0.17	54200	21100	1300	(3)	IC
22-Aug-85		45	0.23	53000	24500	1200	(2)	Wet chemical analysis
02-May-86	M-763	38	n.d.	55000	22500	550	(1)	IC
02-May-86		38	0.2	40100	16500	970	(3)	IC
02-May-86		38	0.3	47000	15400	830	(2)	Wet chemical analysis
31-Oct-86		54	0.14	52000	23200	1240*	(3)	IC
31-Oct-86		54	0.15	52500	27800	975*	(2)	Wet chemical analysis
27-Feb-87	M-759	62	n.d.	91900	38000	1400	(1)	IC
27-Feb-87		62	-0.03	78600	33700	1800	(3)	IC
19-Mar-87	M-760	62	< 0	90900	39000	1640	(1)	IC
19-Mar-87		62	< 0	82900	35900	1800	(3)	IC
02-Mar-88	M-346	60	-0.32	118300	51700	1600*	(1)	IC
02-Mar-88		60	-0.31	118000	51300	2100*	(3)	IC
13-Mar-92	M-746	65	-0.85	100400	92000	9840	(1)	IC
13-Mar-92		65	n.d.	119000	87400	8800	(4)	IC and wet chemical analysis
13-Mar-92		65	-0.7	103000	94800	7400	(2)	Wet chemical analysis
24-Jun-92		73	n.d.	78700	53100	7140	(4)	IC and wet chemical analysis
24-Jun-92		73	-0.54	82000	53500	n.d.	(5)	IC
18-Sep-92	M-327	70	n.d.	82300	68400	8200	(1)	IC
18-Sep-92		70	n.d.	93100	74400	8400	(4)	IC and wet chemical analysis
18-Sep-92		70	-0.6	96000	70200	n.d.	(5)	IC
07-Oct-92	M-743	75	n.d.	50000	68100	4600	(1)	IC
07-Oct-92		75	n.d.	52400*	71600	5100	(4)	IC and wet chemical analysis
07-Oct-92		75	-0.5	42000*	64900	n.d.	(5)	IC
19-Nov-92	M-328	80	n.d.	36900	76800	5000	(1)	IC
19-Nov-92		80	n.d.	38400	73000	5700	(4)	IC and wet chemical analysis
19-Nov-92		80	-0.5	33000	65000	n.d.	(5)	IC
23-Jan-93	M-356	65	n.d.	65000	67600*	4300	(1)	IC
23-Jan-93		65	n.d.	56100	54000*	4500	(4)	IC and wet chemical analysis
23-Jan-93		65	< 0	54000	49100	n.d.	(5)	IC
06-Jan-95	M-316	50	n.d.	16700	10800	1100	(1)	IC
06-Jan-95		50	0.22	16000	10200	n.d.	(5)	IC
05-Jan-96	M-706	29	n.d.	8300	3100	200	(1)	IC
05-Jan-96		29	1.35	9100	3600	n.d.	(5)	IC
24-Jul-96	M-719	36	1.75	7400	4700	270	(1)	IC
24-Jul-96		36	n.d.	7500	4500	n.d.	(5)	IC
08-Aug-96	M-252	34	n.d.	7200	4200	360	(1)	IC
08-Aug-96		34	1.45	7000	4500	n.d.	(5)	IC
27-Sep-96	M-304	40	n.d.	7100	4700	220	(1)	IC
27-Sep-96		40	1.65	6800	4300	n.d.	(5)	IC
28-Nov-96	M-724	31	n.d.	7100	5200	300	(1)	IC
28-Nov-96		31	1.55	6800	5100	n.d.	(5)	IC

Overall deviations between analytical results from different laboratories were 15% at most, except for data pairs indicated by an asterisk, which show random differences between 20 and 25%. Concentrations are in mg/kg (ppm). n.d.: no data available.

Data sources: (1) This work; (2) OVSICORI; (3) Rowe et al., 1992b; (4) Nicholson et al., 1993; (5) LAQAT

Appendix photo documentation



Figure 1.1. Engineer Rodolfo Olmos from University of El Salvador, El Salvador Central America, measuring SO₂ fluxes by using a miniDOAS system during a traverse along the southern rim of the active crater of Poás volcano. Photograph taken by Eliécer Duarte on 6 April 2006.



Figure 2.4. Aerial view of the summit of Poás, looking northwest. The currently active crater with the acid lake (Laguna Caliente) is visible in the background and the neutral lake of Botos volcano at the front. Photograph taken on 27 February 2007 by Eliécer Duarte from an aircraft of Project Lighthawk.



Figure 2.8. View of Poás crater looking north on 2 March 1980 with the eastern terrace on the right. Photograph courtesy of Jorge Quirós Umaña.

Figure 1.2. View of Fumarole Norte located at the foot of the eastern terrace at the active crater of Poás volcano, discharging significant amounts of elemental sulphur and water vapour. Temperature of this fumarole ranged within 67 and 290°C between 1999 and 2007. View looking from the northern edge of the acid crater lake captured by Eliécer Duarte on 27 March 2007.



Figure 2.9. Incandescence (960°C) at the north side of the CPC on the night of 19 March 1981. Photograph courtesy of Eduardo Malavassi.



Figure 2.10. View of Poás crater looking north from the lookout point. Note the bluish fumes issued from the CPC, which was the main site of fumarolic degassing between mid 1980 and mid-1986. Photograph taken in 1985 by Jorge Barquero.



Figure 2.12. Poás acid crater lake in June 1988, showing up to 50m-high jets of steam and sediment. Intense activity of the lake by the end of the 1970s, between mid-1987 and early 1990, in the first half of 1994, and 2006–2008 was accompanied by frequent phreatic eruptions. Photograph courtesy of Jorge Enrique Valverde Sanabria.



Figure 2.14. View of the active crater of Poás with a very shallow lake during the rainy season in 1991. Photograph taken by Jorge Barquero.



Figure 2.13. (A) Bottom of the dried lake with "sulphur volcanoes" on 19 April 1989 (Fernández, 1990). (B) One of the "sulphur volcanoes" topped by a chimney-like sulphur structure (photograph taken by Jorge Barquero, April 1989).



Figure 2.15. View of the active crater of Poás with the new lake that started forming in August 1994. Phreatic eruptions had stopped, but strong subaerial degassing from the crater bottom continued until late 1994. Photograph taken on 2 September 1994 by Enrique Valverde Sanabria.



Figure 2.16. Poás acid crater lake was fairly quiescent in May 1995, after a period of phreatic activity and strong fumarolic degassing that ended in late 1994. Photograph courtesy of Jorge Barquero.



Figure 2.17. In late 1995 and early 1996 fumaroles appeared at the western edge of the lake (small fumarole in the background), and fumarolic degassing increased on the north side of the CPC (on the left). Photograph taken by Jorge Barquero.



Figure 2.18. Westward view into the crater of Poás volcano. A prominent water-rich plume rose above the CPC between mid 1999 and mid 2000. Photograph taken from an aircraft in February 2000 by Federico Chavarría Kopper.



Figure 2.19. Between September 2002 and December 2003 a constant emanation of white acidic fumes (HCl evaporation?) formed a fog over the lake that covered all of it at times. This fog was very dense and ~5 m thick in November 2002, as shown in this photograph taken on the 6th by Eliécer Duarte. The persons near the lake edge needed to wear gas masks for in-situ measurement of dissolved gases in the lake water.



Figure 2.21. Northward view of the active crater of Poás volcano from the lookout point (El Mirador). Note the milky turquoise colour of the lake, in contrast to the greenish colour that it had between 2003 and 2004 (cf., Figs. 4.10A and B in Chapter 4). The unusual high volume reached record levels in December 2004-January 2005, flooding an eastern sector of the crater floor and submerging some fumaroles for several weeks. Photograph taken by Milena Berrocal on 29 March 2005.



Figure 2.23. Closer view of the lake from the lookout point. Note the grey colour and the froth of molten sulphur floating on the surface (see also Fig. 2.26). Photograph taken on 10 July 2005 by Rodolfo van der Laat.



Figure 2.22. In April 2005 subaerial fumaroles at the CPC and in the eastern sector of the crater (right side of photograph) showed an increase in activity (see also Fig. 2.21). The colour of the lake was milky turquoise. Photograph taken on 1 April 2005 by Eliécer Duarte.



Figure 2.24. North-westward view of the crater lake. From March 2005 till present the lake has shown an unusual grey colour and moderate evaporation and upwelling. Photograph taken on 25 August 2005 by Wendy Sáenz.



Figure 2.26. Large amounts of sulphur globules of various sizes, shapes, colours, and many with “tails” floated on the lake surface between June and November 2005, i.e. several months before renewal of phreatic activity in March 2006. Grey globules and globules with tails are rarely seen at Poás lake. Photograph taken by the author.



Figure 2.27. Aerial panorama of the acid lake of Poás volcano looking southwest. Vaporous concentric rings indicate the release of a series of large gas bubbles through a subaqueous conduit near the northern edge of the lake. The CPC fumaroles are seen in the upper left. Photograph taken from an aircraft in November 2005 by Federico Chavarría Kopper.



Figure 2.28 and Figure 4.11. View from the lookout point (El Mirador) at the southern rim of the crater, just a few hours after the renewal of phreatic activity, some time on the night of 23 March or the morning of 24 March 2006. Note the grey colour of the lake. This photo captures the moment when dense whitish columns of vapour and gas, issued from the lake and from the Fumarole Norte near the north-eastern edge of the lake, showed a simultaneous increase in vigour. Rock fragments and wet sediments that were ejected from the lake can be seen on the surrounding flat crater floor. Photograph taken on 24 March 2006 around 3:30 p.m. by Geerke Floor.



Figure 2.30. Aerial view of the crater lake looking west, apparently showing a strong upwelling event in the central part of the lake. Photograph taken from an aircraft on 25 March 2006 at 9:35 a.m. by Federico Chavarría Kopper.



Figure 2.31. Aerial view of the active crater of Poás looking north. The mud plume in the central part of the lake points to a strong discharge of fluids and upwelling of suspended dark material. The dark-grey rings and streaks might be sulphur and/or sulphide particles derived from a high-temperature region (Takano, written comm. 2006; Takano et al., 1994). Note the weak degassing at the CPC. Photograph from an aircraft taken on 1 October 2006 at 9:35 a.m. by Federico Chavarría Kopper.

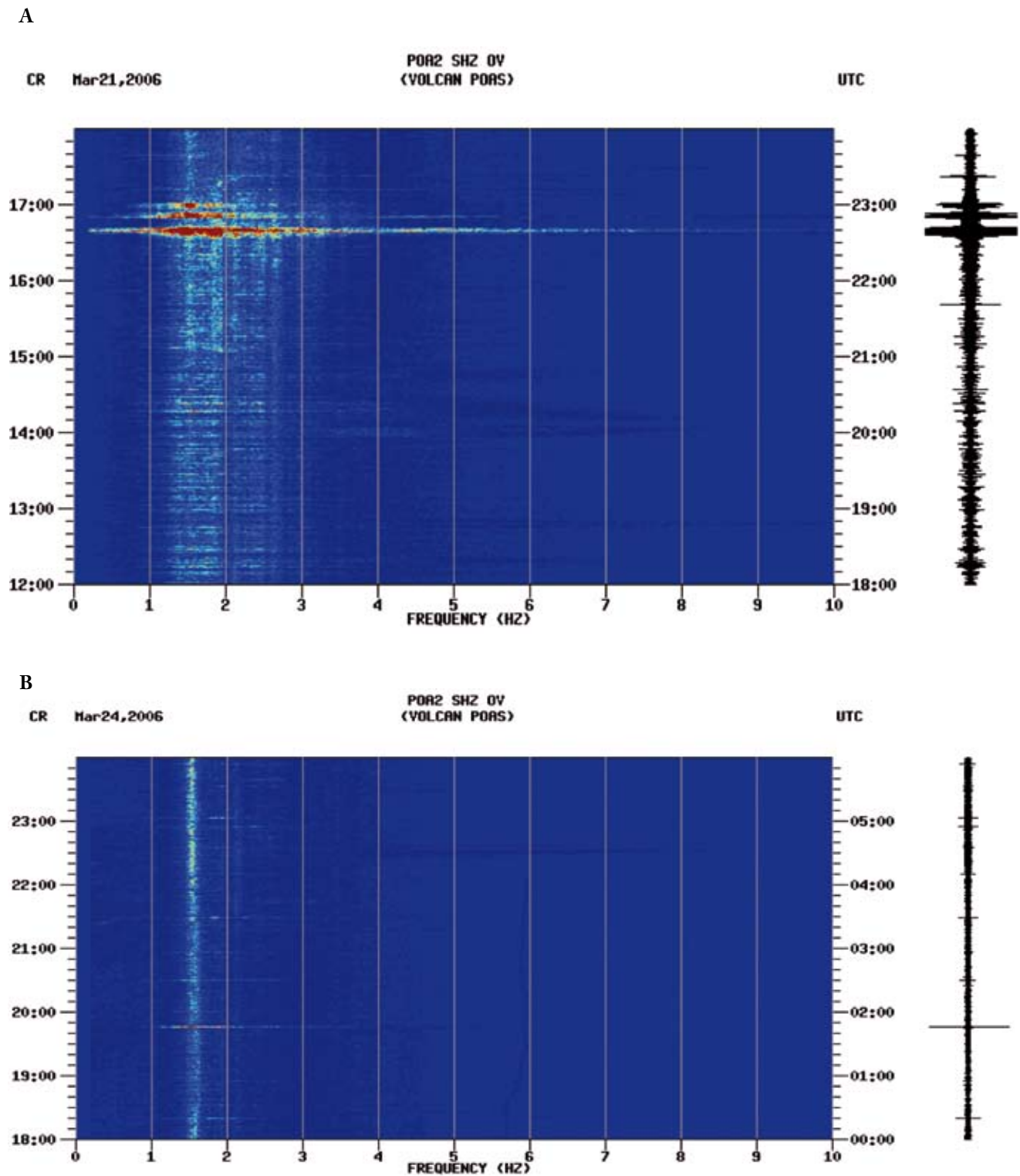


Figure 2.29. (A) Seismic signal of “seal rupture” recorded on 21 March 2006 at 22:39 hrs GMT at the POA2 seismic station; (B) Seismogram of the phreatic eruption of 24 March 2006 at 19:51 hrs local time (01:51 hrs GMT). The dominant frequency (1.5 Hz) corresponds to monochromatic harmonic tremor.



Figure 4.9. Aerial view of the active crater of Poás volcano (~1.3 km diameter along its E-W axis). The vapour-rich plume rising from the CPC, located on the southern shore of the lake, are fumaroles with temperatures usually around 90–100°C. Photograph taken from an aircraft by Federico Chavarria Kopper in mid 1999.



Figure 4.10. (A) The acid crater lake of Poás with a diameter of about 300 m and a temperature of 26°C; view looking north on 13 April 2004. (B) Close up of the lake looking west. Unusual greenish-turquoise colour observed in 2004 is unique in ca. 30 years of continuous monitoring, and corresponds to geochemical changes in the hydrothermal system between late 2003 and early 2005. Notice the weak fumarolic degassing through the CPC and at the eastern terrace. Photographs courtesy of Eliécer Duarte.

References

- Aguilar, E., Peterson T. C., Ramírez, P., Frutos, R., Retana, J. A., Solera M., Soley, J., González, I., Araujo, R. M., Santos, A. R., Valle, V. E., Brunet, M., Aguilar, L., Álvarez, L., Bautista, M., Castañón, C., Herrera, L., Ruano, E., Sinay, J. J., Sánchez, E., Hernández, G. I., Obed, F., Salgado, J. E., Vázquez, J. L., Baca, M., Gutiérrez, M., Centella, C., Espinoza, J., Martínez, D., Olmedo, B., Ojeda, C. E., Núñez, R., Haylock, M., Benavides, H., Mayorga, R. 2005. Changes in precipitation and temperature extremes in Central America and northern South America, 1961-2003. *J. Geophys. Res.* Vol. 110, No. D23, 107, doi:10.1029/2005JD006119.
- Aki, K., Fehler, M., Das, S. 1977. Source mechanism of volcanic tremor: Fluid-driven crack models and their application to the 1963 Kilauea eruption. *J. Volcanol. Geother. Res.* 2: 259-287.
- Alvarado, G. E. 2000. Los volcanes de Costa Rica: Geología, historia y riqueza natural. Segunda Edición. Editorial Universidad Estatal a Distancia, San José, Costa Rica.
- Alvarado, G.E., Kussmaul, S., Chiesa, S., Gillot, P.Y., Appel, H., Wörner, G., Rundle, C. 1992. Resumen cronoestratigráfico de las rocas ígneas de Costa Rica basado en dataciones radiométricas. *J. South Am. Earth Sciences*, Vol. 6 (3): 1-168.
- Allen, A. G., Oppenheimer, C., Ferm, M., Baxter, P. J., Horrocks, L. A., Galle, B., McGonigle, A. J. S., Duffell, H. J. 2002. Primary sulfate aerosol and associated emissions from Masaya Volcano, Nicaragua. *J. Geophys. Res.*, Vol. 107, No. D23, 4682, doi:10.1029/2002JD002120.
- Andres, R.J., Barquero, J., Rose, W.I. 1992. New measurements of SO₂ flux at Poás Volcano, Costa Rica.. 49: *J. Volcanol. Geother. Res.* 49: 175-177.
- Andres, R. J., Rose, W.I. 1995. Remote sensing spectroscopy of volcanic plumes and clouds. In: Monitoring Active Volcanoes: Strategies, Procedures, and Techniques. Edited by B. McGuire, C. Kilburn, and J. Murray, pp. 301-314, UCL Press, London, England.
- Armienta, M.A., De la Cruz-Reyna, S., Macias, J.L. 2000. Chemical characteristics of the crater lakes of Popocatepetl, El Chichon, and Nevado de Toluca volcanoes, Mexico. *J. Volcanol. Geotherm. Res.*, 97: 105-125.
- Badrudin, M. 1994. Kelut volcano monitoring: Hazards, mitigation and changes in water chemistry prior to the 1990 eruption. *Geochem. J.*, 28: 233-241.
- Bandy, M.C. 1938. Mineralogy of three sulphate deposits of Northern Chile. *Amer. Mineral.* 23: 6771-759.
- Barquero, J.A., 1980. Estado de los volcanes. *Bol. Vulcanol.* Ovsicori-UNA, 6: 2-4.
- Barquero, J.A., Malavassi, E. 1981a. Estado de los volcanes, diciembre 1980-febrero 1981. *Bol. Vulcanol.* 10: 6-7.
- Barquero, J.A., Malavassi, E. 1981b. Estado de los volcanes, marzo-junio 1980. *Bol. Vulcanol.* 11: 3-4.
- Barquero, J.A., Malavassi, E. 1982. Estado de los volcanes, julio 1981-marzo 1982. *Bol. Vulcanol.* 12: 1.
- Barquero, J.A., Fernández, E. 1983. Poás volcanic activity reports: Strong continuous gas emission. *SEAN*, 8(10).
- Barquero, J.A., Malavassi, E. 1983. Estado de los volcanes, mayo 1982-abril 1983. *Bol. Vulcanol.* 13: 3.
- Barquero, J.A., Segura, J. 1983. La actividad del Volcán Rincón de la Vieja. *Bol. Vulcanol.* 13. Escuela de Ciencias Geográficas, Universidad Nacional. Heredia, Costa Rica.
- Barquero, J.A., Fernández, E. 1988. Estado de los volcanes, enero-diciembre 1987. *Bol. Vulcanol.* 19: 5.
- Barquero, J.A., Fernández, E. 1990. Erupciones de gases y sus consecuencias en el Volcán Poás, Costa Rica. *Bol. Vulcanol.* 21: 13-18.
- Barquero, J.A. 1998. Volcán Poás, Costa Rica. First edition. San José, Costa Rica. ISBN 9977-12-298-9.
- Barrancos, J., Rosello, J.I., Calvo, D., Padro, E., Melián, G., Hernández, P.A., Pérez, N.M., Millán, M.M., Galle, B. 2008. SO₂ emission from active volcanoes measured simultaneously by COSPEC and mini-DOAS. *Pure appl. geophys.* 165: 115-133.
- Baxter, P., Alfaro, M.R., Moreno, N., Solís, P. 1997. Poás volcano acid precipitation assessment project. Final report No. 2-07-97. Universidad Nacional, Heredia-Costa Rica.
- Bennett, F., Raccichini, S. 1978a. Nuevos aspectos de las erupciones del Volcán Poás. *Rev. Geogr. Am. Centr.* 5-6: 37-54.
- Bennett, F., Raccichini, S. 1978b. Subaqueous sulphur lake in Volcan Poás. *Nature*, 271: 342-344.
- Bennett, F.D. 1979. Fumarolas y pozos subacuáticos de azufre en el volcán Poás, Costa Rica. *Rev. Geogr. Am. Centr.*, 11-12: 125-130.
- Bernard, A., Escobar, C.D., Mazot, A., Gutiérrez, R.E. 2004. The acid volcanic lake of Santa Ana volcano, El Salvador. Geological Society of America, special paper, 375: 121-133.
- Boza, M.A., Mendoza, R. 1981. The national parks of Costa Rica: Industrias Gráficas Alui. S.A.Madrid, Spain.
- Brantley, S.L., Borgia, A., Rowe, G., Fernández, J.F., Reynolds, J.R. 1987. Poás volcano crater lake acts as a condenser for acid metal-rich brine. *Nature*. 330: 470-472.
- Brown, G., Rymer, H., Dowden, J., Kapadia, P., Stevenson, D., Barquero, J., Morales, L.D. 1989. Energy budget analysis for Poás Crater Lake: implications for predicting volcanic activity. *Nature* 339: 370-373.
- Brown, G.C., Rymer, H., Stevenson, D.S. 1991. Volcano monitoring by microgravity and energy budget analysis. *J. Geol. Soc. (London)* 148: 585-593.
- Calderón, T. 2005. Valoración cuantitativa de la corrosividad de materiales metálicos expuestos al ambiente del volcán Poás. Tesis Lic. Ingeniería en Metalurgia. Instituto Tecnológico de Costa Rica. Escuela de Ciencias e Ingeniería de los Materiales. Cartago, Costa Rica.

- Calvert, A. S., Calvert, P. P. 1917. A Year of Costa Rican Natural History. Mac Millan, New York, p. 577 chap. XVII.
- Carr, M.J., Feigenson, M.D., Bennett, E.A. 1990. Incompatible element and isotopic evidence for tectonic control of source mixing and melt extraction along the Central American arc. *Contribs. Mineral. Petrol.* 105:369-380.
- Carr, M.J., Feigenson, M.D., Patino, L.C. Walker, J.A. 2003. Volcanism and geochemistry in Central America: Progress and Problems. In: Inside the subduction factory, Geophysical monograph 138. J. Eiler (ed.). American Geophysical Union. United States of America.
- Carr, M.J., Saginor, I., Alvarado, G.E., Bolge, L.L., Lindsay, F.N., Milidakis, K., Turrin, B.D., Feigenson, M.D. Swisher III, C.C. 2007. Element fluxes from the volcanic front of Nicaragua and Costa Rica. *G³:Geochem. Geophys. Geosyst.* 8 (6), Q06001. doi: 10.1029/2006GC001396. ISSN: 1525-2027.
- Casadevall, T., Rose, W.I., Fuller, W. H., Hart, M.A., Moyers, J.L., Woods, D.C., Chuan, R.L., Friend, J.P. 1984a. Sulfur dioxide from Poás, Arenal, and Colima volcanoes, Costa Rica and Mexico. *J. Geophys. Res.*, 89: 9633-9641.
- Casadevall, T., de la Cruz-Reyna, S., Rose, W.I., Bagley, S., Finnegan, D., Zoller, W.H. 1984b. Crater lake and post-eruption hydrothermal activity, el Chichón volcano, Mexico. *J. Volcanol. Geotherm. Res.*, 97: 1-30.
- Casertano, L., Borgia, A., Cigolini, C. 1983. El volcán Poás, Costa Rica: Cronología y características de la actividad. *Geofis. Int.* 22(3): 215-236.
- Casertano, L., Borgia, A., Cigolini, C., Morales, L., Montero, W., Gómez, M., Fernández, J. 1985. Investigaciones geofísicas y características geoquímicas de las aguas hidrotermales: Volcán Poás, Costa Rica. *Geofis. Int.*, 24 (2): 315-332.
- Casertano, L., Borgia, A., Cigolini, C., Morales, L.D., Gómez, M., Fernández, J.F. 1987. An integrated dynamic model for the volcanic activity at Poás Volcano, Costa Rica. *Bull. Volcanol.* 49: 588-598.
- Castillo, E., Batiza, R., Vanko, D., Malavassi, E., Barquero, J., Fernández, E. 1988. Anomalously young and old hot-spot traces: I. Geology and petrology of Cocos Island. *Bull. Geol. Soc. America* 100, 1400-1414.
- Cheminée, J.L., Delorme, H., Barquero, J., Ávila, G., Malavassi, E., Güendel, F. 1981. Some physical and chemical aspects of the activity of Poás and Arenal volcanoes, *Bol. Vulcanol. No. 11*. Escuela de Ciencias Geográficas, Universidad Nacional. Heredia, Costa Rica.
- Christenson, B.W., Wood, C.P. 1993. The evolution of a volcano-hosted hydrothermal system beneath Ruapehu Crater Lake, New Zealand. *Bull. Volc.* 55, 547 – 565.
- Christenson, B.W. 1994. Convection and stratification in Ruapehu crater lake, New Zealand: implications for lake Nyos-type gas release eruptions. *Geochem. J.*, 28: 185-197.
- Christenson, B.W. 2000. Geochemistry of fluids associated with the 1995-1996 eruption of Mt. Ruapehu, New Zealand: signatures and processes in the magmatic-hydrothermal reservoir. *J. Volcanol. Geotherm. Res.*, 97: 1-30.
- Churakov, S.V., Tkachenko, S.I., Korzhinskii, M.A., Bocharnikov, R.E., Shmulovich, K.I. 2000. Evolution of composition of high temperature fumarolic gases from Kudryavy volcano, Iturup, Kuril Islands: the thermodynamic modeling. *Geoch. Intern.* 38(5): 436-451.
- Craig, H. 1961. Isotopic Variations in Meteoric Waters. *Science.* 133: 1702-1703.
- Day, A.L., Allen, E.T. 1925. The volcanic activity and hot springs of Lassen Peak, Carnegie Institute of Washington Publ. 360.
- Delmelle, P., Bernard, A. 1994. Geochemistry, mineralogy, and chemical modelling of the acid crater lake of Kawah Ijen Volcano, Indonesia. *Geochim. et Cosmochim. Acta.* 58 (11): 2445-2460.
- Delmelle, P. 1995. Geochemical, isotopic and heat budget study of two volcano hosted hydrothermal systems: the acid crater lakes of Kawah Ijen, Indonesia, and Taal, Philippines, volcanoes. *Ph.D. dissertation*. Université Libre de Bruxelles, Belgium.
- Delmelle, P., Bernard, A. 2000. Volcanic Lakes. In: Encyclopedia of Volcanoes. H. Sigurdson, Houghton, B., McNutt, S.R., Rymer, H., Stix, J. (eds.). Academic Press., United States of America.
- Delmelle, P., Bernard, A., Kusakabe, M., Fischer, T.P., Takano, B. 2000. Geochemistry of the magmatic-hydrothermal system of Kawah Ijen volcano, East Java, Indonesia. *J. Volcanol. Geotherm. Res.*, 97: 31-53.
- Delorme, H. 1983. Composition chimique et isotopique de la phase gazeuse de volcans calcoalcalins: America Centrale et Soufriere de la Guadeloupe, Application al la surveillance volcanologique. *PhD dissertation*, University of Paris VII.
- De Mets, C., Gordon, R.G., Argus, D.F., Stein, S. 1990. Current plate motions. *Geophys. J. Int.*, 101: 425-478.
- De Mets, C., 2001. A new estimate for present-day Cocos-Caribbeanplate motion: Implications for slip along the Central American volcanic arc. *Geophys. Res. Letters*, 28: 4043-4046.
- Díaz, J.A., Giese, C., Gentry, R. 2002. Mass spectrometry for in situ volcanic gas monitoring. *Trends in Analytical Chemistry*, vol. 21, No. 8: 498-514.
- Druschel, G.K., Hamers, R.J., Banfield, J.F. 2003. Kinetics and mechanism of polythionate oxidation to sulfate at low pH by O₂ and Fe³⁺. *Geoch. Cosm. Acta.* 67(23): 4457-4469.
- Duarte, E., Fernández, E., Sáenz, W., Malavassi, E., Martínez, M., Barquero, J. 2003a. Wall instability and fumarole migration from 1999 to 2002, Poás Volcano, Costa Rica. *Proceedings of the Eighth Field Workshop on Volcanic Gases Nicaragua and Costa Rica 2003*. IAVCEI-CCVG.
- Duarte, E., Fernández, E., Barquero, J., Martínez, M., Valdés, J., Sáenz, R., Malavassi, E., Sáenz, W., van der Laat, R., Barboza, V. 2003b. Poás Volcano: impacts of recent extraordinary events. *Proceedings of the Eighth Field Workshop on Volcanic Gases Nicaragua and Costa Rica 2003*. IAVCEI-CCVG.
- Duarte, E., Fernández, E., Tassi, F., Vaselli, O., Bergamaschi, F. 2003c. Geochemical study and bathymetric analysis of Poás volcano crater lake, Costa Rica. *Proceedings of the Eighth Field Workshop on Volcanic Gases Nicaragua and Costa Rica 2003*. IAVCEI-CCVG.
- Duarte, E., Fernandez, E., Vaselli, O. 2008. http://www.ovsicori.una.ac.cr/informes_prensa/2008/Inf_CampoPoa10marzo08.pdf

- Eggar, M. 2007. Costa Rica weather and climate. Worldheadquarters. <http://www.worldheadquarters.com/cr/climate/>. Accessed in April 2007.
- Fan, G.W., Beck, S.L., Wallace, T.C. 1993. The seismic source parameters of the 1991 Costa Rica aftershock sequence: evidence for a transcurrent plate boundary. *Jour. Geophys. Res.*, 98: 15,759-15,778.
- Fernández, M. 1990. Actividad del Volcán Poás, Costa Rica: Análisis sísmico durante el período 1980-1989. *Tesis de Licenciatura*, Escuela Centroamericana de Geología, Universidad de Costa Rica, San José, Costa Rica América Central.
- Fernández, E., Barquero, J., Barboza, V., van der Laat, R., Marino, T., Obaldía, F. 1994. Estado de los Volcanes, 1992. *Bol. Volcanol.* 23, 5-11 OVSICORI-UNA: Costa Rica.
- Fernández, E., Duarte, E., Sáenz, W., Malavassi, E., Barboza, V., Martínez, M., Valdés, J. 2003a. Volcanic gas condensates from Poás Volcano 1999-2000. *Book of Abstracts Eighth Field Workshop on Volcanic Gases Nicaragua and Costa Rica 2003*. IAVCEI-CCVG.
- Fernández, E., Duarte, E., Sáenz, W., Malavassi, E., Barboza, V., Martínez, M., Valdés, J. 2003b. Acid rain impact at Poás Volcano during 1999 (effects on vegetation and socio-economic interest areas). *Proceedings of the Eighth Field Workshop on Volcanic Gases Nicaragua and Costa Rica 2003*. IAVCEI-CCVG.
- Ferrucci, F. 1995. In: Mc Guire, W.J., Kilburn, C., Murray, J.B. (Eds.), Seismic monitoring at active volcanoes. UCL, London.
- Fischer, T., Taran, Y. 2004. Report on the Eighth Field Workshop on Volcanic Gases Nicaragua-Costa Rica 2003. IAVCEI Commission on the Chemistry of Volcanic Gases. *Newsletter* No. 18, March 2004.
- Fisher, D.M., Gardner, T.W., Marshall, J.S., Montero, W. 1994. Kinematics Associated With Late Tertiary and Quaternary Deformation in Central Costa Rica: Western Boundary of the Panamá Microplate. *Geology*, 22: 263-266.
- Fischer, T. P., N. C. Sturchio, J. Stix, G. B. Arehart, D. Counce, and S. N. Williams. 1997. The chemical and isotopic composition of fumarolic gases and spring discharges from Galeras Volcano, Colombia. *J. Volcanol. Geotherm. Res.*, 77: 229-253.
- Fournier, N., Williams-Jones, G., Rymer, H. 2001. Sulphur budget at Poás Volcano. *Eos. Trans. AGU*, 82 (47), Fall Meet. Suppl., Abstract V22E-12.
- Fournier, N., Williams-Jones, G., Rymer, H. 2002. Sulphur budget at Poás Volcano, Costa Rica: A multidisciplinary approach. *Book of abstracts of the Volcanic and Magmatic Studies Group Annual Meeting*, 3-4 January 2002, University College London, England.
- Fournier, N. 2003. Shallow volcanic processes at persistently active volcanoes: Evidence from multidisciplinary study at Poás volcano, Costa Rica. *PhD dissertation*, The Open University, Milton Keynes, United Kingdom.
- Fournier, N., Rymer, H., Williams-Jones, G., Brenes, J. 2004. High-resolution gravity survey: Investigation of subsurface structures at Poás Volcano, Costa Rica. *Geophys. Res. Lett.* 31, L15602.
- Francis, P.W., Thorpe, R.S., Brown, G.C. and Glasscock, J. 1980. Pyroclastic sulphur eruption at Poás volcano, Costa Rica. *Nature*, 283: 754-756.
- Fujiwara, Y., Ohsawa, S., Watanuki, K., Takano, B. 1988. Determination of polythionates in an active crater lake by nitrate ion-selective electrode. *Geochem. J.* 22: 249-256.
- Fujiwara, Y. 1989. Dynamic mobility of sulphur compounds in active crater lakes. *Master dissertation*. Dept. of Chemistry, Faculty of Earth Sciences. University of Tokyo, Japan.
- Fulginiti, P., Gioncada, A., Sbrana, A. 1999. Rare earth element (REE) behaviour in the alteration facies of the active magmatic hydrothermal system of Vulcano (Aeolian Islands, Italy). *J. Volcanol. Geother. Res.* 88: 325-342.
- Galle, B. 2002. Preliminary report from studies of volcanic SO₂ emission in Nicaragua and Costa Rica, March 2002, using DOAS spectroscopy. Department of Radio and Space Science, Chalmers University of Technology, S-412 96 Gothenburg, Sweden 2002.
- Galle, B., Oppenheimer, C., Geyer, A., McGonigle, A.J.S., Edmonds, M., Horrocks, L.A., 2003. A miniaturised UV spectrometer for remote sensing of SO₂ fluxes: a new tool for volcano surveillance. *J. Volcanol. Geother. Res.* 119: 241-254.
- García, R., Fernández, E., Duarte, E., Castro, C., Monnin, M., Malavassi, E., Barboza, V. 2003. Radon gas concentration monitoring: anomalies correlation found with volcanic activity after year 2000. *Proceedings of the Eighth Field Workshop on Volcanic Gases Nicaragua and Costa Rica 2003*. IAVCEI-CCVG.
- Gemmell, B. 1987. Geochemistry of metallic trace elements in fumarolic condensates from Nicaraguan and Costa Rican volcanoes. *J. Volcanol. Geother. Res.* 33: 161-181.
- Giggenbach, W.F. 1983. Chemical surveillance of active volcanoes in New Zealand, in Tazieff, H., and Saborux, J.C. (eds.). *Forecasting volcanic events*, Elsevier, Amsterdam: 311-322.
- Giggenbach, W.F. 1974. The chemistry of Crater Lake, Mt Ruapehu (New Zealand) during and after the 1971 active period. *New Zealand J.Sc.* 17: 33-45.
- Giggenbach, W.F., Glover, R.B. 1975. The use of chemical indicators in the surveillance of volcanic activity affecting the crater lake on Mt Ruapehu, New Zealand. *Bull. Volc.* 39(1): 70.
- Giggenbach, W. 1975. A simple method for the collection and analysis of volcanic gas samples. *Bull. Volcanol.*, 39: 132-145.
- Giolito, C. 2000. Geochimica dei fluidi del vulcano Rincón de la Vieja (Costa Rica). *Tesi di Laurea Univerita' degli Studi di Firenze, Italia*.
- Goehring M., Feldmann, U. 1948. Neue Verfahren zur Darstellung von Kaliumpentathionat und von Kaliumhexathionat. *Zeit. anorg. allg. Chem.* 257: 223-226.
- Goehring M. 1952. Die Chemie der Polythionsäuren. *Fortschr. chem. Forsch.*, Bd. 2, S. 444-483.
- Goes, S.D.B., Velasco, A. A., Schwartz, S., Lay, T. 1993. The April 22, 1991, Valle de la Estrella, Costa Rica (Mw=7.7) earthquake and its tectonic implications: a broadband seismic study. *J. Geophys. Res.*, 98: 8127-8142.
- Güendel, F., Pacheco, J. 1992. The 1990-1991 seismic sequence across central Costa Rica: evidence for the existence of a

- micro-plate boundary connecting the Panama deformed belt and the Middle America trench, *Eos Trans., Am. Geophys. Un.*, 73: 399.
- Hilton, D., Ramírez, C., Mora, R., Fischer, T., Fueri, E., Barry, P., Shaw, A., Alvarado, G. 2008. Variations in gas emission rates and gas chemistry at Poás volcano, Costa Rica (2001-2008). IAVCEI 2008 General Assembly Understanding volcanoes. Reykjavik, Iceland.
- Husen, S., Quintero, R., Kissling, E., Hacker, B. 2003. Subduction-zone structure and magmatic processes beneath Costa Rica constrained by local earthquake tomography and petrological modelling, *Geophys. J. International*, 155.
- IUPAC, 1983. In: Young, C.L. (Ed.), Solubility Data Series. Sulfur Dioxide, Chlorine, Fluorine and Chlorine Oxides, vol. 12. Pergamon, Oxford.
- IUPAC, 1988. In: Fogg, P.G.T., Young, C.L. (Eds.), Solubility Data Series. Hydrogen Sulfide, Deuterium Sulfide and Hydrogen Selenide, vol. 32. Pergamon, Oxford.
- Jacob, K.H., Pacheco, J. 1991. The M-7.4 Costa Rica earthquake of April 22, 1991: tectonic setting, teleseismic data, and consequences for seismic hazard assessment, *Earthquake Spectra*, 7- B.
- Kempton, K.A., Rowe, G.L. 2000. Leakage of active crater lake brine through the north flank at Rincón de La Vieja volcano, northwest Costa Rica, and implications for crater collapse. *J. Volcanol. Geotherm. Res.*, 97: 143-160.
- Kikawada, Y., Oosaka, T., Oi, T., Honda, T. 2001. Experimental studies on the mobility of lanthanides accompanying alteration of andesite by acidic hot spring water. *Chemical Geology*, 176: 137-149.
- Kikawada, Y., Uruga, M., Oi, T., Honda, T. 2004. Mobility of lanthanides accompanying the formation of alunite group minerals. *J. Radioanalytical Nuclear Chemistry*, 261: 651-659.
- Krushensky, R.D. and Escalante, G. 1967. Activity of Irazú and Poás volcanoes, Costa Rica, Nov. 1964- Jul. 1965. *Bull. Volcanol.* 31: 75-84.
- Kussmaul, S. 1987. Petrología de las rocas intrusivas neógenas de Costa Rica, *Rev. Geol. Am. Cent.* 7: 83-111.
- Leeman, W.P., Carr, M.J., Morris, J.D. 1994. Boron geochemistry of the Central American Volcanic Arc: constraints on the genesis of subduction-related magmas. *Geochim. Cosmochim. Acta* 58: 149.
- Lewis, A.J., Palmer, M.R., Sturchio, N.C., Kemp, A.J. 1997. The rare earth element geochemistry of acid-sulphate and acid-sulphate-chloride geothermal systems from Yellowstone National Park, Wyoming, USA. *Geochim. Cosmochim. Acta* 61: 695-706.
- Liao, A. 1997. Climatología de las áreas circunvecinas al Volcán Poás. Reporte técnico, Instituto Meteorológico Nacional de Costa Rica (IMN), San José, Costa Rica.
- Locke, C.A., Rymer, H., Cassidy, J. 2003. Magma transfer processes at persistently active volcanoes: insights from gravity observations. *J. Volcanol. Geother. Res.* 127: 73-86.
- MacLaurin, J.S. 1911. Occurrence of pentathionic acid in natural waters. *Proc. Chem. Soc. (London)*, 27: 10-12.
- MacMillan, I., Gans, P.B., Alvarado, G. 2004. Middle Miocene to present plate tectonic history of the southern Central American Volcanic Arc. *Tectonophysics* 392: 325- 348.
- Maekawa, T. 1991. The behaviour of aqueous polythionates originating from volcanic activity at crater lakes. *Master dissertation*. Dept. of Chemistry University of Tokyo, Japan.
- Malavassi, E., Barquero, J. 1982. Excursión al Volcán Poás. Proceedings of the First US-Costa Rica Joint Seminar in Volcanology. *Bol. Vulcanol.* 14: 119-131 OVSICORI-UNA: Heredia-Costa Rica.
- Malavassi, E. 1991. Magma sources and crustal processes at the southern terminus of the Central American Volcanic Arc. *Ph.D. dissertation*. University of California Santa Cruz, California. United States of America.
- Malavassi, E., Barquero, J., Fernández, E., Barboza, V., Van der Laat, R., Marino, T., De Obaldía, F. 1993. Excursión al Volcán Poás. IV Taller Regional sobre Metodologías de Vigilancia Volcánica con Énfasis en Gases Volcánicos. OVSICORI-UNA: Costa Rica, 1-26.
- Marshall, J.S., Idleman, B.d., Gardner, T.W., Fisher, D.M. 2003. Landscape evolution within a retreating volcanic arc, Costa Rica, Central America. *Geology* 31(5): 419-422.
- Martínez, M., Fernández, E., Valdés, J. 1993. Manual for Laboratory and Field Work. 4th Regional Course on Watch Volcanic Methodologies with emphasis in volcanic gases. OVSICORI-LAQAT: Universidad Nacional: Heredia, Costa Rica.
- Martínez, M., Sandoval, L., Valdés, J., Valverde, J., Fernández, E., Duarte, E., Barquero, J., Malavassi, E. 1997. Changes in the Chemical Characteristics of Poás Volcano's Crater Lake between 1993-1996, Costa Rica. *Newsletter IAVCEI Commission on Volcanic Lakes, U.K.* No. 10.
- Martínez, M., Fernández, E., Valdés, J., Barboza, V., van der Laat, R., Duarte, E., Malavassi, E., Sandoval, L., Barquero, J., Marino, T. 2000. Chemical evolution and volcanic activity of the active crater lake of Poás Volcano, Costa Rica, 1993-1997. *J. Volcanol. Geother. Res.* 97: 127-141.
- Martínez, M., van Bergen, M.J., Fernández, E., Malavassi, E., Marino, T., Barquero, J., Valdés, J., Barboza, V., Duarte, E., van der Laat, R., Sáenz, R., Sáenz, W., Chavarría, F. 2003. Two Decades of Crater-Lake Monitoring and Implications for the Degassing History of Poás Volcano. Proceedings IAVCEI-CCVG Eighth Field Workshop on Volcanic Gases Nicaragua-Costa Rica 2003.
- Martínez, M., van Bergen, M. J., Segura, J., Fernández, E., van der Laat, R., Berrocal, M., Malavassi, E., Rodríguez, H., Brenes, J., Valdés, J. 2004a. Volatile fluxes from surface waters at Poás volcano. Proceedings of the 32nd International Geological Congress 2004, Florence-Italy. Abs. Vol, pt. 2, abs. 221-20.
- Martínez, M., van Bergen, M.J., Fernández, E., Bokuichiro, T.; Barboza, V., Miura, Y., Sáenz, W., van der Laat, R., Valdés, J., Malavassi, E., Rodríguez, H., Chavarría, F. 2004b. A long-term record of polythionates in the acid crater-lake of Poás volcano: Changes in the subaqueous input of fumarolic gases. Proceedings of the IAVCEI 2004 Meeting. Crater Lakes scientific session, Pucón-Chile, November 2004.
- Martinelli, B. 1990. Seismic pattern observed at Nevado del Ruiz. In: S.N. Williams (editor), Nevado del Ruiz volcano, Colombia, I. *J. Volcanol. Geotherm. Res.* 41: 297-314.

- Mastin, L.G., Witter, J.B. 2000. The hazards of eruptions through lakes and seawater. *J. Volcanol. Geotherm. Res.* 97: 195-214.
- McNutt, S. R., Harlow, D.H. 1983. Seismicity at Fuego, Pacaya, Izalco and San Cristóbal volcanoes, Central America. *Bull. Volcanol.*, 46: 283-297.
- McNutt, S. R. 1991. Volcanic Tremor. *Encyclopedia of Earth System Science*, Volume 4. Academic Press.
- McNutt, S. R. 1996. Seismic monitoring and eruption forecasting of volcanoes: A review of the state-of-the-art and case histories. In: Scarpa, R., and Tilling, R.I. (eds.): *Monitoring and mitigation of volcano hazards*. Springer-Verlag, Berlin Germany.
- McNutt, S. 2000. Seismic monitoring. In: Sigurdsson, H. (ed.). *Encyclopaedia of Volcanoes*. Academic Press, California, U.S.A.
- Melián, G., Galindo, I., Salazar, J., Hernández, P., Pérez, N., Ramírez, C., Fernández, M., Notsu, K. 2001. Spatial and secular variations of diffuse CO₂ degassing from Poás Volcano, Costa Rica, Central America. *Eos. Trans. AGU*, 82 (47), Fall Meet. Suppl., Abstract V31A-0951.
- Melián, G., Galindo, I., Salazar, J., Pérez, N., Hernández, P., Fernández, M., Ramírez, C., Mora, R., Alvarado, G.E. 2003. Anomalous changes in diffuse hydrogen emission from Poás Volcano, Costa Rica, Central America: A premonitory geochemical signature of volcanic unrest? *Proceedings of the Eighth Field Workshop on Volcanic Gases Nicaragua and Costa Rica 2003*. IAVCEI-CCVG.
- Melián, G., Galindo, I., Pérez, N., Hernández, P., Salazar, J., Fernández, M., Ramírez, C., Mora, R., Alvarado, G.E. 2004. Emisión difusa de hidrógeno en el Volcán Poás, Costa Rica, América Central. En: Soto, G.J. and Alvarado, G.E. (eds.): *La Vulcanología y su entorno geoambiental*. *Rev. Geol. América Central*. 30: 167-177.
- Minakami, T. 1969. Earthquakes originating from volcanoes. *Atti. XVIII, Conv. Ass. Geof. Italy, Napoli*.
- Miura, Y., Kawaoi, A. 2000. Determination of thiosulphate, thiocyanate and polythionates in a mixture by ion-pair chromatography with ultraviolet absorbance detection. *J. Chrom. A.*, 884: 81-87.
- Mora, R., Ramírez, C. 2004. Physical changes in the hyperacidic hot lake of Poás volcano (2002-2004, Costa Rica). Abstracts of the Sixth Meeting of the IAVCEI Committee on Volcanic Lakes, Caviabue, Argentina. November 2004.
- Mora, R., Ramírez, C., Fernández, M. 2004. La actividad de los volcanes de la Cordillera Central, 1998-2002, Costa Rica. En: Soto, G.J. and Alvarado, G.E. (eds.): *La Vulcanología y su entorno geoambiental*. Número especial, *Rev. Geol. América Central*, 30: 189-197.
- Morris, J., Leeman, W.P., Tera, F. 1990. The subducted component in island arc lavas: constraints from Be isotopes and B-Be systematics. *Nature* 344, 31-36.
- Neshyba, S., Fernández, W., Andrade, J.D. 1988. Temperature profiles from Poás crater lake, *Eos* 69 (19), 588-589.
- Nicholson, R.A., Howells, M.F., Roberts, P.D., Baxter, P.J. 1992. Gas geochemistry studies at Poás Volcano, Costa Rica, November 1991. British Geological Survey. Overseas Geology Series. Technical report No. WC/92/10.
- Nicholson, R.A., Howells, M.F., Baxter, P.J., Clegg, S.L., Barquero, J. 1993. Gas geochemistry studies at Poás Volcano, Costa Rica, March 1992-January 1993. British Geological Survey. Overseas Geology Series. Technical report No. WC/93/21.
- Ohba, T., Hirabayashi, J., Nogami, K. 1994. Water, heat and chloride budgets of the crater lake, Yugama at Kusatsu-Shirane volcano, Japan. *Geochem. J.* 28: 217-231.
- Ohba, T., Hirabayashi, J., Nogami, K. 2000. D/H and ¹⁸O/¹⁶O ratio of water in the crater lake at Kusatsu-Shirane volcano, Japan. *J. Volcanol. Geotherm. Res.*, 97: 329-346.
- Ohba, T., Hirabayashi, J., Nogami, K. 2008. Temporal changes in the chemistry of lake water within Yugama Crater, Kusatsu-Shirane Volcano, Japan: Implications for the evolution of the magmatic hydrothermal system. *J. Volcanol. Geotherm. Res.*, in press.
- Ohsawa, S. 1992. Geochemical studies on the behaviour of intermediate sulphur compounds in aqueous solutions- Application to volcanology. *Ph.D. Dissertation*. The University of Tokyo, Japan. 29-36.
- Okita, T. 1971. Detection of SO₂ and NO₂ gas in the atmosphere by Barringer spectrometer. Rep. 8/7, JASCO, Tokyo, Japan.
- Oppenheimer, C., Stevenson, D. 1989. Liquid sulfur lakes at Poás Volcano. *Nature*, 342: 790-793.
- OVSICORI. 1995. Actividad eruptiva del volcán Rincón de la Vieja durante los días 6 y 13 de Noviembre, 1995. Open Report, OVSICORI-UNA. http://www.ovsicori.una.ac.cr/vulcanologia/volcanes/rincon_vieja.htm. Accessed in October 2006.
- OVSICORI. 1998. Actividad eruptiva del volcán Rincón de la Vieja en Setiembre de 1998. Open Report, OVSICORI-UNA. http://www.ovsicori.una.ac.cr/informes_prensa/1998/oldeprensaErupcionenelVolRincondeLaVieja9setiembre1998.pdf. Accessed in April 2008.
- OVSICORI. 2006a. Colada de azufre fundido de 160 m de largo se produjo en el Volcán Poás 2 de junio del 2006. Open Report, OVSICORI-UNA. http://www.ovsicori.una.ac.cr/informes_prensa/2006/coladaazufre02junio2006.pdf. Accessed in November 2006.
- OVSICORI. 2006b. Poás volcano activity during 2006. Special report to the Global Volcanism Program. Smithsonian Institution. http://www.ovsicori.una.ac.cr/informes_prensa/2006/indice_2006.htm
- OVSICORI. 2006c. Experto en medición remota de SO₂ en plumas volcánicas de la Universidad de El Salvador comparte experiencia con vulcanólogos del OVSICORI-UNA, Costa Rica. 25 de Abril de 2006. http://www.ovsicori.una.ac.cr/informes_prensa/2006/Experto_en_medicion_de_SO2_nos_visita25abril2006.pdf
- OVSICORI. 2008a. Small phreatic eruption on January 13, 2008: Poás Volcano, Costa Rica. Open Report OVSICORI-UNA. http://www.ovsicori.una.ac.cr/informes_prensa/2008/FieldInfPoa180108Eng.pdf. Accessed in January 2008.
- OVSICORI. 2008b. Erupción freática se produjo por la tarde del Lunes 28 de enero 2008. Open Report OVSICORI-UNA. http://www.ovsicori.una.ac.cr/informes_prensa/2008/InfCPoa29108.pdf. Accessed in January 2008.

- Pasternack G.B., Varekamp J.C. 1994. The geochemistry of the Keli Mutu crater lakes, Flores, Indonesia. *Geoch. J.* 28: 243–262.
- Pasternack, G., Varekamp, J. 1997. Volcanic lake systematics I. Physical constraints. *Bull. Volcanol.* 58: 534–535.
- Peacock, S.M., van Keken, P., Holloway, S., Hacker, B., Geoffrey, A., Ferguson, R.L. 2005. Thermal structure of the Costa Rica – Nicaragua subduction zone. *Physics of the Earth and Planetary Interiors* 149: 187–200.
- Pichler, H., Weyl, R. 1975. Magmatism and crustal evolution in Costa Rica (Central America), *Internat. J. Earth Sciences*, 64: 457–475.
- Ponce, D.A., Case, J.E. 1987. Geophysical interpretation of Costa Rica, in: Mineral Resources Assessment of the Republic of Costa Rica, U.S. Geol. Surv., *Misc. Invest.* I-1865: 8–17.
- Prosser, J.T. 1983. The geology of Poás Volcano, Costa Rica. *Master dissertation*. Dartmouth College, Hanover, New Hampshire.
- Prosser, J.T. 1985. Geology and medium-term temporal magmatic variation found at the summit region of Poás volcano, Costa Rica. *Bol. Volcanol.*, 15: 21–39.
- Prosser, J.T., Carr, M.J. 1987. Poás volcano, Costa Rica: Geology of the summit region and spatial and temporal variations among the most recent lavas. *J. Volcanol. Geotherm. Res.* 33: 131–146.
- Protti, M., Schwartz, S. 1994. Mechanics of back arc deformation in Costa Rica: Evidence from an aftershock study of the April 22, 1991, Valle de la Estrella, Costa Rica, earthquake (M_w=7.7). *Tectonics*, Vol. 13, No. 5: 1093–1107.
- Protti, M., McNally, K., Pacheco, J., González, V., Montero, C., Segura, J., Brenes, J., Barboza, V., Malavassi, E., Güendel, F., Simila, G., Rojas, D., Velasco, A., Mata, A., Schillinger, W. 1995. The March 25, 1990 (M_w = 7.0, M_L = 6.8), earthquake at the entrance of the Nicoya Gulf, Costa Rica: Its prior activity, foreshocks, aftershocks, and triggered seismicity. *J. Geophys. Res.*, 100 (20): 345–358.
- Protti, M., Güendel, F., Malavassi, E. 2001. Evaluación del Potencial Sísmico de la Península de Nicoya. Editorial Fundación UNA, Universidad Nacional. Primera edición: Heredia, Costa Rica.
- Raccichini, S., Bennett, F.D. 1977. Nuevos aspectos de las erupciones del volcán Poás. *Rev. Geogr. Am. Centr.* 5–6: 37–53.
- Reed, M.H., 1982. Calculations of multicomponent chemical equilibria and reaction processes in systems involving minerals, gases and an aqueous phase. *Geochim. Cosmochim. Acta* 46: 513–528.
- Reed, M.H., Spycher, N.F. 1984. Calculation of pH and mineral equilibria in hydrothermal waters with application to geothermometry and studies of boiling and dilution. *Geochim. Cosmochim. Acta* 48: 1479–1492.
- Rouwet, D., Taran, Y., Inguaggiato, S., Varley, N., Santiago, J.A. 2008. Hydrochemical dynamics of the lake spring system in the crater of El Chichón volcano (Chiapas, Mexico). *J. Volcanol. Geotherm. Res.*, doi:10.1016/j.jvolgeores.2008.06.026.
- Rowe, G.L., Brantley, S.L., Fernández, J.F., Barquero, J., Borgia, A. 1989. Observaciones preliminares del sistema hidrotermal del Volcán Poás, Costa Rica. *Bol. Volcanol. OVSICORI-UNA*. 20: 23–31.
- Rowe, G.L. 1991. The acid crater lake system of Poás Volcano, Costa Rica: Geochemistry, hydrology and physical characteristics. *Ph.D. dissertation*. The Pennsylvania State University, Pennsylvania.
- Rowe, G.L., Brantley, S.L., Fernández, M., Fernández, J.F., Borgia, A., Barquero, J. 1992a. Fluid volcano interaction in an active stratovolcano: the crater lake system of Poás Volcano, Costa Rica. *J. Volcanol. Geother. Res.*, 49: 23–51.
- Rowe, G.L., Ohsawa, S., Takano, B., Brantley, S.L., Fernández, J.F., Barquero, J. 1992b. Using Crater Lake chemistry to predict volcanic activity at Poás Volcano, Costa Rica. *Bull. Volcanol.*, 54: 494–503.
- Rowe, G.L. 1994. Oxygen, hydrogen, and sulfur isotope systematics of the crater lake system of Poás Volcano, Costa Rica. *Geochim. Journal* 28: 263–287.
- Rowe, G.L., Brantley, S.L., Fernández, J.F., Borgia, A. 1995. The chemical and hydrologic structure of Poás Volcano, Costa Rica. *J. Volcanol. Geother. Res.*, 64: 233–267.
- Rymer, H., Brown, G.C. 1987. Causes of microgravity changes at Poás volcano, Costa Rica: an active but non erupting system. *Bull. Volcanol.* 49: 389–398.
- Rymer, H., Brown, G.C. 1989. Gravity changes as a precursor to volcanic eruption at Poás volcano, Costa Rica. *Nature*, 342: 902–905.
- Rymer, H., Cassidy, J., Locke, C., Barboza, V., Barquero, J., Brenes, J., van der Laat, R. 2000. Geophysical studies of the recent 15-year eruptive cycle at Poás Volcano, Costa Rica. *J. Volcanol. Geother. Res.* 97: 425–442.
- Rymer, H., Fournier, N., Williams-Jones, G. 2004. Persistent activity and its effect on microgravity variations at Poás volcano, Costa Rica. Abstracts of the 2004 IAVCEI Meeting, Pucón Chile, November 2004.
- Rymer, H., Locke, C., Brenes, J., Williams-Jones, G. 2005. Magma plumbing processes for persistent activity at Poás volcano, Costa Rica. *Geophys. Res. Lett.* 32, LXXXIX, doi: 10.1029/2004GL022284.
- Salguero, M. 1980. Volcanes de Costa Rica. Tercera edición. Imprenta Nacional, San José. Costa Rica.
- Sandoval, L. 1996. Efecto de las emisiones volcánicas sobre la vegetación del Parque Nacional Volcán Poás. *Tesis de licenciatura*, Escuela de Biología Universidad Nacional. Heredia Costa Rica.
- Sanford, W.E., Konikow, L.F., Rowe, G.L., Brantley, S. 1995. Groundwater transport of crater lake brine at Poás volcano, Costa Rica. *J. Volcanol. Geotherm. Res.* 64: 269–293.
- Shriver, D.F., Atkins, P.W. 1999. The nitrogen and oxygen groups. In: *Inorganic Chemistry*. Third edition. Oxford University Press, UK.
- Sigurdsson, H. 1977. Chemistry of the crater lake during the 1971–72 Soufrière eruption. *J. Volcanol. Geother. Res.* 2: 165–186.
- Silver, E.A., Reed, D.L., Tagudin, J.E., Heil, D.J. 1990. Implications of the north and south Panama thrust belt for the origin of the Panama orocline. *Tectonics*, 9: 261–281.
- Smithsonian Institution, 1989. *Bull. Global Volcanism Network*, Poás Volcano 14 (4), 7–10.

- Smithsonian Institution, 1990. *Bull. Global Volcanism Network*, Poás Volcano 15 (4), 6-9.
- Smithsonian Institution, 1991. *Bull. Global Volcanism Network*, Poás Volcano 16 (1-11).
- Smithsonian Institution, 1992. *Bull. Global Volcanism Network*, Poás Volcano 17 (1-12).
- Smithsonian Institution, 1993. *Bull. Global Volcanism Network*, Poás Volcano 18 (2), 3.
- Smithsonian Institution, 1994a. *Bull. Global Volcanism Network*, Poás Volcano 19 (5), 12-13.
- Smithsonian Institution, 1994b. *Bull. Global Volcanism Network*, Poás Volcano 19 (4), 4.
- Smithsonian Institution, 1996a. *Bull. Global Volcanism Network*, Poás Volcano 21 (3), 5.
- Smithsonian Institution, 1996b. *Bull. Global Volcanism Network*, Poás Volcano 21 (5), 10.
- Soto, G. J., Alvarado, G.E., Goold, S. 2003. Erupciones <3800 a.P. del volcán Rincón de la Vieja, Costa Rica. *Rev. Geológica América Central, Costa Rica*, 29: 67-86.
- Sriwana, T., van Bergen, M.J., Varekamp, J.C., Sumarti, S., Takano, B., van Os, B.J.H., Leng, M.J. 2000. Geochemistry of the acid Kawah Putih lake, Patuha Volcano, West Java, Indonesia. *J. Volcanol. Geother. Res.* 97: 77-104.
- Stamm H., Goehring, M., Feldmann, U. 1942. Zur Kenntnis der Polythionsäuren und ihrer Bildung-Neue Verfahren zur Darstellung von Kaliumtrithionat und von Kaliumtetrathionat. *Zeit. Anorg. Allgem. Chem.* 250: 226-228.
- Steudel, R., Holdt, G. 1986. Ion-Pair Chromatographic Separation of Polythionates $S_nO_6^{2-}$ with up to Thirteen Sulfur Atoms. *J. Chromatogr.* 361: 379-384.
- Stimac, J.A., Goff, F., Counce, D., Larocque, A.C.L., Hilton, D.R., Morgenstern, U. 2003. The crater lake and hydrothermal system of Mount Pinatubo, Philippines: evolution in the decade after eruption. *Bull. Volcanol.* 66 (2): 149-167.
- Stoiber, R.E., Rose, W.I. 1970. The geochemistry of Central American volcanic gas condensates, *Geol. Soc. Amer. Bull.*, 81: 2891-2912.
- Stoiber, R. E., Malinconico, L.L., Williams, S. N. 1983. Use of the correlation spectrometer at volcanoes. In: Tazieff, H., Sabroux, J.C. (eds). *Forecasting Volcanic Events*. Elsevier, New York, 1983.
- Stoiber, R. E., Williams, S. N., Huebert, B. J. 1986. Annual contribution of sulfur dioxide to the atmosphere by volcanoes. *J. Volcanol. Geotherm. Res.* 33: 1-8.
- Strahler, A. 1974. *Geografía Física*. Editorial Omega, S.A. Barcelona, España.
- Sugimori, K., Takano, B., Matsuo, M., Suzuki, K., Fazlullin, S.M. 1995. Activity of sulphur-oxidizing bacteria in the acidic crater lake of Maly Semiachik Volcano, Kamchatka. In: Kharaka, Y.K., Chudaev, O.V. (eds.). *Proceedings of the 8th. International Symposium on Water-Rock Interaction*, Vladivostik, Russia. Balkema, Rotterdam.
- Sugimori, K., Martínez, M., Malavassi, E., Fernández, E., Duarte, E., Segura, J., Sáenz, W., van Bergen, M.J., Valdés, J. 2001. Microorganisms living in the acid lake of Poás volcano. Book of Abstracts of the 54th. Annual Meeting of the Balneological Society of Japan, Shirakama, Wakayama, 22-25 August 2001.
- Sumarti, S. 1998. Volcanogenic pollutants in hyperacid river water discharged from Ijen crater lake, East Java, Indonesia: Concentrations, seasonal variations, and possible environmental consequences. *Thesis* Utrecht University, The Netherlands, unpublished.
- Sun, S.S., McDonough, W.F. 1989. Chemical and isotopic systematics of oceanic basalts; implications for mantle composition and processes. In: *Magmatism in the ocean basins*. Saunders, A.D. and Norry, M.J. (Editors), Geological Society of London, London.
- Symonds, R.B., Rose, W.I., Gerlach, T.M., Briggs, P.H., Harmon, R.S. 1990. Evaluation of gases, condensates, and SO_2 emissions from Augustine volcano, Alaska: the degassing of a Cl-rich volcanic system. *Bull. Volcan.* 52: 355-374.
- Symonds, R.B., Rose, W.I., Bluth, G.J.S., Gerlach, T.M. 1994. Volcanic-gas studies: methods, results, and applications. *Rev. Mineral.* 30: 1-66.
- Symonds, R.B., Gerlach, T.M., Reed, M.H. 2001. Magmatic gas scrubbing: implications for volcano monitoring. *J. Volcanol. Geotherm. Res.*, 108, 303-341.
- Takano, B. 1987. Correlation of volcanic activity with sulfur oxyanion speciation in a crater lake. *Science* 235: 1545-1712.
- Takano, B., Watanuki, K. 1988. Quenching and liquid chromatography determination of polythionates in natural water. *Talanta* 35: 847-854.
- Takano, B., Watanuki, K. 1990. Monitoring of volcanic eruptions at Yugama Crater Lake by aqueous sulfur oxyanions. *J. Volcanol. Geotherm. Res.*, 40: 71-87.
- Takano, B., Saitoh, H., Takano, E. 1994a. Geochemical implications of subaqueous molten sulfur at Yugama Crater Lake, Kusatsu-Shirane volcano, Japan. *Geochem. J.* 28: 199-216.
- Takano, B., Ohsawa, S., Glover, R. B. 1994b. Surveillance of Ruapehu crater lake, New Zealand, by aqueous polythionates. *J. Volcanol. Geotherm. Res.* 60: 29-57.
- Takano, B., Matsuo, M., Suzuki, K. 1995. Bathymetry and chemical investigation of crater lake at Maly Semiachik Volcano, Kamchatka. In: Kharaka, Y.K., Chudaev, O.V. (eds.), *Proceedings of the 8th. International Symposium on Water-Rock Interaction*, Vladivostik, Russia. Balkema, Rotterdam.
- Takano, B., Koshida, M., Fujiwara, Y., Sugimori, K., Takayanagi, S. 1997. Influence of sulfur-oxidizing bacteria on the budget of sulfate in Yugama crater lake, Kusatsu-Shirane volcano, Japan. *Biogeochemistry*. 38(3): 227-253.
- Takano, B., Maekawa, T., Zheng, Q. 2001. Kinetic study on aqueous polythionates and its application to active crater lake systems. In: Cidu (ed.), *Proceedings of the 10th. International Symposium on Water-Rock Interaction*. Swets and Zeitlinger, Lisse.
- Takano, B., Suzuki, K., Sugimori, K., Ohba, T., Fazlullin, S.M., Bernard, A., Sumarti, S., Sukhyar, R., Hirabayashi, M. 2004. Bathymetric and geochemical investigation of Kawah Ijen Crater Lake, East Java, Indonesia. *J. Volc. Geoth. Res.* 135: 299-329.

- Takano, B., Kuno, A., Ohsawa, S., Kawakami, H. 2008. Aqueous sulfur speciation possibly linked to sublimic volcanic gas-water interaction during a quiescent period at Yugama crater lake, Kusatsu-Shirane volcano, Central Japan. *J. Volcanol. Geotherm. Res.* (in press).
- Taran, Y., Fischer, T.P., Pokrovsky, B., Sano, Y., Armienta, M.A., Macías, J.L. 1998. Geochemistry of the volcano hydrothermal system of El Chichón volcano, Chiapas, Mexico. *Bull. Volcanol.* 59: 436-449.
- Tassi, F., Bergamaschi, F., Vaselli, O., Fernández, E., Duarte, E. 2003. Crater lakes of Costa Rica: A geochemical survey. Proceedings of the 8th Field Gas Workshop Nicaragua and Costa Rica 26 March-1 April 2003. The Commission on the Chemistry of Volcanic Gases, CCVG-IAVCEI.
- Tassi, F., Vaselli, O., Capaccioni, B., Giolito, C., Duarte, E., Fernández, E., Minissale, A., Magro, G. 2005. The hydrothermal-volcanic system of Rincón de la Vieja Volcano (Costa Rica): a combined (inorganic and organic) geochemical approach to understanding the origin of the fluid discharges and its possible application to volcanic surveillance. *J. Volcanol. Geother. Res.* 148: 315-333.
- Tassi, F., Vaselli, O., Duarte, E., Fernández, E., Martínez, M., Sáenz, W., Delgado, A., Bergamaschi, F. 2006. Crater Lakes of Costa Rica: A Geochemical Survey. Proceedings of the Meeting Cities on volcanoes 4, Quito Ecuador. January 2006.
- Thomas, P. 1990. Reiseführer Costa Rica. Tucan Verlag. München, Germany.
- Thorpe, R.W., Locke, C.A. Brown, G.C., Francis, P.W., Randal, M. 1981. Magma chamber below Poás volcano, Costa Rica. *J. Geol. Soc. London*, 138: 367-373.
- Togano, T., Ochiai, M. 1987. Quantitative analysis of sulfide ions in hot spring waters. Kagaku to Kyoiku. *Chem. Educ.* 35: 346-347.
- Varekamp, J.C., Ouimette, A.P., Herman, S.W., Bermúdez, A., Delpino, D. 2001. Hydrothermal element fluxes from Copahue, Argentina: A "beehive" volcano in turmoil. *Geology*, 29(11): 1059-1062.
- Vargas, C.A. 1979. Antología: El volcán Poás. Universidad Estatal a Distancia, San José, Costa Rica.
- Vaselli, O., Tassi, F., Minissale, A., Montegrossi, G., Duarte, E., Fernández, E., Bergamaschi, F. 2003. Fumarole migration and fluid geochemistry at Poás Volcano (Costa Rica) from 1998 to 2001. In: Oppenheimer, C., Pyle, D.M., Barclay, J. (eds.) Volcanic Degassing. The Geological Society of London special publications. 213: 247-262.
- Vaselli, O., Tassi, F., Duarte, E., Fernández, E., Minissale, A., Bergamaschi, F., Montegrossi, G. 2004. Geochemical insights on the fumaroles of Poás Volcano (Costa Rica) from 1998 to 2004: Chemical variations, migration and volcanic implications. Proceedings of the IAVCEI General Assembly 2004, Pucón, Chile.
- Venzke, E., Wunderman, R.W., McClelland, L., Simkin, T., Luhr, J.F., Siebert, L., Mayberry, G. (eds.) (2002-). Global Volcanism, 1968 to the present. Smithsonian Institution, Global Volcanism Program Digital Information Series, GVP-4 (<http://www.volcano.si.edu/reports/>). Accessed in February 2005.
- Vogel, T. A., Patino, L.C., Alvarado, G.E., Gans, P.B. 2004. Silicic ignimbrites within the Costa Rican volcanic front: evidence for the formation of continental crust. *Earth and Planetary Science Letters* 226 (2004) 149- 159.
- Weiss, J. 1986. Dionex: Handbook of ion chromatography. Dionex Corp.: California, U.S.A.
- Werner, C., Hurst, T., Scott, B., Sherburn, S., Christenson, B.W., Britten, K., Cole-Baker, J., Mullan, B. 2008. Variability of passive gas emissions, seismicity, and deformation during crater lake growth at White Island volcano, New Zealand, 2002-2006. *J. Geophys. Res.* 113, B01204. doi: 10.1029/2007JB005094.
- Williams-Jones, G., Stix, J., Heiligmann, M., Charland, A., Sherwood Lollar, B., Garzón V., G., Barquero, J., Fernández, E. 2000. A model of diffuse degassing at three subduction-related volcanoes. *Bull. Volcanol.*, 62: 130-142.
- Wilson, S.H. 1941. Natural occurrence of polythionic acids. *Nature* 148: 502-503.
- Wilson, S.H. 1953. The elemental investigation of the hot springs of the New Zealand thermal region. South Pacific Sci. Congress, New Zealand. 2: 449-469.
- Wilson, S.H. 1959. Physical and chemical investigations (White Island) 1939-1955. *New Zealand Dept. Sci. Indus. Res. Bull.* 127: 32-50.
- Wood, S.A. 2006. Rare earth element systematics of acidic geothermal waters from the Taupo Volcanic Zone, New Zealand. *J. Geoch. Exploration*, 89: 424-427.
- Xia, J., Rumpf, B., Maurer, G. 1999. The solubility of sulfur dioxide in aqueous solutions of sodium chloride and ammonium chloride in the temperature range from 313 to 393 K at pressures up to 3.7 MPa: experimental results and comparisons with correlations. *Fluid phase equilibria*. 165: 99-119.
- Xia, J., Pérez, A., Rumpf, B., Maurer, G. 2000. Solubility of hydrogen sulfide in aqueous solutions of single strong electrolytes sodium nitrate, ammonium nitrate, and sodium hydroxide at temperatures from 313 to 393 K and total pressures up to 10 MPa. *Fluid phase equilibria*. 167: 263-284.
- Zimmer, M. M., Fischer, T. P., Hilton, D.R., Alvarado, G.E., Sharp, Z.D., Walker, J.A. 2004. Nitrogen systematics and gas fluxes of subduction zones: Insights from Costa Rica arc volatiles. *Geochem. Geophys. Geosyst.* 5, Q05J11. doi: 10.1029/2003GC000651.

Summary

This thesis describes the evolution of Laguna Caliente, an acid crater lake at the summit of Poás, a persistently active volcano in central Costa Rica. The appearance, volume, temperature and chemical composition of the lake have continuously changed over the entire known period of its existence. Occasionally, the lake completely disappeared, which occurred for the last time in 1953-1954 and 1989-1994. These intervals were accompanied by eruptions, which at Poás are usually restricted to expulsion of steam, ash and lake bottom sediments. Such eruptions may also go through the lake, as was the case in 1968-1980, 1987-1994, and most recently in 2006-2008. The latest eruption of fresh magma occurred in 1953-1954, a phenomenon that is rare for this volcano. The periods of eruptive activity alternate with relatively quiet intervals. They go together with changes in the altitude of the volcanic plume and the amount of gases emitted into the atmosphere. In addition, gas and particles are also emitted almost continuously from vents in the crater area, which vary in vigour and location with time. Because the gas contains large amounts of sulphur and chlorine, and is transported through the air, there are also variations in the environmental effects produced by acid rain, gases, and particles around the volcano. Hence, the intermittently strong activity not only pose direct dangers in the crater area at the summit, but may also be harmful to the health of residents and livestock, and may impact agriculture, infrastructure and ecosystems on the flanks of Poás.

In order to better predict the nature and timing of future eruptive events, it is necessary to know the particular processes that operate in the interior of the volcano and that are responsible for its activity at the surface. The accompanying movement of fluid materials and heat effects are rapidly transmitted upward by rising vapour and circulating groundwater. The crater lake intercepts these signals and transforms them into measurable chemical and physical properties. The results of this study show that Laguna Caliente provides a detailed record of ongoing processes at depth. The lake-water temperature and a large number of dissolved chemicals show systematic but not equal variations over longer and shorter periods of time, which makes their interpretation a challenging exercise.

A comprehensive inventory of new and existing data is presented, covering the history of the lake between 1978 and 2008. Based on field observations and virtually continuous monthly sampling of the lake water, the following five periods were distinguished, reflecting major changes in the state of activity of the volcano:

Stage I (~1972 – August 1980). The lake was a highly acid (pH below 0), hot (average 49°C) grey brine, voluminous (about $1.5 \times 10^6 \text{ m}^3$) and carrying a high concentration of total dissolved solutes (average TDS $1.5 \times 10^5 \text{ mg/kg}$). Moderate fumarolic discharge and sporadic small geyser-like phreatic explosions took place within the lake.

Stage II (September 1980 – April 1986). This period was marked by relative quiescence in the lake compared to Stage I. No phreatic activity occurred, but there was intense emission of high-temperature gas (up to 1020°C) from fumarole vents on the southern border of the lake, i.e. at the composite pyroclastic cone (CPC). Nonetheless, the lake maintained a stable volume (about $1.4 \times 10^6 \text{ m}^3$), while its temperature, pH, and TDS fluctuated around 49°C, 0.16, and $8.7 \times 10^4 \text{ mg/kg}$, respectively.

Stage III (May 1986 – August 1995). This period is marked by vigorous activity in the lake and intense phreatic eruptions. The maximum volume was only $\sim 93 \times 10^3 \text{ m}^3$ (if the transitions to stages II and IV are ignored), and the lake dried out on several occasions, leaving mud pools only. The temperature averaged around 66°C and peaked to boiling point values of $\sim 94^\circ\text{C}$, while average pH values of -0.2 point to extremely acid conditions. TDS averaged around $1.6 \times 10^5 \text{ mg/kg}$.

Stage IV (September 1995 – February 2005). This stage represents the most quiescent period of the last three decades, although numerous fluctuations in the properties of the lake were observed. Average temperature and TDS values were fairly low, about 33°C and $2 \times 10^4 \text{ mg/kg}$, respectively, and the pH was generally highest, on average ~ 1 . The lake reached the highest levels ever in 1997 ($\sim 1.7 \times 10^6 \text{ m}^3$) and in 2004-2005 ($> 1.9 \times 10^6 \text{ m}^3$). During this period, a new field of vigorous subaerial fumaroles and minor seeps of thermal water developed at the eastern terrace in the crater.

Stage V (March 2005 – Present). The main characteristic of this stage is the return of high-activity conditions and phreatic eruptions, following a sharp rise in temperature up to $\sim 58^\circ\text{C}$, a steady drop in pH down to values of ~ 0 , and a 10-fold increase in TDS to $> 1.5 \times 10^5 \text{ mg/kg}$ in September 2007. The input of heat and volatiles through the lake continues to be significant, so that the lake level decreases rapidly, despite the input of heavy rainfall. Recurrence of phreatic explosions may occur anytime in the near future, given the similarity in conditions to those observed after the transition between Stages II and III.

The subdivision into five stages is seen in the concentration trends of both the major anions (S, Cl, F) and the major cations (rock-forming elements), although these element groups have a different origin: the anions are mainly derived from degassing magma and the cations from the interaction between water and rock. Their concentrations in the lake water thus reflect different processes in the interior of the volcano.

Interpretations of the anion patterns indicate that variable concentrations and relative proportions are not only caused by changes in the release from a magma body. Usually, their output is also modulated by the overlying hydrothermal system. Free influx of hot magmatic gas into the lake only occurred in

the early years of Stage III, prior to its desiccation. In contrast, strongest deviations from primary magmatic gas signatures (e.g. low S/Cl ratios) and lowest concentrations point to a noticeable interference of the hydrothermal system during the quiet Stage IV.

Concentrations of the major cations generally follow the anion trends, except for those taken up by minerals that precipitate in the lake. Cation proportions do not remain constant depending on the degree of rock dissolution as well. Almost complete rock dissolution explains the cation budget during Stage III, while a relatively strong divergence was observed during Stage IV. This deviation resulted from the uptake of elements by alunite and several other alteration minerals. Chemical modelling indicates that their formation requires higher temperatures than observed in the lake. Therefore, influx of hot brine water derived from the underlying hydrothermal system is largely responsible for cation budgets in the lake.

Rare earth elements appear to be sensitive monitors of water-rock interaction and fluid cycling. A marked trend in europium anomalies from the first half of Stage III on suggests that water interacted with progressively more altered rocks. This points to maturation of the hydrothermal system and no exposure of water to fresh rocks since then (perhaps until the transition between stages IV and V). Short-lived fluctuations in cerium/ytterbium ratios during Stage IV are consistent with rapid recycling of the lake water through this underlying reservoir.

Polythionates usually constitute a significant part of the total sulphur budget of the crater lake. These polymeric sulphur compounds proved to be sensitive indicators of SO_2 and H_2S input at the bottom. Large amounts (up to 7400 mg/L) were present when fumarolic activity was centred within the lake area or at the CPC (i.e. at the transition of Stages II-III, the transition of Stages III-IV, and in Stage V). They have been virtually absent (a) due to high lake temperatures ($>60\text{--}65^\circ\text{C}$) and/or excess injection of SO_2 when fumarolic activity in the lake area was strongest (Stage III and part of Stage V), and (b) when fumarolic input into the lake was interrupted, due to partial sealing of feeding conduits (several intervals in Stage IV). In general, high polythionate concentrations tend to coincide with transitions in the discharge rate of gas through the crater area, either from weaker to stronger or from stronger to weaker.

The polythionates provide strong signals of renewed input of SO_2 -rich gas into the lake that may be followed by phreatic eruptions. Such intervals were found to coincide with increases in seismicity. A rise in polythionate concentrations and a change in the distribution of different species, possibly followed by a sharp drop are likely to precede eruptive events. However, a similar sequence may also occur without subsequent phreatic eruptions, at occasions when fumarolic inputs become temporarily blocked. In the latter case this will be accompanied by decreases in lake temperatures and concentrations of dissolved SO_4 , Cl and F. Hence, the monitoring of polythionates is a valuable tool for predicting future eruptive events as long as it is accompanied by simultaneous monitoring of other parameters.

Over the last 30 years the sites of main fumarolic outgassing within the active crater have been shifting between the lake area and the CPC on its southern shore. This suggests that the magma body that drives the volcanic-hydrothermal activity

is located directly below the area that comprises the lake and the CPC. It also suggests that most of the fluids and heat are transferred toward the surface through permeable layers and fracture zones that are concentrated below this area.

Shifts in the location of fumarolic activity are also marked by the appearance of low-temperature vents and associated thermal springs in the eastern part of the crater from late 1998 on. Both had a transient existence throughout Stage IV until their disappearance in the beginning of Stage V. Consistent with the observed behaviour of the lake, their lifetime heralds a temporary expansion of the volume of hydrothermal groundwater in the summit area, and has no magmatic origin.

Porosity and permeability in the subsurface are likely affected by the formation of alteration minerals in pore spaces, fractures and channels. Sealing effects are therefore important in regulating the chemical and thermal properties of the lake. They were most efficient during Stage IV, leading to almost complete shutdown of input during brief intervals. Sealing is also a likely agent in the movement of fumarole locations, and possibly in the triggering of explosive events if seals are suddenly broken.

The combined geochemical and field observations indicate that Poás is a prime example of a volcano where persistent activity is regulated by the presence of a sizeable hydrothermal system situated between a magma body and the crater area. The successive stages of activity and quiescence lead to the concept of a hydrothermal system wherein vapour and liquid alternate in prevalence. Conditions during the active Stage III ("dry") and the quiet Stage IV ("wet") represent the extremes.

Resurging input of heat and volatiles, eventually leading to eruptive activity, could be triggered by magma, either via intrusion of a fresh batch or through fracturing of the brittle chilled margin around a cooling body. Alternatively, rupture of an impermeable seal in the overlying sequence of altered lavas and pyroclastics may release large quantities of accumulated volatiles. From the lake properties alone, if fresh magma intrusion has played a role in the last decades, it likely occurred at the transitions between Stages II and III, and between Stages IV and V. A local intrusion of magma may also have been responsible for a steep temperature rise of CPC fumaroles at the transition between Stages I and II. Whether a minor intrusion was also responsible for the resumption of phreatic explosions in 1994 after almost three years of quiescence that followed the phreatic period of 1987-1990 (Stage III) is uncertain, given the virtual absence of a lake at that time. Perhaps a more plausible cause is the breaking of seals or unclogging of conduits that may have been blocked by mineral deposits in the hydrothermal system during the previous phreatic period. The evidence that hydrothermal water has not been exposed to fresh rock from the early years of Stage III on, argues against the intrusion of fresh magma, at least until the end of Stage IV.

The relative quiescence of Stage IV highlights conditions when liquid dominates in the hydrothermal system, as evidenced by relative weak fumarolic degassing and by the record rise in the lake level. Due to the expansion of the subsurface volume of hydrothermal and meteoric water rising magmatic gas species were intercepted, hampering their free release to the atmosphere and reducing volatile concentrations in the lake. The Stage IV-V transition in the lake's properties and enhanced fumarolic degassing, culminating in phreatic activity from early 2005 on,

followed a scenario comparable to that observed at the Stage II-III transition. The combined observations are indicative of desiccation of the hydrothermal system and a return to the conditions of Stage III.

Discharge rates of magmatic volatiles (S, Cl, F) issued by the Agrio springs on the northwest flank of the volcano are of the same order of magnitude but much more stable than those directly emitted into the atmosphere from vents in the active crater.

Combined data obtained during intervals in Stages III and IV indicate that the minimum total flux of SO_2 from Poás volcano ranges roughly between 150 and 250 ton per day. In

periods when the hydrothermal system inhibits free atmospheric emissions of volatiles via the crater area, larger fluxes through the Agrio springs might keep the overall output in balance.

The presence or absence of the lake, the volume of the associated water body below the crater, and the overall level of outgassing play a critical role in determining the type and intensity of acid deposition on the flanks of Poás and its environmental impact. Economic damage and adverse health effects are likely to occur when the lake declines or disappears, as was demonstrated by the events during Stage III, or when the combined vigour of subaerial fumarolic venting increases, as observed in some periods of Stage IV (1999-2000).

Resumen

Esta tesis describe la evolución del lago cratérico ácido (conocido como Laguna Caliente), ubicado en la cima del volcán Poás, localizado en la parte central de Costa Rica. El Poás ha manifestado actividad fumarólica persistente y fluctuante lo cual ha dado como resultado que la apariencia, volumen, temperatura y composición química del lago cambien continuamente y en forma drástica durante todo el período en el cual se ha tenido conocimiento de su existencia. Ocasionalmente, el lago ha desaparecido completamente, las últimas veces que esto ha ocurrido fue entre 1953-55 y 1989-1994. Esos intervalos durante los cuales el lago inclusive se ha secado, han sido acompañados por erupciones, las cuales están restringidas en el Poás a expulsión de vapor, ceniza y sedimentos del fondo del lago. Estas erupciones típicamente se han producido a través de la región ocupada por el lago ácido, las últimas de ellas se han observado entre 1968-1980, 1987-1994, y más recientemente entre el 2006-2008. Erupciones magmáticas en el Poás, la última ocurrida en 1953-1954, constituyen un evento raro en este volcán. Los períodos de actividad eruptiva en el Poás se han alternado con intervalos de relativa quietud caracterizados por actividad fumarólica débil o moderada. Durante los períodos eruptivos se han producido plumas volcánicas de considerable altitud y una considerable cantidad de gases y partículas han sido emitidos hacia la atmósfera. Gases y partículas son emitidos prácticamente en forma continua desde las aberturas fumarólicas ubicadas dentro del cráter activo, las cuales varían en vigor y ubicación en el tiempo. Debido a que los gases contienen grandes cantidades de azufre y cloro y los mismos son transportados por el viento, estos producen cambios en el ambiente por efecto de lluvia ácida, gases y las partículas emitidas desde el cráter y los cuales son dispersados sobre los flancos del volcán. Por lo tanto, la actividad fumarólica intensa intermitente no solo representa peligros directos para la región ubicada en la cima del volcán, sino que también puede resultar perjudicial para la salud de pobladores, animales domésticos y ganado, e inclusive impactar las actividades agrícolas, forestales, turísticas, así como la infraestructura y los ecosistemas existentes en los flancos del volcán Poás.

Con el fin de predecir mejor la naturaleza y el momento de futuros acontecimientos eruptivos, es necesario conocer los procesos particulares que operan en el interior del volcán, los cuales son últimamente responsables de la actividad hidrotermal que se manifiesta en la superficie. La circulación de fluidos magmáticos-hidrotermales y los efectos de la energía térmica que acompañan a esos procesos, rápidamente se transmiten hacia la superficie por medio de vapor en expansión y mediante la circulación subterránea de fluidos. El lago cratérico del Poás intercepta esas señales y las transforma en propiedades químicas y físicas medibles. Los resultados de este estudio demuestran que la Laguna Caliente provee un registro detallado de los procesos que se desarrollan en profundidad dentro del edificio volcánico. La temperatura de la laguna, así como una gran

variedad de compuestos químicos disueltos en las aguas de la misma, muestran variaciones sistemáticas, sin embargo, las variaciones observadas en los períodos de tiempo largos no son las mismas que en los períodos de tiempo corto, lo cual hace la interpretación de los procesos que producen estos cambios sistemáticos todo un reto.

Un inventario comprensivo de datos nuevos así como publicados es presentado en esta tesis, cubriendo de esta forma la historia del lago ácido cratérico del Poás entre 1978 y 2008. Basado en observaciones de campo y el muestreo mensual, prácticamente continuo, de las aguas del lago, se reconocen cinco estadios que reflejan los cambios principales en el lago, de acuerdo al estado de actividad del volcán:

Estadio I (~1972 – agosto 1980). El lago era sumamente ácido (pH menor que 0), caliente (temperatura promedio 49°C), con una salmuera de color gris, voluminoso (aproximadamente $1.5 \times 10^6 \text{ m}^3$), y presentaba una alta concentración total de solutos disueltos (promedio TDS $1.5 \times 10^5 \text{ mg/kg}$). Durante este periodo la actividad fumarólica estuvo principalmente centrada en el lago, fue moderada y esporádica, con pequeñas explosiones freáticas tipo géiser.

Estadio II (setiembre 1980 – abril 1986). Este período fue marcado por una quietud relativa en el lago comparado con el Estadio I. No hubo actividad freática, sin embargo, hubo una emisión intensa de gases de alta temperatura (hasta 1020°C) a través de fumarolas ubicadas en el borde sur del lago, propiamente en el cono piroclástico compuesto (CPC) formado en 1954-55. A pesar de las altas temperaturas de las fumarolas en el CPC, el lago mantuvo un volumen estable (alrededor de $1.4 \times 10^6 \text{ m}^3$), en tanto su temperatura, pH, y TDS fluctuaron alrededor de 49°C, 0.16, y $8.7 \times 10^4 \text{ mg/kg}$, respectivamente.

Estadio III (mayo 1986 – agosto 1995). Este período es caracterizado por numerosas erupciones freáticas intensas y actividad fumarólica vigorosa en el lago. El volumen máximo del lago fue de sólo $\sim 93 \times 10^3 \text{ m}^3$ (si las transiciones entre los estadios II y IV son ignoradas), además, el lago se secó en varias ocasiones, dejando solo charcos de lodo en el fondo. La temperatura del lago se mantuvo alrededor de los 66°C y alcanzó máximos alrededor del punto de ebullición correspondiente a la altitud en la cima del volcán Poás, i.e. $\sim 94^\circ \text{C}$, en tanto el pH promedio (pH = -0.2) indicó condiciones de extrema acidez. El TDS promedio estuvo alrededor de $1.6 \times 10^5 \text{ mg/kg}$.

Estadio IV (septiembre 1995 – febrero 2005). Este estadio representa el período en el cual el lago ha mostrado la mayor quietud respecto a los demás estadios, aunque numerosas fluctuaciones en las propiedades del lago fueron también observadas. Los promedios de temperatura y de TDS han sido los más bajos registrados a lo largo de todo el período bajo

estudio, alrededor de 33°C y 2×10^4 mg/kg, respectivamente. Por otra parte, el pH fue en general el más alto registrado, en promedio ~1. El lago alcanzó los niveles más altos desde que se tienen registros. El volumen en 1997 alcanzó $\sim 1.7 \times 10^6$ m³ y en 2004-2005 el mismo fue aún mayor, es decir alrededor de 1.9×10^6 m³. Durante este período, una nueva área fumarólica con descargas vigorosas de vapor de agua, y en menor grado escapes de agua termal, se desarrolló en la terraza Este del cráter activo.

Estadio V (marzo 2005 – Presente). La característica principal de este estadio es el regreso de actividad fumarólica vigorosa y de erupciones freáticas a la región ocupada por el lago cratérico ácido, luego de un incremento rápido en la temperatura del mismo (desde 22° hasta $\sim 58^\circ\text{C}$), así como un descenso continuo del pH hasta alcanzar valores cercanos a cero, y un incremento de 10 órdenes de magnitud en los valores de TDS, $> 1.5 \times 10^5$ mg/kg en setiembre del 2007. En la actualidad, el flujo de calor y de volátiles a través del lago continúa siendo significativo, de modo que el nivel del lago continúa disminuyendo, a pesar del aporte cuantioso de agua que proveen las fuertes lluvias en la cima del volcán Poás durante los meses más lluviosos del año. De esta manera, la ocurrencia de más explosiones freáticas podría repetirse en cualquier momento, considerando que las condiciones actuales del lago ácido del Poás se asemejan a aquellas observadas durante la transición entre los Estadios II y III.

La subdivisión de la actividad en el lago cratérico en cinco estadios es definida claramente por las tendencias en función del tiempo mostradas por la concentración de los aniones (S, Cl, F) y los cationes mayoritarios (elementos formadores de rocas volcánicas) en las aguas del lago, aunque estos dos grupos de elementos tienen un origen diferente: los aniones son derivados primordialmente de la fase gaseosa liberada desde el magma y los cationes provienen de la interacción entre fluidos ácidos acuosos y rocas. Así, las concentraciones de iones en las aguas del lago reflejan por lo tanto, diferentes procesos ocurriendo en el interior del volcán.

La interpretación de las tendencias mostradas por los aniones en el lago ácido del Poás indican que las variaciones en las concentraciones y proporciones relativas no sólo son causadas por cambios en los flujos de volátiles liberados por un cuerpo de magma. Por lo general, el flujo de volátiles magmáticos es también modulado por la presencia de un sistema hidrotermal ubicado alrededor del cuerpo magmático. De los resultados de este estudio se infiere que gas caliente magmático fue inyectado en el lago ácido en los primeros años del Estadio III, antes de su desecamiento. Por el contrario, las desviaciones más fuertes respecto a las señales primarias de gas magmático (por ejemplo, bajas relaciones S/Cl) y las bajas concentraciones registradas sugieren una notable interferencia del sistema hidrotermal durante el Estadio IV el cual fue caracterizado por calma relativa.

Por otro lado, las concentraciones de los cationes mayoritarios, siguen en general las tendencias mostradas por los aniones, excepto aquellos cationes que forman parte de minerales que precipitan en el lago. Las relaciones mostradas por los cationes no permanecen constantes pues dependen del grado de disolución de la roca presente. La disolución casi completa de

roca explica la concentración de cationes observada durante el Estadio III, mientras una divergencia relativamente fuerte es observada durante el Estadio IV. Esta desviación se ha atribuido a la formación de alunita y otros minerales de aluminio resultantes de la alteración de rocas. Resultados obtenidos a través del modelaje del equilibrio geoquímico de las aguas del lago ácido, indican que la formación de estos minerales requiere temperaturas más altas que las observadas en la superficie del lago. Por lo tanto, se infiere que las concentraciones de cationes observadas en el lago son resultado de la mezcla de una salmuera caliente originada en zonas profundas del sistema hidrotermal subyacente con las aguas someras del lago.

Los elementos tierras raras parecen ser sensibles monitores de la interacción roca-agua y de la circulación de fluidos. La aparición de anomalías del elemento químico Europio, a partir de la primera mitad del Estadio III, sugiere una interacción progresiva entre fluidos magmáticos-hidrotermales y roca fresca que gradualmente fueron cada vez más alteradas. Esto sugiere la ocurrencia de una intrusión de un cuerpo de magma fresco interactuando con el sistema hidrotermal así como una maduración gradual del sistema hidrotermal. La tendencia general mostrada por el Europio también sugiere la ausencia de nuevas interacciones entre fluidos hidrotermales y rocas frescas desde entonces hasta quizás la transición entre los estadios IV y V. Fluctuaciones efímeras observadas en las relaciones entre cerio/iterbio durante el Estadio IV son compatibles con el reciclaje rápido del agua del lago en el reservorio hidrotermal subyacente.

Los politionatos por lo general constituyen una parte significativa de la cantidad total de compuestos de azufre disueltos en el lago cratérico. Estos compuestos poliméricos de azufre han demostrado ser indicadores sensibles de la inyección de SO₂ y H₂S hacia el lago cratérico. Cantidades significativas de politionatos (hasta 7400 mg/L) han estado presentes en el lago ácido del Poás cuando la actividad fumarólica ha estado centrada predominantemente en la región ocupada por el lago o en el cono piroclástico compuesto CPC (por ejemplo, en la transición entre los Estadios II-III y III-IV, y en el Estadio V). Los politionatos han estado prácticamente ausentes debido a: (a) temperaturas del lago relativamente altas ($> 60\text{--}65^\circ\text{C}$) y a la excesiva inyección de SO₂ cuando la actividad fumarólica en el lago era la más fuerte (Estadio III y parte del Estadio V), y (b) cuando la inyección de gases fumarólicos en el lago fue interrumpida o débil, debido posiblemente al sellamiento parcial de conductos fumarólicos (como parece haber ocurrido en intervalos de gran calma en el lago observados durante el Estadio IV). En general, la presencia temporal de altas concentraciones de politionatos en el lago tiende a coincidir con transiciones en el flujo de volátiles descargados a través de las fumarolas en el cráter activo, variando este de más débil a más fuerte o de más fuerte a más débil.

Los politionatos constituyen señales contundentes de que gases ricos en SO₂ están siendo inyectados en el lago cratérico ácido, por lo cual pueden ser considerados potenciales precursores de erupciones freáticas. Se ha encontrado que los periodos en los cuales los politionatos muestran un aumento o disminución debido a la inyección de gases ricos en SO₂, coinciden con aumentos en la actividad sísmica. Un aumento en la concentración de los politionatos y un cambio en la

distribución de las diferentes especies de los mismos donde predomine el tetratiónato, seguido por una disminución repentina en la concentración de politionatos, podría preceder eventos eruptivos en el volcán Poás. Sin embargo, secuencias similares también se han observado en el Poás sin que ocurran posteriormente erupciones freáticas. Por otra parte, en el Poás se han observado secuencias de esta naturaleza luego de que los conductos fumarólicos parecen haberse sellado temporalmente. En este último caso, se ha observado además una disminución en la temperatura del lago, así como en las concentraciones de especies químicas disueltas. Por consiguiente, el monitoreo de politionatos es una herramienta valiosa para predecir eventos eruptivos futuros en el volcán Poás en tanto el mismo sea realizado conjuntamente con otros parámetros de cruciales para el monitoreo.

Durante los últimos 30 años, la ubicación de las principales fumarolas dentro del cráter activo ha estado cambiando entre el área ocupada por el lago y el cono piroclástico compuesto (CPC) en el borde sur del lago. Esto sugiere que el cuerpo magmático del cual se deriva la actividad volcánica hidrotermal del Poás está localizado directamente debajo de la región donde están ubicados el lago y el CPC. También sugiere que la mayoría de los fluidos y del calor son transferidos hacia la superficie a través de capas permeables y zonas de fractura que se concentran debajo de esta área.

Cambios en la ubicación de la actividad fumarólica se observaron durante el Estadio IV, con la aparición de fumarolas de baja temperatura y algunas fuentes termales asociadas en el sector este del cráter activo a partir de finales de 1998. Tanto las fumarolas de baja temperatura como las fuentes termales en este sector tuvieron una existencia transitoria durante el Estadio IV hasta que las mismas desaparecieron a principios del Estadio V. En consistencia con el gran volumen de agua mostrado por el lago como resultado de un aumento significativo en la tabla de agua observado durante el Estadio IV, la ocurrencia temporal de estas fumarolas y fuentes termales en el sector este del cráter parece ser resultado de la acumulación excesiva de aguas subterráneas hidrotermales en la región subyacente al cráter activo del volcán, y no resultado de degasificación magmática debajo del sector este del cráter activo.

La porosidad y permeabilidad de la estructura interna en los alrededores de la cima del volcán, son probablemente afectadas por la formación de minerales dentro de los espacios porosos, fracturas y canales. Así, los efectos de sellamiento de conductos y fracturas en el edificio volcánico juegan un papel en la regulación de las propiedades químicas y térmicas del lago. El sellamiento de conductos parece haber sido muy eficiente durante el Estadio IV, y esto pudo haber causado el cese o debilitamiento de la inyección de fluidos y calor hacia el lago durante los breves intervalos de mayor calma que se observaron a lo largo del Estadio IV. El sellamiento de conductos es probablemente también un agente importante en el desplazamiento de la ubicación de fumarolas y posiblemente juega también un papel en el disparo de eventos explosivos cuando estos sellos son súbitamente rotos.

La combinación de observaciones geoquímicas y de campo indican que el volcán Poás representa un buen ejemplo de como la actividad fumarólica persistente es regulada por la presencia de un importante sistema hidrotermal situado entre el cuerpo

magmático en enfriamiento y la región subyacente al cráter activo. La sucesión alternada de estadios activos y de quietud relativa conducen al concepto de un sistema hidrotermal en el cual regiones constituidas mayormente por vapor y líquido se alternan en cuanto a su predominio. Las condiciones durante el Estadio más activo III ("seco") y el Estadio de calma relativa en el lago IV ("húmedo") representan los extremos.

El resurgimiento de un aumento en el flujo de calor y de volátiles, conducente a una eventual actividad eruptiva, puede ser disparada por el magma mismo, ya sea mediante la intrusión de un volumen de magma fresco o a través de la inducción de fracturamiento de la parte externa quebradiza del cuerpo magmático en enfriamiento. Alternativamente, la ruptura de sellos impermeables en la secuencia de rocas sobreyacentes, lavas alteradas y piroclastos, podría liberar cantidades significativas de fluidos y calor acumulados en niveles profundos. Considerando solamente las propiedades físico-químicas del lago ácido del Poás observadas a lo largo del período estudiado, se tiene que si una intrusión de magma fresco ha jugado un papel en las últimas décadas, es posible que la misma ocurriera en las transiciones entre los Estadios II y III y los Estadios IV y V. Una intrusión local de magma podría también haber sido responsable del brusco aumento de temperatura de las fumarolas alrededor del CPC, en la transición entre los Estadios I y II. Es incierto aún, si una intrusión menor podría haber causado la reanudación de explosiones freáticas en el lago en 1994, luego de casi tres años de quietud que siguieron al periodo de erupciones freáticas de 1987-1990 (Estadio III), dada la virtual ausencia del lago en ese momento. Algunas de las causas plausibles que podrían explicar las erupciones freáticas de 1994, es el rompimiento de rocas creando nuevas rutas por las cuales fluidos y calor migraron hacia la superficie hasta alcanzar la región del lago, o quizás el desbloqueo repentino de conductos fumarólicos que pudieron haber sido obstruidos por depósitos minerales formados en el sistema hidrotermal subterráneo durante el período freático previo de 1987-1990. La evidencia de que fluidos magmático-hidrotermales no han estado expuestos a roca fresca a partir de los primeros años del Estadio III, argumenta en contra de la ocurrencia de una intrusión de magma fresco, al menos hasta el final del Estadio IV.

La quietud relativa observada en el Estadio IV llama la atención sobre las condiciones que se producen cuando una zona rica en líquidos domina el sistema hidrotermal, como es evidenciado por la relativamente débil degasificación fumarólica y el incremento sin precedentes del nivel del lago. En el Estadio IV, la penetración y acumulación de volúmenes importantes de agua meteórica debajo de la superficie del cráter activo, dio como resultado una mejor captación de fluidos magmáticos y calor por el sistema hidrotermal, obstaculizando así su liberación hacia la atmósfera y reduciendo las concentraciones de especies químicas disueltas en el lago. Los cambios en las propiedades del lago observados durante la transición entre los Estadios IV-V, así como el incremento significativo en la degasificación fumarólica a través del lago, la cual culminó con la reanudación de actividad freática a principios del 2006, han mostrado un escenario comparable al observado durante la transición de los Estadios II-III. Las condiciones observadas en el Estadio V son indicativas de un proceso de desecamiento del sistema hidrotermal y del establecimiento de condiciones en el lago y

el sistema hidrotermal similares a las observadas en el Estadio III.

Los flujos de volátiles magmáticos (S, Cl, F) transportados por las aguas de la cuenca del río Agrio, ubicada sobre el flanco noroeste del volcán, son del mismo orden de magnitud, pero mucho más estables que los flujos de volátiles emitidos a la atmósfera a través de las fumarolas del cráter activo del Poás. La combinación de datos obtenidos durante ciertos períodos de los Estadios III y IV indican que el flujo mínimo total de SO_2 emitido por el volcán Poás varía entre 150 y 250 toneladas por día. En períodos cuando el sistema hidrotermal inhibe la emisión de volátiles y calor hacia la atmósfera a través del cráter activo, flujos mayores de volátiles parecen ser liberados a través de las aguas del río Agrio, lo cual permite mantener el balance en el flujo total de volátiles en el sistema magmático hidrotermal del volcán Poás.

La presencia o ausencia del lago cratérico, así como el volumen del cuerpo de agua subterránea asociado al lago que se encuentra debajo del cráter, y el grado de desgasificación a través del cráter activo, juegan un papel crucial en la determinación del tipo y la intensidad de depositación ácida sobre los flancos del volcán Poás y sus alrededores, así como el nivel de impacto sobre el ambiente. Los efectos adversos sobre la salud humana y animal, los ecosistemas, las actividades económicas, y la infraestructura en zonas aledañas al volcán Poás, principalmente en los sectores oeste y suroeste, han sido más severos cuando el volumen del lago se ha reducido significativamente o cuando el mismo se ha evaporado, tal y como fue observado durante el período más activo, es decir, Estadio III, o cuando el vigor combinado de las fumarolas subaéreas aumenta, tal y como se observó a mediados del Estadio IV (años 1999-2000).

Samenvatting

Dit proefschrift beschrijft de ontwikkeling van Laguna Caliente, een zuur kratermeer op de top van Poás, een permanent actieve vulkaan in Costa Rica. Sinds het bestaan van het meer bekend is zijn de samenstelling, het volume, de temperatuur en het uiterlijk ervan voortdurend veranderd. Soms was het meer zelfs geheel verdwenen, wat voor het laatst gebeurde in 1953-1954 en in 1989-1994. Deze perioden gingen gepaard met erupties, die in het geval van Poás gewoonlijk beperkt blijven tot de uitstoot van stoom en as. Dit soort uitbarstingen gaat veelal via het meer, zoals onder meer het geval was in de late jaren zeventig en recentelijk in 2006-2008. De laatste eruptie waarbij nieuw magma naar buiten kwam, een verschijnsel dat bij deze vulkaan zelden voorkomt, vond plaats in 1953-1954. Deze eruptieperioden wisselen af met tijden van relatieve rust. De wisselingen gaan samen met veranderingen in de hoeveelheid gasuitstoot en de hoogte die de emissies in de atmosfeer bereiken. Met fluctuerende kracht worden vrijwel voortdurend gassen uitgestoten door fumarolen in het kratergebied die in de loop van de tijd veranderen van plaats. Vanwege de grote hoeveelheden zwavel en chloor in het gas zijn er daardoor ook veranderingen in de neerslag van zure regen en andere milieuschade rond de vulkaan. Behalve de directe gevaren in het kratergebied op de top, zijn er zodoende met regelmaat schadelijke effecten voor de gezondheid van de bevolking, de veestapel, landbouwgewassen en infrastructuur op de flanken van de vulkaan.

Om de aard en het tijdstip van toekomstige erupties beter te kunnen voorspellen is het nodig de onderliggende processen te kennen die zich in het binnenste van de vulkaan afspelen. De vloeistofbewegingen en warmte-effecten die deze met zich meebrengen worden via opstijgende gassen en circulerend groundwater efficiënt naar de oppervlakte doorgegeven. Het kratermeer vangt deze signalen op en zet ze om in meetbare chemische en fysische eigenschappen. De resultaten van dit onderzoek tonen aan dat Laguna Caliente deze diepe processen nauwkeurig weergeeft. De watertemperatuur en een grote aantal opgeloste chemische bestanddelen laten systematische, maar ongelijkwaardige veranderingen zien over langere zowel als kortere tijdintervallen. De interpretatie ervan vormt een complexe uitdaging.

Deze dissertatie presenteert een uitgebreide inventaris van nieuwe en bestaande gegevens die de geschiedenis van het meer tussen 1978 en 2008 beslaan. Gebaseerd op veldwaarnemingen en vrijwel ononderbroken maandelijkse bemonstering van het meer, konden vijf perioden worden onderscheiden die grote veranderingen in de activiteitstoestand van de vulkaan vertegenwoordigen:

Periode I (~1972 – augustus 1980): Gematigde gasemissies en, sporadisch, kleine geyser-achtige freatische explosies in het meer.

Periode II (september 1980 – april 1986): Relatief rustige omstandigheden in het meer, zonder freatische activiteit, maar met intense uitstoot van zeer hete gassen (tot 1020°C) uit fumarolen op de zuidoever.

Periode III (mei 1986 – augustus 1995): Heftige activiteit in het meer en intense freatische erupties, waarbij het meer volledig opdroogde en alleen modderpoelen overbleven. De watertemperatuur lag gemiddeld rond 66°C en bereikte zo nu en dan het kookpunt, terwijl de gemiddelde pH-waarde negatief was.

Periode IV (september 1995 – februari 2005): De rustigste periode van de laatste dertig jaar, hoewel talrijke fluctuaties in de eigenschappen van het meer werden waargenomen. Het meerniveau bereikte de hoogste standen ooit; nieuwe krachtige fumarolen en kleine warmwaterbronnen ontwikkelden zich op terrassen aan de oostzijde van de krater.

Periode V (maart 2005 – vandaag): hervatting van sterke activiteit en freatische erupties; belangrijke toevoer van warmte en gassen, en snelle daling van het waterniveau ondanks heftige regenval. Nieuwe freatische uitbarstingen kunnen elk moment plaatsvinden, gelet op de gelijkenis met de omstandigheden na de overgang van Periode II naar Periode III.

De onderverdeling in vijf perioden wordt gemarkeerd door duidelijke veranderingen in de concentraties van anionen (S, Cl, F) en kationen (gesteentevormende elementen), ook al hebben deze groepen opgeloste elementen een verschillende herkomst: de anionen komen van ontgassend magma en de kationen van de interactie tussen water en het gesteente waaruit de vulkaan is opgebouwd. Hun concentraties weerspiegelen dus verschillende processen binnen de vulkaan.

De patronen die de anionen laten zien worden niet alleen veroorzaakt door veranderingen in de ontgassing van een magmabron. Deze wordt gemoduleerd door het hydrothermale systeem dat daarboven aanwezig is. Een onbelemmerde toevoer van heet magmatisch gas naar het meer vond alleen plaats in de eerste jaren van Periode III, voordat het meer opdroogde. Daarentegen duiden sterke afwijkingen van de signatures van een magmatisch gas (o.m. een lage S/Cl verhouding) en lage concentraties in het meer tijdens de rustige Periode IV op een sterke wisselwerking met het hydrothermale systeem.

De kationen volgen de trend van de anionen, behalve degenen die opgenomen worden in mineralen die neerslaan in het meer. Ook de mate waarin het gesteente oplost zorgt ervoor dat de verhoudingen tussen verschillende kationen niet constant blijven. De waargenomen concentraties kationen tijdens Periode III komen grotendeels overeen met een vrijwel volledig oplossen van het gesteente, terwijl ze daarvan het sterkst afwijken tijdens Periode IV. Deze afwijkingen kunnen verklaard worden door de vorming van nieuwe mineralen. Chemische modelberekeningen laten zien dat de betreffende mineralen echter niet in het meer ontstaan, omdat de temperaturen daarin niet hoog genoeg

zijn. Daarom kan geconcludeerd worden dat instromend heet grondwater uit het hydrothermale systeem voor een groot deel verantwoordelijk is voor het budget aan kationen in het meer.

Polythionaten (polymerische zwavelverbindingen) blijken gevoelige indicatoren te zijn van de aanvoer van SO_2 en H_2S via de bodem van het meer. In het algemeen werden hoge concentraties gevonden bij overgangen in de doorstroom van gas door het kratergebied, hetzij van zwakker naar sterker, hetzij van sterker naar zwakker. De polythionaten signaleren een hernieuwde aanvoer van SO_2 -rijk gas die gevolgd kan worden door freatische erupties. Zulke perioden bleken samen te vallen met een toename in de seismische activiteit. Het monitoren van polythionaten is dan ook belangrijk voor het voorspellen van toekomstige uitbarstingen, mits dit vergezeld gaat van het gelijktijdig monitoren van andere parameters.

De afgelopen 30 jaar is de locatie waar de meeste fumarolische ontgassing plaatsvond voortdurend verschoven tussen het meer en een pyroclastische kegelvormige heuvel (CPC) op de zuidoever. Dit wijst erop dat het magmalichaam dat de vulkanisch-hydrothermale activiteit aandrijft precies ligt onder het gebied dat het meer en de CPC beslaat. Hier lijken ook de meeste vloeistoffen en warmte via doorlaatbare lagen en breukzones naar de oppervlakte te komen.

Dat fumarolische activiteit zich verplaatst wordt ook gemarkeerd door het verschijnen van nieuwe fumarolen (met een lage temperatuur) en warme bronnen in het oostelijke deel van de krater vanaf 1998. Hun bestaan gedurende Periode IV was van voorbijgaande aard, en ze verdwenen dan ook weer in het begin van Periode V. Deze levensduur weerspiegelt een tijdelijke expansie van het volume aan hydrothermaal grondwater en heeft geen magmatische oorsprong.

De vorming van omzettingsmineralen in poriën, barsten en kanalen heeft de porositeit en permeabiliteit in de ondergrond waarschijnlijk beïnvloed. Natuurlijke afdichting is daarom een belangrijke regulerende factor voor de chemische en thermische eigenschappen van het meer. Dit verschijnsel was het meest effectief tijdens Periode IV toen het zelfs voor kortstondige, volledige onderbrekingen van de instroom zorgde. Afdichting is waarschijnlijk ook een oorzaak voor de verplaatsingen van fumarolen, en speelt mogelijk eveneens een rol als aanzet tot explosieve activiteit wanneer ondoorlatende lagen plotseling doorbroken worden.

De combinatie van geochemische gegevens en veldwaarnemingen laat zien dat Poás een sleutelvoorbeeld is van een vulkaan waar ononderbroken activiteit wordt gemoduleerd door de aanwezigheid van een omvangrijk hydrothermaal systeem tussen het magmalichaam en het kratergebied. De opeenvolgende stadia van activiteit leiden tot het concept van een hydrothermaal systeem waarin damp en vloeistof beurteilungen de overhand hebben. De omstandigheden tijdens de actieve Periode III ("droog") en de rustige Periode IV ("nat") vertegenwoordigen de uitersten.

Een plotselinge nieuwe stroom van gassen en warmte, die mogelijk tot een eruptie leidt, kan worden veroorzaakt door magma, hetzij doordat er een nieuwe hoeveelheid intrudeert, hetzij wanneer er barsten ontstaan in de gestolde omhulling van een reeds aanwezige hoeveelheid die afkoelt en kristalliseert. Een andere mogelijkheid is een plotselinge doorbraak van een afgedichte, ondoordringbare laag in het pakket lava's en pyroclastische afzettingen, waardoor een grote hoeveelheid gas dat zich daaronder verzameld had plotseling vrijkomt. Gebaseerd op de eigenschappen van het meer hebben intrusies van vers magma hoogstwaarschijnlijk plaatsgevonden bij de overgangen van Periode II naar III, en van Periode IV naar V. De bewijzen voor locale intrusies op andere momenten zijn minder eenduidig. Aanwijzingen dat hydrothermaal water niet meer in contact geweest is met vers gesteente sinds de eerste jaren van Periode III pleiten tegen een intrusie van nieuw magma op enig moment daarna.

De betrekkelijke rust tijdens Periode IV weerspiegelt omstandigheden waarbij vloeistof domineert in het hydrothermale systeem, zoals ook blijkt uit de tamelijk zwakke fumarolische ontgassing en de record-waterstanden die het meer bereikte. Door de expansie van het ondergrondse volume hydrothermaal en meteorisch water werd opstijgend magmatisch gas onderschept, hetgeen de vrije doorstroom naar de atmosfeer belemmerde en leidde tot lagere concentraties anionen in het meer. De veranderingen in de eigenschappen van het meer bij de overgang van Periode IV naar V en de toenemende fumarolische ontgassing, uitmondend in de freatische activiteit vanaf begin 2005, volgen een scenario dat vergelijkbaar is met de overgang van Periode II naar III. De waarnemingen wijzen op een uitdroging van het hydrothermale systeem en terugkeer naar de omstandigheden van Periode III.

Magmatische bestanddelen (S, Cl, F) komen ook naar buiten via warmwaterbronnen op de noordwestelijke flank van de vulkaan. De hoeveelheden die deze bronnen produceren zijn van de zelfde orde van grootte als de fumarolische emissies in de krater, maar ze zijn veel stabielier door de tijd heen. Bij elkaar opgeteld is de totale minimum uitstoot van SO_2 door de Poás vulkaan ruwweg tussen de 150 en 250 ton per dag. In perioden wanneer het hydrothermale systeem een vrije emissie naar de atmosfeer belemmert, lijkt een grotere uitstroom via de bronnen dit te compenseren, zodat de totale uitstoot in balans blijft.

De aan- of afwezigheid van het meer, zowel als het volume van het grondwater onder de krater bepalen in belangrijke mate de aard en intensiteit van zure neerslag op de flanken van Poás en daarmee samenhangende milieu-effecten. Economische schade en gezondheidproblemen zullen vooral optreden wanneer het meer krimpt of geheel verdwijnt, zoals de gebeurtenissen tijdens Periode III hebben aangetoond.

Acknowledgements

First of all, I would like to express my sincere gratitude to my academic advisor at Utrecht University, Dr. Manfred van Bergen, for giving me the great opportunity to do research on the geochemistry of volcanic lakes in The Netherlands, for helping me initiate and expand this project by providing numerous facilities, and for sharing his ability to give light to many scientific ideas and issues through which this work could proceed. I also thank him for his help and critical advice during the successive research stages and the preparation of this dissertation. I very much appreciate his constant enthusiasm, encouragement, support and consideration, which made my life immensely easier during all the years I worked on this thesis. It was always comforting to have his support when I went through a difficult period.

I am also very much indebted to Professor Bernard de Jong, my other academic advisor at Utrecht University, who always encouraged me by stimulating discussion and constructive criticism, and who taught me about the importance to always ask questions when I do not understand something. I greatly appreciate his help and sponsorship that supported my stay in Utrecht. I enjoyed very much the warm and charming atmosphere of that attic there at Achter Sint Pieter. I also appreciate very much the hospitality, patience and kindness of Auke de Jong.

I am grateful to Paul Mason, Harry Oonk, Cees Woensdregt, Michel Jacobs, Igor Nikogosian, Matthias Barth, Gijs Nobbe, Pien van Minnen, Jason Herrin, Sri Sumarti, Sander van den Boorn, Marjolijn Stam and Kristen Mitchell, all members of the Petrology Group for their kind support, assistance and help, and for their valuable comments to improve my research.

I would also like to acknowledge the nice times I shared with my officemates in Utrecht, Sri Sumarti, Jason Herrin and Sander van den Boorn; if it were not for them I would not have kept my sanity, being so many long days 5000% busy in what we called “Happy Valley” (Room O222). I also appreciate the support and friendship of Iwona Rejniewicz.

I am very grateful to Ronald van Miltenburg, Helen de Waard, Erick van Vilsteren, Dineke van de Meent, Pieter Kleingeld, Gijs Nobbe, Christelle Hyacinthe, Herman van Roermund, Tilly Bouten, Anita van Leeuwen, Ton Zalm and Otto Stiekema for their technical and analytical support in the chemical analysis of large numbers of samples from Poás volcano at the laboratories of the Department of Earth Sciences.

I specially thank Maaïke Blau for her excellent and delicate work doing manual measurements on hundreds of polythionate chromatograms. Thanks also to Geerke Floor and Geertje Pronk

for contributing to the study of Costa Rican volcanoes through their graduate research projects.

I am very indebted to Margot Stoete, Ton Markus, Isaac Santoe, Jaco Bergenhenegouwen and Fred Trappenburg of the GeoMedia Office for their support and willingness to construct all of the drawings and for creating the layout of this proefschrift.

I also owe many thanks to Roy Pieris (thanks Roy for fixing my fiets!) and to Manolita Cabrera, the charming Spanish lady who shared her enthusiasm and “joie de vivre” every time I took a meal at the canteen of the Minnaertgebouw. Thanks to Boudewijn ‘t Hart for his friendship and nice coffee breaks. I also thank Mark van Alphen and Joop Hoofd without whom computers and printers would never run smoothly.

Thanks to the whole Department of Earth Sciences of Utrecht University, in case I have forgotten anyone there.

I give my special thanks to Jaap, Gonne, Piet Hein, and Eugénie Drabbe and the relatives of the Dutch Drabbe Family, and all of the descendants of Michiel de Ruyter, for their support and friendship, and for sharing with me the delights of being immersed in the warm atmosphere of Dutch family homes during the time I studied and lived in Holland. This thesis is also dedicated to the memory of Dirk Johannes de Ruyter and Cornelia Mooy Vermeulen who were my “Dutch grandparents”.

Thanks to all these people in the Netherlands for all of their support and hospitality.

I gratefully thank Dr. Eduardo Malavassi (OVSI-CORI-UNA), Prof. Dr. Bokuichiro Takano (University of Tokyo, Japan), Prof. Dr. Alain Bernard (Université Libre de Bruxelles, Belgium), Prof. Dr. Johan C. Varekamp (Wesleyan University Connecticut, USA), Dr. Marino Protti (OVSI-CORI-UNA), Dr. Gary L. Rowe Jr. (U.S. Geological Survey), Dr. Peter Neeb (Max Planck Institut, Germany), Dr. Wendy Harrison (Colorado School of Mines, USA) and Dr. Juan Valdés (Universidad Nacional Costa Rica) for their prompt and thorough reviews of my thesis or parts of it.

I am grateful to Erick Fernández, Jorge Barquero, Wendy Sáenz, Jorge Brenes, Eduardo Malavassi, Vilma Barboza, Rodolfo van der Laet, Enrique Hernández, Eliécer Duarte, Henry Rodríguez, Rodrigo Sáenz, Juan Segura, Tomás Marino, Milena Berrocal, Javier Pacheco, María Miranda, Christian Garita, Ronnie Quintero, Emma Peñaranda, Jeannette Arauz, Zayda Campos, Carlos Montero, Yadira Solís, Marino Protti, Víctor González, Floribeth Vega, Walter Jiménez, Antonio Mata, Daniel Rojas, Federico Chavarría, Rodrigo del Potro, Francesca Martini, all

colleagues at the Volcanological and Seismological Observatory of Costa Rica at Universidad Nacional (OVSICORI-UNA) who in so many ways contributed to this work.

I am indebted to the Centro de Servicios y Estudios Básicos de Ingeniería del Instituto Costarricense de Electricidad (ICE) for generously providing long-term Poás-summit rainfall data. The valuable help from the people in charge of the administration of Poás Volcano National Park is gratefully acknowledged.

My thanks are also due to Dr. Alain Bernard, Dr. Fátima Africano and Saskia Gevaert at the Université Libre de Bruxelles, Belgium, for teaching me how to handle the computer code SOLVEQ, which I used to model the chemical equilibria in the lake waters, and for their hospitality when I stayed with them in Bruxelles learning about this technique. I also thank Dr. Christian Hensen from the Leibniz Institute of Marine Sciences at the University of Kiel (IFM-GEOMAR), who kindly introduced me into the use of the Grapher programme, which was used to construct the graphs for this thesis.

I very much appreciate the encouragement and support provided by Dr. Gary Rowe Jr., Dr. Joop Varekamp, Dr. Chris Newhall, Dr. Hazel Rymer, Dr. Ana Lilliam Martin, Dr. Hugo Delgado Granados, Dr. Eduardo Malavassi, the Commission of Incentives of the Ministry of Science and Technology, the National Council of Science and Technology of Costa Rica (MICIT-CONICIT), the Italian Organizing Committee of the International Geological Congress Florence-Italy 2004, and the Roegiers Family in Sausalito, California, that allowed me to attend great volcano meetings and geological expeditions in the USA, Indonesia, Mexico, Nicaragua, Costa Rica, Germany and Italy.

Special thanks are due to Prof. Dr. Bokuichiro Takano and Mrs. Etsu Takano, Prof. Dr. Kenji Sugimori, Prof. Dr. Takeshi Ohba and Prof. Dr. Yasuyuki Miura, as well as the scientific and technological support provided by the Japanese International Cooperation Agency JICA, which have contributed substantially to strengthen the volcano monitoring development and capabilities of OVSICORI-UNA. This thesis especially benefited from the pioneering work of Professor Takano in the analysis and interpretation of polythionates in acid volcanic lakes. I am very grateful for his expert advice and for his willingness to analyse samples, even after his retirement in his state-of-the-art home-kitchen laboratory.

The photographic material in this dissertation has been kindly provided by Federico Chavarría Kopper, Jorge Barquero, Enrique Valverde Sanabria, Jorge Quirós Umaña, Eduardo Malavassi, Eliécer Duarte, Bernhard Edmaier, Manfred van Bergen, Milena Berrocal, Wendy Sáenz, Rodolfo van der Laet and Geerke Floor.

I also acknowledge the financial and academic support provided by the American Endowment for the Arts, through Dr. Richard Stoiber from Dartmouth College (Hanover, NH), about 30 years ago that permitted to set up the geochemistry laboratory of OVSICORI. The support provided by the Laboratory



of Atmospheric Chemistry of the School of Chemistry of Universidad Nacional to the Volcano Monitoring Programme of OVSICORI-UNA throughout a fruitful 8-year joint project is also acknowledged.

This thesis benefited from technological support provided by DAAD (Deutscher Akademischer Austauschdienst), CEPREDENAC (Centro de Coordinación para la Prevención de los Desastres Naturales en América Central), Fondo de Incentivos para la Investigación del Ministerio de Ciencia y Tecnología-Consejo Nacional de Investigaciones Científicas y Tecnológicas de Costa Rica-MICIT-CONICIT, Dr. Karen McNally of the Tectonics Organised Research Unit at UCSC (University of California in Santa Cruz), and Dr. Randy White of the Volcano Disaster Assistance Programme of the USA (VDAP).

OVSICORI-UNA is very grateful for the extraordinary contribution from the Costa Rican citizens through a large budget made available by the Government of Costa Rica and the Authorities of Universidad Nacional to construct a 0.66 million dollars new building to host the observatory, as well as to purchase state-of-the-art instrumentation that is essential for systematic research and monitoring of seismic, tectonic and volcanic processes in the region. This contribution has been of great importance to strengthening the capabilities of OVSICORI-UNA. It also gave a major impulse to the development of its Laboratory of Volcano Geochemistry, enabling the implementation of modern sampling and analytical

techniques for the monitoring and study of volcanic fluids and processes.

This research was financially supported by scholarship programmes of Utrecht University and Universidad Nacional, by the Petrology Group of the Department of Earth Sciences, OVSICORI and the Laboratory of Atmospheric Chemistry of the School of Chemistry of Universidad Nacional, as well as by grants provided by the Commission of Incentives of the Costa Rican Council for Scientific and Technological Research (CONICIT) of the Ministry of Science and Technology of Costa Rica (MICIT). I very much appreciate the financial contributions of the Department of Earth Sciences of Utrecht University, Federico Chavarría Kopper, Dr. Ronnie Quintero, Dr. Jorge Marino Protti, Lic. Jorge Brenes, Dr. Karen Mc Nally and the GeoForschungsZentrum, Potsdam to cover my travel

and stay in Holland for the PhD defence, as well as the printing cost of this dissertation, which makes a broad dissemination possible.

I am indebted to Dr. Sandra Kinghorn, Dr. Helga Jiménez, and Elisa Zeledón (La Niña Elisa) for keeping faith in me and for encouraging and supporting me and my relatives all these years.

Finally, I am deeply grateful to my Mom Isabella, my brother Jose Manuel and my sister Mayra, as well as my nieces and nephews for their unconditional love, understanding, and constant support. Of Uli Schmidt, Dr. Jason Scott Herrin ("my paranympnette"), and Calvin Tullos I have many fond memories and I thank them very much for encouraging and inspiring me over the years I dedicated to this research.

Curriculum Vitae

María Martínez Cruz was born in Guanacaste Province, Costa Rica in a little village at the foot of Rincón de la Vieja Volcano, a remote active volcano that is not easy to access.

She received Bachelor and Licentiate degrees in chemistry from the School of Chemistry of Universidad de Costa Rica in San José, Costa Rica in 1998 and 2000, respectively.

From 1993 to 2001 she worked at the Laboratory of Atmospheric Chemistry of the School of Chemistry as a research assistant and as an analytical chemist supporting a joint project on Volcanogenic Emissions developed by this laboratory and the Volcanological and Seismological Observatory of Costa Rica (OVSICORI), both entities of Universidad Nacional in Heredia, Costa Rica.

Between 2001-2008 she worked intermittently on this research with the Petrology Group of the Department of Earth Sciences at Utrecht University in The Netherlands.

She currently works as a geochemist/volcanologist in the Volcano Surveillance Programme of OVSICORI at Heredia, Costa Rica. She is the coordinator of the Laboratory of Volcano Geochemistry of OVSICORI, which supports its Volcano Surveillance Programme.

Author's address

María Martínez Cruz

Coordinator of the Laboratory of Volcano Geochemistry
(Geochemistry and Volcano Surveillance Programmes)
Volcanological and Seismological Observatory of Costa Rica
OVSICORI, Universidad Nacional
P.O. Box 86-3000 Heredia
Costa Rica

E-mail: mmartine@una.ac.cr
maria.martinez.cruz@gmail.com

Website: www.ovsiori.una.ac.cr

Telephone: (506) 2-562 4030/2-562 4001

Fax: (506) 2-261 0303